TRANSPORTATION RESEARCH

RECORD

No. 1317

Materials and Construction

Asphalt Mixtures: Design, Testing, and Evaluation 1991

A peer-reviewed publication of the Transportation Research Board

TRANSPORTATION RESEARCH BOARD
NATIONAL RESEARCH COUNCIL
WASHINGTON, D.C. 1991

Transportation Research Record 1317
Price: $26.00

Subscriber Category
IIIB materials and construction

TRB Publications Staff
Director of Publications: Nancy A. Ackerman
Senior Editor: Naomi C. Kassabian
Associate Editor: Alison G. Tobias
Assistant Editors: Luanne Crayton, Norman Solomon
Graphics Coordinator: Diane L. Ross
Production Coordinator: Karen S. Waugh
Office Manager: Phyllis D. Barber
Production Assistant: Betty L. Hawkins

Printed in the United States of America

Library of Congress Cataloging-in-Publication Data
National Research Council. Transportation Research Board.

Asphalt mixtures : design, testing, and evaluation, 1991.
p. cm. — (Transportation research record, ISSN 0361-1981 ; no. 1317)
Papers from the 70th annual meeting held in 1991 in Washington, D.C.
ISBN 0-309-05155-X
1. Asphalt emulsion mixtures. 2. Asphalt—Testing. 3. Pavements, Asphalt—Testing. 4. Pavement, Asphalt concrete—Testing. I. National Research Council (U.S.). Transportation Research Board. Meeting (70th : 1991 : Washington, D.C.) II. Series: Transportation research record ; 1317.
TE7.H5 no. 1317
[TE275]
388 s—dc20
[625.8'5] 91-44016
CIP

Sponsorship of Transportation Research Record 1317

GROUP 2—DESIGN AND CONSTRUCTION OF TRANSPORTATION FACILITIES
Chairman: Raymond A. Forsyth, Sacramento, California

Bituminous Section
Chairman: Leonard E. Wood, Purdue University

Committee on Characteristics of Bituminous Paving Mixtures to Meet Structural Requirements
Chairman: Dallas N. Little, Texas A&M University, Texas Transportation Institute
Secretary: Robert N. Jester, Federal Highway Administration, U.S. Department of Transportation
David A. Anderson, Benjamin Colucci, Dale S. Decker, R. N. Doty, Jack N. Dybalski, R. G. Hicks, R. J. Holmgreen, Jr., Vincent C. Janoo, Rudolf A. Jimenez, Ignat V. Kalcheff, N. Paul Khosla, Kang-Won Wayne Lee, J-M Machet, Michael S. Mamlouk, Harold R. Paul, R. D. Pavlovich, James A. Scherocman, Tony Stock, Ronald L. Terrel, David G. Tunnicliff, Bernard A. Vallerga, James P. Walter, John S. Youtcheff

Frederick D. Hejl, Transportation Research Board staff

The organizational units, officers, and members are as of December 31, 1990.

Transportation Research Record 1317

Contents

Foreword

This Record contains information on the design, testing, and evaluation of asphalt mixtures. It should be of interest to state and local engineers of materials and construction, as well as to contractors and materials producers.

Four papers deal with polymer-modified asphalts—the specifications for these asphalts and their performance in the field. Little discusses the performance of binder-rich polyethylene-modified asphalt mixtures (Novophalt). He reports that binder-rich modified asphalt concretes are significantly less sensitive to permanent deformation and have significantly greater resistance to fracture. Khosla reports from his study that carbon black was the most significant modifier in reducing pavement rutting and the polymer styrelf was the most significant in reducing fatigue cracking. He and Button have developed a laboratory procedure using a Fourier transform infrared analyzer for determining the polyethylene content of modified asphalt concrete mixtures. They report that the procedure provides reasonable accuracy and precision and is suitable for use as a quality assurance test for highway and airport agencies. Ahlrich and Anderton evaluate the resin-modified paving process and conclude that it provides an alternative surfacing material for many army pavement applications, including tracked-vehicle roads, hardstands, and aircraft parking aprons.

Five papers deal with concepts in asphalt mix design. Cooper et al. discuss the development of a method for the design of hot-mix asphalt using the Nottingham asphalt mix tester. Elliott et al. report on their investigation of the effects of aggregate gradation variations on asphalt mix properties. Harvey et al. discuss the effects of sample preparation and air void measurements on asphalt concrete. Al-Abdul Wahhab and Khan evaluate the Marshall and Hveem mix design procedures for use in Saudi Arabia. Their study indicates that Hveem-designed mixes possess better engineering properties than mixes designed by the Marshall method. Scholz et al. discuss their evaluation of cold in-place recycled (CIR) mixes. Their study compared the mix properties of field cores with those of laboratory-prepared samples and compared CIR mixes with dense-graded hot mixes.

Six papers deal with fracture and deformation characterization of asphalt mixtures. Jenq and Perng discuss the development of a cohesive crack model to simulate progressive crack development in asphalt concrete. Krutz et al. concluded from a rutting research project that strains observed in creep testing depend on the location of instrumentation and the boundary conditions imposed on the sample and that permanent strains after moisture conditioning appear to be a good indicator of possible moisture damage. Hadley presents the results of a repetitive (fatigue) testing program to evaluate the inherent variation in the fundamental resilient properties of field cores representative of in-service conditions and to develop material characterization information concerning the three types of asphaltic materials: wearing, binder, and black base. Al-Qadi and Sebaaly report on a new technique developed to measure the moisture content in hot-mix asphalt concrete. The technique involves measuring the dielectric properties of the hot-mix asphalt concrete using electromagnetic waves in the microwave range. Kim et al. discuss the results of controlled-stress diametral fatigue testing to evaluate the influence of temperature and mixture variables on the fatigue life of asphalt concrete mixtures. Almudaiheem and Al-Sugair report on a comprehensive test program undertaken to investigate the effect of the loading magnitude of the diametral resilient modulus test on the measured results of the test.

Performance Assessment of Binder-Rich Polyethylene-Modified Asphalt Concrete Mixtures (Novophalt)

DALLAS N. LITTLE

A 7-in. overlay of polyethylene-modified asphalt concrete (using the Novophalt process) was placed at the William Hobby Airport in Houston, Texas, in December 1988. The mixture was somewhat binder-rich according to traditional mixture design methodology (i.e., Marshall and Hveem). The binder-rich mixture and the optimally designed polyethylene-modified mixture (optimum binder content according to Marshall design) were evaluated. This evaluation included compressive uniaxial creep compliance testing, uniaxial repeated-load permanent deformation testing, tensile creep testing, tensile strength testing, and resilient modulus testing. Binder-rich polyethylene-modified asphalt concrete proved to be significantly less sensitive to permanent deformation than the control mixture. The binder-rich mixture also demonstrated significantly greater resistance to fracture as verified by indirect tensile test data (toughness) over a range of temperature from 32°F to 104°F and by the slope of the steady-state region of indirect tensile creep plots. The response of the binder-rich mixtures also demonstrated a strong sensitivity to the initial level of compaction. Binder-rich mixtures compacted to air void contents between 5.0 and 6.5 percent were not substantially more susceptible to permanent deformation than the optimally designed mixture at the 104°F test temperature. Data from Italy verify the hypothesis that binder-rich polyethylene-modified asphalt concrete mixtures can perform successfully in certain specialized applications with acceptable resistance to permanent deformation, potentially superior resistance to fracture (reflection cracking and thermal cracking), and potentially superior durability of the low-permeability, binder-rich mixture.

Reconstruction of runway 17-35 at the William Hobby Airport in Houston, Texas, used 20,000 tons of Novophalt modified asphalt concrete. The Novophalt mixture was laid to depths of 7 in. below the surface of the central runway section and 3.2 in. below the shoulder sections. Construction took place between October 1988 and January 1989.

Novophalt modified asphalt cement is a biphase binder system containing polyolefin additives and paving-grade asphalt cement. Novophalt is prepared by incorporating polyolefins, primarily low-density polyethylene (LDPE), into paving-grade asphalt using a patented blending process. The properties of the polyethylene used for modification may vary. Virgin or recycled polyethylene characterized as follows is used:

Characteristic	*Description*
Physical	
Melt index:	1.0–15.0
Melting point (°C)	115–125
Density	0.910–0.940
Fire hazard	Noncombustible
Chemical	Inert hydrocarbon polymer

Department of Civil Engineering, Texas A&M University, College Station, Tex. 77843.

The mix design was carried out by an independent quality control laboratory before construction. The laboratory recommended a binder content of 4.8 to 5.0 percent. In the actual construction, Novophalt hot mix was placed at binder contents ranging from 4.8 percent (the optimum as established in the laboratory) to about 5.8 percent (20 percent above the optimum).

A laboratory evaluation of the actual mixtures used at Hobby Airport was conducted at the Texas Transportation Institute (TTI) of Texas A&M University. The objectives were to verify the mixture design and to investigate the ramifications of using binder-rich mixtures in the runway. Specifically, the effects of high binder contents on deformation potential and fracture potential were investigated. In addition, the effects of initial compaction on deformation potential of the binder-rich Novophalt mixtures were investigated.

PAVEMENT STRUCTURE AND DESIGN CRITERIA

Runway 17-35 at Hobby Airport lies over a native plastic clay with an approximate average annual resilient modulus of 4,900 psi. The subbase consists of a mixture of sand and shells. The main structural layer for most of the life of the pavement was a plain portland cement concrete pavement that had been subsequently overlayed with asphalt concrete to a depth of approximately 4 in.

The reconstruction process called for milling off the existing 4 in. of asphalt in the central runway section and replacing it with 7 in. of Novophalt. The shoulders were overlayed with approximately 3.2 in. of Novophalt. Before the Novophalt overlay was placed, a stress-absorbing membrane interlayer (SAMI) was laid to minimize the potential of crack reflection from the existing portland cement concrete through the Novophalt surface.

Because of the nature of the structural pavement design (i.e., Novophalt laid over the existing primary structural section of portland cement concrete), load-induced flexural fatigue cracking in the surface was not considered a design problem; tensile flexural stresses in the asphalt concrete surface are not induced by load in this type of pavement struc-

ture. The major concern and primary design criterion was permanent deformation in the surface layer under the DC-9 aircraft. Permanent deformation in asphalt concrete surfaces is of primary concern in Houston because of the high pavement temperatures induced by the hot Texas summers.

MATERIALS SELECTED FOR RUNWAY OVERLAY

The aggregate selected for the asphalt mixture used in the overlay was a Scottish granite. The blend of aggregate used at the plant was approximately 35 percent coarse crushed granite particles, approximately 57.5 percent granite screenings, and approximately 7.5 percent clean sand. The job mix formula tolerances for the mixture are as follows:

Sieve Size	*Job-Mix Formula Tolerances (% passing)*
¾ in.	93.0–100.0
½ in.	86.6–100.0
⅜ in.	73.1–87.1
No. 4	56.0–69.3
No. 10	39.6–47.6
No. 40	21.2–29.2
No. 80	10.0–14.6
No. 200	3.0–7.0

The job mix range for the asphalt binder content was between 5.0 and 5.6 percent by total weight of the mixture.

A Novophalt binder consisting of an AC-20 asphalt cement modified with 5 percent recycled LDPE was selected for the mixture. The asphalt was modified with the polyethylene using a Novophalt high-shear blender at the mix plant.

MIXTURE ANALYSIS

The mixture of granite aggregate and Novophalt was evaluated using Marshall and Texas mixture design procedures. These evaluations produced approximately the same optimum binder content of approximately 4.8 to 5.0 percent. The Marshall stability at this range of binder content ranged from 3,700 to 3,800 lb. The air void in this range of binder contents was approximately 4.0 percent. Marshall flow and voids in the mineral aggregate for the mixture meet requirements established by the Asphalt Institute (*1*).

When the binder content of the mixture was raised to 5.8 percent, the Marshall stability of the Novophalt mixture dropped to about 3,300 lb; the average air void content of the binder-rich specimens compacted at 280°F using 75-blow Marshall compaction was approximately 2.2 percent.

Hveem stabilities were above 40 for the mixture with optimum binder content and dropped to approximately 35 for the binder-rich mixture. Once again compaction was performed at about 280°F. Hveem stabilities and air void contents were also determined on samples compacted at 250°F for the Novophalt mixture. The reduction in compaction temperature significantly affected Hveem stability and air void content of the samples. The result of this effect is that the optimum binder content of the samples compacted at the lower temperature was about 6 percent higher than that of samples compacted at the higher temperature (4.6 versus 4.9 percent). This effect of temperature of compaction on optimum binder content indicates that the initial level of compaction affects the performance of the mixture. This concept has been espoused by Foster (*2*). The influence of level of compaction was evaluated in this study.

The compaction temperatures discussed refer to laboratory compaction. Substantially higher field compaction temperatures may be required to achieve satisfactory results.

STUDY APPROACH

Because the prime objective in this research was to evaluate the effect of binder-rich Novophalt mixtures in the Houston environment specifically for the Hobby runway reconstruction project, primary attention was given to mixture properties related to permanent deformation of the mixture at high temperatures. To evaluate deformation potential of the mixtures, the following tests were performed: (a) uniaxial compressive creep compliance, (b) repeated-load permanent deformation, and (c) incremental static compressive loading. During this testing the following variables were considered ("optimum" refers to optimum according to Marshall mix design):

Test	*Variables*
Creep compliance	Void content (level of compaction): optimum, low (standard, modified) Binder content: optimum, high Asphalt type: modified, unmodified Temperature: high
Repeated-load permanent deformation	Void content (level of compaction): optimum, low (standard, modified) Binder content: optimum, high Asphalt type: modified, unmodified Temperature: high
Incremental static compression	Void content (level of compaction): optimum, low (standard, modified) Binder content: optimum, high Asphalt type: modified, unmodified Aggregate: river gravel

In concert with the evaluation of mixture properties in compressive deformation testing, mixture properties were evaluated during testing in the tensile mode of loading. Specifically, indirect tensile testing (IDT Texas Test Method 226-F) (*3*) was performed at 32°F, 77°F, and 104°F; diametral resilient modulus testing (ASTM D4123) was performed at 4°F, 32°F, 68°F, 77°F, and 104°F; and indirect tensile creep testing was performed at 77°F. Each test was performed at two levels of binder content: optimum (approximately 4.8 percent) and binder-rich (approximately 5.8 percent).

All creep and repeated-load deformation testing results were based on the average of at least two replicate specimens per combination of variables (matrix cell). All tensile test results were based on the average of three replicate specimens per combination of variables.

COMPRESSIVE DEFORMATION TESTING

Testing Techniques and Sample Fabrication

Three types of compressive deformation testing were used: uniaxial compressive creep compliance, uniaxial repeated-load

permanent deformation, and uniaxial incremental static creep. Testing was performed on mixtures with optimum binder content (4.8 percent binder) and on binder-rich mixtures (5.8 percent binder). All testing was performed at 104°F. This temperature was determined to be a representative average daily temperature of the upper 2 in. of an asphalt concrete pavement subjected to the climatic conditions in the Houston area during the hottest 180 days of the year (*4*).

All specimens tested were prepared according to the method in the VESYS Users Manual (*5*). The Cox kneading compactor was used for compaction. After compaction, each sample was conditioned in accordance with VESYS procedures. This conditioning consisted of subjecting the sample to three ramp loads and holding these loads for 10 min with minimal unload time between loads. The magnitude of the ramp load was selected so as to remain in the region of loading that would not produce excessive deformation of the sample (i.e., less than 2,500 microstrain). The load used in preconditioning was 10 psi at the 104°F test temperature. The conditioning exercise attempted to simulate the effects of thousands of wheel loads on the pavement. Although the proper conditioning methodology is controversial, the conditioning is expected to affect the final air void contents of the two mixture groups in a manner proportional to their susceptibility to traffic densification.

The initial test philosophy was to compact all mixtures, regardless of binder content, to within the same range of air void content (5.0 to 7.0 percent) and to condition the samples according to the VESYS procedure. This process was intended to simulate construction compaction followed by traffic densification, simulated by the conditioning phase. However, average final air void contents after conditioning and creep testing for the two binder levels were 5.1 and 6.3 percent for the 5.8 and 4.8 percent binder content mixture groups, respectively. The 5.1 percent void content for the mixture with high binder content was *not* thought to be representative of the level of air voids that could be achieved at this high binder content with greater compactive effort. Thus, an increased level of compactive effort was applied using the Cox compactor at 250°F and 280°F.

The level of compactive effort required to produce ultimate densification was determined by trail and error. The compactive efforts used in sample preparation are summarized as follows:

Standard Effort	*Modified Effort*
Layer 1: 30 tamps at 250 psi/tamp	Layer 1: 30 tamps at 600 psi/tamp
Layer 2: 60 tamps at 250 psi/tamp	Layer 2: 60 tamps at 600 psi/tamp
Layer 3: 140 tamps at 250 psi/tamp, 1,000 psi leveling load	Layer 3: 140 tamps at 250 psi/tamp, 1,000 psi leveling load

The average air void contents of the Novophalt mixtures produced by the modified compactive effort were as follows: 4.0 percent (4.8 percent binder, 250°F compaction temperature); 3.8 percent (4.8 percent binder, 280°F compaction temperature); 2.3 percent (5.8 percent binder, 250°F compaction temperature); and 1.6 percent (5.8 percent binder, 280°F compaction temperature). Control mixtures of crushed granite aggregate and AC-20 asphalt (unmodified) were compacted at 250°F using standard compaction efforts. The resulting average air void contents were 5.8 percent for the mixtures with optimum binder content and 1.8 percent for the binder-rich mixtures.

Findings

Results of uniaxial compressive creep testing are summarized in Figures 1 and 2. The data in Figure 1 demonstrate a very small change in creep compliance for the optimum and binder-rich Novophalt mixtures when the mixtures were compacted to air void contents from 5.0 to 6.5 percent. Note the very

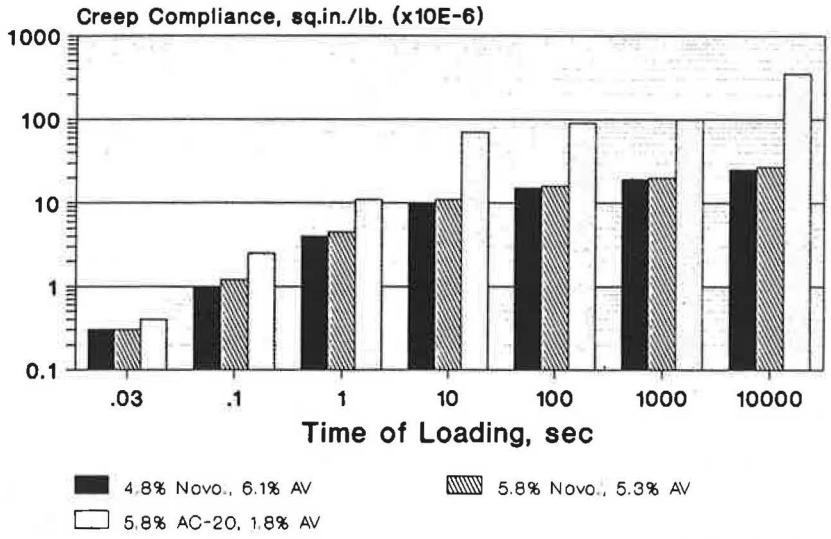

FIGURE 1 Creep compliance versus time of loading for optimally designed and binder-rich Novophalt mixtures compacted to 5.0 to 6.5 percent air void content and binder-rich control mixture.

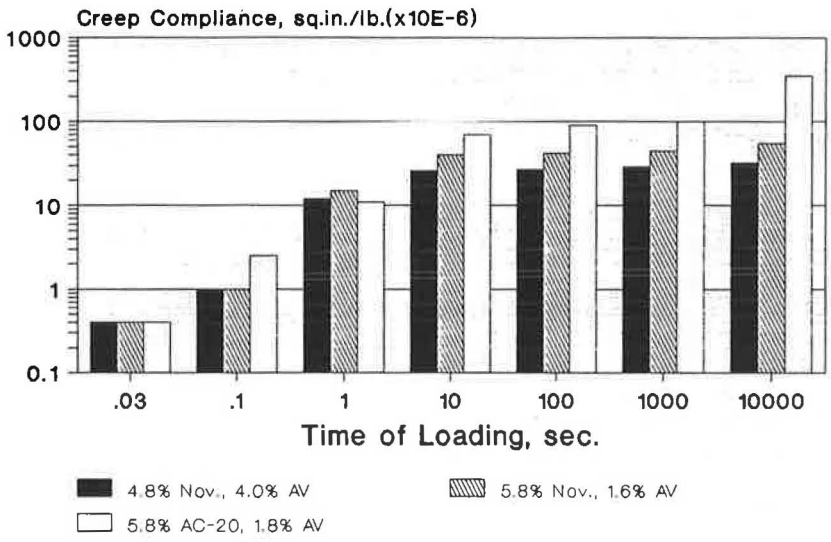

FIGURE 2 Creep compliance versus time of loading for optimally designed and binder-rich Novophalt mixtures compacted to ultimate (low) air void content and binder-rich control mixture.

high compliance for the control mixture, which is a binder-rich AC-20 mixture with a low air void content (1.8 percent). Figure 2 shows creep compliance data following compaction to ultimate air void contents. In this case, the difference between optimum and binder-rich Novophalt mixtures is more noticeable. However, the compliance of the binder-rich Novophalt mixture at 1.6 percent air voids remains substantially less than that of the AC-20 control mixture compacted to an air void content of 1.8 percent.

A critical level of creep compliance was calculated using the modified Shell procedure (*6*), cross-sectional data for the Hobby runway pavement, and contact tire pressure data for the DC-9 aircraft (100,000 passes). The modified Shell equation states

$$\Delta h_{\text{Total}} = \sum_{i=1}^{n} \Delta h_i = \sum_{i=1}^{n} h_i \cdot A_i \cdot \sigma_i \cdot D_i$$

where

Δh_i = change in height of each sublayer;
h_i = thickness of each sublayer; and
A_i = stress factor relating laboratory stress (σ_{lab}, used in obtaining creep compliance D_i) to in situ stress within the sublayer σ_i, $A_i = (\sigma_i/\sigma_{\text{lab}})^{1.61}$ after Regress 6.

By assigning a maximum tolerable deformation within the pavement of 0.125 in. for 100,000 applications of the DC-9 aircraft and by assuming an average annual daytime temperature of 104°F in the hottest 180 days of the year, a design or critical average creep compliance was calculated as 0.000060 in.²/lb. This value is plotted in Figures 1 and 2. The plot of this value can be used to judge the adequacy of the mixture based on creep compliance data. The time of loading of 10,000 sec corresponds to 100,000 load applications (100,000 applications times 0.1 sec of dwell time per load application).

Based on the critical level of compliance (0.000060 in.²/lb), both optimum and binder-rich Novophalt mixtures are quite acceptable when air void contents of the mixture are within the 5.0 to 6.5 percent range (Figure 1). When compacted to ultimate air void contents (Figure 2), the Novophalt mixture with optimum binder content is quite adequate; the binder-rich Novophalt mixture is adequate, although it approaches the design compliance at 10,000 sec; and the binder-rich AC-20 mixture compacted to ultimate air voids demonstrates a compliance at 10,000 sec (approximately 0.000350 in.²/lb), which is approximately six times the design compliance (0.000060 in.²/lb).

Figures 3 and 4 show accumulated permanent strain data versus loading applications. Once again, data in Figure 3 are for samples compacted using a standard compaction effort, and data in Figure 4 are for the modified compactive effort resulting in minimum air void levels. The trend is essentially the same as for the creep compliance testing. There is essentially no difference in the optimum binder content and the binder-rich Novophalt data when the samples are compacted to air void contents within the 5.0 to 6.5 percent range, as shown in Figure 3. However, when the samples are compacted to ultimate or low air void contents, as shown in Figure 4, a greater difference in deformation results between the optimum binder content mixture and the binder-rich mixture. However, the binder-rich Novophalt mixture is still substantially more resistant to permanent deformation than the control mixture, which failed at 20,000 cycles of loading.

Figure 5 further illustrates mixture sensitivity to binder content of polyethylene-modified binders. This figure shows the changes in the permanent strain determined from incremental static deformation testing on a siliceous river gravel mixture. The height of each bar in the figure represents the increase in permanent strain for the particular mix in question over the control mix at the same time of incremental loading. The control mixture was an optimally designed river gravel mixture with binder of either AC-20 or AC-20 plus LDPE (Novophalt). In the figure, binder-rich mixtures with the traditional and Novophalt binders were compared with the optimal

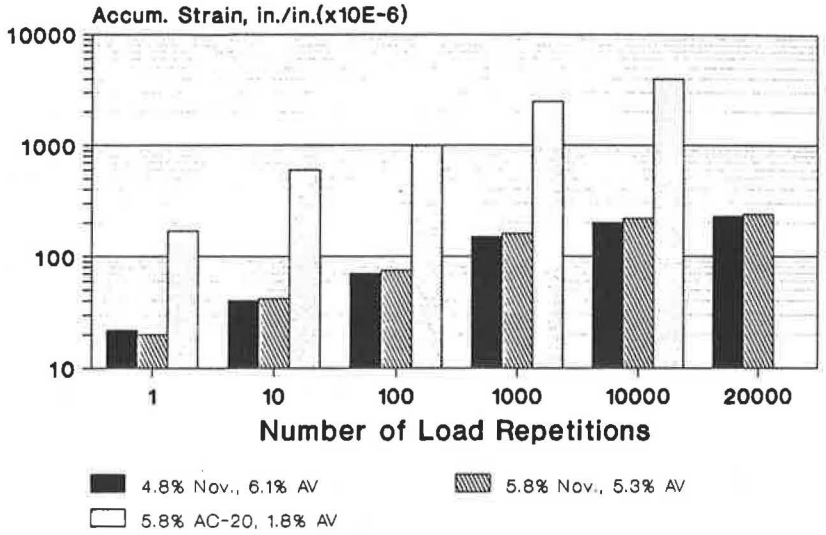

FIGURE 3 Accumulated permanent strain versus loading repetitions for optimally designed and binder-rich Novophalt mixtures compacted to 5.0 to 6.5 percent air void content and binder-rich control mixture.

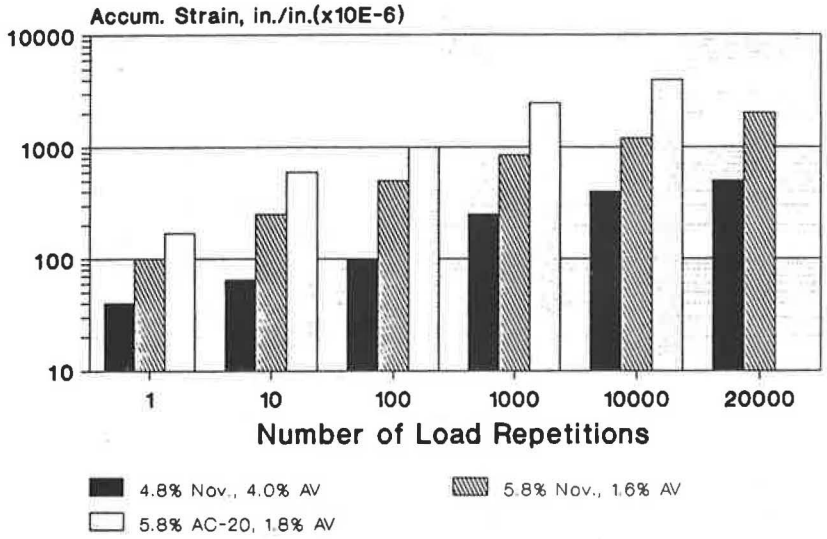

FIGURE 4 Accumulated permanent strain versus loading repetitions of optimally designed and binder-rich Novophalt mixtures compacted to ultimate (low) air void content and binder-rich control mixture.

(control) mix with the traditional and Novophalt binders, respectively. In each case (traditional and Novophalt) the binder-rich mixture consisted of 1.15 percent of the optimum level of binder.

Figure 5 clearly shows the significant influence of binder type (Novophalt versus unmodified AC-20) and level of compaction. For the granite mixture, Novophalt is substantially more resistant to deformation than the traditional mix for all conditions evaluated. Of most significance is the level of increase in deformation for the binder-rich Novophalt mixture compared with the level of increase for the binder-rich traditional mixture.

TENSILE TESTING

Resilient Modulus

Diametral resilient modulus testing was performed in accordance with ASTM D4123 at the nominal high average surface temperature of 104°F for a mixture containing the granite aggregate used at Hobby Airport and a river gravel aggregate used as a laboratory standard at TTI because of its sensitivity to binder properties and binder content. Figure 6 shows that the binder-rich modified mixture retains a resilient modulus that is substantially greater than that of the control mixture

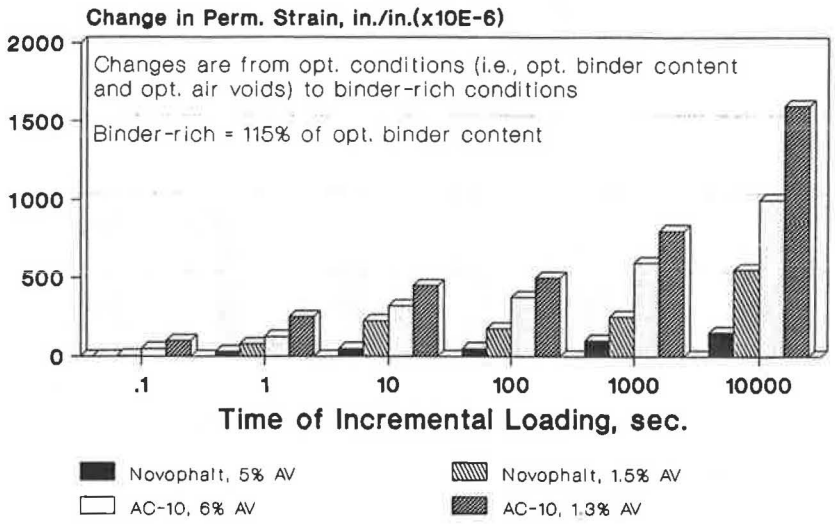

FIGURE 5 Changes in permanent strain comparing two binder-rich Novophalt mixtures (low and high levels of densification) with an optimally designed Novophalt mixture and two binder-rich traditional mixtures (low and high levels of densification) with an optimally designed traditional mixture.

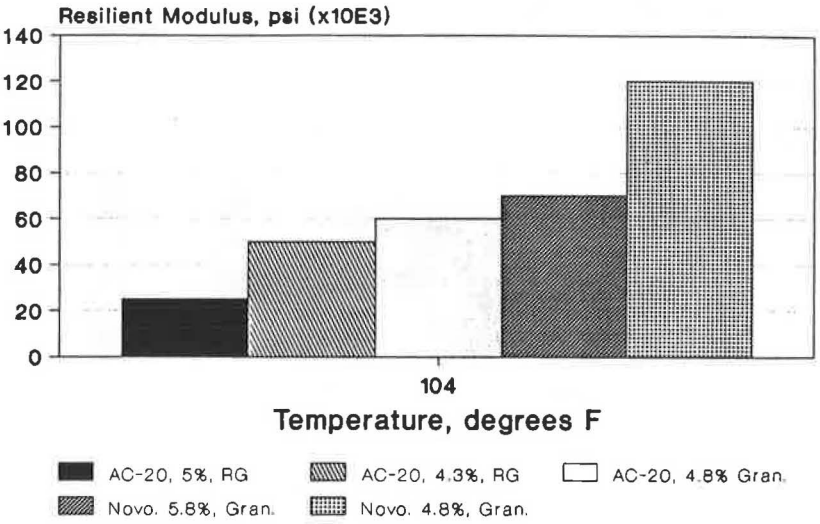

FIGURE 6 Comparison of resilient moduli at 104°F for selected mixtures of Novophalt and traditional asphalt.

at the optimum binder content. The optimum and binder-rich river gravel mixtures are included in the analysis simply to demonstrate the sensitivity of mixtures to binder content when traditional, unmodified binders are used. The ability of binder-rich polyethylene-modified mixtures to retain a higher level of resilient modulus is significant because this higher level indicates an improved load-spreading capability of the asphalt layer.

Indirect Tensile Testing

Indirect tensile strength testing was performed at three temperatures: 32°F, 77°F, and 104°F at a stroke rate of 2 in./min. Figure 7 summarizes the results of this testing for the optimum and binder-rich mixtures. All samples were compacted to ultimate (low) air void contents. This figure shows that the toughness, or area under the stress-strain plot, is significantly greater for the binder-rich mixtures than for the optimum mixtures of the polymer-modified (Novophalt) mixture.

Toughness is often used as a relative indicator of the resistance of an asphalt concrete mixture to fracture, either fatigue-related or temperature-related (*7*). High toughness values indicate greater resistance to fracture, and low toughness values indicate lower resistance to fracture. Materials with high toughness values have high potential to absorb energy without fracture. The primary significance of the data plotted in Figure 7 is that the binder-rich Novophalt mixture provides signifi-

cantly higher toughness and thus greater resistance to fracture across the entire temperature range evaluated.

The trend toward greater resistance to fracture due to the use of higher binder contents is substantiated by the results of indirect tensile creep testing data, shown in Figure 8. These tests were performed at 77°F under a constant stress level of 20 psi. The slope of the binder-rich Novophalt mixtures in the steady-state region of the creep test is substantially higher than the comparative slope for the Novophalt mixtures with the optimum binder content. This slope indicates the rate of energy dissipation of the mixture under load. A faster rate of energy dissipation indicates the ability to absorb energy without fracture. Thus, mixtures with steeper slopes in the steady-state region of the tensile creep test indicate mixtures with lower fracture potential.

Schapery (*8*) has demonstrated that by applying viscoelastic fracture principles, the constants K_1 and k_2 in the phenomenological fatigue relationship [$\log N = \log K_1 + k_2 \log (1/e_t)$, where N is number of loading applications and e_t is the repeated level of tensile strain] can be calculated as a function of the slope of the steady-state region of the tensile creep curve. In fact, Schapery has shown the parameter K_2 to be very simply related to the slope of the steady-state region of the creep compliance curve (m) as $k_2 = 2/m$. Also, Al-Balbissi and Little (*9*) have established that the magnitude of the shift factor between laboratory and field fatigue data is directly related to the slope of the steady-state creep curve because this slope indicates the rate at which the mixture can relax and dissipate residual stresses.

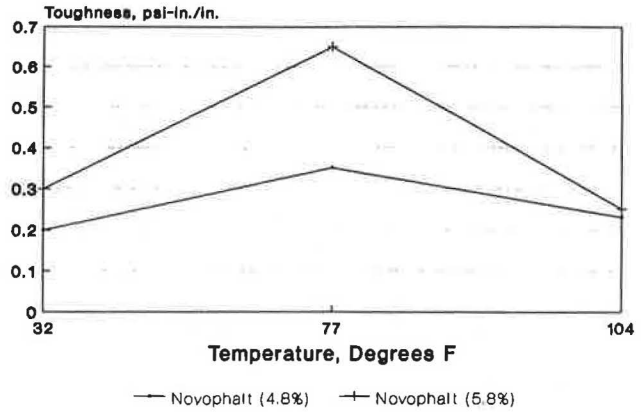

FIGURE 7 Comparison of toughness of optimally designed and binder-rich Novophalt mixtures determined from indirect tension testing at 32°F, 77°F, and 104°F.

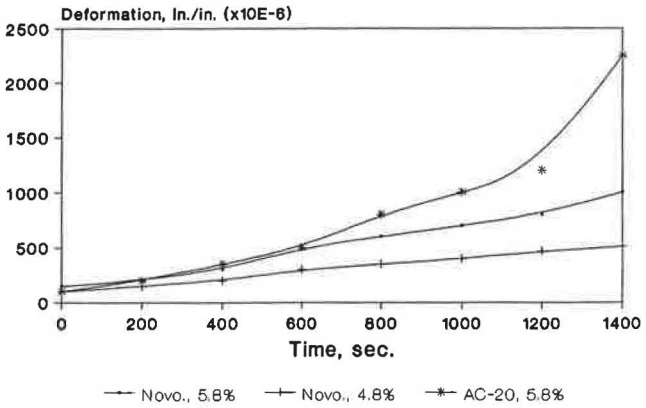

FIGURE 8 Indirect tensile creep data at 77°F, 20 psi stress level, comparing optimally designed and binder-rich Novophalt mixtures and unmodified AC-20.

The control mixture shown in Figure 8 is a binder-rich AC-20 mixture. This mixture exhibits an even higher slope than the binder-rich Novophalt sample. However, the steady-state region of this mixture is substantially less under the 20-psi stress level. The time to rupture of the binder-rich control mixture is substantially shorter than the time to rupture for either Novophalt mixture. Time to rupture indicates flexural fatigue potential. Kennedy (*10*) has empirically demonstrated a relationship between time to rupture in the indirect tensile creep test and number of loading cycles to failure in repeated-load indirect tensile fatigue tests. Thus, a middle ground must be sought in optimizing mixture properties related to fracture and fatigue. This middle ground is characterized by the ability to effectively dissipate energy without fracture and at the same time resist accumulated damage (plastic damage) leading to fatigue failure. In this case, the binder-rich Novophalt mixture appears to achieve this middle ground.

Another indication of the linkage between fracture potential and binder content is work done by Molenaar (*11*). Molenaar demonstrated the relationship between fracture toughness (K_{1c}) and air void content for a gravel and sand mixture (Figure 9). Note that reducing the air void content substantially improves the value of K_{1c}. Of course, reducing binder content lowers air void content.

DISCUSSION OF FINDINGS

This study indicates that the binder-rich Novophalt mixtures used at Hobby Airport should perform well and resist rutting and *may* have improved fracture resistance compared to the Novophalt mixture with optimum binder content. The results of this study point out some interesting general trends:

1. Binder-rich polymer-modified asphalt (Novophalt) mixtures are substantially less susceptible to rutting or permanent deformation than are binder-rich traditional mixtures even when the polymer-modified mixtures are compacted to air void contents well below the level producing plastic flow (less than 3 percent air voids) and are tested at high temperatures (104°F).
2. The level of initial compaction has a pronounced influence on the deformation potential of the polymer-modified mixtures.
3. Binder-rich polymer-modified mixtures demonstrate a higher resistance to fracture than do mixtures with optimum binder contents.

These trends indicate that certain specific pavement applications may be better satisfied by polymer-modified mixtures (Novophalt) that are slightly binder-rich. These mixtures would provide increased resistance to cracking due to thicker binder films and improved durability mainly because of substantially

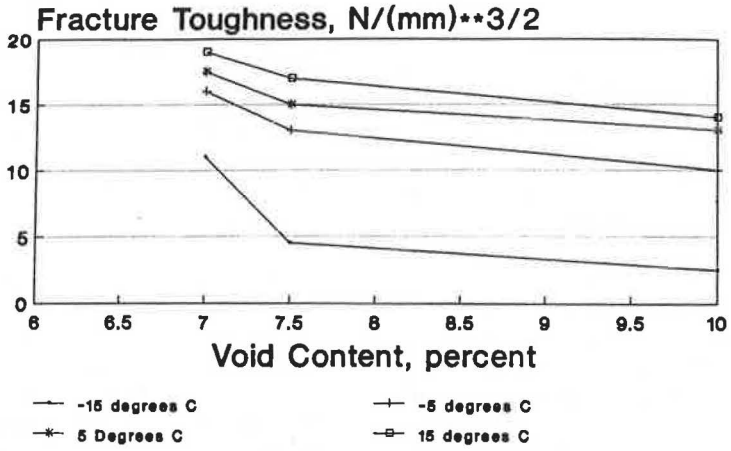

FIGURE 9 Influence of void content and temperature on fracture toughness of gravel sand asphalt mixes (*11*).

reduced permeability to air (oxidation) and water (stripping). Pallotta (*12*) has provided evidence that supports the use of binder-rich polyethylene-modified asphalt concrete on bridge decks in Europe. Pallotta reported on Novophalt in Italy with binder contents in the range of 20 to 25 percent above the optimum binder level; these mixtures were still mechanically more stable than a comparable unmodified mixture at the optimum binder content. Based on these Italian data, binder-rich Novophalt mixtures have been laid whenever impermeability and durability were a major concern. The preferred air void content range was 2 to 3 percent for the binder and wearing courses, based on the Italian data (*12*). Actual air void contents in the range of 1 to 2 percent provided stable Novophalt mixtures.

A U.S. Army Corps of Engineers study (*13*) provides additional evidence that binder-rich mixtures provide better resistance to permanent deformation even at very low air void contents than do traditional mixtures. This study compared properties of asphalt mixtures modified with several different modifiers including oxidants, styrene-butadiene-styrene, ethylene–vinyl acetate, polyethylene, and AC-40 asphalt cement. Three variables were evaluated in mixtures with each modifier: (a) binder content, (b) modifier content, and (c) asphalt cement source. Binder contents evaluated were optimum, 80 percent of optimum, and 120 percent of optimum.

The Corps of Engineers study (*13*) states that "the polyethylene-modified blends were less sensitive to all three matrix variables as a whole when compared to most of the modifiers of this study."

The variation in air void contents in this study produced by varying the compactive effort and compaction temperature had a pronounced effect on the susceptibility of the mixtures to uniaxial compressive repeated-load permanent deformation. Binder-rich polyethylene-modified mixtures compacted to air void contents of 5.0 to 6.5 percent produced substantially reduced permanent deformation when compared with binder-rich mixtures compacted to ultimate (low) air voids (1.0 to 2.0 percent). In fact, the binder-rich mixtures compacted to high air void contents demonstrated a permanent deformation potential that was essentially identical to that of the optimally designed mixture.

The influence of level of compaction on ultimate air void content, and hence rutting potential, has been addressed by Foster (*2*) for traditional (unmodified mixtures). In this study, Foster states:

> Review of existing literature shows that densification occurred at a very rapid rate in the first few months of traffic followed by a much slower rate for the next five years after which no further densification occurred. This review shows *conclusively* that the density to which a pavement is rolled controls the density that develops in both stages.

Foster further presents data demonstrating that the ultimate densities of mixtures with both soft and stiff binders are controlled by the construction density. The stiffer binders, as expected, allow considerably less additional densification than do the soft binders. These results are shown in Figure 10. This trend indicates not only the importance in initial compaction but also the influence of binder stiffness. It is logical to extend this trend to polymer-modified binder systems, which are less resistant to plastic deformation than are traditional mixtures at high temperatures. Thus, the deformation of the polymer-modified asphalt may well be more greatly influenced by initial compaction than would traditional mixtures.

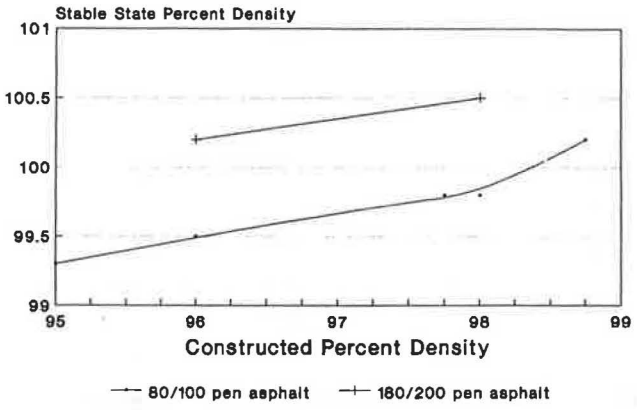

FIGURE 10 Evaluation of effect of construction densification on stable-state air void content of asphalt concrete (*2*).

CONCLUSIONS

1. Binder-rich polyethylene-modified mixtures (Novophalt) are substantially more resistant to permanent deformation than are binder-rich traditional systems.

2. Even when binder-rich polyethylene-modified mixtures are compacted to air void contents below 3 percent, their resistance to permanent deformation is substantially superior to that of binder-rich traditional mixtures.

3. Binder-rich Novophalt mixtures are sensitive to the level of initial densification. Reducing the level of initial densification from the 1.0 to 2.0 percent air void range to the 5.0 to 6.5 percent air void range results in permanent deformation in binder-rich Novophalt mixtures that is not significantly greater than that of optimum binder content Novophalt mixtures. It appears that mixtures prepared using modified binders are substantially more resistant to densification than are traditional (unmodified) mixtures even if the mixtures are binder-rich. This conclusion is based on results of repeated-load permanent deformation testing of polyethylene-modified and unmodified mixtures. Apparently the rheological change in the binder caused by polyethylene modification is responsible for the resistance of the mixture to postconstruction densification and hence superior resistance to rutting. This finding indicates that the resistance to permanent deformation of binder-rich polyethylene-modified mixtures can be significantly improved by controlling the level of density achieved at construction.

4. Binder-rich Novophalt mixtures with low air void contents, because of their ability to absorb energy, possess greater potential to resist fracture than do optimum binder content mixtures.

5. Binder-rich Novophalt mixtures may have applications in specialized situations that require lower air and water permeability and greater resistance to fracture while still maintaining acceptable resistance to permanent deformation. These applications have been demonstrated successfully in field applications in Italy.

6. These results in no way suggest that traditional mixture design methodologies and criteria be abandoned. The results simply indicate that polymer-modified binder systems such as Novophalt are very different rheological systems than traditional binder systems. Consequently, for certain applications, a polyethylene-modified mixture with a higher binder content may provide a more effective system.

7. Runway 17-35 at Houston Hobby Airport continues to perform well 2 years after construction with no signs of cracking or permanent deformation.

REFERENCES

1. *Mix Design Methods for Asphalt Concrete and Other Hot Mix Types*. Manual Series No. 2 (MS-2), Asphalt Institute, College Park, Md., 1984.
2. C. R. Foster. Traffic Densification of Asphalt Pavements. Presented at the Annual Meeting of the Association of Asphalt Paving Technologists, Albuquerque, N.M., Feb. 1990.
3. *Manual of Testing Procedures*. Section 226-F, Texas State Department of Highways and Public Transportation, Austin, Aug. 1984.
4. J. Li, M. J. P. Olsen, and D. N. Little. *Use of Climatic Data for the Prediction of Permanent Deformation in Flexible Pavements*. Texas Transportation Research Report 452-2. Nov. 1989.
5. W. J. Kenis. *Predictive Design Procedures, VESYS Users Manual—An Interim Design Manual for Flexible Pavements Using the VESYS Structural Subsystem*. Final Report FHWA-RD-77-154, FHWA, U.S. Department of Transportation, 1978.
6. K. Mahmoud and D. N. Little. *Improved Asphalt Concrete Mixture Design Procedure for Texas*. Research Report 474-1F. Texas Transportation Institute, Texas A&M University, College Station, Nov. 1988.
7. D. N. Little and B. L. Richey. A Mixture Design Procedure Based on the Failure Envelope Concept. *Proc., Association of Asphalt Paving Technologists*, Vol. 52, 1983.
8. R. A. Schapery. Models for Damage Growth and Fracture in Nonlinear Viscoelastic Particulate Composites. *Proc., North U.S. National Congress of Applied Mechanics*. Book No. H0022B. ASME, 1982.
9. A. Al-Balbissi and D. N. Little. Effects of Fracture Healing on Laboratory-to-Field Shift Factor. In *Transportation Research Record 1286*, TRB, National Research Council, Washington, D.C., 1990, pp. 173–183.
10. T. W. Kennedy and B. W. Porter. *Comparison of Fatigue Test Methods for Asphalt Materials*. Research Report 183-4. Center for Transportation Research, University of Texas, Austin, 1975.
11. A. A. A. Molenaar. *Structural Performance and Design of Flexible Road Constructions and Asphalt Concrete Overlays*. Ph.D. dissertation. 1983.
12. S. Pallotta. I Conglomorati Bituminous Modificati. *Rassegna Del Bitume*, April 1985.
13. G. L. Anderton. *Evaluation of Asphalt Binder Modifiers*. Miscellaneous Paper GL-90-1, U.S. Army Engineer Waterways Experiment Station, Vicksburg, Miss., Jan. 1990.

Effect of the Use of Modifiers on Performance of Asphaltic Pavements

N. PAUL KHOSLA

The effects of two commercially available asphalt modifiers in improving the mechanical properties of asphalt paving mixtures were explored, and the abilities of these modifiers to mitigate pavement distress and improve overall pavement performance were evaluated. Nine binders were formulated with three asphalt grades and two modifiers. The modifiers investigated were carbon black and polymerized asphalt (styrelf). The dense-graded asphalt paving mixture specimens were subjected to dynamic and creep tests at temperatures of 0°, 40°, 70°, 100°, and 140°F, and the mechanical properties determined were resilient modulus, creep, permanent deformation parameters, and fatigue life. On the basis of these properties, the VESYS IIIA pavement performance prediction model was used to assess any improvement of the modifier on pavement distress and overall performance. The results indicate that the effect of the modifier on the paving mixture properties is not significant at low temperatures but pronounced at high temperatures. The predicted performance shows that carbon black is the most significant in reducing pavement rutting and polymer is the most significant in reducing fatigue cracking. Both modifiers show some degree of improvement in the overall pavement performance.

Choosing a suitable asphalt is of primary importance in the construction of a satisfactory pavement. The various grades and qualities of asphalt produced from different crudes and manufacturing processes show a marked difference in weathering resistance and durability. Because the highway engineer usually has a limited selection of asphalt, there is a need for a practical way to improve asphalt quality by adding ingredients. It is believed that asphalt cements modified with polymer (styrelf) and with carbon black may provide mixtures with improved durability, wear resistance, and general performance (*1–5*). Accordingly, the effectiveness of these two modified binders in improving the structural properties of asphaltic mixtures was verified, namely, their resilient modulus, fatigue life, resistance to rutting, and mitigation of low-temperature cracking.

MATERIALS AND SPECIMEN PREPARATION

The base asphalts used include AC-5, AC-10, and AC-20. These asphalts were sent to the Elf Aquitaine Laboratory in Terre Haute, Indiana, for blending with polymer. After blending, the modified asphalt is called "styrelf." Styrelf is a polymer system in which the polymer (styrene-butadiene block copolymer) undergoes an irreversible chemical reaction with asphalt through a patented vulcanizing process. MICROFIL8—pelletized carbon black using 8 percent maltenes—was also blended with each of the base asphalts. The amount of MICROFIL8 that should be used depends on the desired consistency of the binder and the viscosity of the original asphalt. Thus, to have the desired stiffening effect, a slightly higher amount of modifier is mixed with softer asphalts. Consequently, AC-5 was blended with 12 percent MICROFIL8, and AC-10 and AC-20 were blended with 10 percent MICROFIL8. The properties of the binders are summarized in Table 1.

Dense-graded granite aggregate was used. The gradation of the aggregates conforms to the North Carolina specifications for I-1 mix. The gradation of the aggregates is as follows:

Sieve Size	*Percent Passing*
3/4 in.	100
1/2 in.	96
3/8 in.	92
No. 4	66
No. 8	50
No. 16	39
No. 40	24
No. 80	10
No. 200	3

The mixtures were designed in accordance with the Marshall method of mix design (*6*); a summary of the mixture properties is given in Table 2. The specific gravity of the base asphalts ranged from 1.020 to 1.035 and the specific gravity of polymer-modified binders ranged from 1.029 to 1.044; the specific gravity of the pelletized carbon black was assumed to be 1.740. To keep the volume of the binder constant in all the mixtures, the binder contents used in the mixtures were varied, as shown in Tables 2 and 3.

Specimens for the resilient modulus and fatigue tests were 4 in. in diameter and 2.5 in. high and fabricated using the mechanical Marshall compactor. Specimens for the creep tests were 4 in. in diameter and 8 in. high and prepared with a modified Rainhart mechanical compactor. The mixture was compacted in four layers. The sequence of weight of the mixture, starting at the bottom was 1200, 1000, 800, and 600 g, and the corresponding numbers of blows on each layer were 60, 70, 80, and 85. This procedure was developed as part of a previous study (*7*) to provide uniform density from top to bottom of the specimen and produce a specimen with the same density as that prepared by the mechanical Marshall compactor.

Department of Civil Engineering, North Carolina State University, Box 7908, Raleigh, N.C. 27695.

TABLE 1 BINDER PROPERTIES

Property	Binder AC-5	AC-5+P	AC-5+ 12%C	AC-10	AC-10+P	AC-10+ 10%C	AC-20	AC-20+P	AC-20+ 10%C
penetration, 100g, 5 sec, 77°F	140	102	104	130	89	122	82	61	72
viscosity, abs, 140°F, P	741	2940	2250	1050	4285	1900	2220	8255	3840
viscosity, kin, 275°F, cst	315	544	616	412	797	614	502	1178	1170
Pen - vis number (PVN)pp	-0.2	0.3	0.5	0.2	0.7	0.7	-0.1	0.8	1.0

TABLE 2 SUMMARY OF MIXTURE PROPERTIES

Property	Binder AC-5	AC-10	AC-20
Percent asphalt by wt. aggregate	5.87	5.88	5.94
Percent asphalt by wt. mixture	5.55	5.56	5.61
Mix bulk Sp. Gr.	2.30	2.30	2.30
Absorbed asphalt (percent)	0.70	0.70	0.70
Aggregate bulk Sp. Gr.	2.58	2.58	2.58
Asphalt Sp. Gr.	1.020	1.023	1.035
VMA (percent)	15.78	15.71	15.85
Air Void (percent)	4.75	4.80	4.86
Marshall Stability (lb)	2190	2380	2550
Flow (0.01 IN)	11	10	10

TEST PROCEDURES

The procedures for creep, fatigue, and resilient modulus tests are briefly described. A detailed description of the test procedures and equipment is given elsewhere (7).

Creep Test

The incremental static creep tests were conducted on specimens 4 in. in diameter and 8 in. high to determine the permanent deformation coefficients to be used in the VESYS computer program. Test specimens at temperatures of −20°, 0°, 20°, 40°, 70°, 90°, and 120°F were tested under a creep stress of 20 psi. However, specimens at 140°F were tested under a creep stress of 10 psi. Furthermore, specimens made with AC-5 and AC-10 were too soft to be tested even under a creep stress of 10 psi at 120° and 140°F, so no creep test data were generated for these mixture specimens at these temperatures.

The total permanent strain at the end of each rest period following load increment, as shown in Figure 1, was calculated. The total permanent strain versus the incremental time of loading was plotted on log-log paper, as shown in Figure 2. A best-fit straight line is constructed through the plotted points intersecting the vertical axis at a 0.1-sec loading time. The permanent deformation coefficients of layer material were calculated as follows:

$$\mu = \frac{IS}{e} \qquad \alpha = 1 - S$$

where e is the resilient strain. The resilient strain is determined from a repetitive loading test conducted after the creep test.

TABLE 3 BINDER SPECIFIC GRAVITY AND BINDER CONTENT OF MIXTURES

	Binder					
Property	AC-5+P	AC-5+C	AC-10+P	AC-10+C	AC-20+P	AC-20+C
Specific Gravity	1.029	1.107	1.036	1.095	1.044	1.098
% Asphalt by wt. agg.	5.929	6.389	5.955	6.306	5.992	6.361
% Asphalt by wt. mix.	5.599	6.005	5.647	5.932	6.653	5.981

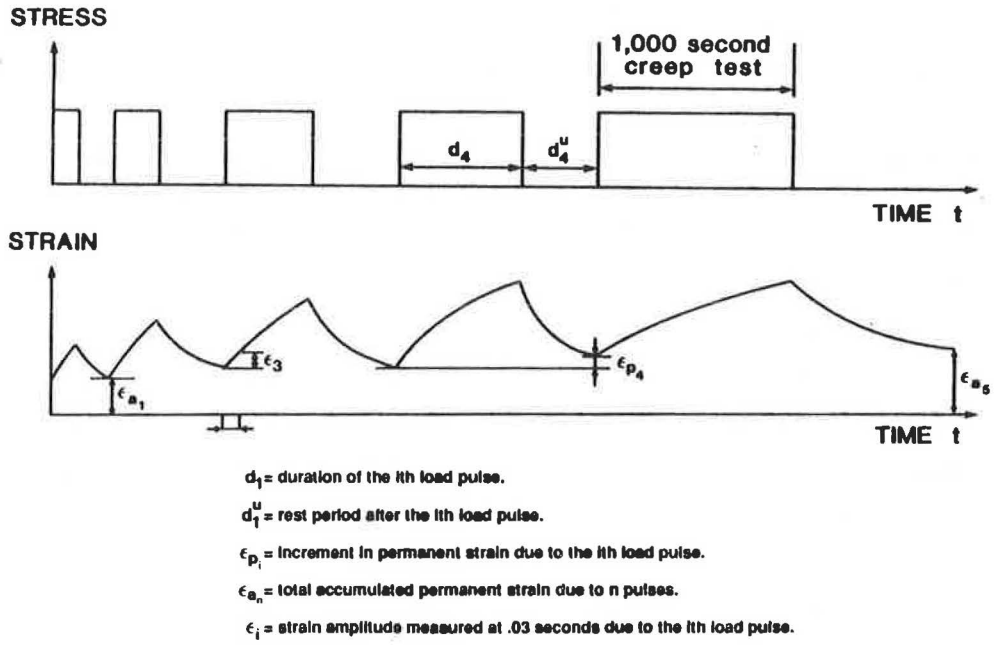

FIGURE 1 Stress and strain of incremental static test series.

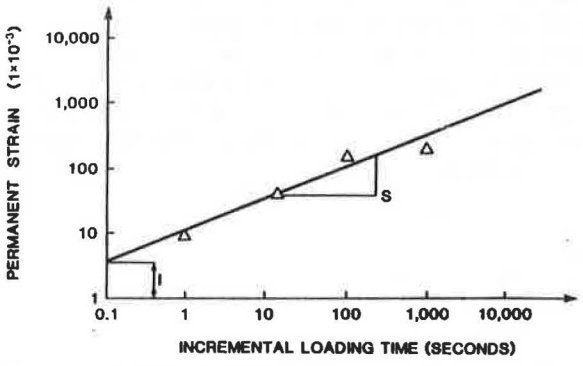

FIGURE 2 Permanent strain curve using incremental static creep test.

Resilient Modulus Test

The resilient modulus tests were conducted on diametral specimens (4 in. × 2.5 in.) in the indirect tension mode at 0°, 40°, 70°, 100°, and 140°F. A test load was applied along the vertical diameter of the test specimen, and the corresponding deformation was measured across the horizontal diameter. The resilient modulus was calculated as follows:

$$M_R = \frac{P(\nu + 0.2734)}{Dt}$$

where

P = load in (lb),

ν = Poisson's ratio (assumed to be 0.35),
t = thickness of specimen (in.), and
D = total horizontal resilient deformation.

Fatigue Test

Fatigue response of the mixtures was measured on diametral specimens in the indirect tension mode. The controlled stress mode of loading with square wave form was used, which included a 0.1-sec loading period and 2.9-sec unloading period. Stresses in the range of 15 to 50 psi were used, and the tests were conducted at 70°F.

In the fatigue test, a repetitive load was applied, and the initial strain was measured between 100 and 200 repetitions. The number of cycles to failure (N_f) was represented by the load's reaching a limiting value of 70 percent of the original load. The number of cycles to failure (N_f) versus the initial tensile strain (e) was plotted on log-log paper. Then a best-fit straight line was drawn through the points. The slope of the line was denoted as S, and the strain value corresponding to 100 load applications was denoted as I. The straight line was shifted horizontally to the right by a factor of 13.03, as suggested by Finn (*8*), to adjust for field fatigue properties. This is because laboratory tests do not take into account several important factors, such as healing of the pavement between stress applications, rest time between stresses, and variability in the position of the load within the wheel path resulting in a reduction of stress due to the passage of a certain number of vehicles. The mean value of fatigue coefficients was calculated as follows:

$$K_2 = \frac{1}{S} \qquad K_1 = 100(I)^{1/S}$$

ANALYSIS OF TEST RESULTS

The analysis of the data and plots of the test results pertaining to resilient modulus, creep, and fatigue characteristics are described. Two replicate specimens for each test condition were used.

Creep Test Results

As discussed, the total permanent strain at the end of each rest period was plotted on a log-log paper at a function of incremental loading times: 0.1, 1, 10, 100, and 1,000 sec. The permanent deformation plots of incremental static loading tests at 40°F and 100°F are shown in Figures 3 and 4.

An analysis of the plot in Figure 3 reveals that the mixtures containing the conventional asphalts AC-5, AS-10, and AC-20 exhibited significantly higher deformation than the mixtures modified with polymer and carbon black. Thus, it can be inferred that these modified mixtures will result in less rutting. An analysis of the rutting potential of these mixtures supports this premise.

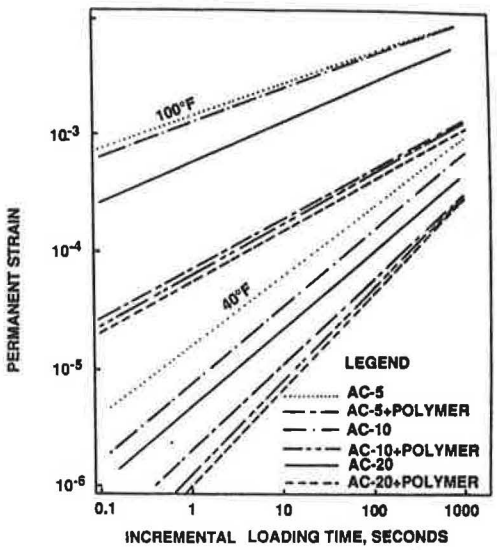

FIGURE 3 Permanent strain from incremental static loading test: AC-5, AC-5+P, AC-10, AC-10+P, AC-20, and AC-20+P.

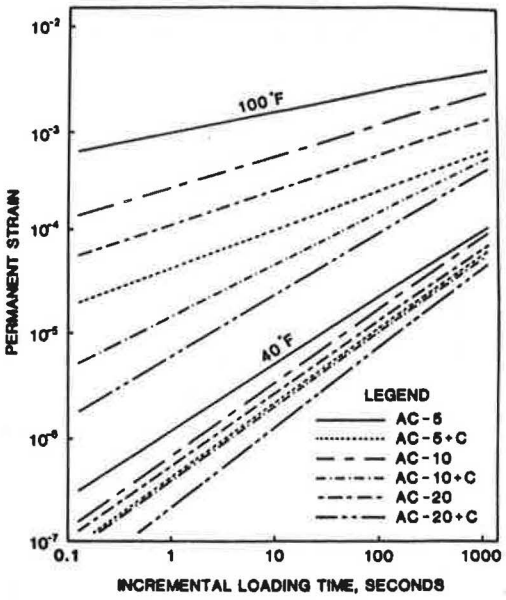

FIGURE 4 Permanent strain from incremental static loading test: AC-5, AC-5+C, AC-10, AC-10+C, AC-20, and AC-20+C.

Resilient Modulus Test Results

The plot of the resilient modulus values versus temperature for the mixture types is shown in Figures 5 and 6. Because the mixture specimens made with AC-5 and AC-10 were too soft to be tested above 100°F, no resilient modulus data were generated for these mixtures at 120°F and 140°F. The data in Figures 5 and 6 indicate that at low temperatures, mixtures made with AC-5, AC-10, AC-5+P, AC-10+P, AC-5+C, and AC-10+C have almost the same modulus values, whereas

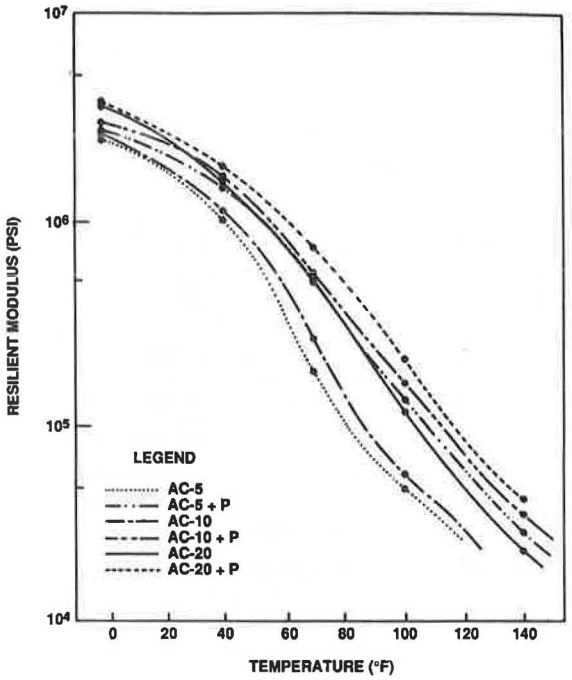

FIGURE 5 Resilient modulus versus temperature: AC-5, AC-5+C, AC-10, AC-10+C, AC-20, and AC-20+C.

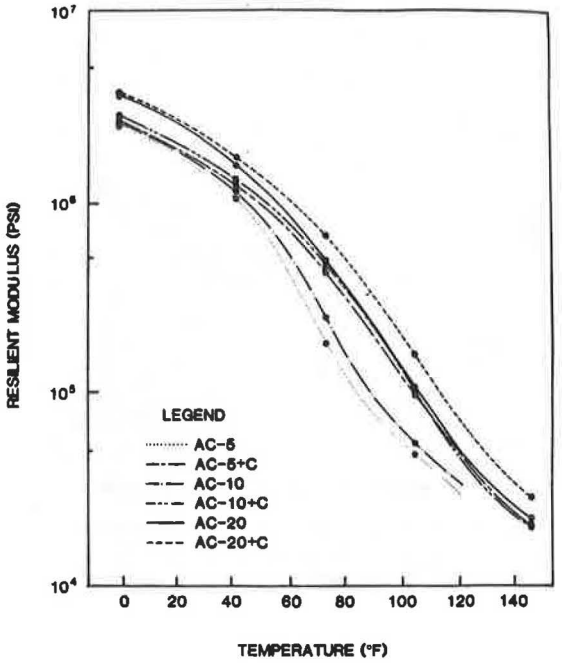

FIGURE 6 Resilient modulus versus temperature: AC-5, AC-5+P, AC-10, AC-10+P, AC-20, and AC-20+P.

AC-20, AC-20+P, and AC-20+C provide mixtures with slightly higher modulus values. At high service temperatures, mixtures made with AC-5 and AC-10 have the lowest resilient modulus values. In addition, at temperatures above 100°F, mixtures made with AC-5+P, AC-10+P, AC-5+C, AC-10+C, and AC-20 have no significant difference in their resilient modulus values, whereas AC-20+P and AC-20+C provide mixtures with the highest resilient modulus values. It can be concluded that adding polymer and carbon black to the asphalt reduces the temperature susceptibility and gives mixtures higher resilient modulus at high temperatures without affecting the modulus values at low temperatures.

Fatigue Test Results

The fatigue lives are plotted in Figures 7 and 8. The data in Figures 7 and 8 suggest that mixtures containing AC-5 and AC-10 have relatively shorter fatigue lives than other mixtures. Furthermore, the mixtures made with AC-5+P, AC-

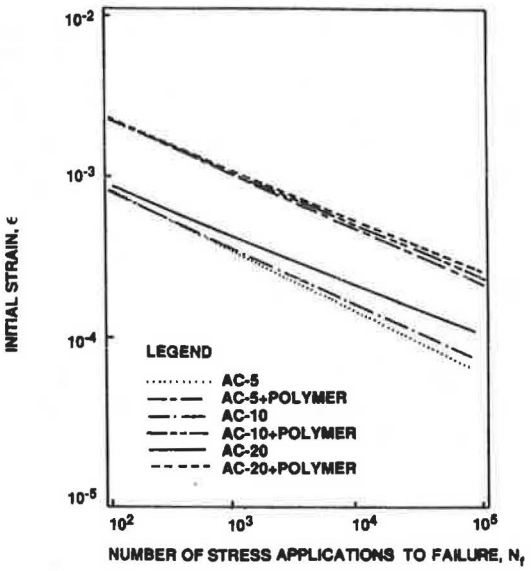

FIGURE 7 Strain versus cycles to failure at 70°F: AC-5, AC-5+P, AC-10, AC-10+P, AC-20, and AC-20+P.

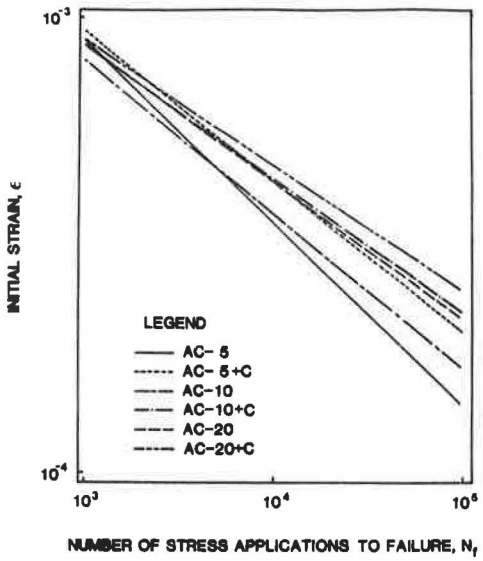

FIGURE 8 Strain versus cycles to failure at 70°F: AC-5, AC-5+C, AC-10, AC-10+C, AC-20, and AC-20+C.

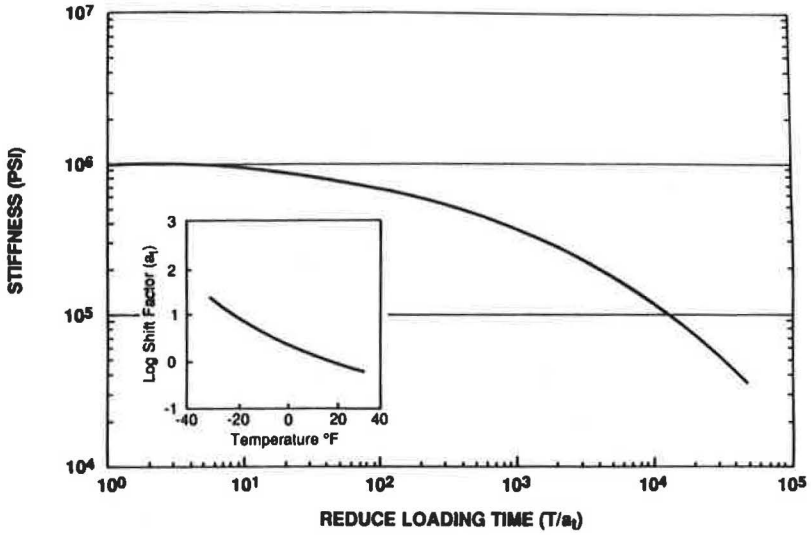

FIGURE 9 Master curve for AC-5.

10+P, AC-5+C, AC-10+C, and AC-20 exhibit similar fatigue life. AC-20+P and AC-20+C provide mixtures with the longest fatigue life. This trend is reflected in and supported by the analysis of performance of a representative pavement section.

Low-Temperature Characteristics

The low-temperature cracking phenomenon is a function of ambient air temperature and thermal loading time. Loading times in the range of a half-hour to several hours are considered reasonable. McLeod (*9*) has suggested a loading time of 20,000 sec as the nominal rate at which the pavement may be stressed because of chilling to low temperature. The experimental stiffness values from creep tests at −20°, 0°, 20°, and 40°F were measured up to a loading time of roughly 1,000 sec. To extend the data to the loading time of 20,000 sec at low temperatures, time-temperature superposition techniques were used. The experimental stiffness curves were moved along the loading time axis until all of them were superimposed and formed one master curve. An example of such a master curve for stiffness versus reduced loading time for mixture with AC-5 binder, along with the corresponding shift factor (a_t) versus temperature curve shown as an inset, is shown in Figure 9.

Similar master curves were prepared for other mixture types, and, for the loading time of 20,000 sec, the stiffness values at −30°, −20°, −10°, and 0°F were calculated and are reported in Table 4. To eliminate transverse pavement cracking, McLeod (*9*) has suggested limiting stiffness values given in Table 5. In this regard, the stiffness values in Table 4 suggest that at −30°F, only the mixtures containing AC-5, AC-5+P, AC-10+P, and AC-5+C would be able to mitigate low-temperature cracking. At −20°F and −10°F, in addition to the aforementioned binders, mixtures with AC-10 and AC-10+C would also be able to perform well. At 0°F, all the binders except AC-20 would be able to eliminate transverse pavement cracking under these criteria.

ANALYSIS OF PERFORMANCE OF REPRESENTATIVE PAVEMENT WITH AND WITHOUT POLYMER MODIFICATION

In order to assess the influence of the modified mixtures on the pavement performance, a representative pavement section was selected for analysis. The composition of this pavement section is shown in Figure 10. The VESYS IIIA structural subsystem was used to predict the pavement performance (*10*). On the basis of the mechanical properties of the materials in different layers of the flexible pavement, a typical traffic volume, and different environmental conditions, VESYS IIIA predicts the performance of a given pavement in terms of rutting, cracking, and present serviceability index.

The mechanical properties for the granular base course and the subgrade were determined as a part of a previous study (*7*) and are given in Tables 6 and 7. In addition, the mechanical properties of the mixtures for the surface course with and without modifiers are given in Tables 8 and 9. An analysis period of 20 years was chosen for this purpose; a hypothetical value of average daily traffic of 110 equivalent 18-kip axle loads (EAL_{18}) was selected for the analysis period. To predict the performance of the selected representative pavement under different environmental conditions, four regions were selected as shown in Table 10.

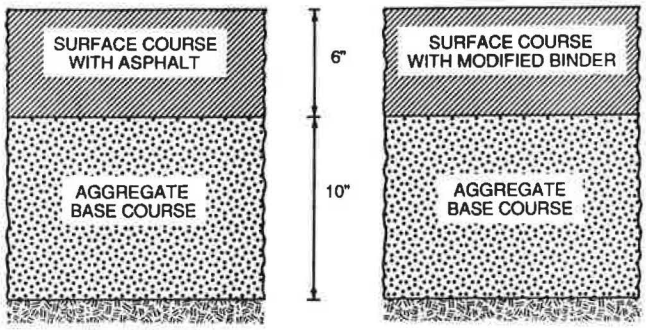

FIGURE 10 Layer thickness of representative pavement section.

TABLE 4 STIFFNESS VALUES IN POUNDS PER SQUARE INCH FOR LOADING TIME OF 20,000 SEC

	Temperature (°F)			
Binder	**-30**	**-20**	**-10**	**0**
AC5	3.5×10^5	2.7×10^5	1.8×10^5	3.4×10^4
AC5+P	2.4×10^5	1.0×10^5	7.2×10^4	1.6×10^4
AC5+C	2.9×10^5	2.1×10^5	7.8×10^4	3.1×10^4
AC10	7.32×10^5	2.9×10^5	1.9×10^5	6.1×10^4
AC10+P	4.1×10^5	1.4×10^5	9.3×10^4	3.4×10^4
AC10+C	6.7×10^5	2.4×10^5	1.10^5	5.7×10^4
AC20	1.6×10^6	8.7×10^5	6.5×10^5	1.7×10^5
AC20+P	9.1×10^5	5.1×10^5	3.3×10^5	8×10^4
AC20+C	1.5×10^6	8.1×10^5	6.3×10^5	1.6×10^5

TABLE 5 INFLUENCE OF MINIMUM PAVEMENT TEMPERATURE ON PAVEMENT MODULUS OF STIFFNESS TO BE USED FOR SELECTING ASPHALT GRADE (*9*)

Minimum Temperature of the Pavement (°F)	**Stiffness at Which Transverse Cracking Can be Expected**	**Pavement at Which Transverse Cracking Can be Eliminated**
-30	800,000	400,000
-20	600,000	300,000
-10	400,000	200,000
0	250,000	125,000

TABLE 6 RESILIENT MODULUS VALUES IN POUNDS PER SQUARE INCH FOR NONASPHALTIC LAYERS (*7*)

	Temperature (°F)					
Layer	**0**	**40**	**70**	**90**	**120**	**140**
Granular Base Course	54,000	27,000	26,000	27,000	29,000	29,000
Subgrade Soil	8,000	4,000	3,000	9,000	9,000	7,000

TABLE 7 PERMANENT DEFORMATION PARAMETERS FOR NONASPHALTIC LAYERS (7)

Layer	Temperature (°F) 0		40		70		90		120		140	
	Parameter											
Layer	μ	α	μ	α	μ	α	μ	α	μ	α	μ	α
Granular Base Course	.01	.81	.01	.81	.01	.84	.005	.87	.005	.87	.005	.87
Subgrade Soil	.16	.85	.16	.85	.16	.85	.04	.72	.06	.72	.06	.72

TABLE 8 RESILIENT MODULUS VALUES IN THOUSANDS OF POUNDS PER SQUARE INCH FOR I-1 MIX

Binder	Temperature (°F) 0	40	70	90	120	140
AC5	2,273	1,170	208	98	28	*
AC5+P	2,466	1,457	485	268	81	34
AC5+C	2,523	1,278	480	234	90	23
AC10	2,328	1,228	283	129	31	*
AC10+P	2,664	1,687	599	315	85	38
AC10+C	2,643	1,300	488	238	91	22
AC20	2,647	1,620	517	243	75	23
AC20+P	3,272	2,024	853	483	123	45
AC20+C	2,657	1,706	712	327	120	33

* Not Available

TABLE 9 PERMANENT DEFORMATION PARAMETERS FOR I-1 MIX

Temperature (°F)	0		40		70		90		120		140	
Parameter	μ	α	μ	α	μ	α	μ	α	μ	α	μ	α
Binder												
AC5	.031	.756	.297	.404	.512	.673	.709	.710	.717	.728	*	*
AC5+P	.035	.743	.054	.270	.126	.542	.506	.562	.249	.525	.269	.697
AC5+C	.024	.762	.031	.175	.080	.513	.134	.697	.130	.620	.203	.724
AC10	.028	.757	.148	.34	.495	.636	.560	.686	.705	.715	*	*
AC10+P	.028	.753	.038	.218	.128	.517	.520	.588	.250	.546	.263	.689
AC10+C	.023	.773	.031	.174	.068	.603	.118	.634	.132	.640	.204	.748
AC20	.027	.762	.128	.34	.411	.617	.522	.665	.597	.674	.604	.690
AC20+P	.024	.760	.036	.201	.102	.514	.190	.511	.237	.544	.250	.656
AC20+C	.021	.793	.022	.140	.060	.640	.110	.510	.141	.650	.169	.741

* Not Available

TABLE 10 SEASONAL TEMPERATURE IN DEGREES FAHRENHEIT

Region	Winter	Spring	Summer	Fall
1	0	40	90	70
2	40	70	90	70
3	40	70	120	70
4	40	70	140	90

Rut Depth

Rut depth is a measure of the permanent deformation in the wheel path created by traffic loads. In the rut depth model, rutting is primarily a function of the laboratory-determined permanent deformation characteristics and stiffness of the materials in pavement layers and of the truck-traffic volume. The predicted rut depths for the different cases of the binders are shown in Table 11.

The pavement sections constructed with AC-5, AC-10, and AC-20 will reach the limiting value of rut depth of 0.6 in. in 4 to 6 years of service life. The same pavement sections constructed with the polymer-modified binders will take 8 to 10 years to reach a rut depth of 0.6 in., and those constructed with carbon black–modified binders will take 10 to 12 years to reach a depth of 0.6 in.

Fatigue Cracking

Table 12 indicates that the mixtures made with polymer-modified binders exhibit a much lower fatigue damage index than the conventional asphalts and carbon black–modified asphalts.

The predicted cracking index using the VESYS IIIA program indicates the expected fatigue cracking. The predicted

TABLE 11 RUT DEPTH IN INCHES

Region	Binder	Time (Year) 1	5	10	15	20
	AC5	.26	.56	.78	.95	1.01
	AC5+C	.17	.39	.56	.69	.80
	AC5+P	.23	.47	.64	.77	.87
	AC10	.22	.48	.67	.82	.94
1	AC10+C	.16	.38	.55	.68	.79
	AC10+P	.21	.45	.61	.74	.84
	AC20	.20	.43	.60	.73	.84
	AC20+C	.15	.32	.52	.62	.72
	AC20+P	.18	.39	.55	.68	.78
	AC5	.31	.66	.92	1.1	1.3
	AC5+C	.18	.41	.58	.72	.83
	AC5+P	.24	.50	.68	.81	.92
2	AC10	.28	.58	.80	.97	1.11
	AC10+C	.18	.41	.58	.71	.77
	AC10+P	.22	.46	.63	.75	.86
	AC20	.23	.48	.66	.80	.92
	AC20+C	.17	.37	.54	.66	.77
	AC20+P	.18	.41	.58	.70	.81
	AC5	.37	.73	.98	1.18	1.34
	AC5+C	.20	.44	.63	.77	.89
	AC5+P	.25	.52	.71	.84	.95
	AC10	.35	.67	.89	1.06	1.21
3	AC10+C	.18	.41	.59	.73	.84
	AC10+P	.23	.48	.64	.80	.91
	AC20	.26	.52	.71	.84	.96
	AC20+C	.16	.37	.52	.65	.75
	AC20+P	.20	.44	.62	.73	.83
	AC5	*	*	*	*	*
	AC5+C	.21	.46	.65	.80	.92
	AC5+P	.27	.53	.72	.89	.98
4	AC10	*	*	*	*	*
	AC10+C	.20	.46	.65	.79	.92
	AC10+P	.24	.48	.66	.77	.87
	AC20	.36	.65	.80	.98	1.10
	AC20+C	.19	.42	.59	.73	.84
	AC20+P	.20	.46	.63	.76	.89

* Not Available

values are mainly a function of fatigue curve parameters K_1 and K_2, primary response properties, traffic loading, pavement temperature variations, and layer thickness. The cracking index is a dimensionless parameter that estimates the occurrence of fatigue cracking; a value of 1 corresponds to the time when the cracks are initiated at the bottom of the asphaltic layer. The predicted cracking indexes for different regions are shown in Table 12.

The sections constructed with AC-5 and AC-10 will show severe cracking in the first 5 years of service life in all the regions; in the same period, AC-20 will show severe cracking in Regions 3 and 4 only. After 20 years of service life, pave-

TABLE 12 FATIGUE CRACKING DAMAGE INDEX

Region	Binder	Time (Year) 1	5	10	15	20
	AC5	.93	4.68	9.36	14.04	18.73
	AC5+C	.12	.59	1.17	1.76	2.34
	AC5+P	.01	.05	.10	.15	.20
	AC10	.55	2.74	5.48	8.22	10.96
1	AC10+C	.09	.45	.91	1.36	1.82
	AC10+P	.004	.023	.046	.068	.091
	AC20	.073	.366	.731	1.09	1.46
	AC20+C	.03	.15	.29	.44	.59
	AC20+P	.002	.009	.018	.026	.035
	AC5	1.15	5.77	11.54	17.32	23.05
	AC5+C	.09	.44	.88	1.32	1.75
	AC5+P	0.11	.055	.110	.165	.220
	AC10	.675	3.37	6.74	10.12	13.49
2	AC10+C	.07	.35	.70	1.05	1.39
	AC10+P	.005	.025	.050	.075	.099
	AC20	.092	.45	.92	1.37	1.83
	AC20+C	.03	.13	.26	.40	.53
	AC20+P	.002	.010	.019	.028	.037
	AC5	3.54	17.74	35.48	53.22	70.96
	AC5+C	.39	1.94	3.87	5.81	7.75
	AC5+P	.039	.197	.394	.590	.78
3	AC10	3.02	15.14	30.28	45.43	60.57
	AC10+C	.31	1.57	3.13	4.70	6.26
	AC10+P	.027	.136	.272	.407	.543
	AC20	.561	2.80	5.60	8.40	11.21
	AC20+C	.18	.92	1.83	2.75	3.67
	AC20+P	.012	.058	.117	.175	.233
	AC5	*	*	*	*	*
	AC5+C	3.21	15.68	31.36	47.12	54.84
	AC5+P	1.75	8.79	17.5	26.38	35.17
4	AC10	*	*	*	*	*
	AC10+C	3.6	17.84	35.68	53.68	72.28
	AC10+P	1.24	6.20	12.41	18.61	24.82
	AC20	4.51	22.59	45.19	66.77	90.39
	AC20+C	2.80	14.00	28.08	42.08	56.8
	AC20+P	.85	4.27	8.54	12.82	17.09

* Not Available

ment sections constructed with AC-5 + P, AC-10 + P, and AC-20 + P will be expected to have almost no cracking in Regions 1, 2, and 3. However, for Region 4, severe cracking will be anticipated in the first 5 years of service life.

For carbon black–modified mixtures, pavement sections constructed with AC-5 + C and AC-10 + C will experience slight to moderate cracking in 10 to 15 years in Regions 1 and 2, and Regions 3 and 4 will have moderate cracking in approximately 5 years. Sections using AC-20 + C will not be expected to have any cracking in 20 years in Regions 1 and 2, but they will experience moderate cracking in approximately 12 years in Region 3 and 5 years in Region 4.

Present Serviceability Index

The present serviceability index gives an indication of ridability of pavement in relation to present pavement condition. The mean serviceability index at time zero was assigned a value of 4.5, and the terminal serviceability index was assigned a value of 2.5.

A summary of present serviceability indexes is shown in Table 3. Data in Tables 13 and 14 indicate that the service life of the pavement sections will be influenced greatly by the choice of the binder. For the aforementioned service and environmental conditions, AC-5, AC-10, and AC-20 will provide pavements with 5 to 15 years of service life. The pavement sections constructed with polymer-modified binders will

TABLE 13 PRESENT SERVICEABILITY INDEX

		Time (Year)				
Region	Binder	1	5	10	15	20
	AC5	4.00	3.10	2.30	1.68	1.08
	AC5+C	4.37	3.88	3.09	2.62	2.21
	AC5+P	4.26	3.65	3.05	2.57	2.16
	AC10	4.24	3.33	2.71	2.18	1.70
1	AC10+C	4.38	3.88	3.24	2.64	2.23
	AC10+P	4.29	3.71	3.13	2.67	2.27
	AC20	4.32	3.73	3.17	2.50	2.07
	AC20+C	4.36	3.81	3.27	2.81	2.40
	AC20+P	4.34	3.79	3.26	2.82	2.42
	AC5	3.84	2.74	1.80	1.00	.268
	AC5+C	4.21	3.69	3.11	2.49	2.07
	AC5+P	4.22	3.53	2.43	2.44	2.01
	AC10	4.06	2.99	2.21	1.55	.96
2	AC10+C	4.22	3.70	3.13	2.54	2.07
	AC10+P	4.25	3.63	3.08	2.62	2.22
	AC20	4.24	3.57	2.83	2.17	1.73
	AC20+C	4.21	3.66	3.16	2.69	2.29
	AC20+P	4.32	3.76	3.23	2.78	2.38
	AC5	3.64	2.50	1.53	.71	.03
	AC5+C	4.30	3.41	2.82	2.32	1.86
	AC5+P	4.21	3.47	2.81	2.27	1.73
	AC10	3.69	2.68	1.86	1.17	.55
3	AC10+C	4.34	3.50	2.94	2.47	2.05
	AC10+P	4.24	3.58	2.98	2.49	2.05
	AC20	4.08	3.16	2.54	2.04	1.59
	AC20+C	4.37	3.72	3.13	2.73	2.36
	AC20+P	4.29	3.67	3.10	2.62	2.19
	AC5	*	*	*	*	*
	AC5+C	4.00	3.36	2.75	2.23	1.75
	AC5+P	3.90	3.13	2.53	2.04	1.61
	AC10	*	*	*	*	*
4	AC10+C	4.00	3.38	2.76	2.23	1.74
	AC10+P	3.98	3.29	2.75	2.31	1.92
	AC20	3.65	2.74	2.05	1.49	1.00
	AC20+C	4.03	3.48	2.94	2.48	2.06
	AC20+P	4.09	3.40	2.87	2.43	2.04

* Not Available

TABLE 14 PREDICTED SERVICE LIFE IN YEARS

Region	AC5	AC5+P	AC5+C	AC10	AC10+P	AC10+C	AC20	AC20+P	AC20+C
1	8.83	15.90	16.44	11.96	17.13	16.70	15.10	19.01	18.79
2	6.24	14.39	14.91	8.04	16.55	15.38	11.94	18.53	17.34
3	5.02	12.81	13.12	6.04	14.92	14.70	10.40	16.39	18.09
4	*	10.32	12.34	*	12.76	12.41	6.63	14.21	14.72

* Not Available
(TERMINAL PSI = 2.5)

have a service life of 10 to 19 years, and those constructed with carbon black–modified binders will have a service life of 12 to 19 years.

CONCLUSIONS

The following principal conclusions can be drawn:

1. Modifying asphalt with polymer or carbon black reduces the temperature susceptibility of the binders. In this regard, the mixtures made with styrelf and carbon black–modified binders provide higher resilient modulus values at higher temperatures without adversely affecting the modulus values at low temperatures.
2. Mixtures made with styrelf and carbon black–modified binders are most resistant to low-temperature cracking than conventional asphalts.
3. Modifying an asphalt cement with polymer or carbon black reduces the permanent deformation of the paving mixtures at high temperatures and thus reduces the potential for rutting. However, carbon black is more effective in reducing the rutting.
4. Using styrelf significantly improves the fatigue life of the pavements.

REFERENCES

1. D. N. Little, J. W. Button, R. M. White, E. K. Ensley, Y. Kim, and S. J. Ahmed. *Investigation of Asphalt Additives*. Report FHWA-RD-87-001. FHWA, U.S. Department of Transportation, 1986.
2. V. P. Puzinauskas, and E. T. Harrigan. *Modification of Asphalt Cement and Paving Mixes with Styrene and Butadiene Elastomer—Styrelf System*. Asphalt Institute, College Park, Md., 1987.
3. F. S. Rostler, R. M. White, and E. M. Dannenberg. Carbon Black as a Reinforcing Agent for Asphalt. *Proc. Association of Asphalt Paving Technologists*, Vol. 46, 1977, pp. 376–401.
4. A. G. Alliotti. Carbon Black—Its Nature and Possible Effects on the Characteristics of Bituminous Road Binders. *Proc., Australian Road Research Board*, Vol. 1, Part 1, 1962.
5. Z. Yao and C. L. Monismith. Behavior of Asphalt Mixtures with Carbon Black Reinforcement. *Proc. Association of Asphalt Paving Technologists*, Vol. 55, 1986, pp. 564–585.
6. *Mix Design Methods for Asphalt Concrete*. Manual Series No. 2 (MS-2). Asphalt Institute, College Park, Md., 1984.
7. N. P. Khosla. *Investigation of Premature Distresses in Flexible Pavements*. Report FHWA-NC-85-001. FHWA, U.S. Department of Transportation, 1985.
8. F. Finn et al. The Use of Distress Prediction Subsystems for the Design of Pavement Structures. *Proc., 4th International Conference on the Structural Design of Asphalt Pavements*, Vol. 1, University of Michigan, Ann Arbor, 1977.
9. N. W. McLeod. A 4-Year Survey of Low Temperature Transverse Pavement Cracking on Three Ontario Test Roads. *Proc. Association of Asphalt Paving Technologists*, Vol. 41, 1972.
10. W. J. Kenis. *Predictive Design Procedures: VESYS Users Manual*. Report FHWA-RD-77-154. FHWA, U.S. Department of Transportation, 1978.

Methods To Determine Polymer Content of Modified Asphalt

LING YU HE AND JOE W. BUTTON

A laboratory procedure using a Fourier transform infrared (FTIR) analyzer to quantitatively determine the polyethylene content of modified hot-mixed asphalt concrete paving mixtures was developed. FTIR provides a reasonably accurate and precise method for measuring polymer content of modified mixtures and is suitable for quality assurance testing for highway and airport agencies. However, certain factors limit the accuracy of the test, which is of concern when highly precise quantitative determinations are required. An attempt as made to develop a gravimetric procedure for quantitative analysis of polymer in asphalt paving mixtures. Although no successful procedure was generated, the findings were important because they revealed that the solubility of polyethylene is altered upon high-shear blending and exposure to hot asphalt cement.

Federal, state, and municipal highway and airport agencies purchase and apply paving materials using a variety of specifications and test procedures. To satisfy governmental regulations, the agency often must be able to accurately determine not only quality of materials but also content of certain components. In fact, certain highway agencies have expressed the desire for a test to accurately determine the polyethylene content of Novophalt in order to verify that their specifications are being met. Novophalt America, Inc., responded to this need by initiating a study at the Texas Transportation Institute at Texas A&M University to develop a test procedure to quantitatively measure the polyethylene content of modified binders and/or paving mixtures. The results of this work are applicable to any polymer-modified asphalt binder.

The primary objective of this research was to develop a test procedure using the Fourier transform infrared (FTIR) analyzer to quantitatively determine polyethylene (PE) content in Novophalt and paving mixtures containing Novophalt. A secondary objective was to investigate the merits of a gravimetric procedure using selected solvents to determine polyethylene content in Novophalt and paving mixtures containing Novophalt.

FTIR spectroscopy is routinely used to aid in analysis of binary compatible polymer blend systems. FTIR is used to qualitatively identify the presence of chemical functional groups. By measuring relationships between absorbance intensity and concentration and preparing calibration curves using known concentrations of materials of interest, accurate quantitative analyses can also be accomplished using FTIR. A procedure was developed to extract polyethylene-modified asphalt binder (Novophalt) from asphalt-aggregate mixtures, prepare calibration curves, and measure polyethylene content of asphalt cement.

A gravimetric method to physically separate polyethylene from asphalt cement using selected solvents was evaluated. Although polyethylene is normally insoluble in the selected solvent, the polyethylene was finely divided and exposed to asphalt in the presence of heat (i.e., the Novophalt process), becoming mostly soluble. This work was preliminary and further effort is needed to fully understand the findings.

Texas Transportation Institute, Texas A&M University, College Station, Tex. 77843.

DESCRIPTION OF MATERIALS

The materials used in this study include asphalt cement, recycled polyethylene (mostly), aggregates, hot-mixed asphalt concrete, and organic solvents.

Asphalt Cement

The AC-10 asphalt used in this study was supplied by West Houston Asphalt in Houston, Texas. This asphalt was used in reconstruction of runways at Hobby Airport in Houston in fall 1988.

Polymer

A recycled polymer consisting mostly of polyethylene was used in this study. The same polyethylene had been used in the latter part of the runway reconstruction project at Hobby Airport. The polyethylene was produced by Bamberger Polymers, Inc., and contained some ethylene–vinyl acetate and carbon black as follows:

- Vinyl acetate, 3.0 percent,
- Carbon black, 2.5 percent,
- Density, 0.92 g/cc, and
- Melt index, 1.0 g/10 min.

Aggregates

Three aggregates were used in the various segments of the study. Washed coarse sand and washed river gravel were obtained from Gifford-Hill near College Station, Texas. These are siliceous, subrounded, nonporous materials used locally in construction of asphalt concrete pavement.

Crushed limestone was obtained from a White's Mines quarry near Brownwood, Texas. This material is characterized as a

very hard, low-porosity, low-absorption, and somewhat dolomitic limestone.

Gradation-specific gravity of the river gravel and limestone used in this study were approximately the same. Therefore, surface area per unit weight should be approximately equivalent.

Hot-Mixed Asphalt Concrete

Hot-mixed asphalt concrete was prepared in the laboratory, using the asphalt and aggregates described, to simulate paving mixtures. The aggregate was dried to constant weight in an oven at 325°F. The hot aggregate was mixed with hot Novophalt. The ratios of components in the mixture were as follows:

- Sand, 3000 g; Novophalt, 180 g; binder content, 5.66 percent
- River gravel, 1000 g; Novophalt, 53 g; binder content, 5.03 percent
- Limestone, 1000 g; Novophalt, 53 g; binder content, 5.03 percent.

Solvents

Solvents included trichloroethylene and methylene chloride, which have relatively low boiling points, and toluene and xylene, which have comparatively high boiling points.

FTIR METHOD

FTIR Equipment

The FTIR analyzer used in this investigation was a Nicolet Model 60 SX single-beam spectrometer. Specular reflectance was adapted as an accessory in the analysis of undiluted, opaque asphalt cement and polymer-modified asphalt. Infrared spectra with a bandwidth of 400 to 4000 cm^{-1} and 32 scans at a resolution of 4 cm^{-1} were signal-averaged and stored on a magnetic disk system.

Development of Calibration Curve

Sample Preparation

To simulate a binder extracted from a paving mixture, a sample of the pelletized black recycled polyethylene of known weight was dissolved in 20 ml of trichloroethylene at 70 ± 5°C using a reflux condenser and stirred for 30 min. To identical solutions, samples of hot asphalt of different weights were added and stirred for 2 hr at 70°C until the blend became a homogeneous system. Specimens were removed from this solution and placed on specially prepared aluminum plates, and the trichloroethylene was removed by evaporation under vacuum at room temperature.

Calibration Curve

Using this procedure, 10 different blends of the polymer in asphalt were prepared. The dosages of polymer in asphalt included 1.6, 1.8, 3.0, 4.6, 5.1, 6.4, 7.1, 8.1, and 9.9. Selected vertical peak heights on the FTIR absorbance plot were measured manually from the baseline. The most informative bands for these particular materials were between 1755 and 1530 cm^{-1} for asphalt and between 1820 and 1725 cm^{-1} for the polymer. The ratio of the peak heights representing absorbance at two distinct wavelengths was used to construct the calibration curve. For routine testing, approximately four points should produce a satisfactory calibration curve.

The infrared spectra for the asphalt used in this study show distinct, relatively interference-free absorption band peaks at frequencies of 1601, 1461, and 1376 cm^{-1} in the 400- to 2000-cm^{-1} region with a high degree of reproducibility (Figure 1). For this particular polymer, peaks occur at 1738, 1462, and 1376 cm^{-1} (Figure 1). The peaks at 1460 and 1376 cm^{-1} are common to both the polymer and the asphalt and therefore cannot be used as an accurate measure of polymer content in this particular Novophalt product. The small peak at 1738 cm^{-1} in the spectra of the polymer is attributed to the carbonyl functional group in the polyvinyl acetate. The peak at 1601 cm^{-1} for the asphalt is attributed to double bonds in benzene rings (aromatic hydrocarbons).

These unique frequencies at 1601 and 1738 cm^{-1} were chosen for determining the relative concentration of polymer in asphalt using infrared spectroscopy (Figure 2). Ratios of these two absorbance frequencies for asphalt-polymer blends of several known concentrations were determined and plotted (Figure 3). Theoretical considerations for these measurements of absorbance and computations of ratios are given in a subsequent section of this report. Standard linear regression techniques were applied to construct the calibration curve. Polyethylene content was not determined directly; rather, concentration of a component of the polymer, vinyl acetate, was measured. The assumptions were made that polymer components were completely homogeneous and that the extraction process did not preferentially separate out any of the polymer components.

Reference Spectra

In this research, a technique was developed to facilitate FTIR testing of undiluted asphalt. The asphalt samples were mounted on specially designed aluminum plates for FTIR testing. The aluminum plates were chemically treated to remove the oxidized layer and polished to provide an extremely smooth surface. After the instrument and sample compartment of the FTIR was purged with nitrogen for at least 15 min, a blank aluminum plate was placed in the compartment and reference spectra were obtained. FTIR spectra were then obtained for aluminum plates coated with the asphalt blends. The FTIR spectra of the modified asphalts were obtained by subtracting the reference spectra of the blank plate from those of the binder-coated plates. The FTIR analyzer is designed to perform this function automatically.

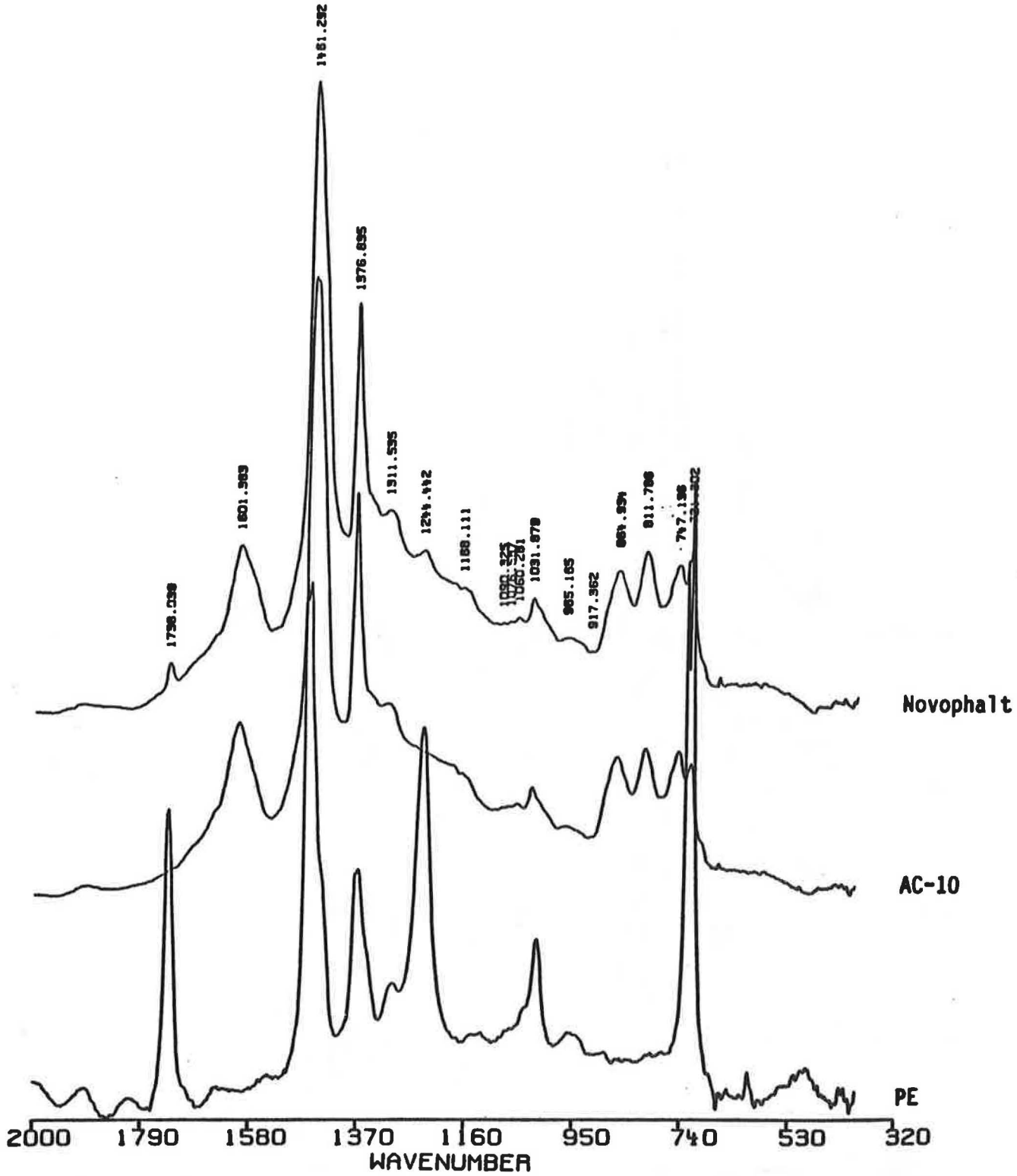

FIGURE 1 Infrared spectra (2000 to 400 cm^{-1}) for Novophalt, asphalt, and polyethylene (black).

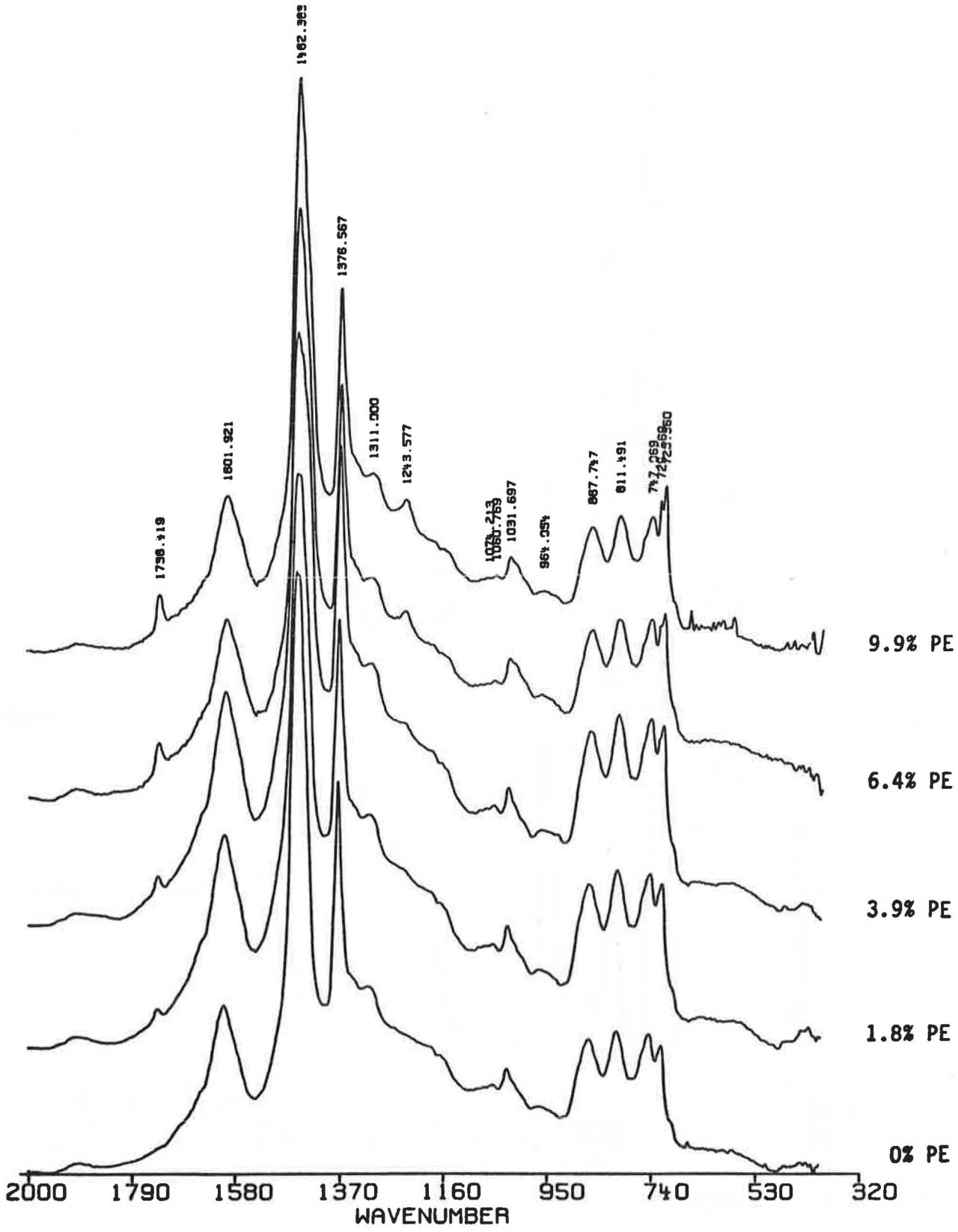

FIGURE 2 Infrared spectra (2000 to 400 cm^{-1}) for different polyethylene contents in asphalt.

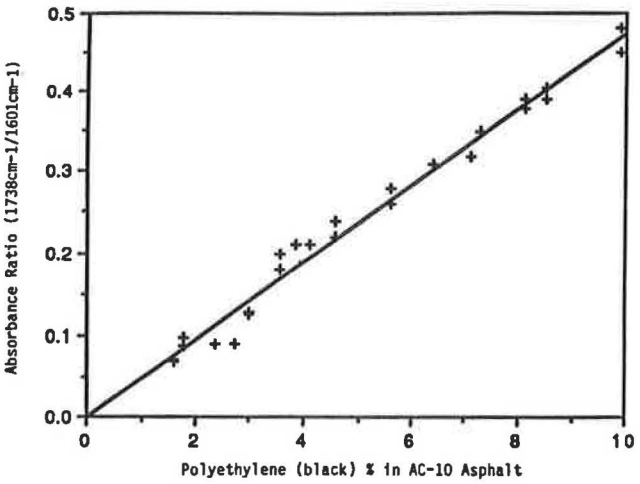

FIGURE 3 Calibration curve for polyethylene (black) content in AC-10 asphalt for —C=0/—C=C— functional group absorbance ratio.

Verification

To verify the utility of the calibration curve, a sample of the polymer was accurately weighed, dissolved in xylene, and mixed with an accurately weighed sample of asphalt. After evaporation of the solvent, the FTIR analyzer measured the polymer content of the asphalt. The known polymer content was 4.72 percent; the FTIR measured 4.69 percent. Therefore, the difference was 0.03 percentage points. Eight measurements were made to obtain the mean, which yielded a standard deviation of 0.083 percent and a coefficient of variation of 1.8 percent. These data indicate that the method is both accurate and precise.

Precautions

FTIR spectra are unique for a particular polyethylene and asphalt; therefore, a new calibration curve must be developed each time new materials are used to produce Novophalt.

The FTIR calibration curve would normally be developed using neat asphalt and polymer. If samples for subsequent analysis are taken from a paving mixture prepared using Novophalt in an asphalt mix plant, significant changes may have occurred in the polymer and asphalt. During the production of Novophalt, chain scission in the polymer can occur. Hot storage of this material may cause certain unknown chemical reactions between the two substances. During plant mixing, both the asphalt and the polymer undergo oxidation, which changes the functionality of both products. Other unknown chemical reactions may occur in the solvent extraction process. These chemical reactions can significantly affect the spectra obtained on the FTIR and thus reduce the accuracy of the quantitative analysis.

Sample Testing

Methodology

Quantitative measurement of polymer in asphalt using FTIR must be preceded by the development of a calibration curve using known concentrations of the materials in question, as discussed earlier. To quantitatively determine the percentage of polyethylene in the modified binder of a sample of asphalt-aggregate mixture, the modified binder must first be extracted from the mixture. Then FTIR spectra are obtained using the aluminum plate method, and the ratios of the peak heights representing absorbance at the appropriate wavelengths are compared with the calibration curve to directly interpolate the polyethylene content.

A reflux extraction process is probably the best method to separate Novophalt and aggregate. This process minimizes the quantity of solvent required. Suitable solvents to extract asphalt and ensure that the polyethylene is also extracted include high boiling point solvents such as xylene (boiling point, 140°C), perchloroethylene (121°C), or toluene (111°C). Toxicity and flash point of the solvents should also be considered. The optimum time period to carry out the reflux process depends on the solvent selected but may be several hours. This limited study did not permit an evaluation of solvent effectiveness or optimization of the extraction time period. Only xylene was examined in this portion of the work. Reflux extraction was allowed to proceed until the filtrate became a light straw color.

Test Results

Asphalt-aggregate mixtures were prepared in the laboratory. An extraction process using xylene at 140°C was used to separate Novophalt from three different aggregates (Table 1). About 8 hr were required to reach the end point (light straw color of filtrate), depending on the type of aggregate. More time was required for the limestone (8 hr), as compared to the coarse sand and river gravel (6 hr).

On the average, about the same proportion of binder was extracted from each of the different aggregates, using the reflux-xylene process. However, based on results of FTIR testing, significantly less polymer was present in the binder extracted from the limestone when compared with that extracted from the siliceous aggregates (Table 1). Slightly less polymer was present in the extract from the sand compared with that from the river gravel. These limited data indicate that the efficiency of extraction of polyethylene depends on aggregate composition, absorbancy, and grain size. Polyethylene may be more strongly adsorbed on calcareous aggregates than on siliceous aggregates. Polyethylene adsorption increases as surface area per unit weight of aggregate increases.

FTIR analysis is an accurate method for determining polymer content of modified asphalt binder. FTIR analysis provides exceptionally good repeatability. The disadvantage of routinely testing a large number of different mixtures is the length of time (20 to 24 hr) required to prepare the calibration curve.

Theoretical Derivation and Practical Application

Quantitative infrared analysis is based on Beer's law. Apparent deviations arise from either chemical or instrumental effects. Low absorbance values were used to minimize the presence of scattered radiation, which makes the direct application of Beer's law inaccurate.

TABLE 1 RESULTS OF EXTRACTION OF ASPHALT MIXTURE WITH XYLENE AND ANALYSIS OF POLYETHYLENE CONTENT OF EXTRACTED BINDER USING FTIR

Test No.	Mix Weight, grams	Aggregate in Mix: Type	Aggregate in Mix: Weight, percent of mix*	Novophalt In Mix, percent of mix*	PE in Novophalt**, percent of mix*	Novophalt Extracted, percent of mix*	PE in Extracted Novophalt, percent of binder*	From FTIR: Weight Change, percent of mix*
1	55.696	Sand	94.34	5.66	5	5.08	4.9	-0.12
2	56.107	Sand	94.34	5.66	5	5.52	4.9	-0.02
3	68.569	Gravel	94.97	5.03	5	4.91	5.1	-0.12
4	71.259	Gravel	94.97	5.03	5	4.86	5.0	0.05
5	57.275	Limestone	94.97	5.03	5	4.86	4.1	-0.51
6	58.612	Limestone	94.97	5.03	5	4.80	4.1	-0.55
7	61.203	Limestone	94.97	5.03	5	4.78	4.2	-0.36
8	64.427	Limestone	94.97	5.03	5	4.67	4.2	-0.35
9	46.646	Sand	94.94	5.66	5	5.32	4.8	+0.02
10	54.094	Sand	94.34	5.66	5	5.49	4.9	-0.04
11	54.505	Sand	94.34	5.66	5	5.62	4.9	-0.14
12	60.484	Sand	94.34	5.66	5	5.59	4.9	-0.07
27	61.426	Sand	94.34	5.66	5	5.43	5.0	-0.07
28	68.936	Gravel	94.97	5.03	5	5.50	5.0	-0.12
30	61.554	Limestone	94.97	5.03	5	4.48	4.1	-0.22

* Indicates percent by weight.
** Novophalt was prepared in Houston, Texas and the value of PE content is approximate.

$$A = alC \tag{1}$$

where

A = absorbance of compound,
a = absorptivity of compound,
l = sample path length (film thickness), and
C = concentration in weight percent of compound.

In the analyses it is imperative, for practical reasons, to use the values for ratios rather than absolute absorbance values. If the absorbance of polyethylene copolymer at 1738 cm^{-1} is defined as $A_{[PE]}$ and the absorbance of asphalt at 1601 cm^{-1} is defined as $A_{[AC]}$ the ratio of the two absorbance values becomes

$$R = A_{[PE]}/A_{[AC]} \tag{2}$$

The concentration (weight percent) of polyethylene and asphalt in a sample of Novophalt is defined as C_{PE} and C_{AC}, respectively, to correspond with the above definitions. According to Beer's law, the absorbance values are related to the concentrations in the following manner:

$$A_{[PE]} = alC_{PE} \tag{3}$$

and

$$A_{[AC]} = blC_{AC} \tag{4}$$

where a and b equal absorptivities of polymer and asphalt, respectively. Dividing Equation 4 into Equation 3 yields

$$\frac{A_{[PE]}}{A_{[AC]}} = \frac{aC_{PE}}{bC_{AC}} \tag{5}$$

If a and b are assumed to be constants, the ratio of a/b must be a constant as well. Let us define

$$K = \frac{a}{b} \tag{6}$$

and the reciprocal

$$K' = \frac{1}{K} = \frac{b}{a} \tag{7}$$

Then

$$R = K\frac{C_{PE}}{C_{AC}} \tag{8}$$

and

$$\frac{C_{PE}}{C_{AC}} = K'R \tag{9}$$

It follows that the ratio of absorbance (R) is directly proportional to the ratio of concentrations of the components. The plot in Figure 3 demonstrates a very good linear relationship between R (abscissa) and the ratio C_{PE}/C_{AC} (ordinate).

This relationship (Figure 3), which has previously been termed a "calibration curve," can be used to readily determine the proportion of polymer to asphalt in an unknown sample, given the ratio of absorbance (R).

The concentration of polymer could be calculated directly from the ratio of concentrations as demonstrated below:

$$C_{PE} = 100\frac{C_{PE}/C_{AC}}{(1 + C_{PE}/C - AC)} \tag{10}$$

where the C_{PE}/C_{AC} ratio is obtained by reading the graph based on the value of R. However, this approach is complicated. Direct reading from a graph of the polymer content is desirable.

In a two-component system, the concentration of one component can be expressed, by definition, in terms of the other:

$$C_{AC} = 100 - C_{PE} \quad (11)$$

Other ratios, such as 1460/1601 or 1376/1601, could have been used to construct a calibration curve, but the $-CH_2$ and $-CH_3$ functional groups were present in both polyethylene and asphalt. Therefore, infrared absorbance was not very sensitive to changes in the $-CH_2$ or $-CH_3$ functional groups with varying concentrations of polyethylene in asphalt. The relative content of the $-CH_3$ group in both polyethylene and asphalt is comparatively low and subject to change during processing. For these reasons, the ratios of 1376/1601 and 1460/1601 were not used in determining polyethylene content of Novophalt.

GRAVIMETRIC METHOD

Two-Step Extraction Procedure

A two-step extraction process was used for quantitative analysis of polyethylene content of Novophalt in hot-mixed asphalt concrete. This method is based on the fact that asphalt and polyethylene have different solubilities in certain solvents at different temperatures. In methylene chloride, asphalt is quite soluble but polyethylene is insoluble. Polyethylene is soluble in certain solvents with high boiling points, such as xylene or toluene at or near their boiling points.

To verify that the polyethylene used in this study is insoluble in methylene chloride, a sample of polyethylene was placed in the soxhlet extractor and allowed to reflux for 24 hr. There was no visible change in the polyethylene. The carbon black in the polyethylene did not cause even the slightest discoloration of the filter.

In Step 1, a sample of Novophalt-aggregate mixture weighing 60 to 70 g was placed in the thimble of a soxhlet extractor and the binder was extracted using methylene chloride at 40°C. This step was stopped when the filtrate became a light straw color, after approximately 4 hr. Step 1 should have removed only the asphalt, leaving the polyethylene with the aggregate. The mass of extract and the material retained in the thimble were dried and weighed separately.

In Step 2, the retained material was again extracted using the soxhlet extractor with xylene at 140°C for approximately 48 hr. This extended extraction time is probably not required but was used to ensure that all soluble material (ideally polyethylene) was removed from the aggregate. The mass of extract and the aggregate retained in the thimble were dried and weighed. Weights of the dry materials were used to calculate binder content of the mix and any weight changes that may have occurred (Table 2). The material extracted in Step 2 appeared to be mostly polyethylene, but an FTIR analysis was not performed because the calibration curve was valid for a maximum polyethylene concentration of 10 percent.

Although considerable care was exercised, unaccountable weight losses occurred. Vacuum distillation of the solvents may have removed some of the lighter hydrocarbons in the asphalt. Certain components in the asphalt may have formed azeotropes with the solvents and evaporated during drying. The limestone mixtures experienced the greatest weight losses by far. This may be explained by decomposition of selected aggregate components (such as hydrates) upon exposure to the high temperatures.

FTIR Analysis of Extract

The extract from Step 1 was analyzed to determine the polyethylene content (Figure 4) using FTIR and the procedures described previously. The result revealed that a significant portion of the polyethylene was extracted by the methylene chloride. This important finding indicates that the nature of the polyethylene was changed significantly during production of Novophalt so that it became partially soluble in methylene chloride. These changes most likely occurred during the high-shear blending process, heating, mixing with aggregate, and storage. Chain scission of the polyethylene may have occurred, which reduced the molecular size and changed the solubility parameters. This is a good reason for not using absorbance bands associated with CH_2 and CH_3 groups. In addition, the oils and resins in the asphalt and the heat likely

TABLE 2 RESULTS OF TWO-STEP GRAVIMETRIC ANALYSIS OF NOVOPHALT USING METHYLENE CHLORIDE AND XYLENE

		Initial Condition			Step 1		Step 2		
Test No.	Mix Weight, grams	Aggregate Type	Aggregate Weight, percent of mix	Novophalt* In Mix, percent of mix	Binder Extracted From Mix, percent of mix	PE In Extracted Binder,** percent of binder	Binder Extracted From Aggr, percent of mix	Aggregate Remaining, percent of mix	Weight Change Of Mix, percent of mix
13	63.699	Sand	94.34	5.66	5.35	5.1	0.17	94.49	+0.01
14	60.546	Sand	94.34	5.66	5.30	5.2	0.11	94.60	+0.01
15	65.803	Sand	94.34	5.66	5.24	4.8	0.24	94.48	-0.04
16	63.388	Sand	94.34	5.66	5.21	4.8	0.08	94.65	-0.06
17	59.184	Sand	94.34	5.66	5.25	4.8	0.16	94.51	-0.08
18	62.611	Sand	94.34	5.66	5.24	4.8	0.20	94.44	-0.12
23	66.061	Gravel	94.97	5.03	4.82	4.3	0.07	94.95	-0.16
25	61.515	Gravel	94.97	5.03	4.90	4.4	0.06	95.00	-0.04
24	60.169	Limestone	94.97	5.03	4.90	3.7	0.08	94.71	-0.39
26	61.337	Limestone	94.97	5.03	4.82	3.6	0.09	94.97	-0.21

* Novophalt was prepared in Houston, Texas and contains approximately 5 percent polyethylene (PE).
** PE content measured using FTIR.

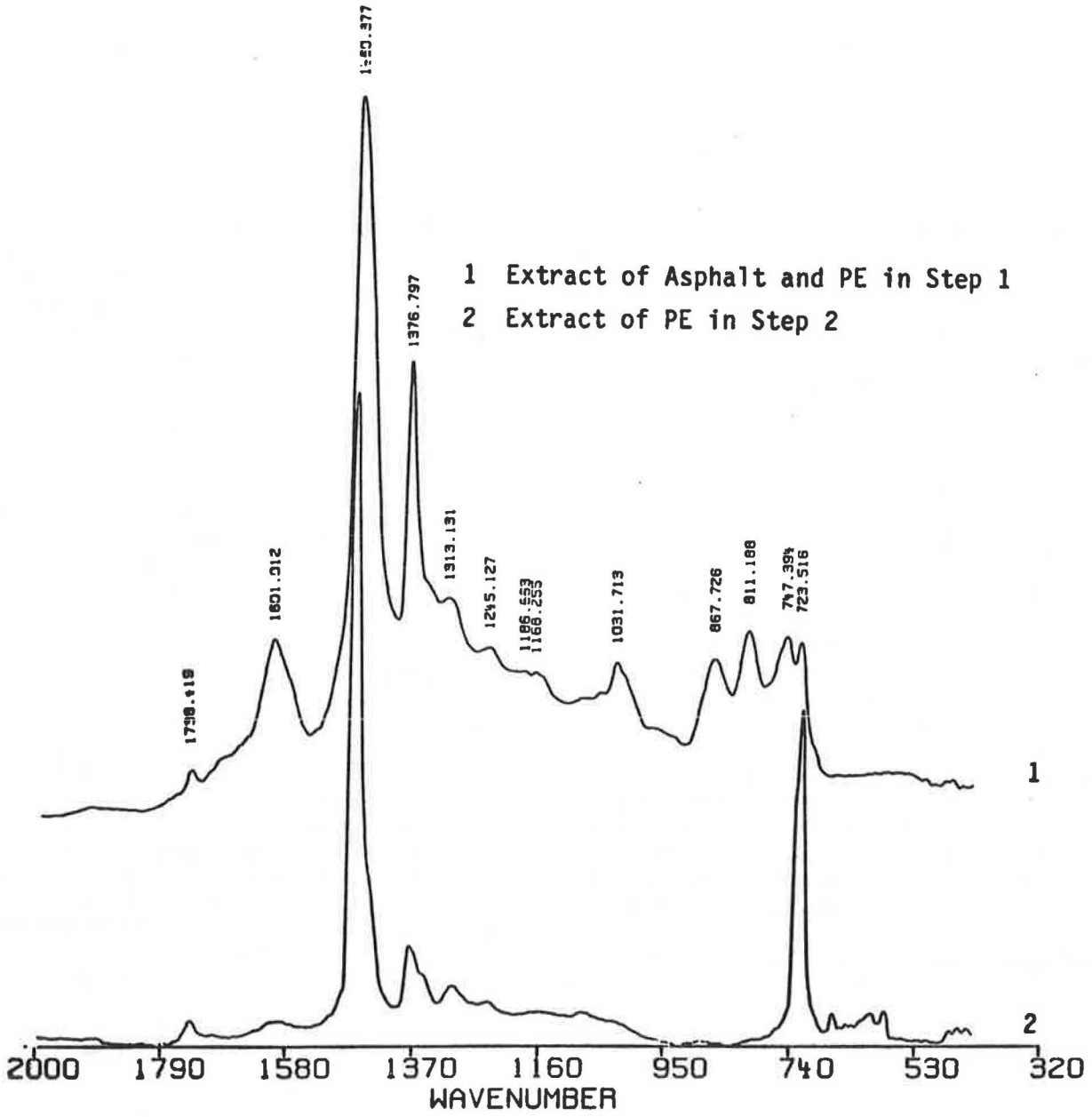

FIGURE 4 FTIR analysis of extracts from Steps 1 and 2 of gravimetric procedure.

caused the polyethylene particles to soften and swell, which further altered the solubility.

Effect of Aggregate Type on Polyethylene Extraction

By using either methylene chloride or xylene as a solvent, more polyethylene was retained by the limestone than by the river gravel or the sand (Table 3). This finding indicates that the polyethylene is more strongly adsorbed on the limestone aggregate than on the siliceous materials. Gradations and thus surface areas per unit weight of the two coarse aggregates were approximately the same. Water absorption tests on aggregates of similar gradation from these two sources has shown only slightly greater absorption for the limestone. The sand and river gravel were obtained from the same source, thus chemical composition of the two should be similar. Therefore, this phenomenon appears to be related to the chemical properties of the aggregates.

CONCLUSIONS

1. FTIR is a reasonably accurate and precise procedure for measuring polymer content of modified asphalt binder. The

TABLE 3 EXTENT OF EXTRACTION OF POLYETHYLENE FROM DIFFERENT AGGREGATES USING DIFFERENT SOLVENTS

Aggregate Type	Solvent	Extraction time, hour	PE in Extracted Binder,* percent	Approximate Quantity of PE Extracted by Solvent, percent
Sand	MC**	4	4.8	96
Sand	MC	4	4.8	96
Sand	MC	4	4.0	80
Gravel	MC	4	4.3	86
Gravel	MC	4	4.4	88
Limestone	MC	4	3.6	72
Limestone	MC	4	3.7	74
Sand	Xylene	6	4.9	98
Sand	Xylene	6	4.9	98
Gravel	Xylene	6	5.1	102
Gravel	Xylene	6	5.0	100
Limestone	Xylene	6	4.1	82
Limestone	Xylene	6	4.1	82
Limestone	Xylene	8	4.2	84
Limestone	Xylene	8	4.2	84

* Measured Using FTIR
** Methylene Chloride

chief disadvantage of the procedure is the time required to prepare the calibration curve necessary for quantitative analysis using FTIR. Typically, at least 1 staff-day is required to prepare a suitable calibration curve.

2. Completeness of the extraction of polyethylene or asphalt from aggregate depends on the aggregate composition and gradation, solvent, temperature, and time.

3. Limited data indicate that polyethylene is more strongly adsorbed on limestone than on siliceous aggregates and, further, that polyethylene is more strongly adsorbed on fine-grained siliceous aggregate than on similar coarse-grained material.

4. A two-step gravimetric procedure using solvents to quantitatively determine the polyethylene content of Novophalt cannot be performed without first finding a solvent that will selectively dissolve asphalt and not affect the polyethylene as it exists in the Novophalt.

5. The solubility of polyethylene is altered when incorporated in asphalt to produce Novophalt. Polyethylene is not normally soluble in methylene chloride, but when exposed to the Novophalt production process and the aggregate mixing process, it becomes mostly soluble.

Evaluation of Resin-Modified Paving Process

RANDY C. AHLRICH AND GARY L. ANDERTON

The U.S. Army Engineer Waterways Experiment Station (WES) was tasked by the headquarters of the U.S. Army Corps of Engineers to evaluate the state of the art of the resin-modified pavement (RMP). This type of pavement is semirigid and semiflexible. RMP is basically an open-graded asphalt concrete mixture that contains 25 to 30 percent voids that are later filled with a resin-modified cement slurry grout. RMP is a tough and durable surfacing material that combines the flexibility characteristics of an asphalt concrete material with the fuel, abrasion, and wear resistance of portland cement concrete. A literature search and background analysis of the RMP process showed that the majority of in-service pavements constructed with this process are in Europe, particularly in France, where this process was developed. Visual observations of these sites indicate that the RMP process has potential for U.S. military applications. The final phase of the WES study involved the construction, trafficking, and evaluation of a 150- × 50-ft test section. Trafficking included both straight passes and pivot steer turns from the M-1 and M-60 tanks. FHWA's Accelerated Loading Facility was used to traffic the RMP test section by simulating heavily loaded, high tire pressure truck traffic. Sections of the test section were also subjected to controlled fuel and oil spillage. The evaluation indicated that RMP does have potential for several pavement uses. At an initial cost somewhere between asphalt concrete and portland cement concrete, RMP provides an alternative surfacing material for many Army pavement applications. These proposed applications include tracked-vehicle roads, hardstands, and aircraft parking aprons.

Asphalt concrete pavements are very susceptible to damage when subjected to fuel and oil spillage or severe abrasion from tracked vehicles. More than 80 percent of the Army's pavements are surfaced with asphalt concrete. Because of the mission of the Army and the equipment in its inventory, Army pavements are routinely subjected to fuel damage and severe abrasion. Tank trails, crossings, hardstands, wash facilities, motorpools, helicopter refueling pads, and aircraft parking aprons are examples of Army pavements susceptible to fuel or abrasion damage. Surfacing materials that are more cost-effective than conventional portland cement concrete are needed for construction and rehabilitation of Army pavements.

A resin-modified pavement (RMP) was developed in France in the 1960s as a fuel- and abrasion-resistant surfacing material. A French construction company, Jean Lefebvre, developed this pavement process as a cost-effective alternative to portland cement concrete. The RMP process has been used on various types of pavements including warehouse floors, tank hardstands, and aircraft parking aprons. RMP has been successfully constructed in numerous countries including Great Britain, South Africa, Japan, Australia, and Saudi Arabia.

RMP is a semirigid, semiflexible pavement. It is a tough and durable surfacing material that combines the flexibility characteristics of an asphalt concrete material with the fuel, abrasion, and wear resistance of portland cement concrete. RMP is basically an open-graded asphalt concrete mixture containing 25 to 30 percent voids that are filled with a resin-modified cement slurry grout. The open-graded asphalt mixture functions as a support layer and determines the RMP thickness. The slurry grout is composed of portland cement, fine aggregate, water, and a resin additive. The grout material is poured onto the open-graded asphalt mixture after the asphalt material has cooled, squeegeed over the surface, and vibrated into the voids with a small (3- to 5-ton) vibratory roller. The curing period can vary between 1 and 28 days depending on the type of portland cement used in the grout and on the loading conditions. Figure 1 is a cut cross section of an RMP field core.

During the mid-1970s, the U.S. Army Engineer Waterways Experiment Station (WES) evaluated the resin-modified pavement (*1*). A test section was constructed to evaluate the effectiveness of this special surfacing material in resisting damage caused by fuel, oil spillage, and abrasion from tracked vehicles. The results of this evaluation were not favorable. The test section did not resist damage caused by tracked vehicles and fuel spillage. The evaluation indicated that the effectiveness of RMP was very construction-sensitive and that if all phases were not performed correctly, the RMP process would not work.

In 1987 the headquarters of the U.S. Army Corps of Engineers tasked WES with reevaluating the RMP process. Good field performance in Europe and improved materials and construction procedures indicated that this process had potential as an alternative to standard paving materials. The evaluation began with a literature search and background analysis into the RMP process. The review indicated that most of the in-service pavements constructed with this process were in Europe, especially in France. Site inspections were conducted to evaluate the field performance of several private and military RMP applications in France, Great Britain, and Australia. Visual observations of these sites indicated that the RMP process had considerable potential for U.S. military applications (*2*).

OBJECTIVE AND SCOPE

The objective of this research was to determine the effectiveness of RMP in resisting damage caused by severe abrasion

U.S. Army Engineer Waterways Experiment Station, Geotechnical Laboratory, 3909 Halls Ferry Road, Vicksburg, Miss. 39180-6199.

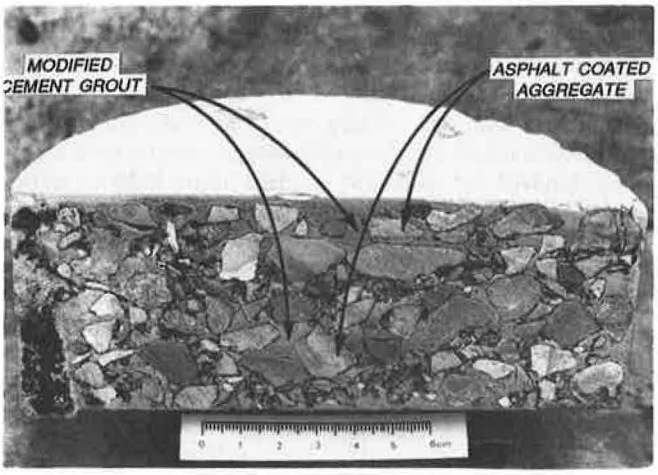

FIGURE 1 Cross section of RMP field core.

from maneuvering tracked vehicles and from fuel and oil spillage. Recommendations for the potential future uses of the RMP were based on its determined effectiveness.

In order to determine the effectiveness of the resin-modified pavement process, an RMP test strip was constructed at WES. A 50- × 150-ft test strip was constructed by a local contractor, APAC of Mississippi, with technical guidance from representatives of the company that developed the RMP process, Jean Lefebvre. The RMP test strip was constructed according to the specifications without any problems. The test strip was allowed to cure for 28 days to obtain full strength before any traffic was placed on the pavement.

The RMP test strip was trafficked with M-1 and M-60 tanks. Straight passes and 180-degree pivot steer turns were applied with the tracked vehicles to evaluate the RMP abrasion resistance. Five different fuels and oils (jet aviation fuel, gasoline, diesel fuel, synthetic oil, and hydraulic oil) were spilled on the RMP. Thirty cycles of controlled fuel and oil spillage were used to evaluate the fuel-resistant properties. FHWA's Accelerated Loading Facility (ALF) was also used to traffic the RMP test strip. ALF simulated heavily loaded, high tire pressure truck traffic. Data drawn from the traffic tests and fuel resistance analysis were the basis for the recommendations made for this new pavement process.

PRECONSTRUCTION ANALYSIS

Site Evaluation and Thickness Design

An old pavement testing area near the Geotechnical Laboratory at WES was chosen as the construction site for the proposed 150- × 50-ft RMP test strip. Various asphalt concrete test pavements had been constructed in this area by WES researchers since World War II. In 1982 approximately 1½ in. of asphalt concrete was placed over the entire area as a leveling course. Since then, the area has been used occasionally to stockpile aggregates and soil samples. This site represents an extremely strong and stiff support for the test section and prevented the possibility of base course or subgrade failure.

Because RMP is essentially a surface course, the underlying layers of the test strip had to be structurally sound. If any load-related failures were to occur during future traffic tests, a structurally sound foundation would leave no doubt that the failure was initiated in the surface course, which was, in this case, the pavement layer being evaluated. A high-quality bituminous mixture placed on top of this paved area was determined to be the most economical means of obtaining a structurally sound foundation.

A thickness design procedure was conducted to determine the required thickness of this asphalt concrete layer. The first step of the design procedure was to determine the strength properties of the existing pavement. Nondestructive tests were conducted using the falling weight deflectometer. The pavement deflection data captured during these tests were entered into a computerized layered-elastic program (BISDEF), which computes strength properties and predicts elastic moduli for each pavement layer. The moduli values were then entered into a computerized pavement thickness design program (AIRPAVE) to determine strengthening overlay requirements. A design load nearly equivalent to the M-1 and M-60 tank loads was used in this thickness design program. The results of this exercise indicated that a total thickness of 3 in. of asphalt concrete surface mixture would provide a structurally sound foundation for the 2-in.-thick RMP wearing course.

Materials Evaluation

Dense-Graded Bituminous Intermediate Course

As previously mentioned, a high-quality bituminous surface mixture was selected as the best means of providing a sound foundation beneath the RMP surface course. The aggregate gradation for this pavement layer was specified in the U.S. Army Standard Practice Manual for a ¾-in. maximum size, high tire pressure surface blend (*3*). An AC-30 grade of asphalt cement was specified for the dense-graded intermediate course. The intermediate course aggregate gradation and asphalt cement properties are shown in Tables 1 and 2.

TABLE 1 AGGREGATE GRADATIONS (PERCENT PASSING)

US Standard	Dense-Graded Intermediate Course		Open-Graded Surface Course	
Sieve Size	Limits	JMF	Limits	JMF
3/4 in.	100	100	100	100
1/2 in.	82-96	95.3	65-75	67
3/8 in.	75-89	88.9	50-65	44
No. 4	59-73	71.3	23-33	22
No. 8	46-60	49.8	9-17	12
No. 16	34-48	38.3		
No. 30	24-38	31.6	5-10	5
No. 50	15-27	18.5		
No. 100	8-18	8.9		
No. 200	3-6	6.7	1-3	2

TABLE 2 AC-30 ASPHALT CEMENT TEST PROPERTIES

Test	Results
Viscosity, 140°F, (P)	3182
Viscosity, 275°F, (cst)	479
Penetration, 77°F, 100g, 5 sec, (0.1 mm)	58
Flash Point, Cleveland Open Cup, (°F)	590
Solubility in Trichloroethylene, (%)	99.9
Specific Gravity at 77°F	1.023
Test on Residue from Thin Film Oven Test	
Viscosity, 140°F, (P)	7523
Ductility, 77°F, 5 cm/min, (cm)	150+

Once the contract for constructing the test strip was awarded, the contractor was asked to provide samples of the aggregates and asphalt cement to WES so that the materials could be tested and a job mix formula developed. The job mix formula presented to the contractor before construction began contained the specific aggregate gradation and asphalt cement content desired. The job mix formula tests indicated that an asphalt content of 4.9 percent with the gradation shown in Table 1, labeled as the intermediate course job mix formula, would provide the optimum mixture for the given materials. These and other requirements for the dense-graded intermediate course were specified in the final construction specifications. The section of the final specifications relating to the intermediate course was designed after the standard U.S. Army Corps of Engineers Guide Specification for Bituminous Intermediate and Surface Courses for Airfields, Heliports, and Tank Roads (*4*).

Open-Graded Asphalt Mixture

A review of the available literature indicated that the mix design of the open-graded asphalt mixture would play a critical role in the proper construction of the RMP (*5*). The majority of the mix design focused on the final void content of the compacted open-graded asphalt mixture. The general requirement is 25 to 30 percent voids in the final compacted mixture. Any amount less than this would not allow the slurry grout to fully penetrate the open-graded mixture, resulting in a structurally unsound surface course that would probably have excessive cracking and deterioration. Void contents greater than this amount would increase the cost of the pavement without providing any significant structural improvements and could reduce the pavement strength by eliminating some of the aggregate-to-aggregate interlock.

A laboratory analysis of the open-graded asphalt mixture was conducted before construction of the test strip to determine the amount of asphalt cement that would produce the proper void content in the final mixture. Although checks against such aggregate properties as fractured faces and particle shapes had to be made, the final void content of the compacted mixture was the main focus of this laboratory analysis. The majority of the laboratory mix design guidance found in the literature was based on French methods, which use nontraditional specimen sizes and compaction methods (*6*). Therefore, a preliminary study was first conducted in the WES laboratories to determine the best mix design method in terms of standard U.S. military practices. This study found that a modified Marshall mix design procedure, which is both a military standard and an ASTM standard, using 25 blows of the hand hammer for the compactive effort indicates the proper asphalt content to achieve the required void criteria.

Twenty-five blows of the 6-in.-diameter Marshall hand hammer are used in the French standards for compacting laboratory samples. A comparative analysis conducted in the WES laboratories validated this compactive effort by examining the changes in void contents versus varying levels of hand hammer compaction. The results of this analysis indicated that the 25 blows would most likely produce void contents in the target range of 25 to 30 percent.

Once the proper mix design method was determined, an estimate of the optimum binder content was made using a French procedure based on material properties and design traffic (*7*). This procedure is outlined below:

$$\text{Optimum binder content} = (\alpha)(K)(\sqrt[5]{\Sigma})$$

where

- $\alpha = 2.65/\gamma_G$ (γ_G is apparent specific gravity of the combined aggregates);
- K = richness modulus, having a value of 3 to 3.5 depending on design traffic;
- Σ = conventional specific surface area $= 0.25G + 2.3S + 12s + 135f$;
- G = percentage of material retained in ¼-in. sieve;
- S = percentage of material passing ¼-in. sieve and retained on No. 50 sieve;
- s = percentage of material passing No. 50 sieve and retained on No. 200 sieve; and
- f = percentage of material passing No. 200 sieve.

Therefore, for the materials and conditions of the WES test section, the following estimate was made:

$$\alpha = \frac{2.65}{\gamma_G} = \frac{2.65}{2.648} = 1.0008$$

$K = 3.25$ (heavy-duty traffic)

$$\Sigma = 0.25G + 2.3S + 12s + 135f = 0.25(0.64) + 2.3(0.32) + 12(0.02) + 135(0.02)$$

$$\Sigma = 3.836$$

$$\therefore \text{Optimum binder content} = (\alpha)(K)(\sqrt[5]{\Sigma}) = (1.0008)(3.25)(\sqrt[5]{3.836})$$

Optimum binder content = 4.26%

The asphalt cement used in the laboratory study and actual construction was the same type as that used in the dense-graded intermediate course, an AC-30 grade. The aggregate gradation specified was taken from the literature as the standard gradation for heavy-duty pavement applications. This gradation is shown in Table 1, labeled as the limits of the open-graded surface course. The job mix formula gradation, which was recommended by the Jean Lefebvre representative, is also shown in Table 1. The coarser gradation was recommended to ensure that the final void content would be sufficient to allow full penetration of the grout.

With all of the aggregate and binder materials in hand, an established aggregate gradation, and an estimate of the optimum binder content, a laboratory job mix formula analysis was conducted. Binder contents at, above, and below the estimated optimum value were evaluated. The laboratory analysis of the open-graded mixture indicated that an asphalt cement content of 4.2 percent would result in a void content of about 30 percent in the final compacted mixture. This asphalt content, along with the surface course aggregate gradation limits shown in Table 1, was specified in the final construction specifications as the open-graded asphalt mixture job mix formula.

Resin-Modified Slurry Grout

A preconstruction laboratory study was also performed on the resin-modified slurry grout. The literature was fairly specific about the types of materials and relative proportions of these materials to produce a satisfactory slurry grout (*7*). Nonetheless, laboratory tests were necessary to ensure that these recommendations would work for the materials to be used in the WES RMP test strip.

The individual components of the slurry grout are cement, sand, filler, water, and a latex resin additive. The additive is generally composed of 5 parts water, 2 parts of a cross-polymer resin of styrene and butadiene, and 1 part water-reducing agent. The type of cement used is purely a design option, as is the case for portland cement concrete. WES used a standard Type I cement. The sand must be clean, sound, and durable, and it must range from the No. 30 to No. 200 sieve sizes. WES used a washed silica sand to meet these requirements. The filler must have a very fine gradation (minimum of 95 percent passing the No. 200 sieve) and may be fly ash, limestone dust, or rock flour. WES used a fly ash. The resin additive acts as a plasticizer to reduce the slurry grout viscosity for better penetration and as a strength-producing agent. The solid constituents of the grout are almost equal proportions of sand and filler with about twice that amount of cement. Enough water is added to produce a water-to-cement ratio of 0.60 to 0.70. The resin additive is added to the mixture last in an amount equal to 2.0 to 3.0 percent of the total batch weight. This combination of ingredients produces a slurry grout that is very fluid and only slightly more viscous than water.

The WES laboratory analysis of the slurry grout consisted of varying the mix proportions within the recommended allowances to determine the best mix formula. The single acceptance criterion for the slurry grout is a Marsh flow cone viscosity of 7.0 to 9.0 sec immediately after mixing. (Water has a Marsh flow cone viscosity of 6.0 sec.) Because this viscosity range is relatively narrow, slight variations of the water-to-cement ratio and amount of resin additive were used to obtain a slurry grout mix formula of the proper viscosity.

After 10 different slurry grout formulations were mixed and tested in the laboratory (Table 3), a final formula was derived that produced a slurry grout viscosity of just over 7 sec. It was thought that a slurry grout in the lower end of the acceptable viscosity range, combined with an open-graded support layer in the upper end of the acceptable voids range, would help to ensure full penetration of the grout during construction. The final slurry grout formulation used on the test strip is shown in Table 4.

CONSTRUCTION

Dense-Graded Bituminous Intermediate Course

Before the construction of the RMP test strip, a 10- × 40-ft trial test section of dense-graded intermediate course was constructed. This test section was tested and evaluated to ensure that the asphalt mixture and construction procedures would conform to all of the specified requirements. Quality control tests conducted on the asphalt concrete mix included asphalt extractions, aggregate gradations, and field compaction. These tests indicated that the construction of the trial test section was acceptable. The results of the quality control tests for the test section are shown in Tables 5 and 6.

The construction of the RMP test strip began with the dense-graded bituminous intermediate course. The existing surface

TABLE 3 SLURRY GROUT LABORATORY ANALYSIS

Trial	Type 1 Cement wt(g) [%]	Sand wt(g) [%]	Filler wt(g) [%]	Water wt(g) [%]	Resin Additive wt(g) [%]	Marsh vis.* (sec.)
1	1835[36.7]	920[18.4]	920[18.4]	1190[23.8]	135 [2.7]	11.0
2a	1820[36.4]	910[18.2]	910[18.2]	1225[24.5]	135 [2.7]	9.7
2b	1820[36.2]	910[18.1]	910[18.1]	1250[24.9]	135 [2.7]	9.0
2c	1820[36.3]	910[18.1]	910[18.1]	1225[24.4]	150 [3.0]	9.0
3a**	1810[36.2]	905[18.1]	905[18.1]	1240[24.8]	140 [2.8]	7.2
3b	1810[36.3]	905[18.1]	905[18.1]	1230[24.6]	140 [2.8]	7.1
3c	1810[36.2]	905[18.1]	905[18.1]	1240[24.8]	135 [2.7]	7.2
4a	1800[36.0]	900[18.0]	900[18.0]	1250[25.0]	150 [3.0]	6.7
4b	1800[36.1]	900[18.0]	900[18.0]	1240[24.8]	150 [3.0]	6.6
4c	1800[36.1]	900[18.0]	900[18.0]	1250[25.0]	140 [2.8]	7.1

* Results shown are average of three viscosity tests.

** This formula chosen as specified job mix formula.

TABLE 4 RESIN-MODIFIED SLURRY GROUT FORMULA

Component	Percent by Weight
Type I cement	36.2
Fly ash	18.1
Sand	18.1
Water	24.8
Cross polymer resin	2.8

was swept clean and a light tack coat of Type SS-1 asphalt emulsion was sprayed on the clean surface by a distributor truck. The tack coat bonded the new dense-graded asphalt mixture with the existing asphalt surface. This tack coat was applied during the afternoon before construction of the intermediate course began to allow enough curing time and to prevent construction delays the next morning.

With the construction equipment already in place, the intermediate course construction was completed in less than 1 day. The hot mix was spread with a mechanical paver and compacted with a 10-ton rubber-tired roller and a 10-ton steel-wheeled roller. Samples of the hot mix were taken at several intervals during the day for determination of mixture properties by WES laboratory personnel. These laboratory quality control tests, along with data obtained from field cores cut out of the test strip early the next day, indicated that both the mix and construction procedures were satisfactory. A final thickness of approximately 3 in. was laid across a 160- × 60-ft area. These dimensions were designed to provide the sound foundation required for the 2-in.-thick, 50- × 150-ft resin-modified surface course.

Resin-Modified Pavement

Open-Graded Asphalt Mixture

After completion of the intermediate course, a trial section for the open-graded asphalt mixture was constructed. Several batches of material were produced at the batch plant before placing the material. After visually observing slight asphalt drainage of the open-graded material, the Jean Lefebvre representative recommended decreasing the asphalt content to 4.0 percent. This change in asphalt content ensured that the mixture had enough void structure to allow full penetration of the slurry grout.

The open-graded asphalt mixture trial section was constructed on top of the dense-graded intermediate course trial section. The asphalt material was sampled and tested for conformance. The test results, shown in Table 7, indicated that the production of the open-graded material and construction procedures used to place the material were satisfactory.

The open-graded asphalt mixture for the RMP test strip was placed on top of the dense-graded bituminous intermediate course 1 week after the intermediate course was placed. A light tack coat was sprayed onto the intermediate course using the same type of asphalt emulsion and application rate as before. The tack coat was allowed to cure for a few hours before the open-graded mixture construction began.

Techniques similar to the quality control techniques used during the construction of the intermediate course were used to take samples of the hot open-graded mix from the haul trucks at several intervals during the day. Laboratory tests on these materials to determine the asphalt content, aggregate gradation, and most importantly the final void content helped to determine the properties of the in-place mix. Additionally, core samples were cut out of the hardened test strip the following morning to recheck these same properties. All loose mix samples and core samples indicated that the open-graded mix was placed with satisfactory material properties and construction techniques.

The open-graded mixture was spread with the same mechanical paver used for placing the intermediate course (Figure 2). Under normal circumstances, open-graded mixes of this nature tend to cool off relatively quickly because of their

TABLE 5 BITUMINOUS INTERMEDIATE COURSE ANALYSIS

Sieve Size	Specified Limits	JMF	Trial Test Section	Test Strip S-1	Test Strip S-2	Test Strip S-3
3/4 in.	100	100	100	100	100	100
1/2 in.	82-96	95.3	97.9	96.0	93.8	97.1
3/8 in.	75-89	88.9	90.2	90.3	86.5	89.0
No. 4	59-73	71.3	67.1	72.3	68.6	69.7
No. 8	46-60	49.8	47.8	52.3	49.8	50.9
No. 16	34-48	38.3	36.3	39.5	37.5	39.1
No. 30	24-38	31.6	29.3	32.0	30.3	32.3
No. 50	15-27	18.5	18.2	19.9	18.9	19.8
No. 100	8-18	8.9	9.2	10.5	10.1	10.0
No. 200	3-6	6.7	6.7	8.1	7.7	7.7
Asphalt Content		4.9	4.4	4.9	4.4	4.6
Marshall Stability (lb)	1800 min	2232	2853	2540	2473	2309
Flow (0.01 in.)	16 max	12	10	12	12	12
Percent Voids Total Mix	3-5	3.6	3.6	2.8	3.9	3.9
Percent Voids Filled	70-80	76.2	74.5	80.7	72.9	73.6
Density (pcf)		150.4	152.1	152.2	151.7	151.2
Theo Density (pcf)		155.9	157.8	156.6	157.8	157.3

TABLE 6 BITUMINOUS INTERMEDIATE COURSE FIELD DENSITY ANALYSIS

Location	Core No.*	Thickness (in.)	Unit Weight (pcf)	Compaction (%)
Trial Test Section	M-1	3	148.3	97.5
	M-2	2 3/4	148.3	97.5
	M-3	3	148.7	97.8
	M-4	2 3/4	146.3	96.2
	M-5	2 3/4	148.4	97.6
	AVG	2 7/8	148.0	97.6
RMP Test Strip	M-1	3 1/4	149.7	98.7
	M-2	3	150.0	98.9
	M-3	3	148.2	97.7
	M-4	3	148.2	97.7
	M-5	2 1/2	148.9	98.2
	M-6	3	149.7	98.7
	M-7	2 7/8	146.2	96.4
	AVG	3	148.7	98.0
	J-1	2 7/8	147.5	97.2
	J-2	2 1/4	148.9	98.2
	J-3	3 1/4	147.7	97.4
	AVG	2 3/4	148.0	97.6

Lab Unit Weight - Test Section - 152.2 pcf
Test Strip - 151.7 pcf

* M-Mat Core, J-Joint Core

TABLE 7 OPEN-GRADED ASPHALT MIXTURE ANALYSIS

Sieve Size	Specified Limits	JMF *	Trial Test Section	Test Strip S-1	Test Strip S-2	Test Strip S-3
3/4 in.	100	100	100	100	100	100
1/2 in.	65-75	67	68.3	74.1	79.4	72.8
3/8 in.	50-65	44	42.2	50.4	52.8	47.2
No. 4	23-33	22	17.9	19.7	21.8	20.5
No. 8	9-17	12	10.2	8.2	9.5	9.0
No. 30	5-10	5	4.7	2.9	3.6	3.0
No. 200	1-3	2	1.1	0.8	1.3	0.8
Asphalt Content		4.0	3.5	3.4	3.5	3.4
Percent Voids Total Mix	French +	30.8	31.2	32.4	31.2	32.6
	Corps #	33.8	34.5	35.9	34.6	35.9
Percent Voids Filled	French +	17.2	15.2	14.1	15.2	14.0
	Corps #	15.9	14.0	12.9	13.9	12.9
Density (pcf)		102.8	102.1	100.1	101.9	100.0
Theo Density (pcf)		154.6	154.9	156.1	155.8	156.1
Temperature (^{0}F)		265	250	240	250	275

* Gradation recommended by Jean Lefebvre representative

\+ French Method - $VTM = 1 - \frac{WTair - WTwater}{volume} \times 100$

\# Corps Method - $VTM = [1 - \frac{WTair}{volume}\left(\frac{1}{SG_T}\right)] \times 100$

VTM = Voids total mix
WTair = Dry weight of specimen
WTwater = Weight of specimen in water after soaking for 15 minutes
Volume = $\pi/4\ D^2H$ (measured)
SG_T = Theoretical specific gravity

FIGURE 2 Placing open-graded asphalt material.

high internal voids and low mixing temperatures (265°F). This tendency usually means that the required compaction must closely follow the paver that is placing the mix. Because the ambient temperatures were so unusually high during the construction of the test strip, rapid heat loss of the asphalt mix was not a problem. To the contrary, the afternoon temperatures, which reached well over 100°F, forced the construction crews to wait several hours before rolling so that the roller would not cut and shove the hot mat.

As is the case for most open-graded asphalt mixes, compaction during construction was not used to achieve any density requirements, but merely to "seat" the asphalt-coated aggregates and smooth over the rough surface. A relatively small (3-ton) steel-wheeled roller was used to accomplish this goal (Figure 3). The static, lightweight, steel-wheeled roller, rather than more traditional heavier models (8 to 10 ton), was used to minimize the loss in voids incurred during the rolling process.

Once the open-graded asphalt mixture had cooled for several hours, a single pass of the small steel-wheeled roller in the static mode was made over the entire 150- × 50-ft area. Small cut marks were left along the edge of the roller wheels after this process. Therefore, after another hour of cooling,

FIGURE 3 Three-ton steel-wheel roller.

another pass of the small roller was used to roll out these marks. After these final passes of the roller, the construction of the open-graded asphalt layer was complete.

Because of the high percentage of voids and the modest slope of the test section, a sand asphalt material was placed on the edges of the open-graded material to prevent seepage of the fluid grout material. The entire freshly paved area was covered with polyethylene sheeting for the night to prevent contaminants (dirt, sand) from blowing onto the pavement surface and falling into the open voids.

Resin-Modified Slurry Grout

A trial application for the resin-modified slurry grout was conducted the day after the open-graded trial section was completed. One batch of slurry grout was produced according to the recommended mixture proportions. The slurry grout had the proper viscosity, but the sand material was settling out before placement was completed. The Jean Lefebvre representative recommended that the amount of sand be decreased to avoid any problems of settling. The final mixture proportions for the resin-modified slurry grout are shown in Table 8.

The resin-modified slurry grout was added to the open-graded asphalt pavement 2 days after the open-graded mix was placed. The slurry grout used in the construction of the test strip was made at a local concrete batch plant. The dry cement, sand, and fly ash were mixed in the plant's pugmill (in their proper proportions) for several minutes before they were dumped into the transient mixer truck. Next, the proper amount of water was dumped into the transient mixer truck and the resulting slurry grout was mixed in the rotating mixing drum for several minutes. At this point, the proper amount of the cross-polymer resin additive was poured into the mixing drum; the truck operator left the plant site and drove toward the test strip job site while the mixing truck continuously rotated.

At the test strip job site, the transient mixing trucks were positioned directly on the open-graded asphalt pavement, which had hardened overnight. A sample of the slurry grout was taken and the Marsh cone viscosity was checked on the test strip job site to ensure that the grout was of the proper viscosity. Samples were taken from each transient mixer truck

TABLE 8 REVISED RESIN-MODIFIED SLURRY GROUT FORMULA AND VISCOSITY TEST RESULTS

Material	Batch Percentage
Type I cement	38.2
Fly ash	19.1
Sand	13.3
Water	26.7
Cross polymer resin	2.7
Viscosity Test - No. 1	6.2 sec
No. 2	7.0 sec
No. 3	7.0 sec
No. 4	7.0 sec

at the test strip job site and approved before the grout was placed. Viscosity test results are shown in Table 8.

The grout was to be placed in the same 10-ft-wide longitudinal lanes that were used during construction of the open-graded asphalt pavement. This pattern gave a sense of order to the grout application and prevented overworking of the crew. This crew consisted of four people working broom-handled squeegees behind the transient mixer truck. The slurry grout was slowly poured onto the open-graded asphalt surface; when an area became saturated with grout, the squeegees were used to pull the grout along the surface to undersaturated areas. The grout was poured down a pivoting delivery chute onto the pavement surface. As the grout was slowly poured onto the pavement, one person continuously directed the chute to dry areas of the pavement. Once an area of a lane was completely saturated with grout, the truck driver slowly moved the truck forward. After a short time at the beginning of the grout application, the squeegee operators, chute operator, and truck driver were able to continue the grouting procedure in an efficient, controlled manner. Figure 4 is a typical view of the grout application procedure used on the test strip.

Immediately behind the grouting operation, the small steel-wheeled roller made several passes over the grout-filled pavement in the vibratory mode to ensure that all subsurface voids were filled. Because the void content of the open-graded asphalt pavement and the slurry grout viscosity were within the specified ranges, most of the internal voids were filled with grout as the pavement was saturated when the grout was poured over the surface. However, a small amount of internal voids seemed to be isolated from the initial grout application, as evidenced by small air bubbles that appeared behind the vibratory roller. These air bubbles usually appeared only after the first pass of the vibratory roller, indicating that all voids were being filled with grout.

After each of the five 10-ft lanes had been saturated with grout and vibrated, all excess grout remaining on the surface was removed by continually pulling the hand squeegees in one direction. This process also filled any undersaturated areas. After this step, the grout application was complete.

FIGURE 4 Resin-modified slurry grout being applied to open-graded asphalt material.

To evaluate whether full penetration of the slurry grout had occurred, 4-in. field cores were taken from the completed RMP test strip. Random cores were taken throughout the RMP test strip. All cores indicated that the slurry grout material had penetrated the total thickness of the open-graded layer. The test results of the field cores are shown in Table 9.

Curing

After the grout application was completed, a curing compound was sprayed over the surface of the wet, grout-filled pavement. The material used was a white pigmented concrete curing compound, which is commonly used in curing Type I portland cement concrete. The white pigments reduce maximum pavement temperatures during the curing period, which in turn reduce the expansion and contraction stresses resulting from extreme temperature changes. An overabundance of

TABLE 9 RMP TEST STRIP FIELD CORES

Location	Core No.	Thickness (in.)	Unit Weight (pcf)	Penetration (%)
Trial Test Section	1	1 3/8	140.6	100
	2	2 1/2	140.5	100
	3	2 3/4	139.7	100
	4	2 3/8	141.0	100
	AVG	2 1/4	140.5	100
RMP Test Strip	1	2 9/16	139.0	100
	2	2 1/4	138.3	100
	3	2 1/8	138.8	100
	4	2 1/2	140.8	100
	5	2 1/8	138.0	100
	6	2	139.0	100
	AVG	2 1/4	139.0	100

these stresses can lead to shrinkage cracking during the curing period. The curing compound was applied by a pressurized, hand-operated sprayer wand with a fan-type nozzle. A light coating of the curing compound (200 sq ft/gal) over the entire test strip completed the construction process. The pavement cured with no traffic for 28 days before traffic testing began.

EVALUATION

In order to determine the effectiveness of the resin-modified pavement, a series of tests and evaluations was conducted on the pavement surface. A layout of the testing areas is shown in Figure 5. To evaluate the abrasion-resistant characteristics of RMP, tracked-vehicle maneuvers were conducted. Controlled fuel and oil spills were conducted to evaluate the fuel-resistant properties. ALF was used to evaluate RMP under heavy rubber-tired vehicular traffic.

Tracked-Vehicle Traffic

As mentioned, the RMP test strip was allowed to cure for 28 days before any traffic was allowed on the pavement. This cure time ensured that the RMP test strip had plenty of time for adequate strength gain. The effectiveness of the RMP greatly depended on its performance during the tracked-vehicle trafficking.

Tracked-vehicle traffic on the RMP test strip consisted of M-1 (gross weight 113,000 lb) and M-60 (gross weight 100,000 lb) tanks. Six hundred 180-degree pivot steer turns at the same point and 5,000 straight passes were applied with the tracked vehicles to the test strip. Excessive wear of the rubber pads on the tank track was noticed during the initial trafficking of the RMP. During the initial stage of trafficking, the RMP withstood the abrasive action of the pivot steer turns very well; only excess grout was worn off. As the tank track turned during the pivot steer, the track pads dragged across the RMP surface (Figure 6). After 420 turns at the same location, the tracked vehicle produced enough rough abrasion and high stresses to start surface raveling. The surface raveling began without any warning. Once the raveling started, the deterioration increased rapidly because the loose debris that had been dislodged caused further damage as it was dragged and scraped across the RMP surface.

At 600 pivot steer turns, the turning traffic was stopped because the abrasive action had produced a raveled area 1 in. deep covering 35 sq ft. It was thought that a large number of concentrated pivot turns of this nature are not commonly applied to one location in the field, making this traffic test much more severe than normal applications. For example, it would require the tanks of two armored divisions performing 180-degree pivot steer turns at the same point to equate this traffic test.

The 5,000 straight passes with the tank traffic caused only slight surface wearing of the grout, which exposed the surface of the coarse aggregate. The tracked vehicle moving forward and in reverse caused no significant damage to the RMP. At the conclusion of the tracked-vehicle trafficking, it was determined that RMP had effectively demonstrated a resistance to severe traffic abrasion and could be used as a pavement surface for tracked vehicles.

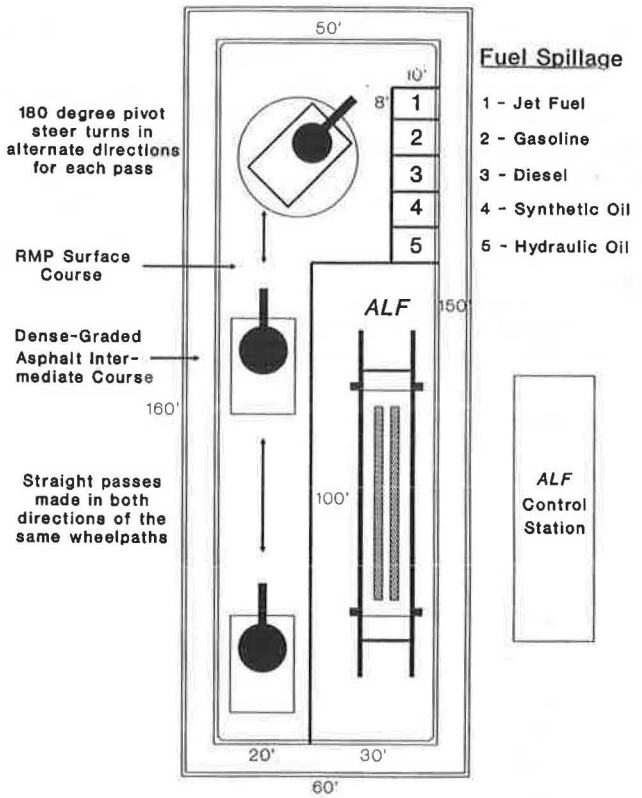

FIGURE 5 Layout of testing areas.

Fuel and Oil Spillage

Five different fuels and oils were used to evaluate the effectiveness of RMP in resisting deterioration caused by fuel and oil spillage. Jet aviation fuel, gasoline, diesel fuel, synthetic oil, and hydraulic oil were spilled on the resin-modified pavement. Thirty cycles of 1 qt of each material were spilled on the RMP surface. Each spill area was 8 ft by 10 ft. The ma-

FIGURE 6 M-1 tank performing pivot steer turns on RMP test strip.

terials were spilled from a height of 30 in. The rate of spillage was set so that each material took 20 to 30 min to drip 1 qt. The fuels and oils were allowed to sit on the RMP surface for 30 days after the spillage cycles were completed.

Visual observations indicated that RMP resisted deterioration from fuel and oil spillage. However, field cores taken from the spillage areas indicated that the fuels and oils had penetrated the resin-modified pavement, causing varying degrees of low-level deterioration. The gasoline and jet aviation fuels had a fast rate of evaporation, which prevented these materials from significantly penetrating the RMP. The diesel fuel had the fastest penetration and caused the most damage. Once again, this test is thought to be an acceleration of typical fuel spillage problems in the field because most spills are cleaned and not allowed to soak into the pavement for a month.

After the fuel and oil penetration was discovered, the stability of RMP was questioned. The maximum penetration was approximately 1 in. in the diesel area. The remaining fuels and oils penetrated less than ½ in. A 1-ton van was used to traffic the fuel spillage areas. Fifty passes and fixed-position, power-steering turns were applied to the contaminated areas by the van. Only slight scuffing was noticed after the van had trafficked the RMP with no appreciable damage.

Accelerated Loading Facility

FHWA's Accelerated Loading Facility was also used to traffic the resin-modified pavement test strip (Figure 7). ALF simulated truck traffic by applying a load of 19,000 lb to a dual wheel assembly with tire pressures of 140 psi. ALF applied 80,000 passes to a 48-in.-wide strip of the RMP. No appreciable deterioration or deformation occurred in the wheel path. Only slight wearing of the excess grout on the RMP surface was observed. The ALF evaluation indicated that vehicular traffic had little effect on the resin-modified pavement and that the RMP should have good field performance when trafficked by rubber-tired vehicles.

SUMMARY

The resin-modified pavement construction process can be used to build new pavements or rehabilitate existing pavements that are subject to heavy, abrasive loads and fuel spillage. RMP can be used to surface areas used by tracked vehicles such as tank trails and crossings, hardstands, and wash facilities. This pavement may also be used in motorpools, refueling pads, and aircraft parking aprons. RMP provides an alternative surfacing material in areas where conventional pavement materials have excessive maintenance problems. The resin-modified pavement can be used in place of asphalt concrete and portland cement concrete in these specialized areas.

RMP provides a tough and durable surfacing material for military pavements. The current data and evaluations indicate that the RMP process has potential for several uses. The variable costs of materials (aggregates, asphalt cement, and portland cement) and variable construction costs throughout the United States make cost estimates for RMP very site-specific. However, the additional cost of the resin additive can range from $4 to $6/sq yd, depending on the void content

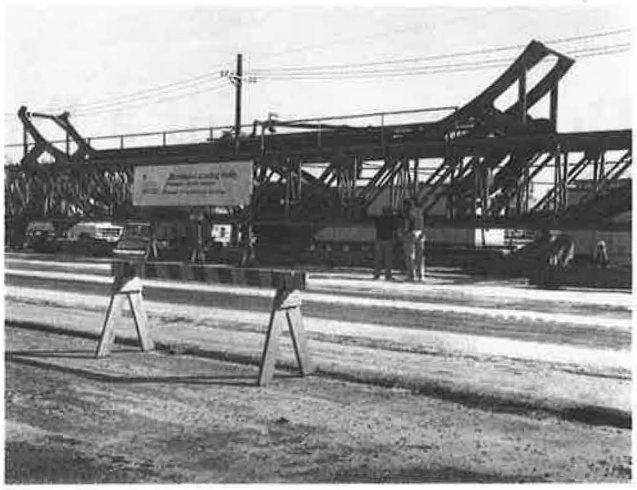

FIGURE 7 ALF trafficking RMP test strip.

of the open-graded support layer and the dosage rate of additive in the slurry grout. Therefore, it is estimated that the initial cost of RMP in 1990 was between $10 and $15/sq yd compared with $15 to $25/sq yd for portland cement concrete. At this price, RMP is a cost-competitive method to construct or rehabilitate many of the Army's abrasion- and fuel-resistant pavements.

ACKNOWLEDGMENTS

The authors wish to express their appreciation to the headquarters of the U.S. Army Corps of Engineers for sponsoring and funding this project and allowing the opportunity to conduct this investigation. The authors also wish to thank Paige Johnson, technical monitor, for his assistance and cooperation during this project. The authors thank their supervisors, the U.S. Army Engineer Waterways Experiment Station, and the headquarters of the U.S. Army Corps of Engineers for allowing publication of this material.

REFERENCES

1. C. L. Rone. *Evaluation of Salviacim Pavement*. Miscellaneous Paper S-76-20. U.S. Army Engineer Waterways Experiment Station, Vicksburg, Miss., Oct. 1976.
2. R. C. Ahlrich. Inspection and Evaluation of Field Test Sites of Salviacim Pavement Process. Letter Report. U.S. Army Engineer Waterways Experiment Station, Vicksburg, Miss., 1988.
3. *Bituminous Pavements Standard Practice*. Report TM 5-822-8. U.S. Department of Defense, July 1987.
4. *Bituminous Intermediate and Surface Courses for Airfields, Heliports, and Tank Roads*. Guide Specification CEGS-02556. U.S. Army Corps of Engineers, Sept. 1984.
5. J. C. Roffe. *Salviacim—Introducing the Pavement*. Jean Lefebvre Enterprise, Paris, France, 1989.
6. *Salviacim Waring Course*. Jean Lefebvre Specification, Paris, France.
7. J. C. Roffe. *Salviacim (Annex 1)—The Paving Process*. Jean Lefebvre Enterprise, Paris, France, 1989.

The contents of this paper reflect the views of the authors and do not necessarily reflect the official position of the Department of the Army or the Department of Defense. This paper does not constitute a standard, specification, or regulation.

Development of a Practical Method for Design of Hot-Mix Asphalt

K. E. COOPER, S. F. BROWN, J. N. PRESTON, AND F. M. L. AKEROYD

The development of a method for the design of hot-mix asphalt is traced. The design of gradations based on aggregate packing characteristics was found to be impractical for routine mix design. Measurement of elastic stiffness and assessment of resistance to permanent deformation was made possible with the development of the Nottingham asphalt mix tester. This development provided a method of designing mixes using relevant mechanical properties as design criteria. The percentage refusal density equipment was used to manufacture specimens at levels of compaction that should be achieved in practice. For a particular source of aggregate, the effect of binder content and aggregate gradation on volumetric composition and mechanical properties can be assessed. Certain volumetric and test criteria are applied to identify the mix or mixes that will perform satisfactorily. The final mix formulation can then be selected on the basis of certain practical and economic considerations.

As the end of the millennium approaches, there is increasing pressure to use more innovative highway construction materials that will result in greater economy, increased service lives, and less disruption to our environment. There have been advances in bitumen modification and significant improvements in the design of production and site plants. The results of research have highlighted the effect of mix variables on the mechanical properties of asphaltic mixes, and many engineers are willing to apply the results of this work. The principal obstacle to real progress is the lack of a reliable and practical method of mix design.

Since the publication of the results of earlier work on the development of a method of mix design for bituminous basecourse and road base materials (*1*), work has continued at Nottingham on developing an improved method of mix design using relatively simple equipment. A preliminary version of the method and associated test equipment was presented to the Eurobitume Conference in Madrid in 1989 (*2*,*3*).

In the United Kingdom, no method of mix design for highway materials is used other than an adaptation of the Marshall method for the "skip" or gap-graded, hot-rolled asphalt wearing course mix that forms the surface of much of the major highway network. The aggregate in this material is normally not greater than 20 mm (¾ in.), but road base mixes may contain sizes up to 37.5 mm (1½ in.); therefore, existing methods of mix design cannot be used because specimens prepared in relatively small molds are not representative. This constraint on the maximum aggregate size may have inhibited the use of mixes with large stone size in the United States. The benefits of using larger stone sizes have been discussed recently (*4*).

Even with conventional 20-mm (¾-in.) down gradations, specimen preparation methods and equipment do not provide the means of producing materials representative of that laid in practice. Moreover, the tests used do not measure relevant mechanical properties. As a consequence, the premature failure of mixes designed using existing methods is becoming increasingly common as the volume of traffic and axle loads increases.

K. E. Cooper, S. F. Brown, J. N. Preston, Department of Civil Engineering, University of Nottingham, Nottingham, U.K. NG7 2RD. F. M. L. Akeroyd, Mobil Oil Company, Ltd., Mobil House, 54/60 Victoria Street, London, U.K. SW1F 60B.

BACKGROUND WORK

Aggregate Packing Characteristics

Previous work (*1*) indicated that gradations could be quantified by the equivalent fines content (EFC), which is the percentage of aggregate passing a sieve with a mesh size 3 percent of that of the smallest sieve through which all the aggregate passes. The voids in mineral aggregate (VMA) and resistance to permanent deformation of a wide range of mixes were found to be related to EFC irrespective of maximum aggregate size.

Work on the compaction of uncoated aggregates suggested the possibility of designing gradings to a target VMA without the necessity of using bitumen in the first instance. Further investigations into the possibility of using spherical ballotinni as a reference aggregate were commenced. It was believed that the packing of gradations of perfect spheres could be compared with that of real aggregates to provide an index of aggregate shape. Materials were compacted in a mold placed on a vibrating table. However, tests indicated that the degree of packing may depend on a relationship between aggregate size and frequency of vibration. It became obvious that a considerable amount of preliminary work would be necessary; as a result, the work on the packing of dry aggregates and spheres was discontinued.

Nottingham Asphalt Mix Tester

Work on the development of simple equipment for measuring mechanical properties continued in parallel with the investigation of aggregate packing characteristics. State-of-the-art techniques in digital interfacing were used so that control and data acquisition could be carried out using a conventional desktop computer and user-friendly software. Load was applied by a pneumatic system with the type of components

commonly used for process control in manufacturing industries. Therefore, the user requires only mains electricity and a compressed air supply of about 7 bar (100 psi). The resultant apparatus is known as the Nottingham asphalt mix tester (NAT).

Currently, three types of test may be carried out using this device. The first is the repeated-load indirect tensile (RLIT) test, otherwise known as the resilient modulus test. The second is the uniaxial creep (UC) test, and the third is the repeated-load axial (RLA) test (also called dynamic creep). The user may first measure elastic stiffness (resilient modulus) of a material using the nondestructive RLIT test and then, using the same specimen, assess resistance to permanent deformation using either the UC or RLA test. Specimens may be 100 mm (4 in.), 150 mm (6 in.), or even 200 mm (8 in.) in diameter, and they may be laboratory molded or cored. The advantage of providing for the use of both molded and cored specimens is that the apparatus used for mix design can also be used for quality control and end product specification testing as well as failure investigation.

Figure 1 shows the NAT set up for the RLIT test. Figure 2 shows the same equipment configured for either the UC or the RLA test. Figure 3 shows schematic layouts of the equipment. NAT is normally situated in a temperature-controlled cabinet with a range of -10°C to 45°C.

To carry out a test, the operator merely responds to questions on the computer screen by typing in specimen dimensions and test conditions. The computer provides information on the steps involved in setting up the specimen and then automatically carries out the test, calculates the results, and presents the data in graphical or tabular form. Alternatively, data can be stored for analysis using spreadsheet software. NATs are currently used in six countries.

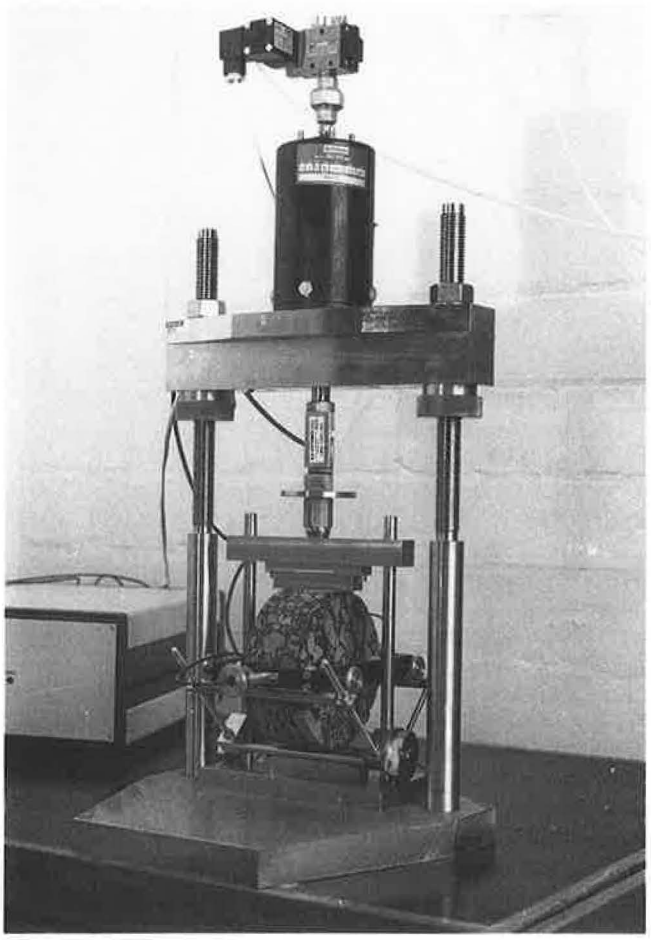

FIGURE 1 NAT set up for repeated-load indirect tensile test.

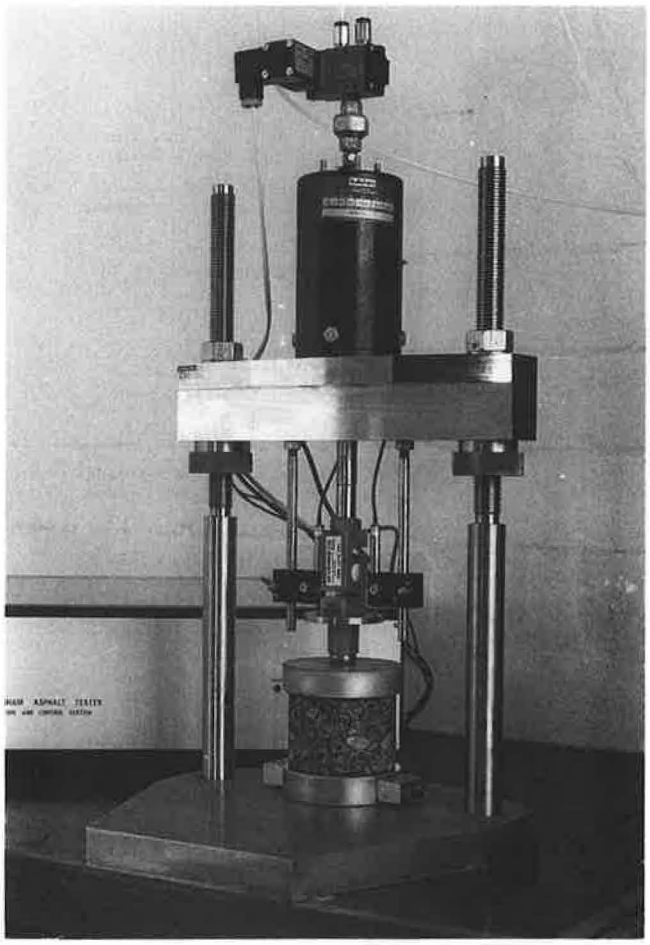

FIGURE 2 NAT set up for uniaxial creep or repeated load axial test.

For the RLIT test, the software enables the operator to select the magnitude of vertical load to be applied and the rise time of the load pulse within the ranges of which the equipment is capable, for example, load up to 3 kN and rise time typically 0.06 to 0.15 sec. Figure 4 shows the output from a typical RLIT test. The dimensionless plots of vertical load and horizontal deformation reflect any errors in specimen setup and indicate the effect of any electrical interference on the results.

Figure 5 shows typical relationships between axial strain and time for the UC test. Currently, the software provides for the following test conditions:

1. An optional 10-min conditioning period during which 10 percent of the test load is applied,
2. A 60-min test period, and
3. An optional 15-min relaxation period during which axial strain is monitored.

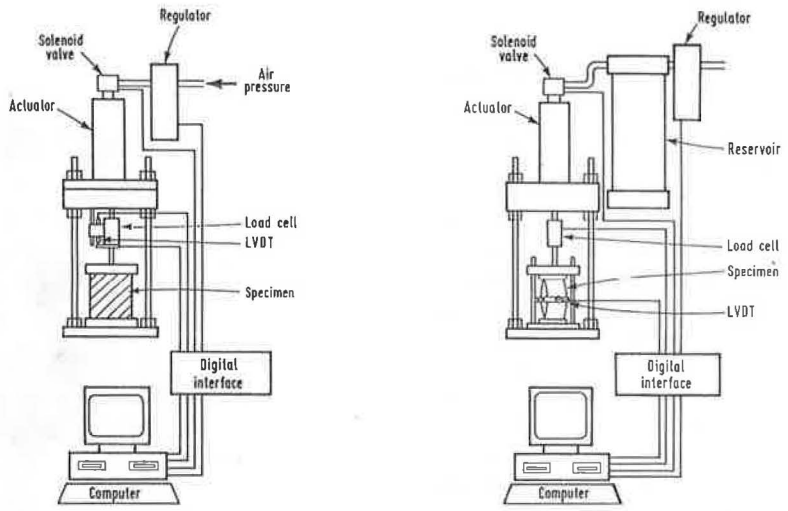

(a) Uniaxial creep and repeated load axial test configuration

(b) Repeated load indirect tensile test configuration

FIGURE 3 Schematic layout of NAT.

NOTTINGHAM ASPHALT TESTER
REPEATED LOAD INDIRECT TENSILE TEST
(calibration factors reviewed on 24 May 90)

Date is 8 Jun 90 -
Temperature = 20 Celsius
Specimen dia. = 100 mm
Poissons ratio = 0.35
No. cond pulses = 5
Pressure scale = 7 Rise time scale = 5

Specimen is PVC
Specimen thickness = 50 mm

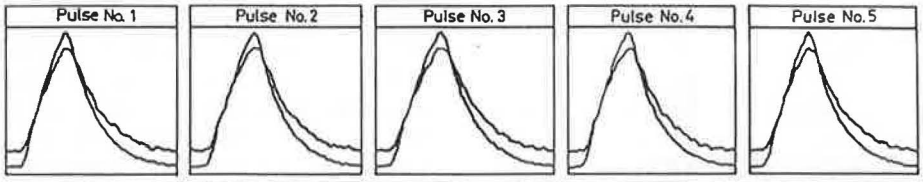

Pulse No.	Vertical Force (kN)	Tensile Stress (kPa)	Rise Time (m.secs)	Elastic Stiffness (MPa)
1	2.13	271.01	103.4	3582
2	2.18	276.99	103.4	3702
3	2.16	274.59	103.4	3647
4	2.12	278.29	103.4	3617
5	2.16	274.85	103.4	3633
Mean	2.16	275.23	103.4	3636

FIGURE 4 Typical output from No. 11 asphalt mix tester (elastic stiffness test).

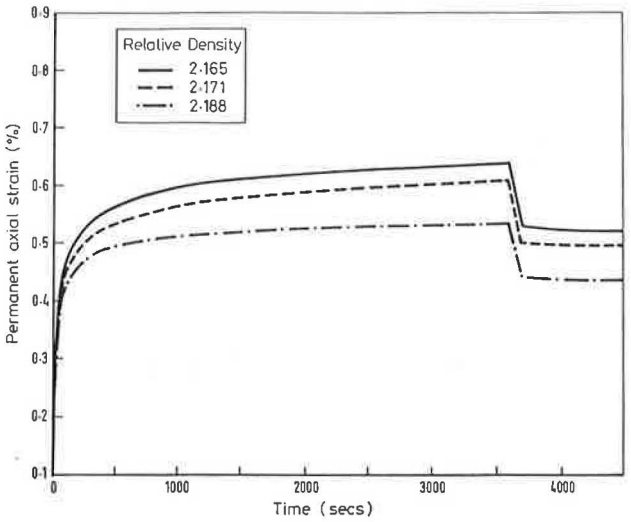

FIGURE 5 Results from typical uniaxial creep tests on bitumen emulsion mixes at 40°C and 100-kPa axial stress.

Software to provide the user with a greater choice of test conditions is being prepared.

Figure 6 shows typical relationships between axial strain and number of load pulses for the RLA test. In this test the specimen is subjected to alternate load applications and rest periods each 1 sec long.

Currently, the software provides for the following test conditions:

1. An optional 10-min conditioning period during which 10 percent of the test load is applied, and
2. A test period of up to 3,600 cycles (2 hr).

Software is being written to allow the user more choice of pulse and rest period length, with the opportunity of applying block periods of pulsed loading followed by rest periods of varying length.

For both the UC and RLA tests, the NAT is capable of applying a maximum vertical force of 3.5 kN.

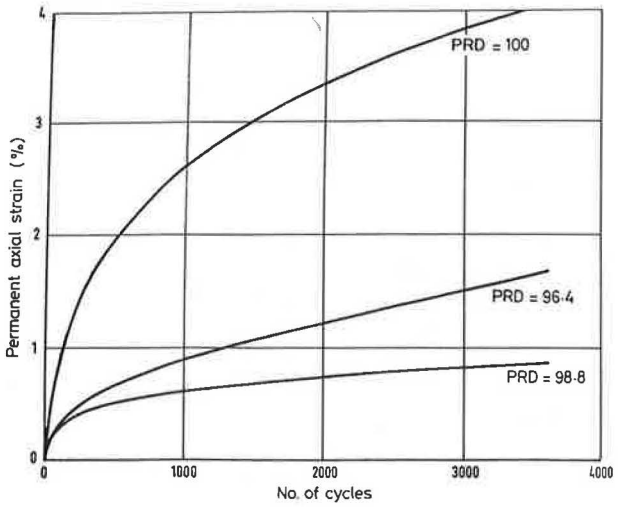

FIGURE 6 Results from typical repeated-load axial tests on hot-mix asphalt specimens at 40°C and 100-kPa axial stress.

Specimen Manufacture

The Nottingham roller compactor was considered for use in the manufacture of slabs from which test specimens could be cored. Some work was carried out with this equipment, but, although the roller compactor is similar to site compaction equipment, it was believed that the device would not be suitable for the routine manufacture of specimens necessary for a widely acceptable method of mix design. Involvement in a project on the problems of Marshall mix design in the Middle East resulted in the use of an alternative method of specimen preparation. The asphaltic concrete rutted seriously soon after the highway was opened to traffic. Investigation showed that good-quality aggregate had been used, the binder contents and gradations were close to those specified, and the bitumen had a penetration of less than 60. Although the mix designs were generally acceptable, the material in the wheel paths of the trafficked highway was found to have virtually zero void content in many cases.

To determine the susceptibility of the mix to overcompaction and subsequent flow under the action of repeated loading, the percentage refusal density (PRD) apparatus was used for specimen compaction (*5*). The PRD test is widely used in the United Kingdom for determining the degree of compaction of materials laid on site. Routinely, 150-mm (6-in.) cores are cut from newly compacted base materials. These cores are dried and coated with wax for density determination. The wax is then removed and the core is placed in a 150-mm-diameter, split PRD mold and put in an oven at 160°C for 3 hr. An electric vibrating hammer with a foot 100 mm (4 in.) in diameter is used to compact the material for 2 min on both ends of the sample. The foot is moved around the mold during compaction to achieve a kneading action. At the end of each 2-min compaction period, a foot 150 mm (6 in.) in diameter is used to flatten the ends of the sample. The density of the material at refusal is then measured. The density of the original core should not be less than a certain percentage of refusal (e.g., 93), otherwise the material from which the cores have been taken should be removed.

At refusal the material is considered to be at the ultimate state of compaction that can be achieved in practice. Refusal density should not be confused with maximum theoretical density, which is calculated on the basis that void content is zero. The advantage of refusal density is that it reflects the compactability of the mix, which depends on a variety of factors including aggregate shape, gradation, binder content, and layer thickness.

The PRD equipment was used to make samples of the deformation-susceptible material. To achieve a range of levels of compaction from 100 PRD to about 93 PRD, compaction temperatures and times were adjusted. This adjustment simulated the causes of variable compaction in the field where low material temperatures and insufficient roller passes can result in poor compaction.

The specimens were about 100 mm (4 in.) high after compaction. From each PRD specimen, a core 100 mm (4 in.) in diameter was cut; this core was trimmed to a height of 70 mm using a diamond-tipped masonry saw blade. Table 1 shows the volumetric proportions and level of compaction obtained for one of the asphalt mix gradations used. Mechanical testing was carried out in the NAT. The elastic stiffness of the cores

TABLE 1 VOLUMETRIC PROPORTIONS OF ASPHALTIC CONCRETE AT DIFFERERENT BINDER CONTENTS AND LEVELS OF COMPACTION

Specimen No.	Mb (%)	Voids (%)	VMA (%)	VFB (%)	PRD
1	4.3	1.9	13.2	85.8	100.0
2	4.3	3.8	15.0	74.3	98.0
3	4.3	4.7	15.7	70.0	97.1
4	4.3	5.7	16.6	65.6	96.1
5	4.3	7.1	17.8	60.2	94.7
6	4.3	9.2	19.7	53.4	92.6
7	3.8	4.1	14.0	70.8	100.0
8	3.8	6.9	16.5	58.3	97.1
9	3.8	9.4	18.7	49.8	94.4
10	4.8	1.3	13.9	90.5	100.0
11	4.8	3.6	15.9	77.3	97.7
12	4.8	6.6	18.6	64.2	94.6

Note: PRD = percentage refusal density; Mb = mass of bitumen; VFB = volume filled with bitumen

was measured using the RLIT test; the relationship between elastic stiffness and degree of compaction (PRD) is shown in Figure 7a, which indicates that, in general, higher elastic stiffness is achieved with well-compacted materials. At the high level of compaction, however, one mix with a high binder content did not follow this trend. The resistance to permanent deformation of the cores was then assessed using the RLA test (Figure 7b). The results generally reflect those of the elastic stiffness tests: higher levels of compaction result in lower levels of permanent deformation. There is a suggestion, however, that overcompaction could result in deformable mixes, as shown in Figure 6.

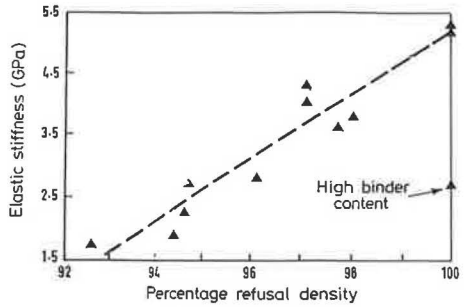

(a) Relationship between PRD and elastic stiffness (temperature = 20°C, load rise time = 0.1 secs)

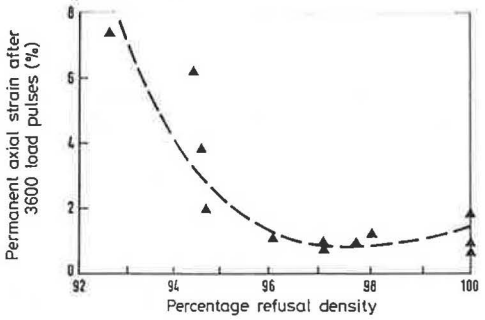

(b) Relationship between PRD and resistance to permanent deformation measured in the repeated load axial test (temperature = 40°C, repeated axial stress = 100 kPa)

FIGURE 7 Effect of compaction level on mechanical properties of asphaltic concrete.

MIX DESIGN

Earlier work (*6*) demonstrated the effect on the mechanical properties of bituminous materials of the interaction of gradation, binder content, and compaction. Therefore, the new mix design method was based on these three parameters by providing the means of examining their effect for a particular aggregate source. This would then enable the engineer to determine the best gradation and binder content for optimum mechanical properties at a target level of compaction.

Gradation

It was decided to concentrate on continuous gradations in the first instance because the use of this type of gradation for the structural layers is widespread. To define the target gradation, a modification of the widely known power law (*7*) was used. The modification allowed gradation and the fines content to be varied while filler (sub-200 mesh) material was maintained at a preselected and practical level. The grading equation is as follows:

$$P = \frac{(100 - F)(d^n - 0.075^n)}{(D^n - 0.075^n)} + F$$

where

P = percentage passing a sieve of size d (mm),
D = maximum aggregate size (mm),
F = filler content (sub-200 mesh material), and
n = exponent between 0 and 1.

Figure 8 shows the effect of varying the exponent n from 0.2 to 0.7 for 28-mm gradations with a filler content of 6.0 percent. The gradation with an exponent of 0.45 approximates the gradation that is generally acknowledged to have maximum density. Experience has shown that such gradations may be too dense, with insufficient void space to accommodate the binder. The solution generally adopted is to increase VMA by moving the gradation away from the maximum density curve. This move may be accomplished by reducing the exponent and, consequently, making the mix finer. This results in a higher binder content caused by the increased surface area of the graded aggregates and, in many cases, increased susceptibility to deformation. An increase in VMA may also be achieved by increasing the exponent and making the gradation coarser. This approach was adopted for the design of the road base and basecourse materials considered in this project; preliminary tests showed that exponents of 0.5, 0.6, and 0.7 were the most appropriate for mixes of this type.

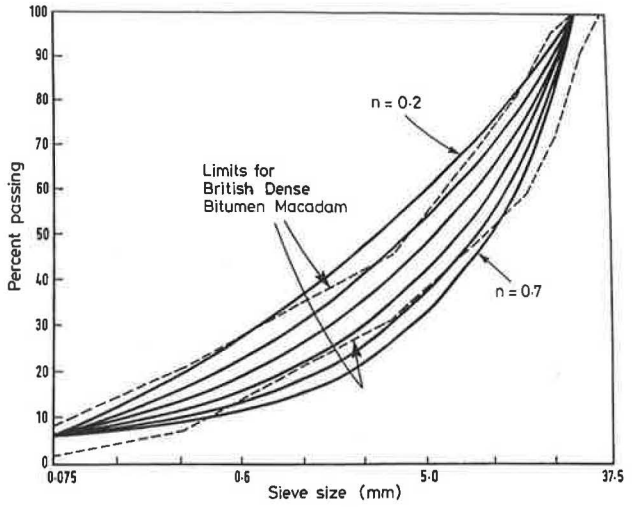

FIGURE 8 Typical grading curves based on Equation 1.

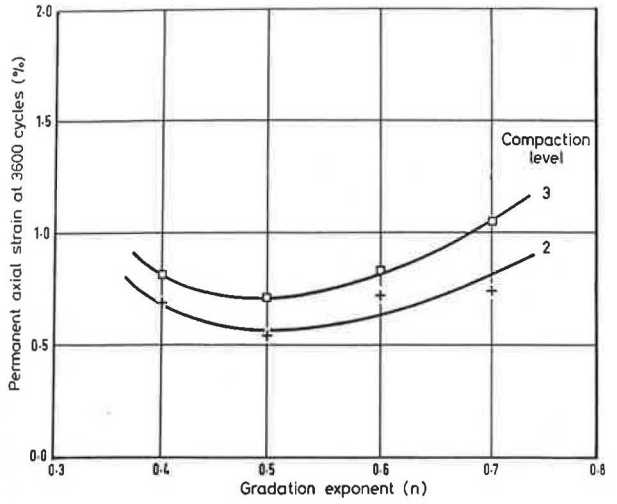

FIGURE 9 Effect of grading exponent *n* on resistance to permanent deformation measured in repeated-load axial test (granite aggregate with 4.1 percent binder).

Figure 9 shows the effect of grading exponent on resistance to permanent deformation measured by the RLA test. It can be seen that, for a certain binder content, aggregate type, and level of compaction, there is an optimum grading exponent for maximum resistance to permanent deformation.

It would not be possible to expect that the aggregate sizes from a particular source could be combined to exactly fit a gradation defined by a theoretical relationship. A simple computer program, however, can be used to determine the blend that minimizes the difference between the theoretical and practical gradations.

Compaction

The compaction was carried out using the PRD equipment to provide three compaction levels. The compaction conditions were as follows:

Compaction Level (approximate value)	*Compaction Time (sec)*	*Compaction Temperature* (°C)
1 (100 PRD)	120	SP + 92
2 (97 PRD)	60	SP + 50
3 (93 PRD)	30	SP + 40

Compaction time is for each end of the specimen, and SP is ring-and-ball softening point (°C).

The 100 PRD level is necessary as a datum for the other levels of compaction. It is also useful because the void content of a mix compacted to refusal reflects the ability of a material to perform adequately in severe conditions, such as the high temperatures combined with very heavy axle loads that occur in the Middle East. A mix with a void content of at least 2 percent at refusal may well be the best for such conditions. For Compaction Level 1, the temperature was that considered ideal for compaction in the field and represents something of an extrapolation assuming typical temperature susceptibilities. For modified bitumens, a more detailed definition of temperature would have to be used. For Compaction Levels 2 and 3, temperatures and compaction times were established by carrying out trials.

The target level of compaction in practice is generally 95 PRD, with 93 PRD being the minimum acceptable. For the purposes of mix design, therefore, 95 PRD is the most appropriate level of compaction.

Binder Content

In the United Kingdom, the binder content of continuously graded basecourse and road base mixes is generally within the range of 3.5 to 4.7 percent of the total mix. These two binder contents, together with the midrange value of 4.1 percent, provide the three levels of binder content that are used in the mix design procedure for the structural layers. For wearing course mixes, however, a finer gradation and higher binder content may be necessary to provide an impermeable, level running surface.

Basis of Mix Design Procedure

The mix design procedure involves an investigation of the effect of gradation, compaction, and binder content for a particular aggregate source. As discussed, three levels of each of the parameters were selected, resulting in nine mix compositions at three levels of compaction (i.e., 27 different mixes).

Specimen Preparation

To simplify the specimen-preparation process, the practice of cutting 100-mm-diameter cores from the PRD samples to produce test specimens was discontinued. Instead, the ends of the PRD specimens were cut, using a diamond-tipped masonry saw, to provide test specimens 70 mm high and 150 mm in diameter.

Volumetric Analysis

The first stage of the design procedure is the measurement and assessment of volumetric proportions when materials that

do not have volumetric proportions within the target ranges can be screened out. Densities are determined from gravimetric measurements without using wax to waterproof the specimens.

For road base and basecourse materials, the mix with a grading exponent of 0.5 and a binder content of 3.5 percent and compacted to 100 PRD is selected as a datum. The void content of this mix reflects the compactability of the aggregate and enables the appropriate volumetric chart (Figures 10–12) to be selected. In each of these charts, an area is defined by constraints on void content, VMA, and binder volume. These constraints are based on experience, practical considerations, and the volumetric proportions at 100 PRD. With the continuously graded basecourse and road base mixtures considered in this work, properly compacted materials have void contents in the range of 3 to 8 percent, as specified to ensure adequate fatigue resistance. Mixes falling within the defined area are considered to be candidates for the measurement of mechanical properties for mix design purposes. Those mixes outside the defined area are rejected, although test data on these materials could provide valuable information in the event of materials' being laid out of specification in practice.

Measurement of Mechanical Properties

NAT measures the elastic stiffness using the RLIT test configured for 150-mm-diameter specimens. The test temperature is 20°C and the rise time is about 120 msec (where rise time is the time between the start and the peak of the load pulse).

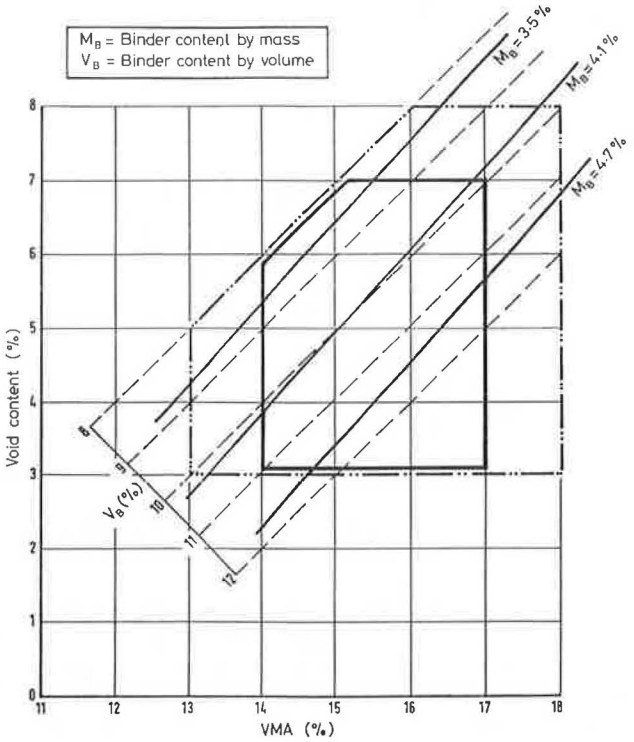

FIGURE 11 Volumetric criteria chart (2 percent voids at 100 PRD).

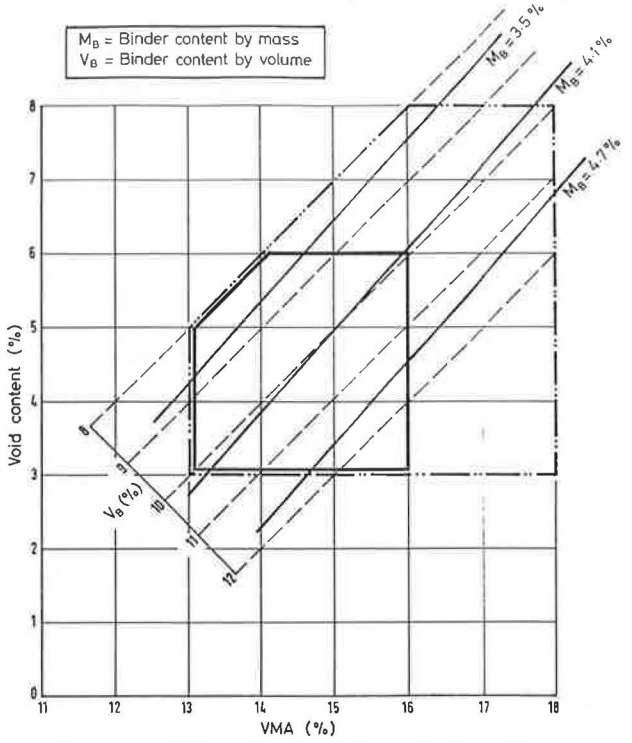

FIGURE 10 Volumetric criteria chart (1 percent voids at 100 PRD).

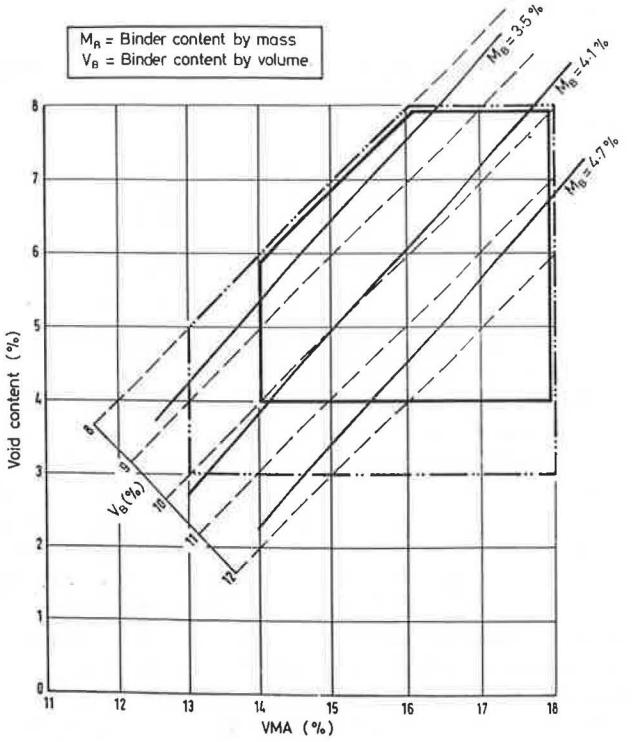

FIGURE 12 Volumetric criteria chart (3 percent voids at 100 PRD).

NAT then assesses resistance to permanent deformation using the RLA test, which, because it uses a pulsed axle load, is considered more simulative of in situ conditions than uniaxial creep. In this test, the 150-mm-diameter specimens are loaded axially between 100-mm-diameter platens as shown in Figure 13. The 25-mm-wide annulus of material outside the directly loaded part of the specimen is considered to impart a degree of lateral constraint that is related to the strength of the material. The test temperature is 40°C and the axial load waveform is virtually square with alternate load and rest periods each 1 sec long. The peak axial stress is 100 kPa and the specimen is normally subjected to 3,600 load pulses, which takes 2 hr. If modified bitumens are to be evaluated, the RLIT test should be carried out at more than one temperature to determine the temperature susceptibility of elastic stiffness.

Additional durability aspects that should be assessed, particularly for surface courses, are water sensitivity and the effects of aging. Measurements of elastic stiffness before and after soaking or freeze-thaw cycling would provide relevant information. New developments in accelerated aging, which involve forcing oxygen-rich air through a mix, could allow ready assessment of the effect of aging on mechanical properties.

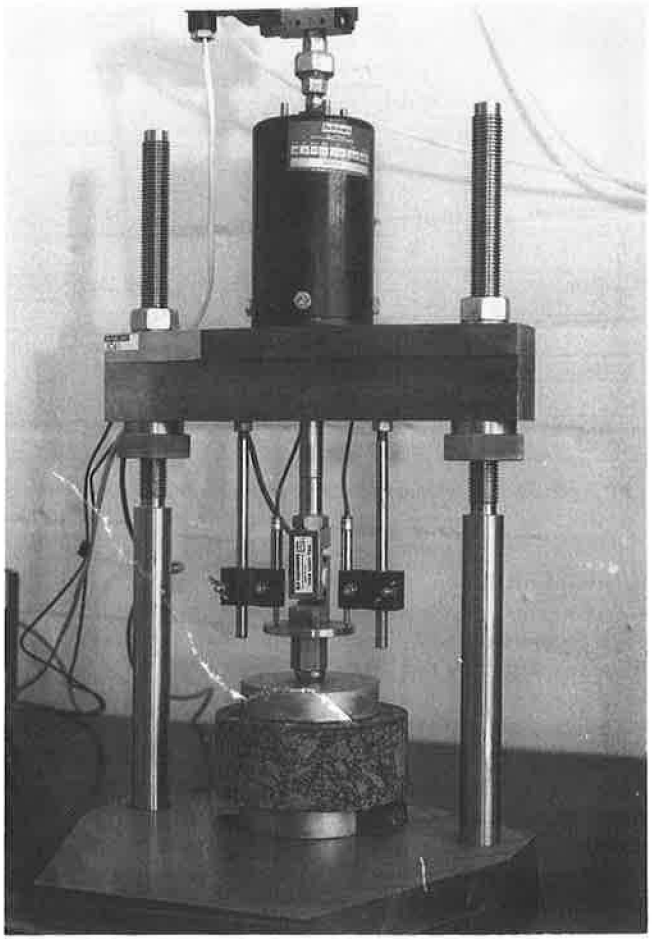

FIGURE 13 Repeated-load axial tests on 150-mm-diameter specimens using 100-mm-diameter platens.

Design Criteria

The development of a new method of mix design has three main problems. The first problem is the method of sample preparation; the second is the test methods; and the third is the selection of design criteria. With this phase of the work, which is primarily concerned with basecourse and road base mixes, the design criteria will be somewhat different from those used for wearing courses. In this project, it was decided not to determine optimum mix proportions for maximum mechanical properties but to specify certain minimum performance levels. This decision enables the engineer to determine the best mix on the basis of additional self-imposed criteria such as workability, the availability of materials, and, inevitably, the associated economic considerations. It is difficult to draw cut-off lines that rule out all materials that fall below, however marginal the shortfall. It is essential to be prudent, however, and ensure that the selected mix exceeds the criteria so that normal variances in composition and compaction do not mean that material is unnecessarily condemned and removed from the works.

For basecourse and road base mixes, the important mechanical properties are resistance to fatigue cracking, resistance to permanent deformation, and elastic stiffness, which reflects the load-spreading ability of the material. Other criteria concerned with volumetric proportions are dealt with in the volumetric charts (Figures 10–12) discussed previously.

Currently, the assessment of resistance to fatigue cracking involves more specimen preparation and testing then is considered practical for routine mix design work. In addition, the test equipment and techniques are generally too complex for a normal materials laboratory. For pavement constructions, which use relatively thick lifts of road base materials made with unmodified bitumens, prediction methods based on mix proportions and bitumen properties (*8*) are considered adequate. The current work on Strategic Highway Research Program Contract A003A may provide the means of assessing fatigue resistance more readily.

For resistance to permanent deformation measured using the RLA test, the criterion currently used is a maximum of 1.0 percent axial strain after 3,600 applications of an axial stress of 100 kPa at 40°C. The strain level was chosen because it appears to form a boundary between those mixes that become stable with a decreasing rate of permanent strain, and those mixes in which strain rate shows no sign of decreasing. Typical results are shown in Figure 14, which also shows the volumetric compositions of the materials used. It is interesting to note, from Figure 14, that overcompaction results in materials that are susceptible to permanent deformation.

For elastic stiffness measured by the RLIT test, the criterion is a minimum of 2500 MPa at 20°C with a load rise time of approximately 0.12 sec. The criterion was based on calculated levels of elastic stiffness related to pavement layer thickness and a background of extensive test data. Table 2 shows typical volumetric compositions and elastic stiffnesses for a particular aggregate type. The results have been sorted on the basis of the magnitude of elastic stiffness. The tabulated results show that, for the aggregate source investigated, higher values of elastic stiffness result from high levels of compaction and the consequently low levels of VMA and void content. In general, higher binder contents result in lower values of elastic stiffness.

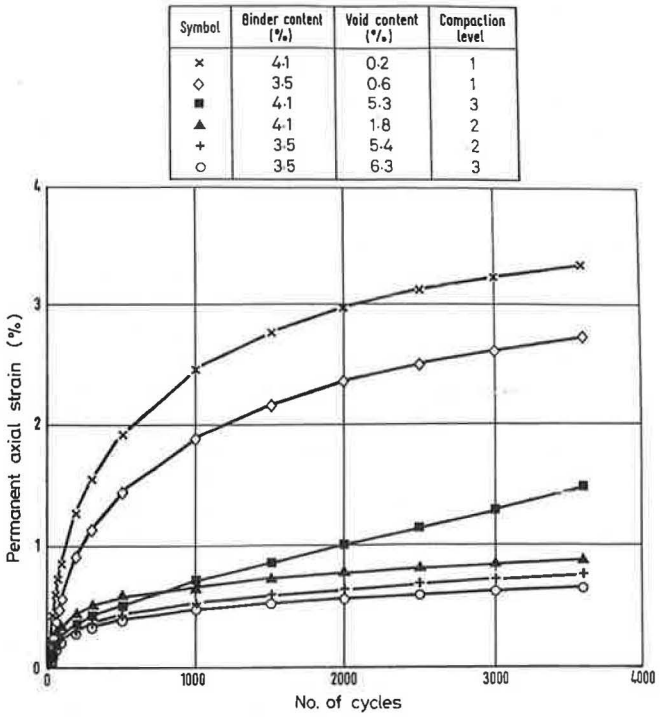

FIGURE 14 Repeated-load axial results for limestone aggregate specimens with gradation exponent n = 0.5.

TABLE 2 VOLUMETRIC COMPOSITIONS AND ELASTIC STIFFNESS OF MIXES MADE WITH CRUSHED LIMESTONE AND 100 PENETRATION BITUMEN

Grading Exponent n	Binder Content (%)	Compaction Level	Voids (%)	VMA (%)	PRD (%)	Elastic Stiffness (MPa)
0.7	3.5	1	0.6	9.6	100.0	5300
0.6	3.5	1	1.2	10.2	100.0	5200
0.5	3.5	1	0.6	9.6	100.0	5100
0.5	4.1	2	1.8	12.1	98.4	4400
0.7	4.1	1	0.1	10.6	100.0	4000
0.6	3.5	2	4.9	13.5	96.3	3700
0.6	3.5	3	6.8	15.3	94.3	3500
0.5	3.5	3	6.3	14.8	94.2	3300
0.5	4.1	1	0.2	10.7	100.0	3300
0.5	3.5	2	5.4	13.9	95.2	3300
0.7	4.7	1	-0.3	11.7	100.0	3300
0.7	3.5	2	4.8	13.4	95.8	3200
0.6	4.1	1	0.3	10.8	100.0	3200
0.5	4.7	1	-0.0	11.9	100.0	3000
0.6	4.7	1	-0.4	11.6	100.0	3000
0.5	4.7	2	1.3	13.0	98.8	2800
0.7	4.1	2	3.8	13.9	96.2	2800
0.6	4.7	2	0.6	12.4	99.4	2800
0.6	4.1	2	4.2	14.2	96.2	2600
0.7	3.5	3	6.9	15.3	93.7	2500
0.6	4.1	3	4.1	14.2	96.2	2400
0.5	4.7	3	3.7	15.1	96.4	2200
0.5	4.1	3	5.3	15.3	94.9	2200
0.7	4.7	2	2.2	13.9	97.8	2000
0.6	4.7	3	3.5	15.0	96.5	1700
0.7	4.7	3	5.3	16.6	94.7	1500
0.7	4.1	3	6.9	16.7	93.2	1400

(Results sorted in order of magnitude of elastic stiffness)

Summary

The basis of a mix design procedure has been established. Relevant volumetric and mechanical properties are used as design criteria. It is envisaged that the complete mix design procedure will take the form represented by the flow chart shown in Figure 15. A complete mix design example is available elsewhere (*9*).

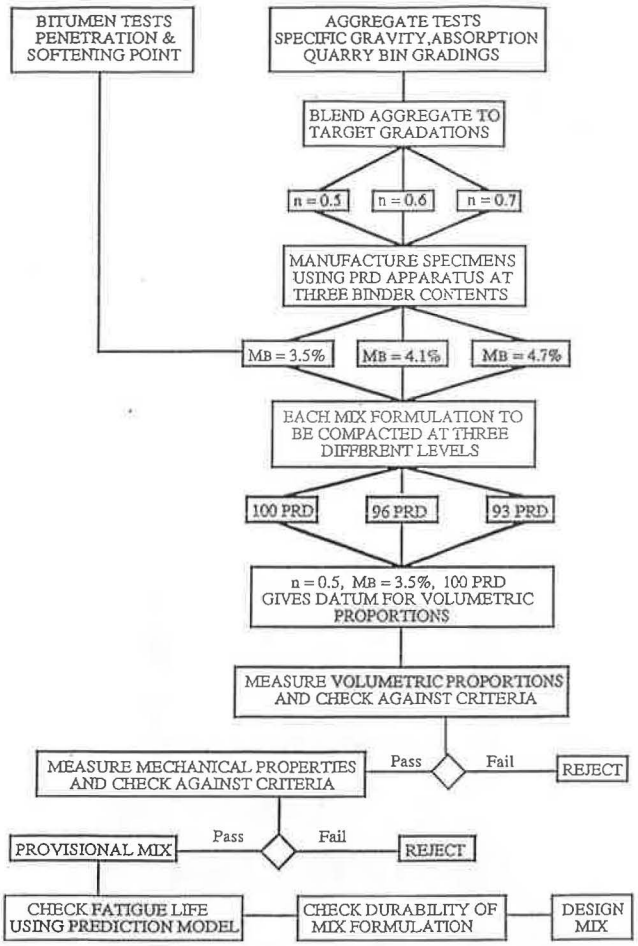

FIGURE 15 Flow chart of mix design procedure.

CONCLUSIONS

The conclusions drawn from this phase of the development of a mix design method are as follows:

1. The compaction of uncoated aggregates to develop appropriate gradations is impractical for routine mix design work.
2. The Nottingham asphalt mix tester provides a convenient method of measuring the elastic stiffness and resistance to permanent deformation of asphaltic mixes. The equipment can be used for mix design and has potential for quality control and end product specification.
3. The percentage refusal density equipment enables asphalt mixes to be compacted in the laboratory to a range of densities typical of those achieved in practice.

4. The framework of a mix design method for road base and basecourse mixes has been established. Design criteria are based on relevant volumetric proportions and mechanical properties. The method is to be developed to take into account flexibility, water sensitivity, and the effect of aging.

ACKNOWLEDGMENTS

The research described in this paper was made possible through the financial support of Mobil Oil Company Limited, the United Kingdom Science and Engineering Research Council, and the National Asphalt Pavement Association. The authors are grateful for the assistance rendered by Chris Bell of Oregon State University.

REFERENCES

1. K. E. Cooper, S. F. Brown, and G. R. Pooley. The Design of Aggregate Gradings for Asphalt Basecourses. *Proc., Association of Asphalt Paving Technologists*, Vol. 54, 1985, pp. 324–346.
2. S. F. Brown, K. E. Cooper, J. N. Preston, and C. A. Bell. Development of a New Procedure for Bituminous Mix Design. *Proc., Eurobitume Symposium*, Madrid, 1989, pp. 499–504.
3. K. E. Cooper and S. F. Brown. Development of a Simple Apparatus for the Measurement of the Mechanical Properties of Asphalt Mixes. *Proc., Eurobitume Symposium*, Madrid, 1989, pp. 494–498.
4. S. M. Acott. Today's Traffic Calls for Heavy Duty Asphalt Mixes. *Roads and Bridges*, Jan. 1988.
5. *The Percentage Refusal Density Test.* TRRL Contractor Report 1. Department of Transport, London, England, 1987.
6. S. F. Brown. Improved Asphalt Pavement Engineering. *Proc., 7th AAPA International Asphalt Conference*, Brisbane, Australia, 1988, pp. 35–48.
7. E. J. Yoder. *Principles of Pavement Design.* John Wiley and Sons, Inc., New York, 1959.
8. K. E. Cooper and P. S. Pell. *The Effect of Mix Variables on the Fatigue Strength of Bituminous Materials.* TRRL Report LR 633. Department of Transport, London, England, 1974.
9. S. F. Brown, J. N. Preston, and K. E. Cooper. Application of New Concepts in Asphalt Mix Design. Presented at Annual Meeting of the Association of Asphalt Paving Technologists, Seattle, Wash., March 1991.

Effect of Aggregate Gradation Variation on Asphalt Concrete Mix Properties

ROBERT P. ELLIOTT, MILLER C. FORD, JR., MAHER GHANIM, AND YUI FEE TU

Six asphalt concrete mixes were tested to investigate the effects of variation in the aggregate gradation on mix properties. The asphalt contents of the mixes were maintained at the job mix design contents. The gradation variations were representative of typical construction extremes. Five gradations were tested from each mix: (a) the job mix formula (JMF) gradation, (b) a fine gradation, (c) a coarse gradation, (d) a coarse-fine gradation, and (e) a fine-coarse gradation. The fine and coarse gradations deviated from the JMF gradation by the maximum amount to the fine or coarse side. The fine-coarse and coarse-fine gradations crossed over the JMF gradation curve from the maximum fine (or coarse) amount on the largest size fraction to the maximum coarse (or fine) amount on the smallest size fraction. Properties investigated were creep stiffness, split tensile strength, resilient modulus, Marshall stability, Marshall flow, air voids, and voids in mineral aggregate. Analysis of the data revealed that the fine-coarse and coarse-fine gradation variations had the greatest impact on mix properties but that none of the variations had a significant effect on resilient modulus. The data also showed that within the range normally encountered, air void content had a greater impact on split tensile strength than did gradation variation.

All highway agencies recognize the need to control the degree of variability of asphalt pavement construction. Specifications controlling the quality of construction typically include limits of acceptability of factors such as asphalt content, density, and gradation. These limits generally have been established over many years and represent the collective experience and opinions of many engineers. Nevertheless, the relationship between mix variation and service life is not well established; however, such relationships are needed to ensure that specification limits are realistic and consistent. The relationships are also needed to establish pay adjustments for construction that does not meet the specification requirements but is not so poor that it warrants removal and replacement.

A study was performed to investigate the effect of variations in the gradation of aggregates on the properties of asphalt concrete mixes. The gradation variations tested represented the extremes for a typical construction project. The specific objectives of the study were to determine the effect of gradation variation on

1. Creep behavior as a measure of rutting resistance;
2. Split tensile strength as an indicator of fatigue resistance potential;
3. Marshall mix properties (stability, flow, air voids, and voids in mineral aggregate) as a measure of mix acceptability; and
4. Resilient modulus as the parameter controlling the AASHTO thickness design structural layer coefficient.

R. P. Elliott and M. C. Ford, Arkansas Highway and Transportation Research Center, 4190 Bell Engineering Center, University of Arkansas, Fayetteville, Ark. 72701. M. Ghanim, American Engineering Company, P.O. Box 690234, Houston, Tex. 77269. Y. F. Tu, California Department of Transportation, 2642 West Lincoln Avenue, Anaheim, Calif. 92801.

SELECTION OF MIXES AND GRADATION VARIATIONS

Six asphalt concrete mixes were tested in the study. Three were surface mixes and three were binder mixes. The mixes were selected to be representative of those typically used in Arkansas. The principal difference between the mixes was in the type of coarse aggregate. Three types of coarse aggregate were used: (a) crushed limestone, (b) crushed syenite, and (c) crushed gravel. The mixes are referred to as limestone surface, limestone binder, syenite surface, syenite binder, gravel surface, and gravel binder. The job mix formulas for the mixes are listed in Table 1.

The gradation variations used in the study represented the extreme variations typically encountered in construction. To identify "typical, maximum" variations, field extraction data were obtained from 11 paving projects. Standard deviations of the gradation percentage for each sieve size were computed for each mix. From these, the typical standard deviations were selected and typical, maximum variations were calculated as three standard deviations. The variations used in the test program were based on these deviations and an examination of the actual maximum variations from the field data. The selected variations are generally about the same as the specification limits set by the Arkansas State Highway and Transportation Department (AHTD).

Each of the six mixes included in the study was tested with five variations in the aggregate gradation (Figure 1 and Table 2). For each mix, only the gradation was varied; the job mix formula asphalt content was held constant for all gradation variations. The control gradation for each mix was the job mix formula (JMF) supplied by AHTD. Two other gradations were the job mix formula plus or minus the maximum variations described. These were referred to as fine and coarse mix gradations. The remaining two gradations were crossover gradations categorized as fine-coarse and coarse-fine.

The fine-coarse gradation had the maximum gradation variation to the fine side for the largest aggregate size fraction (½ in. for surface and ¾ in. for binder) and the maximum gradation variation to the coarse side for the smallest size

Effect of Aggregate Gradation Variation on Asphalt Concrete Mix Properties

ROBERT P. ELLIOTT, MILLER C. FORD, JR., MAHER GHANIM, AND YUI FEE TU

Six asphalt concrete mixes were tested to investigate the effects of variation in the aggregate gradation on mix properties. The asphalt contents of the mixes were maintained at the job mix design contents. The gradation variations were representative of typical construction extremes. Five gradations were tested from each mix: (a) the job mix formula (JMF) gradation, (b) a fine gradation, (c) a coarse gradation, (d) a coarse-fine gradation, and (e) a fine-coarse gradation. The fine and coarse gradations deviated from the JMF gradation by the maximum amount to the fine or coarse side. The fine-coarse and coarse-fine gradations crossed over the JMF gradation curve from the maximum fine (or coarse) amount on the largest size fraction to the maximum coarse (or fine) amount on the smallest size fraction. Properties investigated were creep stiffness, split tensile strength, resilient modulus, Marshall stability, Marshall flow, air voids, and voids in mineral aggregate. Analysis of the data revealed that the fine-coarse and coarse-fine gradation variations had the greatest impact on mix properties but that none of the variations had a significant effect on resilient modulus. The data also showed that within the range normally encountered, air void content had a greater impact on split tensile strength than did gradation variation.

All highway agencies recognize the need to control the degree of variability of asphalt pavement construction. Specifications controlling the quality of construction typically include limits of acceptability of factors such as asphalt content, density, and gradation. These limits generally have been established over many years and represent the collective experience and opinions of many engineers. Nevertheless, the relationship between mix variation and service life is not well established; however, such relationships are needed to ensure that specification limits are realistic and consistent. The relationships are also needed to establish pay adjustments for construction that does not meet the specification requirements but is not so poor that it warrants removal and replacement.

A study was performed to investigate the effect of variations in the gradation of aggregates on the properties of asphalt concrete mixes. The gradation variations tested represented the extremes for a typical construction project. The specific objectives of the study were to determine the effect of gradation variation on

1. Creep behavior as a measure of rutting resistance;
2. Split tensile strength as an indicator of fatigue resistance potential;
3. Marshall mix properties (stability, flow, air voids, and voids in mineral aggregate) as a measure of mix acceptability; and
4. Resilient modulus as the parameter controlling the AASHTO thickness design structural layer coefficient.

R. P. Elliott and M. C. Ford, Arkansas Highway and Transportation Research Center, 4190 Bell Engineering Center, University of Arkansas, Fayetteville, Ark. 72701. M. Ghanim, American Engineering Company, P.O. Box 690234, Houston, Tex. 77269. Y. F. Tu, California Department of Transportation, 2642 West Lincoln Avenue, Anaheim, Calif. 92801.

SELECTION OF MIXES AND GRADATION VARIATIONS

Six asphalt concrete mixes were tested in the study. Three were surface mixes and three were binder mixes. The mixes were selected to be representative of those typically used in Arkansas. The principal difference between the mixes was in the type of coarse aggregate. Three types of coarse aggregate were used: (a) crushed limestone, (b) crushed syenite, and (c) crushed gravel. The mixes are referred to as limestone surface, limestone binder, syenite surface, syenite binder, gravel surface, and gravel binder. The job mix formulas for the mixes are listed in Table 1.

The gradation variations used in the study represented the extreme variations typically encountered in construction. To identify "typical, maximum" variations, field extraction data were obtained from 11 paving projects. Standard deviations of the gradation percentage for each sieve size were computed for each mix. From these, the typical standard deviations were selected and typical, maximum variations were calculated as three standard deviations. The variations used in the test program were based on these deviations and an examination of the actual maximum variations from the field data. The selected variations are generally about the same as the specification limits set by the Arkansas State Highway and Transportation Department (AHTD).

Each of the six mixes included in the study was tested with five variations in the aggregate gradation (Figure 1 and Table 2). For each mix, only the gradation was varied; the job mix formula asphalt content was held constant for all gradation variations. The control gradation for each mix was the job mix formula (JMF) supplied by AHTD. Two other gradations were the job mix formula plus or minus the maximum variations described. These were referred to as fine and coarse mix gradations. The remaining two gradations were crossover gradations categorized as fine-coarse and coarse-fine.

The fine-coarse gradation had the maximum gradation variation to the fine side for the largest aggregate size fraction (½ in. for surface and ¾ in. for binder) and the maximum gradation variation to the coarse side for the smallest size

TABLE 1 JOB MIX FORMULAS OF MIXES TESTED

SIEVE SIZE	AGGREGATE GRADATION, % PASSING AGGREGATE ONLY					
	SURFACE COURSE MIXES			BINDER COURSE MIXES		
	LIMESTONE	SYENITE	GRAVEL	LIMESTONE	SYENITE	GRAVEL
1"				100	100	100
3/4"	100	100	100	88	90	88
1/2"	93	93	96	66	75	69
3/8"	81	84	81	56	62	59
#4	60	61	60	43	40	44
#10	45	42	43	31	30	32
#20	36	28	31	23	25	26
#40	28	21	22	18	19	21
#80	13	12	12	10	11	11
#200	6	7	7	6	6	6
ASPHALT CONTENT, % TOTAL WT.	5.6	5.3	5.4	4.3	4.5	4.4

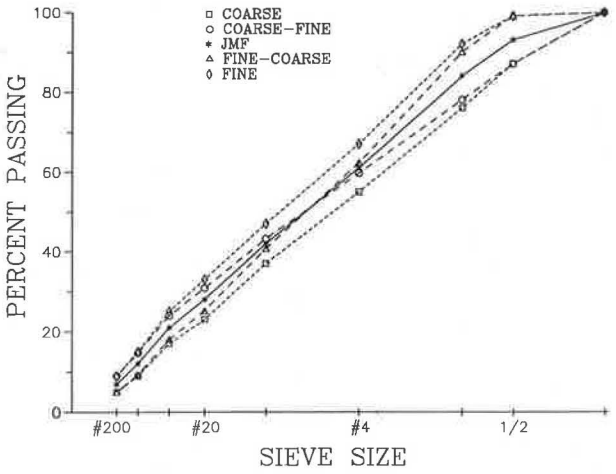

FIGURE 1 Gradation variations tested.

fraction (No. 200 sieve). The variations from the job mix formula for the other sieve sizes were prorated based on the 0.45 power gradation scale. The coarse-fine gradation was similar to the fine-coarse gradation, but the sign of the deviations from the job mix formula was reversed.

SPECIMEN PREPARATION

To control the gradation of the test specimens, all aggregates were separated into the various size fractions (e.g., ½ in. to ⅜ in., ⅜ in. to No. 4) and stored in metal buckets. When test specimens were prepared, the aggregates were recombined to provide the desired gradation with each test specimen batched separately. In the recombination, the composition of each size fraction relative to aggregate sources was held constant. Thus, if the No. 4 to No. 10 material of the job mix formula was composed of 18 percent from the coarse aggregate source, 37 percent from the coarse sand, and 45 percent from the fine sand, these same percentages were used for the No. 4 to No. 10 fraction in all gradation variations of that mix. In this manner, all effects observed from the testing are the result

TABLE 2 GRADATION VARIATIONS USED IN STUDY

SIEVE SIZE	CHANGE IN PERCENT PASSING FROM JOB MIX FORMULA				
	SURFACE COURSE MIXES				
	FINE	FINE-COARSE	JMF	COARSE-FINE	COARSE
1/2"	+6	+6	0	-6	-6
3/8"	+8	+5.93	0	-5.93	-8
#4	+6	+1.29	0	-1.29	-6
#10	+5	-1.24	0	+1.24	-6
#20	+5	-2.80	0	+2.80	-5
#40	+4	-2.95	0	+2.95	-4
#80	+3	-2.68	0	+2.68	-3
#200	+2	-2	0	+2	-2
SIEVE SIZE	BINDER COURSE MIXES				
	FINE	FINE-COARSE	JMF	COARSE-FINE	COARSE
3/4"	+8	+8	0	-8	-8
1/2"	+12	+7.51	0	-7.51	-12
3/8"	+12	+4.99	0	-4.99	-12
#4	+8	-0.10	0	+0.10	-8
#10	+6	-2.33	0	+2.33	-6
#20	+6	-3.85	0	+3.85	-6
#40	+5	-3.93	0	+3.93	-5
#80	+4	-3.65	0	+3.65	-4
#200	+2.5	-2.50	0	+2.50	-2.5

of variations in the gradation rather than variations in aggregate composition.

Two types of test specimens were prepared: standard Marshall specimens and 4 × 4 (4-in. diameter by 4-in. high) cylindrical specimens. The Marshall specimens were molded in accordance with AASHTO T245 using 75 blows of the compaction hammer on each face of the specimens. The 4 × 4 specimens were prepared using rodding and static compaction.

The cylindrical molds for the 4 × 4 specimens were designed to provide a fixed volume for density control. This was accomplished by having end caps that extended a fixed distance into the mold. The distance was controlled by a lip extending beyond the cap. A spacer was used with the bottom end cap to hold it partly out of the mold during rodding. In this way, both end caps were pushed into the mold during the static compaction, obtaining compaction from both ends.

In preparing the 4 × 4 specimens, the amount of mix required to produce a specimen with 5 percent air voids was weighed out and divided into thirds. Each third was placed in the mold and rodded in place. After all three layers had been rodded, compaction was completed on a compression test device by pushing the end caps until the volume control lips were seated on the mold. The objective was to produce specimens with 5 percent air voids that were uniform top to bottom. As will be shown, this objective was not achieved.

MARSHALL SPECIMEN TESTING

Four Marshall specimens were made of each gradation variation for each mix. These specimens were tested for air voids, voids in mineral aggregate (VMA), Marshall stability, Marshall flow, and resilient modulus. Air voids and VMA were

determined based on specimen bulk specific gravities (AASHTO T166) and Rice maximum specific gravities (AASHTO T209).

Resilient modulus was determined using the diametral test developed by Schmidt (*1*). The test temperature was 77°F. The dynamic pulse load was 75 lb, and the radial displacement due to the load was measured at 0.05 sec of loading. Measurements were made on three axes 120 degrees apart, and the average was used as the specimen resilient modulus.

4 × 4 SPECIMEN TESTING

Two 4 × 4 specimens were made for each gradation variation. These specimens were used for creep testing and split tensile strength testing.

The creep testing was conducted at 104°F using the resilient modulus apparatus operated in a static load mode with the specimen loaded in the axial direction. The specimens were placed in an oven set at 104°F for at least 24 hr before testing. For temperature control during testing, an insulated chamber was placed on the test apparatus around the loading head. Temperature was controlled using a thermal couple temperature probe, which was attached as a thermostat to a hair dryer. The test specimens were stored in the chamber at least 1 hr before testing for temperature stabilization.

The top and bottom surfaces of the specimens were coated with graphite before testing to reduce surface friction. Before creep testing, each specimen was conditioned with a set loading history to reduce any influence caused by small surface irregularities. The conditioning consisted of applying the creep loading (15 psi) for 10 min followed by 10 min of no load.

The creep load (15 psi) was then applied for 1 hr with the creep deformation being measured at 5 sec, 30 sec, 2 min, 30 min, and 60 min. The creep stiffness was calculated for each interval as

$$Sx = l*h/d$$

where

Sx = creep stiffness at time x;
l = creep loading stress (15 psi);
h = original height of specimen; and
d = specimen vertical deformation at time x.

After creep testing, each 4 × 4 specimen was sawed in half to provide two specimens for the split tensile strength test. The split tensile strength was determined at 77°F using the Marshall test apparatus but with the Marshall breaking head replaced by loading caps that would apply the diametral load over ½-in. bearing width. The rate of loading was the same as the Marshall loading rate, 2 in./min.

ANALYSES OF MARSHALL SPECIMEN DATA

Methods of Analysis

The data from testing the Marshall specimens were analyzed to identify the effect of gradation variation. Two types of analyses were used: analysis of variance and *t*-test groupings.

Analysis of variance examines the variation in the test parameters (i.e., air voids, VMA, stability, flow, and resilient modulus). It compares the variation observed between replicate mix specimens with the variation observed between mix specimens having different gradations. If gradation has no effect, the degree of variation will be the same for replicate specimens and for specimens of different gradation. However, if gradation does affect the value of the test parameter, the degree of variation for all the test specimens will be greater than the degree of variation for test specimens from a single gradation.

The measure of statistical significance in the analysis of variance is the *F*-ratio. The level of significance is indicated by the probability of finding a higher *F*-ratio if, in fact, no effect due to gradation exists. Low probabilities of a higher *F*-ratio indicate a high probability of an effect attributable to gradation. In this study, probabilities less than 0.05 indicated a statistically significant effect due to gradation.

Analysis of variance provides a statistical determination of whether the test parameter values have differences that might be caused by the gradation variation. However, if differences are identified, analysis of variance does not indicate where those differences occur (i.e., which gradations cause the differences). To make this type of determination, the *t*-test groupings were used.

The *t*-test groupings examine the mean values of the test parameters relative to the various mix gradation categories. The means are compared one by one using the standard *t*-test. Based on the individual comparisons, the gradations are placed in groups having similar means. The separation of the various gradations into two or more groups indicates a significant difference between the mean values of the test parameter being examined. This, then, indicates an effect attributable to the gradation variation.

These two methods were used to analyze the Marshall specimen data from each of the mixes individually and to analyze all of the data together. When all of the data were analyzed together, the analysis of variance was performed to identify effects attributable to the type of aggregate (limestone, gravel, and syenite) and the type of mix (surface and binder).

Air Void Analyses

Analysis of variance showed that air voids were affected by gradation variation, mix type, and aggregate type (Table 3). The *t*-test groupings showed that the fine-coarse gradation had the highest air voids and the coarse-fine mix had the lowest (Table 4). The other gradation variations (fine, coarse, and JMF) tended to have nearly equal air void contents.

These data show that the crossover gradation variations (coarse-fine or fine-coarse) have the greatest effect on air voids. Gradation variations that tend to parallel the job mix gradation do not cause significant changes in the mix air void contents. However, gradation variations that cross from coarse on the large size fractions to fine on the small size fractions cause a significant decrease in air voids. Conversely, gradation variations that cross from fine to coarse cause an increase in the air voids. For the mixes tested, the coarse-fine gradation would be judged to be most detrimental because it resulted in unacceptably low air void contents.

TABLE 3 AIR VOIDS, ALL MARSHALL SPECIMENS: ANALYSIS OF VARIANCE

ANALYSIS OF VARIANCE

Source of Variation	Degrees of Freedom	Sum of Squares	Mean Square	F	Prob. of > F
Gradation (G)	4	60.102	15.025	84.99	0.0001
Aggregate (A)	2	29.119	14.559	82.35	0.0001
Mix Type (M)	1	7.047	7.047	39.86	0.0001
G*A	8	4.450	0.556	3.15	0.0035
G*M	4	1.061	0.265	1.50	0.2088
A*M	2	2.347	1.173	6.64	0.0020
G*A*M	8	4.913	0.614	3.47	0.0016
Error	90	15.911	0.177		
Total	119	124.950			

The level of significance is indicated by the probability of greater F. Probabilities less than 0.05 are generally judged as being indicative of a significant effect.

TABLE 4 AIR VOIDS, ALL MARSHALL SPECIMENS: T-TEST GROUPINGS

T Grouping	Mean (%)	Gradation Variation
A	3.591	FINE-COARSE
B	2.298	FINE
B	2.202	JOB MIX FORMULA
B	2.126	COARSE
C	1.405	COARSE-FINE

Means in the same T Grouping are not significantly different at alpha equal to 0.05.

VMA Analyses

Analyses of the VMA data produced results nearly identical to the air void analyses. VMA content was found to be affected by gradation variation, mix type, and aggregate type (Table 5). The *t*-test groupings showed that the fine-coarse gradation had the highest VMA and the coarse-fine had the lowest (Table 6). The other gradation variations (fine, coarse, and JMF) tended to have nearly equal VMA contents.

Similarly, to the air void analyses, the crossover gradation variations (coarse-fine or fine-coarse) had the greatest effect on VMA. No significant changes in VMA were observed for gradation variations that tend to parallel the job mix gradation. However, coarse-fine gradations caused a significant decrease in VMA, and fine-coarse gradations caused an increase in VMA. The coarse-fine gradation would be judged to be most detrimental because it resulted in an unacceptably low VMA content.

TABLE 5 VMA, ALL MARSHALL SPECIMENS: ANALYSIS OF VARIANCE

Source of Variation	Degrees of Freedom	Sum of Squares	Mean Square	F	Prob. of > F
Gradation (G)	4	45.101	11.275	83.23	0.0001
Aggregate (A)	2	17.834	8.917	65.82	0.0001
Mix Type (M)	1	226.051	226.051	1668.61	0.0001
G*A	8	4.712	0.589	4.35	0.0002
G*M	4	0.877	0.219	1.62	0.1764
A*M	2	1.718	0.859	6.34	0.0027
G*A*M	8	3.548	0.443	3.27	0.0025
Error	90	12.193	0.135		
Total	119	312.033			

The level of significance is indicated by the probability of greater F. Probabilities less than 0.05 are generally judged as being indicative of a significant effect.

TABLE 6 VMA, ALL MARSHALL SPECIMENS: T-TEST GROUPINGS

T Grouping	Mean (%)	Gradation Variation
A	14.721	FINE-COARSE
B	13.575	FINE
B	13.508	JOB MIX FORMULA
B	13.454	COARSE
C	12.829	COARSE-FINE

Means in the same T Grouping are not significantly different at alpha equal to 0.05.

Stability Analyses

Analysis of variance of the Marshall stability data from all the mixes showed significant effects due to gradation, aggregate type, and mix type (Tables 7 and 8). In general, the fine gradation had the highest stability and the fine-coarse gradation had the lowest stability.

These trends, however, were not observed in every mix. The highest stability occurred with the fine gradation in five of the six mixes; the stability was second highest in the sixth mix. Similarly, the fine-coarse gradation had the lowest stability in four of the six mixes and was second lowest in the other two.

The stabilities of all the mixes were quite high, and the lowest stabilities observed would not indicate a mixture problem. Consequently, the effect of gradation variation on the stability of these mixes did not appear to be significant.

Flow Analyses

Marshall flow was also found to be affected by gradation, aggregate type, and mix type (Tables 9 and 10). The *t*-test groupings showed that for five of the six mixes, the coarse-fine gradation had the highest flow and the fine-coarse gradation had the lowest flow. The other gradation variations (fine, JMF, and coarse) did not show any consistent pattern.

The *t*-test grouping analysis for all the data showed the flow data to fit into three gradation groups. The coarse-fine gradations were alone in the high flow group, and the fine-coarse gradations were alone in the low flow group. The other gradations were grouped together.

TABLE 7 STABILITY DATA, ALL MARSHALL SPECIMENS: ANALYSIS OF VARIANCE

Source of Variation	Degrees of Freedom	Sum of Squares	Mean Square	F	Prob. of > F
Gradation (G)	4	12869657	3217414	25.70	0.0001
Aggregate (A)	2	18954544	9477272	75.69	0.0001
Mix Type (M)	1	9403521	9403521	75.10	0.0001
G*A	8	2741912	342739	2.74	0.0095
G*M	4	1249571	312393	2.50	0.0484
A*M	2	4854283	2427141	19.39	0.0001
G*A*M	8	1550071	193759	1.55	0.1522
Error	90	11268529	125206		
Total	119	62892086			

The level of significance is indicated by the probability of greater F. Probabilities less than 0.05 are generally judged as being indicative of a significant effect.

TABLE 8 STABILITY DATA, ALL MARSHALL SPECIMENS: T-TEST GROUPINGS

T Grouping	Mean (lb)	Gradation Variation
A	4206.7	FINE
A & B	3966.5	COARSE-FINE
B & C	3807.3	JOB MIX FORMULA
C & D	3471.8	COARSE
D	3302.8	FINE-COARSE

Means in the same T Grouping are not significantly different at alpha equal to 0.05.

TABLE 9 FLOW DATA, ALL MARSHALL SPECIMENS: ANALYSIS OF VARIANCE

Source of Variation	Degrees of Freedom	Sum of Squares	Mean Square	F	Prob. of > F
Gradation (G)	4	221.686	55.421	19.76	0.0001
Aggregate (A)	2	86.565	43.283	15.43	0.0001
Mix Type (M)	1	71.765	71.765	25.59	0.0001
G*A	8	70.329	8.791	3.13	0.0036
G*M	4	33.529	8.382	2.99	0.0229
A*M	2	25.817	12.909	4.60	0.0125
G*A*M	8	15.674	1.959	0.70	0.6920
Error	90	252.430	2.805		
Total	119	777.795			

The level of significance is indicated by the probability of greater F. Probabilities less than 0.05 are generally judged as being indicative of a significant effect.

TABLE 10 FLOW DATA, ALL MARSHALL SPECIMENS: T-TEST GROUPINGS

T Grouping	Mean (.01")	Gradation Variation
A	15.893	COARSE-FINE
B	13.858	JOB MIX FORMULA
B	13.554	FINE
B	13.346	COARSE
C	11.633	FINE-COARSE

Means in the same T Grouping are not significantly different at alpha equal to 0.05.

Thus, similarly to the air void and VMA data, the flow data suggest that gradation variations that parallel the job mix gradation do not significantly affect the mix. The crossover variations that change the shape of the gradation curve do have a significant effect. The flow values of some of the coarse-fine gradations approached and exceeded the maximum value generally considered to be acceptable for heavy traffic conditions.

Resilient Modulus Analyses

Analysis of variance found no significant differences in the resilient modulus values that might be attributed to the gradation variation (Tables 11 and 12). Analysis of all the data indicated significant effects attributable to aggregate type and mix type but no significant effect caused by gradation. Overall, within the range used in this study, gradation variation appeared to have little effect on the resilient modulus of the mix.

TABLE 11 RESILIENT MODULUS DATA, ALL MIXES: ANALYSIS OF VARIANCE

Source of Variation	Degrees of Freedom	Sum of Squares	Mean Square	F	Prob. of > F
Gradation (G)	4	54785	13696	1.43	0.2298
Aggregate (A)	2	521449	260724	27.27	0.0001
Mix Type (M)	1	4443671	4443671	464.71	0.0001
G*A	8	283344	35418	3.70	0.0009
G*M	4	52188	13047	1.36	0.2526
A*M	2	275998	137999	14.43	0.0001
G*A*M	8	266125	33266	3.48	0.0015
Error	90	860602	9562		
Total	119	6758162			

The level of significance is indicated by the probability of greater F. Probabilities less than 0.05 are generally judged as being indicative of a significant effect.

TABLE 12 RESILIENT MODULUS DATA, ALL MIXES: T-TEST GROUPINGS

T Grouping	Mean, ksi	Gradation Variation
A	812	JOB MIX FORMULA
A	809	FINE
A	803	COARSE
A	780	COARSE-FINE
A	755	FINE-COARSE

Means in the same T Grouping are not significantly different at alpha equal to 0.05.

ANALYSES OF 4 × 4 SPECIMEN DATA

Methods of Analysis

The data from the 4 × 4 specimens were analyzed in much the same manner as the data from the Marshall specimen. However, analysis of covariance was used in lieu of analysis of variance for some of the analyses.

Analysis of covariance is quite similar to analysis of variance except that it is used when some of the variables being analyzed are continuous, measured values rather than classifications. Gradation category, aggregate type, and mix type are all classification variables. Data from a given mix fit into specific categories of gradation, mix, and aggregate. Air void content, on the other hand, is a measured value that covers a continuous range.

Because air voids could not be controlled precisely but have a strong impact on strength, the analyses of the 4 × 4 specimen data included examination of the effects of air voids. The analysis of covariance was used, which in effect provides a means to compensate for the influence of differences in air void contents.

The analyses of covariance listings are somewhat different than the analyses of variance listings. The analyses of covariance show both Type I and Type III sums of squares. The Type I sums of squares pertain to the model analysis, and the corresponding F ratios relate to the significance of the mix parameters as they are added sequentially in the analysis. In this respect, they do not necessarily reflect the level of significance for the individual parameters (i.e., gradation, mix type, or aggregate type). The Type III sums of squares and corresponding F ratios provide a measure of the significance of the individual parameters.

Like it is in the analysis of variance, the measure of statistical significance in the analysis of covariance is the *F*-ratio. However, for the individual mix parameters, the *F*-ratio from the Type III sums of squares should be examined.

The analysis of covariance was used primarily with the split tensile strength data. Preliminary analyses of the creep data using analysis of covariance revealed that air void variation did not have a significant effect on the creep stiffnesses. Therefore, analysis of variance was used and is reported for the creep data.

The *t*-test groupings were again used to examine the mean values of the test parameters relative to the various mix gradation categories. In addition, the split tensile strength data were examined with the mean strengths adjusted for the effects of density.

These methods of analysis were used to analyze the 4 × 4 specimen data from each of the mixes individually and to analyze all of the data together. When all of the data were analyzed together, the analysis was performed to identify effects attributable to the type of aggregate (limestone, gravel, and syenite) and the type of mix (surface and binder).

Split Tensile Strength Analyses

Analysis of covariance showed split tensile strength to be affected by gradation variation and air void content (Table 13). Aggregate type and mix type were not found to be significant as individual parameters, but the interaction between them ($A*M$) was found to be significant. An examination of the strength data reveals the reason for this finding. With the limestone and gravel aggregate, the binder mixes had higher strengths than the surface mixes. However, the surface mix was stronger with the syenite aggregate. Also, the syenite aggregate had the highest strength for surface mixes but the lowest for binder mixes.

The *t*-test groupings from all the data show the JMF gradation to have the highest strength (Table 14). The coarse gradation has the lowest strength and is grouped alone, indicating that its strength is significantly lower than any of the other gradation variations. In the individual mix analyses, JMF was found to have the highest strength for four of the six mixes, and coarse was found to be lowest for five of the six. However, because of the very strong influence of air void content on strength, additional analyses were performed to compensate for the influence of differences in air void content.

This testing was done by performing regression analyses on the data for each gradation variation. These analyses produced a series of equations that predict the split tensile strength for any given air void content. The regression equations and the predicted strengths for air void contents of 4 to 7 percent are shown in Table 15. At 6 and 7 percent air voids, the fine gradation is predicted to have the highest strength and the JMF gradation the second highest. The coarse gradation has the lowest predicted strength at each air void content.

TABLE 13 SPLIT TENSILE STRENGTH DATA, ALL MIXES: ANALYSIS OF COVARIANCE

Source of Variation	Degrees of Freedom	Sum of Squares	Mean Square	F	Prob. of > F
Model					
Gradation (G)	4	6781.7	1695.4	15.02	0.0001
Aggregate (A)	2	9084.8	4542.4	40.25	0.0001
Mix Type (M)	1	3809.4	3809.4	33.75	0.0001
G*A	8	1253.1	156.6	1.39	0.2131
G*M	4	591.6	147.9	1.31	0.2725
A*M	2	5632.7	2816.4	24.95	0.0001
G*A*M	8	696.9	87.1	0.77	0.6284
Air Voids	1	19022.5	19022.5	168.55	0.0001
Error	87	9818.7	122.9		
Total	117	56691.5			
TYPE III SUM OF SQUARES					
Gradation (G)	4	9864.2	2466.0	21.85	0.0001
Aggregate (A)	2	25.5	12.7	0.11	0.8935
Mix Type (M)	1	25.7	25.7	0.23	0.6347
G*A	8	371.1	46.4	0.41	0.9115
G*M	4	1064.5	266.1	2.36	0.0597
A*M	2	3800.2	1900.1	16.84	0.0001
G*A*M	8	703.4	87.9	0.78	0.6222
Air Voids	1	19022.5	19022.5	168.55	0.0001

The level of significance is indicated by the probability of greater F. The Type III sum of squares is indicative of individual effects. Probabilities less than 0.05 are generally judged as being indicative of a significant effect.

TABLE 14 SPLIT TENSILE STRENGTH DATA, ALL MIXES: T-TEST GROUPINGS

T Grouping	Mean (psi)	Gradation Variation
A	144.1	JOB MIX FORMULA
A & B	139.0	COARSE-FINE
B & C	134.8	FINE
C	129.5	FINE-COARSE
D	122.0	COARSE

Means in the same T Grouping are not significantly different at alpha equal to 0.05.

TABLE 15 SPLIT TENSILE STRENGTHS ADJUSTED FOR AIR VOID CONTENT

Gradation Variation	Mix Air Void Content 4%	5%	6%	7%
	Predicted Split Tensile Strength, psi			
JMF	181	164	148	132
FINE	172	161	150	139
FINE-COARSE	171	158	144	130
COARSE-FINE	167	154	140	126
COARSE	142	133	124	114

Prediction Equation: $ST = a + b*AV$

where ST = predicted strength
a & b = regression constants that have the following values

	a	b
JMF	245.8	-16.30
FINE	215.5	-10.92
FINE-COARSE	226.0	-13.65
COARSE-FINE	222.7	-13.81
COARSE	180.1	- 9.41

(R^2 = .74, Std. Error of Est. = 11.7)

There is some question about the legitimacy of the air void adjustment. If the air void differences were caused by the gradation variations, the adjustments should not have been made. However, because of manner in which these specimens were made (static compaction to a controlled volume), they were all expected to have the same air void content. Consequently, the air void differences can only be attributed to laboratory procedures, so the adjustments are considered appropriate. In retrospect, a better approach might have been to prepare the specimens using a fixed compactive effort. Any air void variation could have been attributed to gradation variation, and no adjustment for air voids would have been needed.

Creep Data Analyses

Preliminary analyses of the creep data examined the effect of air voids. These analyses showed that air void content variation was not a significant factor relative to creep stiffness. As an example, the analysis of covariance for the 60-min creep stiffness for all the data had a probability of greater F of 0.1474 (Table 16). Similar results were obtained for each of

TABLE 16 ANALYSIS OF COVARIANCE OF 60-MIN CREEP DATA

Source of Variation	Degrees of Freedom	Sum of Squares	Mean Square	F	Prob. of > F
Model					
Gradation (G)	4	2933400	733350	2.84	0.0421
Aggregate (A)	2	24890594	12445297	48.21	0.0001
Mix Type (M)	1	372740	372740	1.44	0.2392
G*A	8	3493348	436668	1.69	0.1430
G*M	4	287244	71811	0.28	0.8897
A*M	2	800213	400107	1.55	0.2293
G*A*M	8	6545629	818204	3.17	0.0105
Air Voids	1	572154	572154	2.22	0.1474
Error	29	7486454	258154		
Total	59	47381776			
TYPE III SUM OF SQUARES					
Gradation (G)	4	3026974	756744	2.93	0.0376
Aggregate (A)	2	2947324	1473662	5.71	0.0081
Mix Type (M)	1	139284	139284	0.54	0.4685
G*A	8	4065483	508185	1.97	0.0871
G*M	4	566694	141673	0.55	0.7013
A*M	2	538552	269276	1.04	0.3652
G*A*M	8	7063870	882984	3.42	0.0069
Air Voids	1	572154	572154	2.22	0.1474

The level of significance is indicated by the probability of greater F. The Type III sum of squares is indicative of individual effects. Probabilities less than 0.05 are generally judged as being indicative of a significant effect.

the other time intervals and in the analyses of the data from the individual mixes.

Subsequent analyses tested variance and examined the influence of gradation variation, aggregate type, and mix type. Tables 17 and 18 show the analyses for the 60-min creep stiffness. The analysis of variance shows that gradation variation and aggregate type had a significant effect on creep stiffness but that mix type was not significant. Analyses of the creep stiffnesses at the other time intervals were similar except gradation was not significant at the 5-sec interval and mix type was significant at 2 min, 30 sec, and 5 sec.

For each time interval, the *t*-test groupings for all the data show that the JMF had the highest creep stiffness and the coarse-fine and fine-coarse gradations had the lowest creep stiffness. Fine and coarse had about the same stiffness and alternated with one another for second and third highest. Thus, similarly to the results from the Marshall specimens, the crossover gradation variations were found to have greater impact on the properties of the mix than do gradation variations that result simply in a finer or coarser mix.

However, the differences between creep stiffnesses for the various gradations are not great and the relative rankings are not consistent when the data from the individual mixes are examined. At the 60-min, 30-sec, and 5-sec intervals, four gradations were placed in a single group, indicating no significant difference. When the individual mixes were examined, JMF is found to have the highest creep stiffness in only two cases; coarse-fine is lowest or second lowest in four cases; and fine-coarse is lowest or second lowest in only three cases.

Comments on Air Voids

Although this study was not intended to study the effect of air voids, the inability to control the air voids in the 4 × 4 specimens and the impact of air voids on the test results warrant comment. The 4 × 4 specimens were molded in a manner intended to produce uniform specimens of controlled (5 percent) air void content. Examination of the creep data showed that the control of air voids was not successful. After the creep testing, the 4 × 4 specimens were sawed in half and used for the split tensile testing. The split tensile data showed that the specimens were also not uniform. In all cases, the top half of the specimen had lower air voids than did the bottom half. The top half also always had the higher split tensile strength.

Regression analysis of all the split tensile strength data showed that, in general, a 1 percent decrease in air voids results in a 12.7 psi increase in split tensile strength. For the individual gradation variations (Table 15), this effect ranged from 9.4 psi/percent for the coarse gradations to 16.3 psi/percent for the JMF gradations. This suggests that, within the typical range of variation encountered on asphalt construction projects, split tensile strength is more sensitive to the density achieved than it is to gradation variation.

TABLE 17 60-MIN CREEP DATA, ALL MIXES: ANALYSIS OF VARIANCE

Source of Variation	Degrees of Freedom	Sum of Squares	Mean Square	F	Prob. of > F
Gradation (G)	4	2933400	733350	2.73	0.0475
Aggregate (A)	2	24890594	12445297	46.33	0.0001
Mix Type (M)	1	372740	372740	1.69	0.2481
G*A	8	3493348	436668	1.63	0.1592
G*M	4	287244	71811	0.27	0.8966
A*M	2	800213	400107	1.49	0.2417
G*A*M	8	6545629	818204	3.05	0.0125
Error	30	8058608	268620		
Total	59	47381776			

The level of significance is indicated by the probability of greater F. Probabilities less than 0.05 are generally judged as being indicative of a significant effect.

TABLE 18 60-MIN CREEP DATA, ALL MIXES: T-TEST GROUPINGS

T Grouping	Mean, psi	Gradation Variation
A	5994	JOB MIX FORMULA
A & B	5702	FINE
A & B	5680	COARSE
B	5442	COARSE-FINE
B	5367	FINE-COARSE

Means in the same T Grouping are not significantly different at alpha equal to 0.05.

RELATIVE LIFE EFFECTS

The split tensile strength and creep tests were performed to provide data that could be used to examine the relative effects of gradation variation on the life of an asphalt pavement. The relative life analyses were to follow procedures established by Elliott and Herrin (*2*). Because the various gradations were examined relative to the job mix formula, the JMF gradation was assigned a relative life of 100 percent.

Fatigue Life Analyses

The split tensile strength data were to be used to estimate the effect of gradation variation on the fatigue life of an asphalt pavement. The fatigue procedure is based on work by Maupin and Freeman (*3*), who showed that the split tensile strength can provide a reasonable estimate of the fatigue properties of a mix. Using Maupin's relationships, Elliott and Herrin developed the following relative life equation:

$$\log (Na/Nb) = SF * (ST_a - ST_b)$$

where

Na/Nb = relative life ratio for two mix variations (a and b);
ST_a and ST_b = split tensile strengths of the two mix variations; and
SF = strain factor, which Elliott and Herrin found to be 0.0163 for typical asphalt pavements.

The relative life equation was applied to the mean strength data and to the split tensile strengths adjusted for air void content. Table 19 shows the relative life predictions based on the mean strength data and on the strengths predicted for 5 percent air voids, which was the target air void content for the study. The relative life predictions for air void contents of 4 to 7 percent are shown in Figure 2.

These results indicate that the relative life prediction is quite sensitive to variations in split tensile strength. They show that the coarse gradation variation can be expected to have a significantly greater detrimental impact on fatigue life than do the other variations. The results also suggest that, within the

TABLE 19 RELATIVE FATIGUE LIFE ANALYSES USING MEAN STRENGTH DATA AND PREDICTED STRENGTH AT 5 PERCENT AIR VOIDS

Gradation Variation	Mean Strength	Relative Life	Predicted Strength, 5% AV	Relative Life
JMF	144 psi	100%	164 psi	100%
FINE	139 psi	83%	161 psi	88%
FINE-COARSE	135 psi	71%	158 psi	78%
COARSE-FINE	130 psi	58%	154 psi	67%
COARSE	122 psi	44%	133 psi	31%

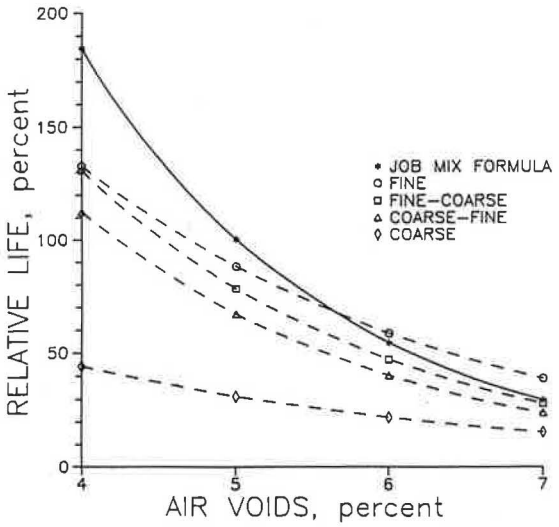

FIGURE 2 Effects of gradation and air void variations on relative fatigue life.

normal range of air void and gradation variation, fatigue life is generally more sensitive to air void content (i.e., compaction) than it is to gradation.

Rut Depth Analyses

The creep data were to be used to examine relative life effects in terms of rut development. The simple creep data are used in the Shell method (*4*) of asphalt pavement design to predict rutting in asphalt layers. In its simplest form, the Shell rut prediction equation is

$$RD = h * s/S_{mix}$$

where

RD = predicted depth of rutting,
h = thickness of asphalt layer,
s = average load-induced stress in the layer, and
S_{mix} = stiffness of mix at total (accumulated) time of all axle loadings applied.

The stiffness of the mix used in the prediction is for the mix at a temperature representative of local climatic conditions and at the accumulated total time of heavy vehicle applications. The stiffness is selected based on a relationship developed from the simple creep test between the stiffness of the mix and the stiffness of the asphalt cement.

Shell has shown that a linear logarithmic relationship exists between mix stiffness and asphalt stiffness. The specific relationship for a given mix is developed by (a) measuring the mix stiffness at various time intervals using the simple creep test, (b) determining the asphalt stiffness at those time intervals and the creep test temperature using Van der Poel's nomograph (*4*), and (c) performing a best fit linear logarithmic regression analysis on the stiffness values.

In the rut depth prediction for a given mix, the total time of axle loading and the representative mix temperature are determined. These are used with Van der Poel's nomograph to determine the asphalt cement stiffness. This asphalt mix stiffness is then used with the linear logarithmic relationship to determine the mix stiffness that goes into the rut depth prediction equation.

The data from this study were analyzed to develop the "typical" linear logarithmic relationships for each gradation variation. The resulting relationships were subsequently used with the Shell method of rut prediction to examine the effect of the gradation variations on rut development in a 6-in. asphalt layer.

The results of the rut depth analyses are shown in Table 20. The table shows the relative depth of rutting for the two traffic levels (1 million and 50 million axle applications). These analyses indicate that, in comparison with the JMF gradation, the fine and coarse gradation variations would experience 7 to 10 percent greater depth of rutting, and the coarse-fine and fine-coarse gradation variations would experience 13 to 19 percent greater depth of rutting.

SUMMARY, CONCLUSIONS, AND RECOMMENDATIONS

This study investigated the effect of aggregate gradation variation on the behavior of asphalt concrete hot mixes. The study was specifically aimed at the effects of typical construction variability. As a result, the gradation variations tested were selected to represent the extremes typically encountered on actual construction projects. If the study had been directed toward a more general determination of gradation effects, a

TABLE 20 RELATIVE RUT DEPTH PREDICTION ANALYSES

	DEPTH OF RUTTING TO FIXED NUMBER OF AXLE LOADS			
	One Million Axle Loads		Fifty Million Axle Loads	
Gradation Variation	Rut Depth	% of JMF	Rut Depth	% of JMF
JOB MIX FORMULA	.160"	100	.210"	100
FINE	.172"	107	.230"	109
COARSE	.172"	107	.232"	110
COARSE-FINE	.180"	113	.246"	117
FINE-COARSE	.186"	116	.249"	119

	PREDICTED APPLICATIONS TO FIXED DEPTH OF RUTTING			
	Rut Depth = .160"		Rut Depth = .210"	
Gradation Variation	Applications	% of JMF	Applications	% of JMF
JOB MIX FORMULA	1,000,000	100	50,000,000	100
FINE	401,000	40	14,960,000	30
COARSE	389,000	39	13,540,000	27
COARSE-FINE	226,000	23	6,810,000	14
FINE-COARSE	165,500	17	5,360,000	11

wider range of gradation would have been tested. In particular, wider ranges of the fine aggregate fractions would have been used because these fractions generally control the mix behavior.

Six mixes were tested: three surfaces and three binders. Each mix was tested at five different aggregate gradations (Figure 1): (a) the job mix formula (JMF); (b) a coarse gradation (coarse); (c) a fine gradation (fine); (d) a gradation that crossed from coarse on the large size fractions to fine on the small size fractions (coarse-fine); and (e) a gradation that crossed from fine on the large size fractions to coarse on the small size fractions (fine-coarse). The job mix formula asphalt content was used with all gradation variations.

The measures of effect were the Marshall mix design parameters (i.e., stability, flow, air voids, and VMA), resilient modulus, tensile strength, and creep stiffness. The tensile strength data and creep stiffness data were used to estimate the relative pavement life effects of the variations.

Based on analysis of the data from this study, the following conclusions are in order:

1. Gradation variations within the magnitude tested have the greatest effect when they result in a change in the general shape of the gradation curve (the fine-coarse and coarse-fine gradations).
2. Fine-coarse gradation variations cause the highest Marshall air voids and VMA. Coarse-fine gradation variations cause the lowest Marshall air voids and VMA.
3. Coarse-fine gradation variations produce the highest Marshall flow and fine-coarse gradation variations produce the lowest.
4. Creep stiffness is lowest for coarse-fine and fine-coarse gradation variations.
5. Relative to air voids, VMA, and flow, the coarse-fine gradation produced the most detrimental effect on the mixes tested. Some of the air void and VMA values were less than those normally considered to be acceptable, and some of the flow values were greater than those normally acceptable.
6. Marshall stability is affected by gradation variations with the fine gradations producing the highest stability and the fine-coarse gradations producing the lowest. However, for the mixes tested, all of the gradations were found to have stabilities that are considered to be more than adequate.
7. Coarse gradation variations produce the lowest tensile strengths. The JMF gradation generally produced the highest strength, but when adjusted for differences in air voids, all gradations except coarse had about the same strength.
8. Within the range of variations normally encountered, tensile strength is more sensitive to air void content (i.e., compaction) than it is to gradation variation.

ACKNOWLEDGMENT

This paper is based on the findings of the Asphalt Gradation Variation Project, which was sponsored by the Arkansas State Highway and Transportation Department and FHWA.

REFERENCES

1. R. J. Schmidt. A Practical Method for Measuring the Resilient Modulus of Asphalt-Treated Mixes. In *Highway Research Record 404*, HRB, National Research Council, Washington, D.C., 1972, pp. 22–32.
2. R. P. Elliott and M. Herrin. Relative Life Effects of Mix Composition and Density Variation. *Proc., Association of Asphalt Paving Technologists*, Vol. 54, 1985, pp. 209–233.
3. G. W. Maupin, Jr., and J. R. Freeman, Jr. *Simple Procedure for Fatigue Characterization of Bituminous Concrete*. Report FHWA-RD-76-102. FHWA, U.S. Department of Transportation, 1976.
4. *Shell Pavement Design Manual*. Shell International Petroleum Company, London, England, 1978.

Effects of Sample Preparation and Air-Void Measurement on Asphalt Concrete Properties

JOHN HARVEY, JORGE B. SOUSA, JOHN A. DEACON, AND CARL L. MONISMITH

A compaction study focusing on the extent to which laboratory compaction methods (gyratory, kneading, and rolling-wheel) affect fundamental mixture properties important to pavement performance has been carried out as part of a project by the Strategic Highway Research Program. The work has shown that besides compaction method, other aspects of specimen preparation significantly affect test results and their interpretation. Of particular importance were the method to measure air void content and the effect of surface condition (cut or as-molded) on both air void measurements and mechanical behavior. Air void content was significantly underestimated by standard procedures that leave the outer surface of the specimen unsealed during submersion. However, difficulties with the standard paraffin wax procedure, coupled with the need to compare dry specimens with partially saturated ones, led to the adoption of a new procedure. By using a surface-dry specimen (wetted and then surface dried) encased in parafilm (a stretchable, waterproof membrane), a consistent measurement of air void content was obtained. Further, it is evident that the surface of the specimen, cut or uncut, influences the measured air voids. Thus, air voids are not uniformly distributed within specimens, a factor that can significantly bias test results. The fact that surface type was found to influence the mechanics of mixture behavior under direct shear loading casts doubt on the accuracy of comparing tests results from field cores and laboratory-compacted specimens when the latter are tested in the as-molded or uncut condition. To obtain reliable and consistent results, it is recommended that laboratory testing be limited to specimens with cut surfaces and that air void measurements use the wet-with-parafilm technique.

The results of a compaction study carried out by the University of California at Berkeley as part of the Strategic Highway Research Program (SHRP) Project A-003A, Performance Related Testing and Measuring of Asphalt-Aggregate Interactions and Mixtures, demonstrate that asphalt-concrete performance in all types of laboratory testing is highly dependent on the air void content of the specimens (*1*,*2*). The direct effect of air voids on mixture performance is clearly shown by the shear creep response of kneading (Figure 1) and gyratory (Figure 2) specimens.

The laboratory work for this study revealed that standard methods of air void measurement present significant problems in comparison of specimens compacted by the various methods included in the study. Significant differences in measured air void contents and in mechanical behavior were observed between uncut specimens (tested as compacted in the mold) and cut specimens (sawed or cored from a larger compacted mass).

Data presented here provide insight into these problems, and recommendations are made for resolving them. Although not included as part of the original study plan for the project, data were collected to examine the issues of air void measurement (Table 1) and effects of cut surfaces. Useful evidence was collected about relationships between measured air voids and specimen preparation method and about the effects of cut surfaces on measured air voids. Shear creep tests were also performed to examine the effects of cut surfaces on specimen performance under loading.

SPECIMEN PREPARATION

Two aggregates with different characteristics were used in the study: Watsonville granite, a completely crushed, nonstripping aggregate with rough surface texture; and Texas Gulf Coast chert, an incompletely crushed, stripping aggregate with a smoother surface texture. The Watsonville granite is softer than the Texas chert and much easier to cut with a masonry saw. The chert is prone to chipping during cutting and coring. Two asphalts were used: Boscan AC-30 and California Valley AR4000.

Two levels of asphalt content were investigated. For each asphalt-aggregate mixture, the lower asphalt content was determined using a modification of standard Hveem procedures (ASTM D1560). The higher asphalt content was set at 0.6 or 0.7 percent more (by weight of aggregate) than was found using the Hveem procedures, which corresponds to approximately the optimum asphalt content found by the U.S. Army Corps of Engineers (Marshall) 75-blow procedure (ASTM D1559).

Three compaction methods were used in the study: Texas gyratory compaction (adapted from Texas Method Tex-206-F and ASTM D4013), kneading compaction (ASTM D1561), and rolling-wheel compaction (procedure not yet standardized). Specimen preparation details are included in a report by Sousa et al. (*1*).

Briquets (4 × 2.5 in.) prepared by gyratory or kneading compaction had compacted or as-molded surfaces that were not cut by coring or sawing. Cylinders (4 × 8 in.) prepared

J. Harvey, J. B. Sousa, and C. L. Monismith, Institute of Transportation Studies, University of California, Berkeley, Calif. 94720. J. A. Deacon, Kentucky Transportation Center, University of Kentucky, Lexington, Ky. 40506-0043.

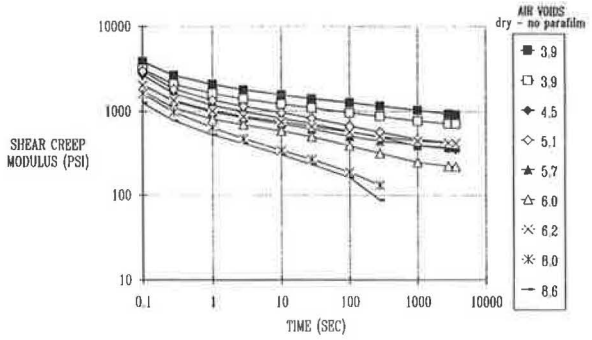

FIGURE 1 Effect of air-void content on shear creep modulus (kneading compaction).

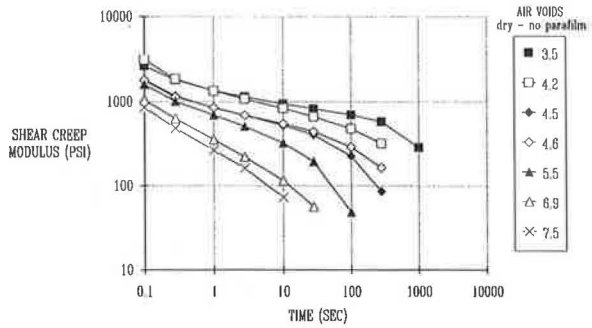

FIGURE 2 Effect of air-void content on shear creep modulus (gyratory compaction).

by kneading compaction had uncut surfaces at the sides and cut surfaces at the ends. Fatigue beams (3 × 3 × 15 in.) prepared by kneading compaction, cylinders prepared by gyratory compaction, and all specimens prepared by rolling-wheel compaction were cut or cored from larger compacted masses and had cut surfaces, that is, surfaces that resulted from removal of all material that touched the compaction mold.

AIR VOID MEASUREMENT

Objectives

The objectives of air void measurement procedures are summarized as follows:

1. To measure the degree of mixture compaction resulting from the application of mechanical energy to the mixture in order to expel air or reorient the aggregate into a denser arrangement;
2. To measure the voids in the aggregate matrix not filled with asphalt;
3. To be fast, simple, and repeatable, and to maintain the original specimen shape so that it can be used for testing; and
4. To allow meaningful comparisons among a variety of specimens with different degrees of compaction, asphalt contents, or fabrication techniques, including field coring.

TABLE 1 SAMPLE SIZE FOR STUDY OF AIR VOID MEASUREMENT

Compaction	Specimen Size (Inches) and Shape	Texas Chert (RL)		Watsonville Granite (RB)		Other
		Valley (AAG-1)	Boscan (AAK-1)	Valley (AAG-1)	Boscan (AAK-1)	
Gyratory	4 × 2.5 (Briquet)			29		
	4 × 8 (Cylinder)			12		
Kneading	4 × 2.5 (Briquet)	12	6	38	15	8
	4 × 8 (Cylinder)	2	9	15	5	
	3 × 3 × 15 (Uncut Beam)	27	7	20	17	
	3 × 3 × 15 (Cut Beam)	12	1	30	71	
	1.5 × 1.5 × 15 (Beam)	105	34	165	143	
Rolling Wheel	4 × 2.5 (Briquet)			11		
	4 × 8 (Cylinder)			18		
Total Number of Specimens 805						

Methods

Bulk specific gravities for air void measurement of specimens prepared early in the compaction study (4- × 2.5-in. briquets using kneading and gyratory compaction) were calculated by weighing the specimens in air and in water, without the use of paraffin wax or other surface coating. The air void content was calculated using the following equation:

$$AV = \left(1 - \frac{G_b}{G_{mm}}\right) \times 100 \quad (1)$$

where

AV = air void content in percent,
G_b = bulk specific gravity, and
G_{mm} = maximum specific gravity determined by the Rice method (ASTM D2041).

The standard method for sealing specimens using paraffin wax (ASTM D1188) was not used because testing after air void measurement requires complete removal of the paraffin wax, a difficult and time-consuming process. These specimens were neither cut nor cored and therefore contained no trapped water. This procedure was later referred to as dry-no-parafilm (dnp) (*1*).

Rolling-wheel specimens and 4- × 8-in. gyratory cylindrical specimens were cored or cut from larger compacted masses, using water cooling to prevent aging of the asphalt and damage to the specimens caused by frictional heat. This process leaves water in the specimen—in varying amounts depending in part on the internal air voids—which may require many

days to remove by drainage and evaporation. Because trapped water is included in the weight-in-air measurement used to calculate G_b in Equation 1, comparison of air void contents for these cut or cored specimens with those measured using the dry-no-parafilm method was questioned. The standard procedure for removal of water (ASTM D2726) requires heating at 110°C (230°F), a potentially destructive process rendering specimens unsuitable for use. This difficulty was surmounted by developing a method to rapidly determine air voids with prewetted specimens in a surface-dry condition. This procedure, referred to as wet-no-parafilm (wnp), uses a compressed air nozzle to remove water from the specimen surface until no moisture can be seen (*1*).

At the same time, it was found that permitting water to enter the specimen during submersed weighing resulted in underestimation of air voids, particularly for specimens with higher air void contents. At high air void contents—above approximately 8.5 percent by the dry-no-parafilm method—it was found that air void content as measured by the dry-no-parafilm or wet-no-parafilm methods was extremely insensitive to compactive effort, and visually obvious differences in void content were undetected by the air void measurements. Experimentation was then carried out with an elastic wax paper, parafilm, as a substitute for paraffin wax (*3*). Measurements of air voids, using the surface-dry condition and parafilm, were found to be sensitive to air void content, applicable to all types of compaction and specimen preparation methods, and convenient for later testing of the specimen. This procedure was referred to as wet-with-parafilm (wwp) (*1*). The equation used to calculate bulk specific gravity using this method is the same as in the standard paraffin wax procedure (ASTM D1188).

Quantitative Differences Between Methods

Wet-with-parafilm measurements are compared to wet-no-parafilm measurements in Figure 3 and to dry-no-parafilm measurements in Figure 4. These results show a significant difference caused by the use of parafilm. As shown in Figure 5, dry measurements (dnp) are not significantly different from the surface-dry measurements (wnp). This indicates that the surface-dry condition results in little water remaining within the specimen. These results are summarized in Figure 6, which shows least square regression lines for each relation.

The effect of parafilm on cut and uncut specimens is similar but not identical, as demonstrated by regression lines for the wet-with-parafilm and wet-no-parafilm methods (both methods used on specimens in both the cut and uncut condition) shown in Figure 7. At higher air void contents, the effect of using parafilm is greater for uncut specimens than for cut specimens. This is because of the generally smoother exteriors of the cut specimens (due to cut aggregate surfaces). At lower air void contents, the effect of using parafilm is greater for cut specimens than for uncut specimens, probably due to smearing of asphalt at the interface between the mold and the specimen surface under heavy compaction.

Specimens prepared using Watsonville granite and Texas chert show no difference between the dry (dnp) and wet (wnp) conditions, as shown in Figure 8. However, the Texas chert specimens with higher air void contents are more sensitive to the use of parafilm than are the Watsonville granite specimens, as shown in Figure 9. This finding is probably the result

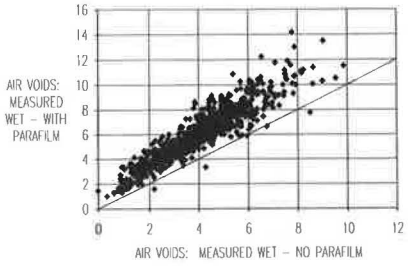

FIGURE 3 Effect of parafilm on surface-dry measurements of air voids (all specimens).

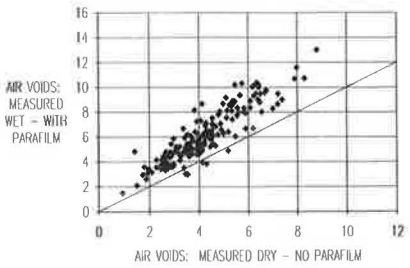

FIGURE 4 Combined effect of parafilm and wetting on air void measurements.

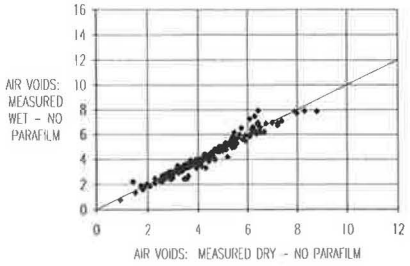

FIGURE 5 Effect of wetting on no-parafilm measurements of air voids.

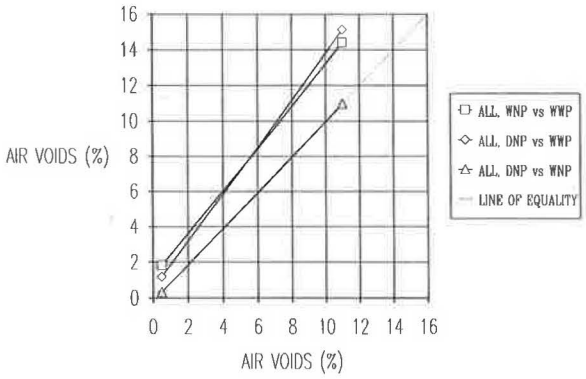

FIGURE 6 Comparison of dry-no-parafilm, wet-no-parafilm, and wet-with-parafilm measurements of air voids (regression lines).

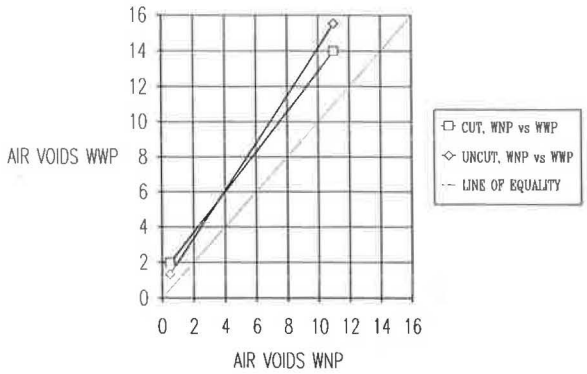

FIGURE 7 Combined effect of cut surfaces and parafilm on air void measurements (regression lines).

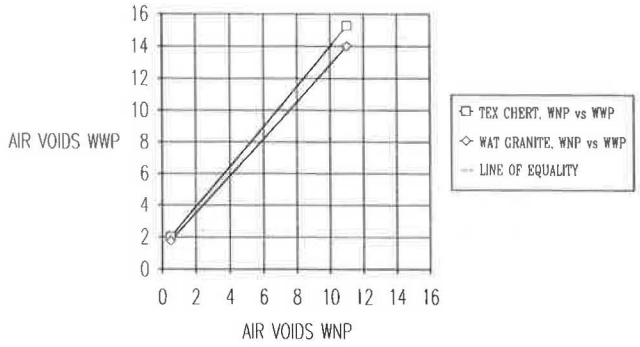

FIGURE 8 Combined effect of wetting and aggregate type on air void measurements (regression lines).

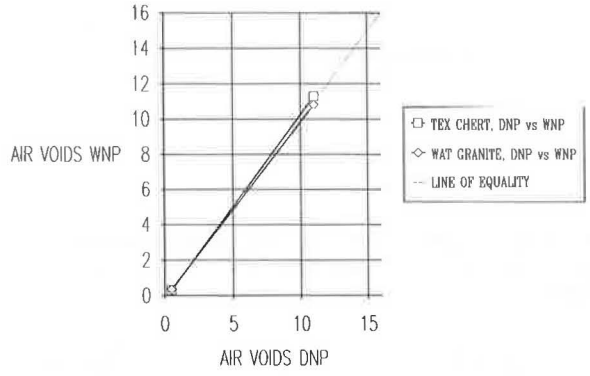

FIGURE 9 Combined effect of parafilm and aggregate type on air void measurements (regression lines).

of the parafilms trapping air in the more irregular, chipped surfaces of the Texas chert specimens.

Critique of Wet-With-Parafilm Procedure

Although the wet-with-parafilm procedure is better than alternatives, it has some problems. The primary problem is arching of the parafilm over surface irregularities caused by chipping of the aggregates during cutting and coring; the result is that air trapped under the parafilm is improperly considered as air voids. This problem occurs most frequently with specimens having thin cross sections or many sharp edges, such as 1.5- × 1.5- × 15-in. fatigue beams, and with specimens made with very hard aggregates or low asphalt contents. The same problem occurs with specimens without surface irregularity if careful attention is not given to the removal of air trapped beneath the parafilm.

The other potential problem with wet-with-parafilm technique is the repeatability with which the surface-dry condition is reached, although a limited comparison with tests from another laboratory showed little problem. Although the general technique used in this study has proven to be suitable, more attention must be given to standardization of the drying equipment and procedure.

EFFECT OF CUT SURFACES

Objectives of Laboratory Specimen Compaction

The objectives of laboratory specimen fabrication are summarized as follows:

1. To fabricate specimens that as closely as possible resemble in-service mixtures, that is, those produced by mixing, placement, and compaction in the field;
2. To fabricate specimens that, under laboratory testing, exhibit the same behavior as in situ mixtures under similar states of stress; and
3. To be as efficient as possible in the use of labor, time, equipment, and material.

Effects of Compaction Method

Slight visual differences were observed between the top and bottom surfaces of all laboratory-prepared specimens. The lower surface was usually rougher, that is, both the aggregate particles and the surface voids were larger. The top of the specimen, which had been in contact with the compacting surface, usually had a smoother surface composed of finer particles. The lateral surfaces of most molded specimens were a smooth matrix of asphalt and the finer fractions of aggregate; there was little honeycombing, and larger particles had migrated inward. Lateral surfaces of specimens with high asphalt contents often contained excess asphalt, especially when compacted to low air void contents.

During compaction, the mold walls constrain the reorientation of surface particles. However, in the interior, the shearing action of the compactor reorients the larger particles, producing a structure that significantly affects engineering properties of the compacted mixture. If the quantities of asphalt and fine particles are limited or the compaction effort is modest, gaps between the larger particles at the surface remain unfilled. The net result is that the aggregate structure at the surface is different from that in the interior.

Some segregation of larger from finer particles often occurs during placement of the hot mixture in the mold. Segregation becomes more pronounced as the size of the compacted specimen or the compactive effort decreases, because the size of the larger aggregates in comparison with the mold dimensions,

or the lack of shearing energy, does not permit the movement of fines to the interstices between the larger aggregates.

Gyratory specimens are subjected to a torsional shear force on their lateral surfaces caused by rotation of the compaction apparatus base plate, while the compaction ram resists rotation at the top surface. This produces surface forces on the specimen, which often results in large aggregates' separating themselves from the surface when the specimen is extruded from the compaction mold. When the large particles are rounded, thin layers of finer material between the large particles and the specimen surface also frequently separate from the specimen after extrusion. The effects of the torsional surface forces in gyratory compaction are recognized in the procedure for the Texas gyratory compactor (Texas Method Tex-206-F and ASTM D4013), which stipulates that large aggregate particles should be pulled away from the mold wall with a large bent spoon before compaction. The mold will rotate if the torsional shear force exceeds the friction between the mixture and the mold wall, smearing excess asphalt and fine material across the lateral surface of the specimen.

Cutting or coring the specimen from a larger compacted mass removes portions of the specimen that have been subjected to these forces and effects. The specimen with cut surfaces has a more homogeneous aggregate and air void structure and does not have a smeared asphalt coating that may otherwise be present at the compacted surface.

The major drawbacks of cut specimens include (a) the need for care during sawing and coring to obtain the required geometric shapes that are free of ripples or other surface imperfections, and (b) possible problems with the exposure of mixtures to water during the sawing and coring process. However, problems with water-sensitive mixtures are encountered with all air void measurements that involve wetting the specimen, and they can usually be solved by timely testing.

Effects on Air Void Determination

The effects of surface condition (cut or uncut) on air void measurements depend on the properties of the mixture (including, for example, asphalt content and aggregate angularity) and the compaction method (gyratory, kneading, or rolling-wheel).

1. The difference between air voids measured with cut surfaces and those measured with uncut surfaces depends on the degree of nonuniformity in the air voids and aggregate structure between the surface and the interior of the specimen: this is a function of the compaction method, the compaction effort, and the aggregate angularity and the asphalt content of the mixture.
2. If the specimen has a large surface area in relation to its volume, the difference between the measured air voids is greater with cut versus uncut surfaces. Thus large specimens, such as 3- × 3- × 15-in. beams and 4- × 8-in. cylinders, will have less difference in the measured air voids than 2.5- × 4-in. briquets compacted using the same method.
3. If the asphalt content or the compaction effort is high, asphalt at the surface of the specimen may form a coating, which prohibits the entry of water into the specimen and affects air void measurements.
4. For high asphalt contents or high compaction efforts, the sealing action at the surface of the specimen is greater for gyratory specimens because of smearing caused by the torsional shear forces on the lateral surfaces.

An example of the difference between the measured air voids for specimens as compacted and after cutting is shown in Figure 10. In this case 3- × 3- × 15-in. beams of all mixture types, prepared by kneading compaction, were tested using the wet-with-parafilm procedure both after compaction and after trimming of the outer 3/16 in. of the surface. The data indicate that the as-compacted specimen has approximately 1 to 2 percent higher air voids than the same specimen after cutting. This conclusion is confirmed by testing the same specimens using the wet-no-parafilm method as shown in Figure 11.

Further evidence of differences between interior and exterior air void contents is shown in Figure 12 for 4- × 8-in. gyratory specimens of identical composition. In this case, specimens were compacted as 6- × 9.5-in. cylinders, then cored and cut to their final dimensions. Comparison of air void measurements using the dry-no-parafilm method for the uncut specimens and the wet-no-parafilm method for the cut specimens—the two methods have previously been shown to produce similar results—indicates that at lower compaction efforts (higher air void contents) the outer portion of the specimen is more densely compacted than the inner portion; at higher compactive efforts (lower air void contents) the reverse is true. At high compactive efforts (low air voids), differences in air voids of up to 3 percent (wwp) have been found between the center third (higher air voids) and top and

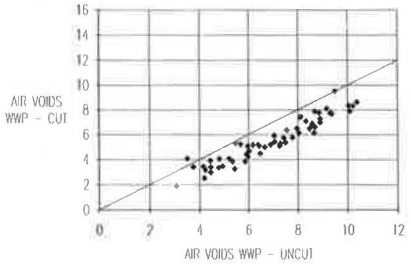

FIGURE 10 Effect of cut surfaces on wet-with-parafilm measurements of air voids in large beams (kneading compaction).

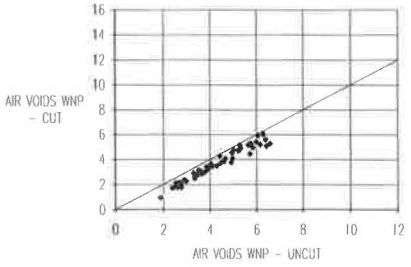

FIGURE 11 Effect of cut surfaces on wet-no-parafilm measurements of air voids in large beams (kneading compaction).

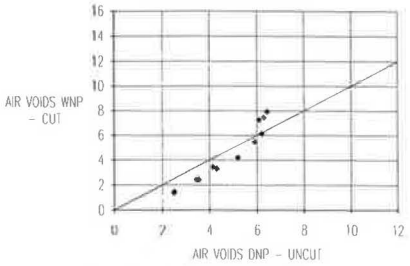

FIGURE 12 Effect of cut surfaces on no-parafilm measurements of air voids in large cylinders (gyratory compaction).

bottom thirds (lower air voids) of 4- × 8-in. gyratory specimens. This finding also indicates specimen nonuniformity along the vertical axis, despite the fact that the specimens have been compacted in one lift.

Effects on Engineering Properties

In some types of tests, cut surfaces may significantly affect the measured response of the mixture. In tests with large shear stress components, the measured values of the strength tend to be larger for specimens with cut surfaces. The cut surfaces of the aggregates rest against the end plates, effectively resisting rotation of the large aggregate particles. Figure 13 shows two examples where this mechanism will produce an effective increase of stiffness modulus, resistance to permanent deformation, and fatigue life. This hypothesis is corroborated by the results of the project compaction study, which show greater modulus, resistance to plastic deformation, and fatigue life for rolling-wheel specimens with cut surfaces, than for kneading specimens with uncut surfaces (*1*,*2*).

Further evidence is provided by comparing simple shear test results for uncut 4- × 2.5-in. gyratory specimens with those for similar specimens cored and cut from 6- × 9.5-in. gyratory cylinders. Figure 14 shows the difference between

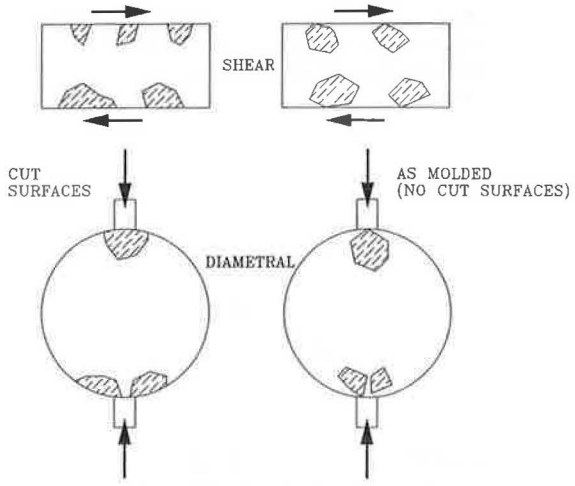

FIGURE 13 Boundary effects of cut specimen surfaces in shear and diametral testing.

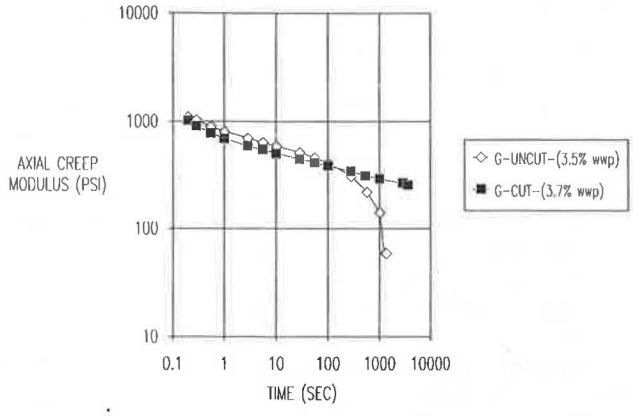

FIGURE 14 Effect of cut surfaces on shear creep modulus (gyratory specimens).

the performance of the two types of specimens. The uncut specimens have a larger proportion of aggregates able to move under stress, leading to rapid failure once aggregate interlock has been overcome by the shearing force.

CONCLUSIONS

Based on the stated objectives of specimens preparation and air void measurement and on the data and observations presented, the following conclusions can be drawn:

1. The surface of a specimen, whether uncut (as-molded) or cut (sawed or cored from a larger compacted mass), significantly affects its mechanical behavior and its measured air void content.
2. In comparison with cut specimens, specimens with uncut surfaces are less homogeneous in their distribution of air voids; during compaction, they experience greater segregation of aggregate and greater migration of fines and asphalt to their surfaces.
3. Cutting the surfaces of laboratory specimens allows more accurate comparison of their properties with those of field cores.
4. Measurement of air void content is critical to understanding specimen performance in testing. The wet-with-parafilm procedure is consistently sensitive and reproducible and easily allows further testing of the specimen after air void determination.

On the basis of these conclusions, it is recommended that laboratory specimens be prepared by coring or cutting from a larger compacted mass and that further study be given to the wet-with-parafilm air void measurement procedure, leading toward standardization.

ACKNOWLEDGMENTS

The work reported herein was conducted as a part of a project of the Strategic Highway Research Program. This project, "Performance Related Testing and Measuring of Asphalt-

Aggregate Interactions and Mixtures," is being conducted by the Institute of Transportation Studies of the University of California, Berkeley. The authors express their appreciation to Akhtar Tayebali, who first identified the limitations of conventional techniques for air void measurement.

REFERENCES

1. J. B. Sousa, J. Harvey, L. Painter, J. A. Deacon, and C. L. Monismith. *Evaluation of Laboratory Procedures for Compacting Asphalt-Aggregate Mixtures*. Report TM-UCB-A-003A-90-5. Institute of Transportation Studies, University of California, Berkeley, 1990.
2. J. B. Sousa and J. A. Deacon. Effect of Laboratory Compaction Method on the Permanent Deformation Characteristics of Asphalt-Aggregate Mixtures. Presented at Annual Meeting of Association of Asphalt Paving Technologists, 1991.
3. H. Del Valle. *Procedure—Bulk Specific Gravity of Compacted Bituminous Mixtures Using Parafilm-Coated Specimens*. Chevron Research Company, Richmond, Calif., 1985.

Evaluation of Marshall and Hveem Mix Design Procedures for Local Use

H. AL-ABDUL WAHHAB AND ZIAUDDIN A. KHAN

Conventional methods of mix design can sometimes result in materials that do not perform satisfactorily. In countries that experience extremes of temperature such as Saudi Arabia, the resultant failures can be severe, often occurring soon after the road is opened to traffic. A laboratory evaluation of Marshall and Hveem mix designs was undertaken with an objective of minimizing permanent deformation in asphaltic layers. Five different gradations were selected based on Ministry of Communications specifications. The design procedures were examined, and the mixes were subjected to dynamic and static testing to evaluate resilient modulus, split tensile strength, stiffness, and creep compliance characteristics. The test results indicated that Hveem mixes possessed better engineering properties than those designed by the Marshall method because the Hveem method can better identify mixes with high rutting susceptibility. Recommendations for additional testing techniques could be used for both mix design and quality control purposes.

Over the past two decades, Saudi Arabia has initiated massive construction programs to modernize and improve its highway network. In the short span of 20 years, Saudi Arabia has built an impressive highway network comparable to that of many developed countries. This network—which includes more than 3,600 km (2,200 mi) of divided highways, more than 30,000 km (18,600 mi) of paved roads, and thousands of bridges, some of which are marvels of engineering achievement—was built at a cost of more than 100 billion Saudi riyals ($27 billion) (*1*). Most of these roads have served for more than a decade, and a number of them have started to fall apart. The rate of deterioration of pavements has been augmented by increasing traffic and axle loads and a lack of good-quality materials. Roads are designed for lives of 15 to 20 years before they need any major maintenance. However, during the past few years these roads have experienced excessive failure (rutting) at an early stage of pavement life.

The rutting problem, because of its extent and importance, has attracted the attention and care of many highway authorities. Khan et al. (*2*) pointed out that the requirements and specifications used in Saudi Arabia allow construction with mixtures susceptible to rutting because of the following factors:

1. Unlimited amount of natural sand,
2. Low voids in mineral aggregate (VMA),
3. High asphalt content, and
4. No measure of shear strength.

H. Al-Abdul Wahhab, Civil Engineering Department, King Fahd University of Petroleum and Minerals, Dhahran 31261, Saudi Arabia. Z. A. Khan, Al-Muhandis Nizar Kurdi Consulting Engineers, P.O. Box 2962, Riyadh 11461, Saudi Arabia.

Most asphaltic paving technologists and literature on the subject agree that for good performance asphaltic concrete must have high stability and durability values. For asphaltic concrete to have good stability (i.e., resistance to stress), it must have adequate strength in tension to prevent cracking and adequate strength in shear to prevent deformation or rutting. The literature has indicated that Hveem stability yields a measure of the angle φ (angle of internal friction in the Coulomb-Mohr equation), which furnishes resistance to rutting, and that the Marshall stability is a measure of c (cohesion in the Coulomb-Mohr equation) of tensile strength to resist cracking in pavement (*3*).

Because the mix design procedure currently used in Saudi Arabia—the Marshall mix design—does not measure shear strength of the paving mixture, an attempt was made to explore and evaluate other design procedures, such as the Hveem mix design method, and to compare their abilities to predict the strength properties of designed mixes (especially rutting resistance) and in-service performance using laboratory tests. Additional laboratory tests, such as static creep and resilient modulus, were used to characterize the mechanical properties of asphalt mix in order to predict the permanent deformation (rutting) that will occur when the mix is used in a pavement of given construction and subjected to the unique traffic loading and climatic conditions in Saudi Arabia.

STUDY APPROACH

A systematic study approach was important in order to achieve the study objectives. The study included three main interconnected tasks. The first task was material collection and mix design. The second task involved laboratory testing and evaluation. The third task involved analyzing data and making conclusions, and recommendations. A schematic for the study approach is shown in Figure 1.

The first task involved material characterization and the design of five mixes for five gradations according to the Ministry of Communications (MOC) specification using the Marshall mix design method (ASTM D1159) and the Hveem mix design method (ASTM D1560 and ASTM D1561). These mixes were subjected to further characterization tests, such as the resilient modulus, split tensile, and static creep tests, in order to provide a better evaluation and basis for comparing the two mix design methods, to develop recommendations to improve local mix design, and to minimize the rutting problem on local roads.

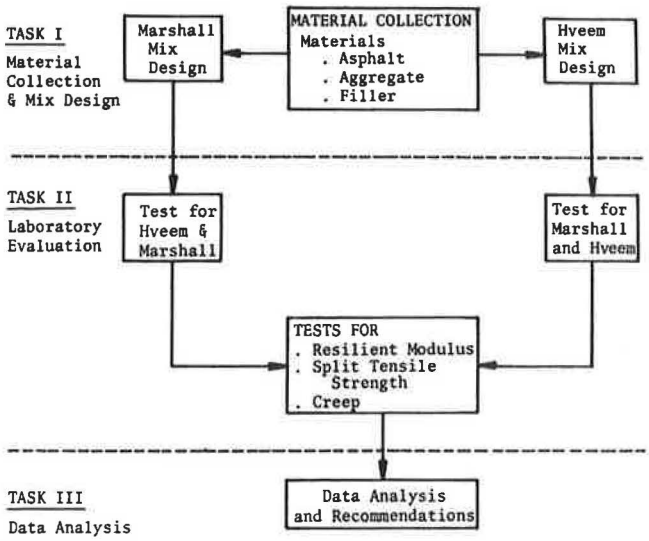

FIGURE 1 Study approach.

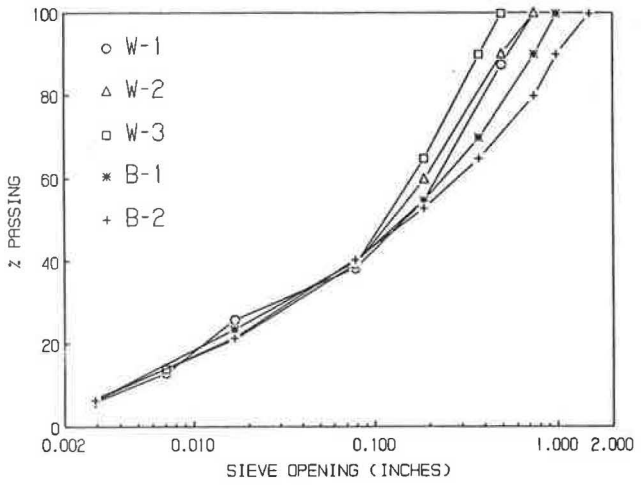

FIGURE 2 Grading curves of aggregates used in mix design.

MATERIAL CHARACTERIZATION AND MIX DESIGN

Material characterization included evaluation of engineering properties of pavement component materials (asphalt and aggregate); the laboratory mix design included determination of optimum asphalt content for different gradations by two mix design procedures. Asphalt cement with 60/70 penetration was used in this study. A series of tests, including penetration, flash point, softening point, specific gravity, and solubility in trichloroethylene, was conducted to identify the basic physical properties of the asphalt.

Five gradations were selected for this study: three gradations for wearing course (W-1, W-2, and W-3) and two gradations for base course (B-1 and B-2) as defined by MOC specifications (*4*), which are shown in Table 1. The adopted gradation for the W-1, W-2, W-3, B-1, and B-2 mixes are shown in Figure 2. The aggregates were subjected to further testing to evaluate other physical properties that are significant in hot-mix asphalt surfaces. These tests included Los Angeles abrasion, soundness, water absorption, and specific gravity tests. Material properties are shown in Table 2. Properties were within the limits specified by MOC.

Marshall Mix Design

The five selected gradations were designed by using the Marshall method and the Hveem method of mix design. To determine the optimum asphalt content for each mix, Marshall testing was conducted at 60°C (140°F). The percentages of air voids in the specimens were determined from the bulk specific gravity of the specimens (ASTM D2726-82) and the maximum theoretical specific gravity of voidless mix (ASTM D2041-82). Stability loss, after immersion in water at 60°C (140°F) for 24 hr, was also determined to check resistance to stripping, which was estimated on the basis of strength index. The optimum asphalt content of the mix was then calculated in accordance with the recommendation of the Asphalt Institute (1981). Marshall properties are shown in Figure 3; optimum

TABLE 1 DESIGN GRADING OBTAINED FOR MIX DESIGN

Sieve Size	Wearing Course (W) Gradation Designation			Base Course (B) Gradation Designation	
	W-1	W-2	W-3	B-1	B-2
1½ inch	-	-	-	100	100
1 inch	-	-	-	100	90
3/4 inch	100	100	-	90	80
1/2 inch	87.5	90	100	-	-
3/8 inch	-	-	90	70	65
No.4	55	60	65	55	53
No.10	38.5	39.5	39.5	40	40.5
No.40	26	21	21	23.5	21.5
No.80	13	14	14	-	-
No.200	6	7	7	6.5	6.5

Saudi Arabian Ministry of Communications Specification

TABLE 2 MATERIAL PROPERTIES

Material	Physical Properties	Mix Designation					Saudi Arabian Ministry of Communications Specification Limits
		W1	W2	W3	B1	B2	
Aggregate	• L.A. Abrasion	22	22	22	23	23	30
	• Soundness 5 cycles						
	- Coarse aggregate	2.86	2.86	2.63	3.2	3.4	10 max
	- Fine aggregate	1.96	1.96	1.95	2.2	2.3	10 max
	• Bulk Specific Gravity (Sat. surface dry)	2.597	2.611	2.592	2.598	2.60	
	• Water Absorption						
	- Coarse aggregate	2.625	2.63	2.64	2.6	2.56	4 max
	- Fine aggregate	3.83	3.82	3.83	3.62	3.61	
Asphalt	• Flash Point, Cleveland open cup	628°F					450 minimum
	• Penetration, 77°F, 100 gm, 5 sec.	61					60-70
	• Specific Gravity, 25°C	1.043					
	• Solubility in Trichloro-ethylene	99.9					99.9 min

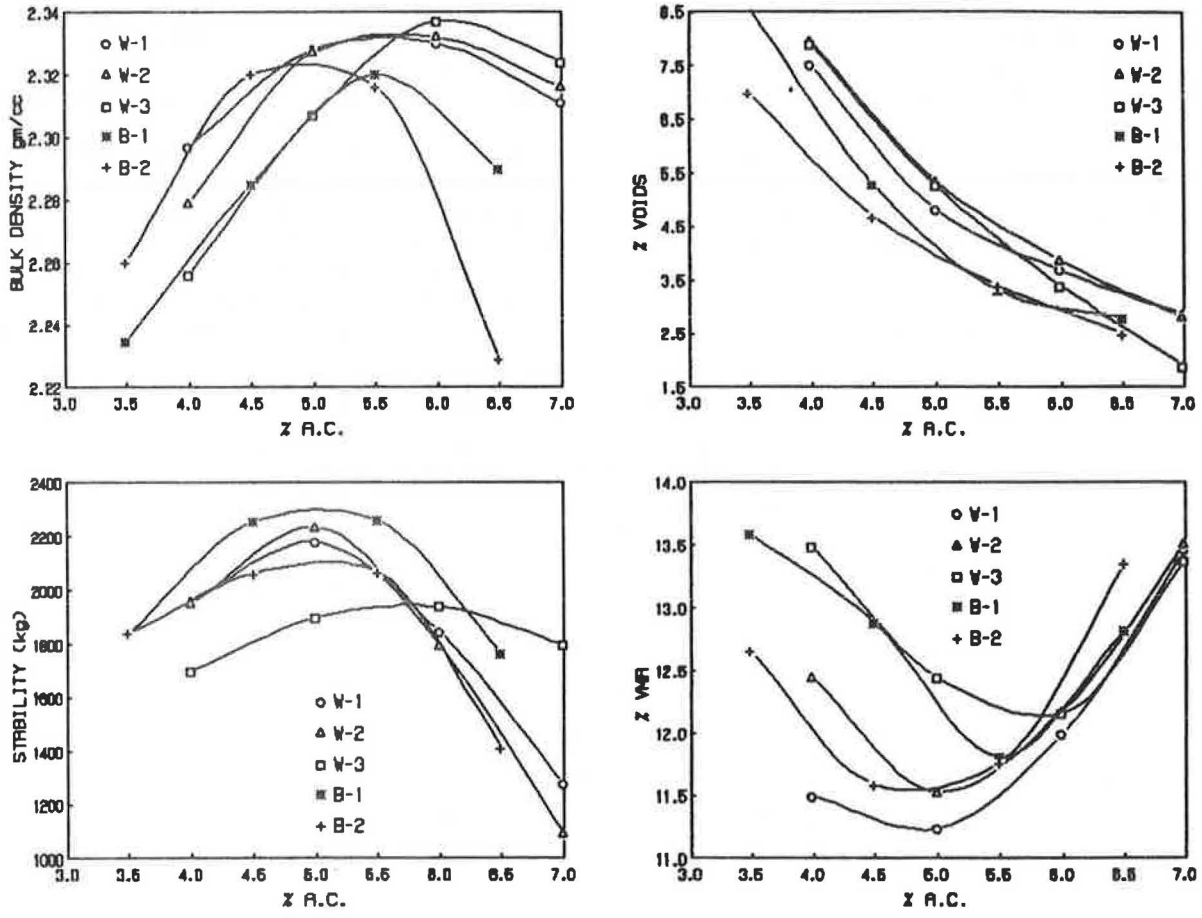

FIGURE 3 Marshall mix design curves.

asphalt content and Marshall properties at these asphalt contents for each mix series are shown in Table 3. The optimum asphalt content for all mixes seems to be affected by the gradation: the finer the gradation, the higher the optimum asphalt content.

Hveem Mix Design

The Hveem mix design procedure used in this study was carried out in the following steps:

1. Centrifuge kerosene equivalent test,
2. Preparation of test specimen (by California kneading compactor), and
3. Hveem stability test.

The specimens prepared by the kneading compactor were tested for Hveem stability. The bulk density test was performed as described in ASTM D2726; the percentage of air voids was determined from bulk specific gravity and maximum theoretical specific gravity of voidless mix. The optimum asphalt content was determined based on stabilometer values, air voids, and surface flushing and bleeding. The pyramid technique (*5*) was used to determine the optimum asphalt content for each mix. The Hveem properties at optimum asphalt (designed by Hveem mix design) are summarized in Table 4 and shown in Figure 4. The Hveem stability for the W-3 mix is 37, which just satisfies the minimum requirement of the Asphalt Institute but does not satisfy the Saudi minimum specification of 40. This low stability value may be attributed to the high percentage of the sand in the mix, which is about 65 percent since the percentages of air voids are above 4 percent in all five mixes.

Comparative Study

The optimum asphalt content predicted by Marshall mix design is about 0.5 percent (0.4 to 0.66 percent) more than the optimum asphalt content predicted by Hveem mix design. A relative comparison of optimum asphalt content determined by both mix design procedures is shown in Figure 5. Further, the Hveem specimens have higher bulk density and lower air void contents than Marshall specimens, indicating that a different orientation of particles is obtained and that more aggregate interlock is achieved. Hveem stability at optimum asphalt content of Marshall mix design, in Hveem mix design curves, showed a very low stability value and was below the specified minimum value of 40 for all five mixes (Figure 6), indicating that the increase in asphalt content from optimum of Hveem mix design affects Hveem stability drastically. For example, the Hveem stability in the W-2 mix dropped from 52 to 38 by increasing asphalt content by only 0.5 percent. Hence, it can be said that Marshall mix design predicts more asphalt content than the Hveem method, which may lead to rutting in the field, especially in hot climates.

TABLE 4 HVEEM PROPERTIES OF VARIOUS MIX SERIES AT OPTIMUM ASPHALT CONTENT

Mix Designation	Optimum Asphalt	Hveem Stability	Air Voids %
W-1	5.0	47	4.3
W-2	5.0	52	4.2
W-3	5.5	37	4.0
B-1	4.5	49	4.4
B-2	4.5	45	4.6
MOC Specifications		40	4-7%

RESILIENT MODULUS TEST

The resilient modulus (M_R) test provides an important input for structural design of pavement systems using multilayer elastic theory. This test is basically a repetitive load test using the stress distribution principle of indirect tensile test. The horizontal deformation of a cylindrical specimen subjected to dynamic vertical loading was measured by two transducers; the load applied was measured by using a flat load cell. In each test, a static load of 10 lb was applied to hold the sample in place. The dynamic load duration was fixed at 0.1 sec, and the load frequency at 60 cycles was fixed at 50°C (122°F) to represent in-service condition. The maximum load applied and the horizontal elastic tensile deformation were recorded to determine the M_R value using the following equation (*6*):

$$M_R(\text{MPa}) = 10^3 P(0.9974\mu + 0.2692)/h\cdot\Delta \quad (1)$$

TABLE 3 MARSHALL PROPERTIES OF VARIOUS MIX SERIES AT OPTIMUM ASPHALT CONTENT

Mix Designation	Optimum Asphalt Content	1/2 hr Stability kgs	Flow 0.25 mm	Air Voids %	VMA %	24 hrs Stability kgs	Strength Index %
W-1	5.5	2090	15.3	4.2	11.5	2060	98.6
W-2	5.6	2060	14.5	4.3	11.8	1953	94.8
W-3	5.9	1940	16.9	3.5	12.1	1832	94.4
B-1	5.2	2307	17.5	3.9	12.3	1960	85.0
B-2	4.9	2120	14.8	4.1	11.5	2040	96.2
MOC Specification		Minimum 700	10-16	4-7			Minimum 80

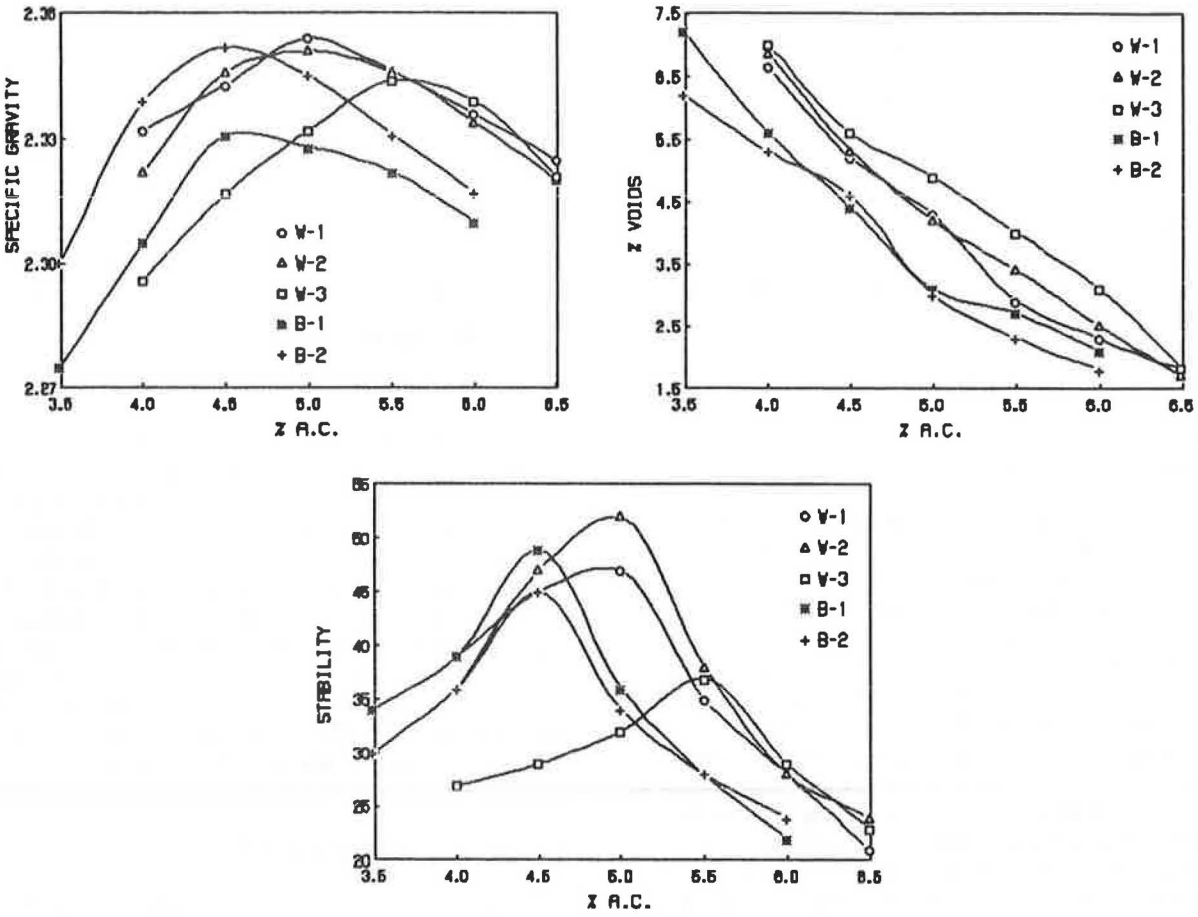

FIGURE 4 Hveem mix design curves.

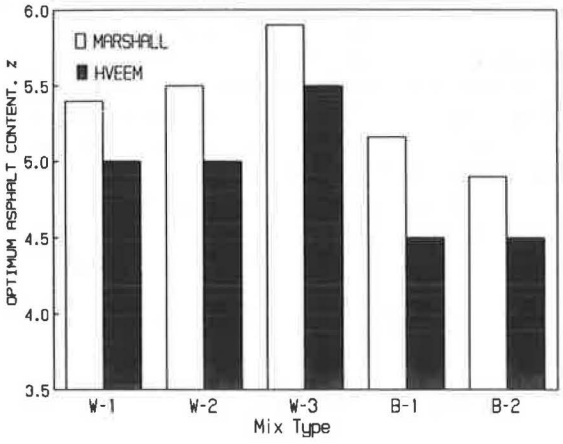

FIGURE 5 Optimum asphalt contents determined by Marshall and Hveem mix design procedures.

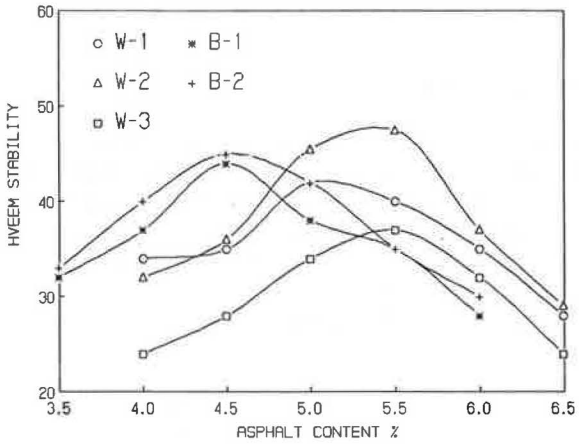

FIGURE 6 Relationship between asphalt content and Hveem stability for Marshall-prepared samples.

where

P = applied load (kN),
h = thickness of specimen (mm),
Δ = recoverable horizontal deformation across sample (mm), and
μ = Poisson's ratio.

The effect of asphalt content on the resilient modulus was studied for mixes compacted by the Marshall hammer and kneading compactor. Table 5 shows asphalt contents at maximum modulus values for all mixes prepared by Hveem and Marshall methods. These asphalt values are about 0.5 percent less than optimum values predicted by both mix design methods. Also, the optimum asphalt contents predicted by the modulus test for samples prepared by Marshall compaction for all five mixes are similar to the optimum asphalt contents predicted by Hveem mix design. The results of resilient modulus at optimum asphalt content of mixes designed by the

TABLE 5 PERCENTAGE OF OPTIMUM ASPHALT CONTENT ESTABLISHED BY RESILIENT MODULUS AND TENSILE STRENGTH TEST FOR MARSHALL AND HVEEM COMPACTIONS

Compaction	Marshall		Hveem	
Test / Mix Type	Resilient Modulus	Tensile Strength	Resilient Modulus	Tensile Strength
W1	5.0	5.3	4.5	5.1
W2	5.0	5.4	4.5	5.3
W3	5.5	5.8	5.0	5.5
B1	4.5	5.0	4.0	4.8
B2	4.5	4.8	4.0	4.7

Marshall or Hveem methods are summarized in Figure 7. The values of resilient modulus at optimum asphalt contents of Hveem mix design are consistently higher than the values of M_R at optimum asphalt contents of Marshall mix design. The higher modulus for mixes designed by the Hveem method can be considered favorable because the mixtures may be less susceptible to cracking and permanent deformation.

SPLIT TENSILE STRENGTH

Specimens prepared by Marshall and Hveem methods for optimum asphalt content and range of asphalt content failed an indirect tensile test at a loading rate of 2 in. (50.8 mm)/min. The test was conducted at 50°C. The specimens failed along the vertical diameter. Split tensile strength was determined by the following equation (*7*):

$$S_T = \frac{2P_{max}}{\pi h D} \quad (2)$$

where

S_T = split tensile strength (psi);
P_{max} = load at failure (lb);
D = diameter of sample (4 in.); and
h = sample thickness (in.).

The split tensile strength at optimum asphalt contents of Marshall and Hveem design are shown in Figure 8. Mixes designed by the Hveem method are about 4 percent higher in strength than those designed by the Marshall method, indicating no significant difference in split tensile strength between both methods. Maximum values of split tensile strength were observed at optimum asphalt contents of Marshall and Hveem mixes, as shown in Table 5.

STATIC CREEP TEST

Present design methods suffer the limitation of accuracy in determining the full effects of variation in environmental and loading conditions and material properties on pavement performance. The major improvement in hot-mix design is the ability to analyze test results quantitatively as well as qualitatively. Qualitatively, the relative improvements between mixes can be evaluated based on creep modulus at the specified temperature.

The permanent deformation of asphalt mixes depends on a number of external and inherent variables in the mix: the main external variables are overall stress condition and the temperature; the inherent variables are the mix composition. In 1973, Hills (*8*) presented a physical deformation model for asphalt mixes using static creep testing as a key tool for predicting pavement rutting.

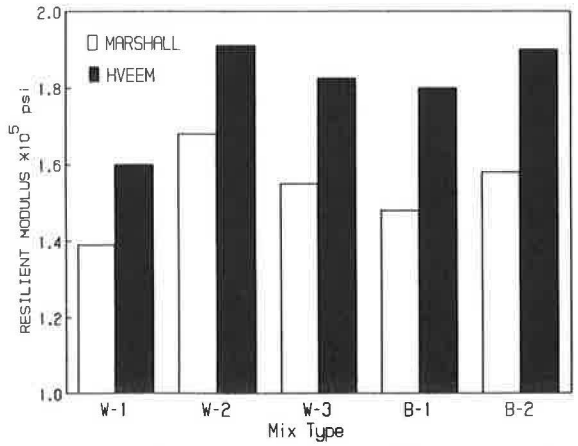

FIGURE 7 Resilient modulus (50°C) at optimum asphalt content of Marshall and Hveem mix design.

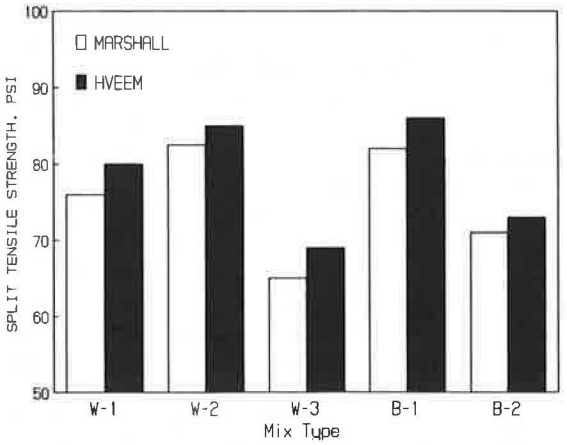

FIGURE 8 Split tensile strength (50°C) at optimum asphalt content of Marshall and Hveem mix design.

Creep test as described in the Shell Pavement Design Manual (*9*) was performed by applying a static load of 14.5 psi. The temperature of test specimens was kept constant as desired by means of an environmental control cabinet. Vertical deformation (displacement) was measured by dial gauges accurate to 0.0001 in.

In this study, the creep test was performed on specimens prepared by the Marhsall and Hveem methods for a range of asphalt contents, including optimum asphalt content at temperature of 50°C. The sample size recommended by Shell investigators (*9*) was governed by maximum aggregate size. For mixes W-1, W-2, and W-3, the sample size was 4 in. (10 cm) in diameter by 2.5 in. (6 cm) high; the sample size for mixes B-1 and B-2 was 6 in. (15 cm) in diameter by 4 in. (10 cm) high. Each specimen was tested at a stress level of 14.5 psi maintained for 3 hr. Before the test, a preconditioning stress of the same magnitude as the test stress was applied for at least 2 min (*10*).

Recorded deformation and applied stress were used to calculate the creep modulus (mix stiffness, S_{mix}) as a function of time of loading using the following equation (*11*):

$$S_{mix}(T,t) = \frac{\sigma}{\varepsilon_t} \quad (3)$$

where

$S_{mix}(T,t)$ = mix stiffness at a specified temperature (T) and time of loading (t);
σ = applied stress (psi); and
ε_t = axial strain at $t = \Delta h/h_o$ where Δh is change in height of specimen, and h_o is original height of specimen.

Further, these results (i.e., ε_t and σ) were used to calculate creep compliance (J_t) in order to study the viscoelastic characteristics of the mixes. Creep compliance (J_t), was calculated by dividing the strain by applied stress as follows:

$$J_t = \frac{\varepsilon_t}{\sigma} \text{ at any test temperature } T \quad (4)$$

where ε_t is strain at time t, and σ is applied stress (psi).

Stiffness results for mix W-1 designed by the Marshall and Hveem methods as a function of loading time at different asphalt contents, including optimum asphalt content, are shown in Figures 9 and 10. Stiffness decreased with loading time. Further, mixes designed by the Hveem method gave relatively higher stiffness values than those obtained from Marshall specimens at loading times greater than 1 hr. Stiffness moduli decrease as the asphalt content increases. The stiffness moduli at optimum asphalt content of both Hveem and Marshall mix design methods (200,000 and 400,000 psi) are comparable with values reported by Finn et al. (150,000 and 550,000 psi) (*12*) in a performance study for Middle East airport pavements.

Creep compliance, which is used to determine viscoelastic properties of pavement materials, was plotted as a function of loading time at different asphalt contents, including optimum asphalt content, for mix W-1 designed by both methods, as shown in Figures 11 and 12. Creep compliance increases with time. Furthermore, mixes designed by the Hveem method

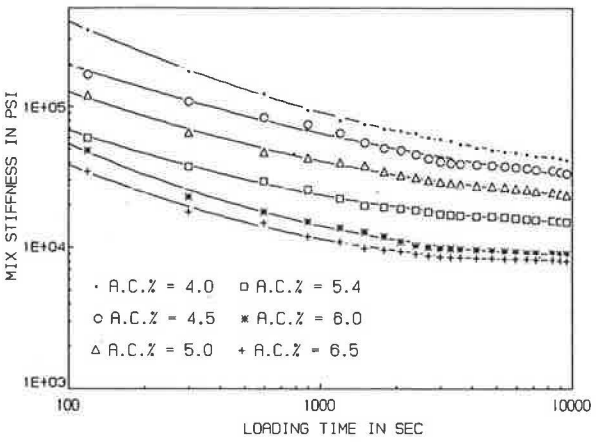

FIGURE 9 Effect of asphalt content on mix stiffness for Marshall specimens, Mix W-1 at 50°C.

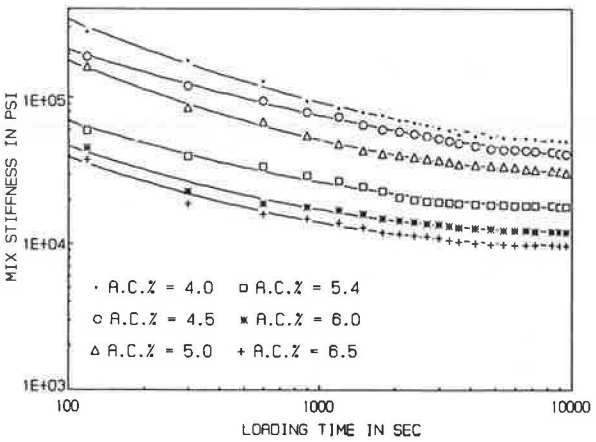

FIGURE 10 Effect of asphalt content on mix stiffness for Hveem specimens, Mix W-1 at 50°C.

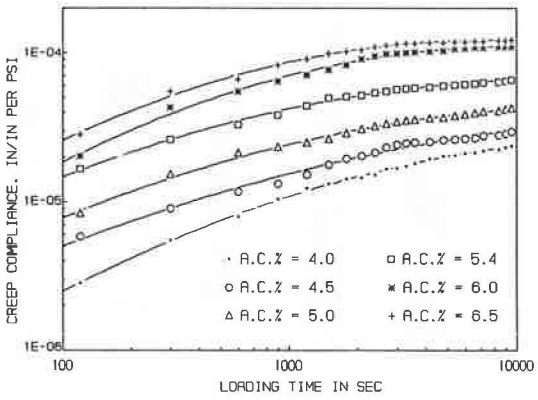

FIGURE 11 Effect of asphalt content on creep compliance for Marshall specimens, Mix W-1 at 50°C.

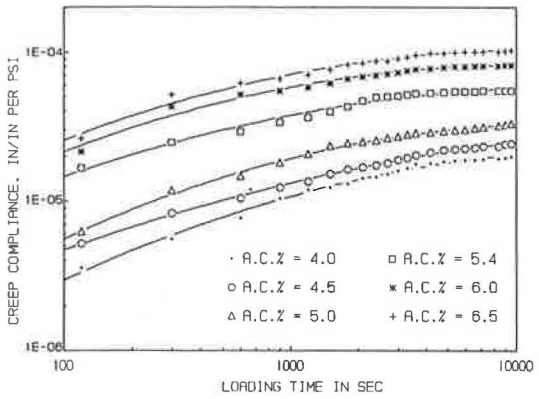

FIGURE 12 Effect of asphalt content on creep compliance for Hveem specimens, Mix W-1 at 50°C.

gave lower values of creep compliance than did mixes designed by the Marshall method at specified asphalt content and loading time.

In order to explore the role of asphalt content on stiffness and creep modulus, bar charts were prepared for a range of asphalt contents in the vicinity of optimum asphalt content predicted by both mix design procedures, as shown in Figures 13–16. The value of stiffness and creep compliance was chosen at the 60-min loading time. Optimum mixes prepared by Hveem had stiffness values twice those of optimum Marshall for wearing course mixes and three times those for base mixes. Moreover, the W-3 mix, which follows the gradation of MOC Type C of wearing course, had very low stiffness values (10,000 and 13,000 psi) and high creep compliance (1,050 and 800 · 10^{-7}/psi) for mixtures designed by the Marshall and Hveem methods, respectively, indicating its high susceptibility to rutting.

CONCLUSIONS

Based on a literature search and experiments conducted in this study, the following conclusions are drawn:

1. Marshall mix design tends to predict optimum asphalt contents that are higher than those predicted by the Hveem

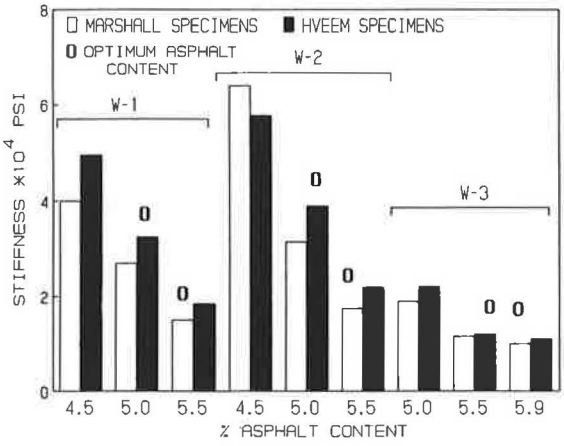

FIGURE 13 Comparison between mix stiffness of Marshall and Hveem specimens for wearing course.

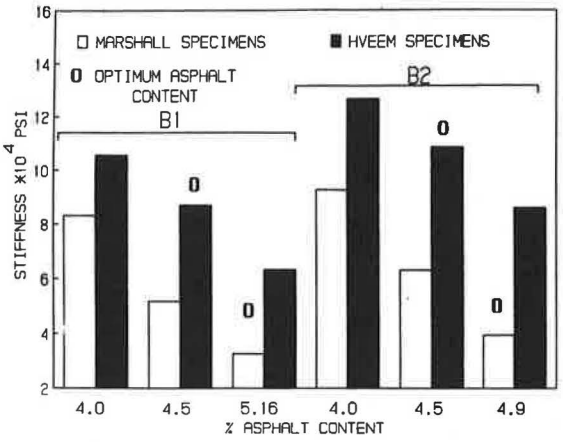

FIGURE 14 Comparison between mix stiffness of Marshall and Hveem specimens for base course.

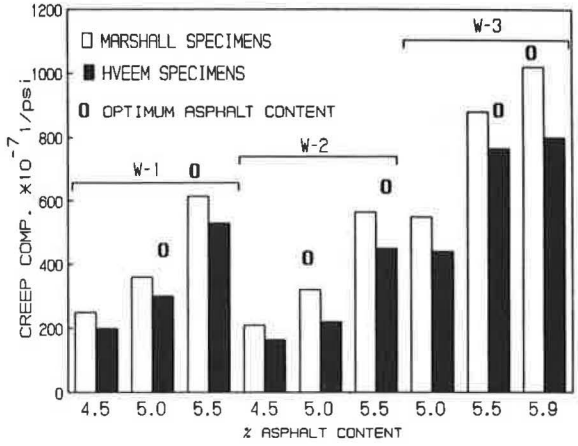

FIGURE 15 Comparison between creep compliance of Marshall and Hveem specimens for wearing course.

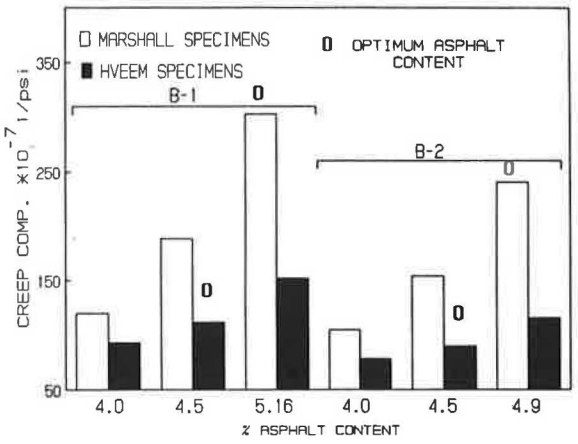

FIGURE 16 Comparison between creep compliance of Marshall and Hveem specimens for base course.

mix design method. In this study, the optimum asphalt contents predicted by the Marshall mix design were about 0.5 percent higher than those predicted by the Hveem mix design method.

2. Hveem specimens have a higher bulk density and a lower air void content than Marshall specimens, indicating that a different orientation of particles is obtained and that more aggregate interlock is achieved by kneading compaction.

3. Mixes designed by the Hveem method gave higher resilient modulus values, higher stiffness values, and lower creep compliance values than those obtained from mixes designed by the Marshall method.

4. Resilient modulus tests on Marshall samples predicted optimum asphalt contents that were similar to those predicted for Hveem samples. The deficiency of the Marshall mix design could be improved by using the resilient modulus test.

5. Hveem mix design seems to have a potential application for Saudi Arabia's roads because it more closely simulates field conditions and can better identify mixes with high rutting susceptibility than does the Marshall method.

ACKNOWLEDGMENT

The authors wish to thank the King Fahd University of Petroleum and Minerals for providing the laboratory space and computer facilities required for this research.

REFERENCES

1. S. A. Ashoor. *Saudi Economic Survey*. June 27, 1984.
2. S. Khan, I. Dubabe, and A. Farouki. *Preliminary Report on Rutting*. Ministry of Communications, Saudi Arabia, Sept. 1986.
3. R. A. Jimenez. A Look at the Art of Asphaltic Mixture Design. *Proc., Association of Asphalt Paving Technologists*, Vol. 55, 1986.
4. *Specifications for Roads and Bridges*. Ministry of Communications, Saudi Arabia, n.d.
5. ASTM. *Road Paving Bituminous Materials, Traveled Surface Characteristics*. Section 4, Vol. 403, 1986.
6. T. W. Kennedy. Characterization of Asphalt Pavement Materials Using Indirect Tensile Test. *Proc., Association of Asphalt Paving Technologists*, Vol. 46, 1977, p. 132.
7. G. Gonzales, T. W. Kennedy, and J. N. Anagnos. *Evaluation of Resilient Elastic Characteristics of Asphalt Mixtures Using Indirect Tensile Test*. Research Report 183-6. Center of Highway Research, University of Texas, Austin, n.d.
8. J. F. Hills. The Creep of Asphalt Mixes. *Journal of the Institute of Petroleum*, Vol. 59, No. 570, London, England, 1973.
9. Shell Pavement Design Manual. *Asphalt Pavements and Overlay for Road Traffic*. Shell International Petroleum Company, London, England, 1978.
10. C. L. Monismith, J. A. Epps, and F. N. Finn. Improved Asphalt Mix Design. *Proc., Association of Asphalt Paving Technologists*, Vol. 54, 1985.
11. J. F. Hills, D. Brein, and P. J. Van de Loo. *The Correlation of Rutting and Creep Tests on Asphalt Mixes*. Paper IP, 74001. Institute of Petroleum, London, England, Jan. 1974.
12. F. N. Finn, C. L. Monismith, and N. J. Markevich. Pavement Performance and Asphalt Concrete Mix Design. *Proc., Association of Asphalt Paving Technologists* Vol. 52, 1983.

Evaluation of Mix Properties of Cold In-Place Recycled Mixes

TODD SCHOLZ, DAVID F. ROGGE, R. GARY HICKS, AND DALE ALLEN

Oregon has used cold in-place recycling (CIR) techniques since 1984 as one alternative to conventional asphalt concrete pavement rehabilitation practices. The initial success of the early CIR projects (1984 and 1985) prompted a joint research effort in 1986 between the Oregon State Highway Division and Oregon State University. This effort, continued in 1988, has focused on developing improved mix design procedures and construction guidelines for cold in-place recycling. One of the goals of the study was to develop a sample preparation procedure for cold recycled mixtures; the samples were to be used for mix design purposes. To validate the procedure, selected mix properties of field cores were compared with those of laboratory-prepared samples. The field and laboratory studies, their results, and a comparison of their results are described. Also, the CIR mix properties are compared with those of conventional hot mixes. Significant findings include (a) laboratory samples can be prepared at void contents similar to those found in the field; (b) laboratory sample mix property test results generally compare well with those of the field cores; and (c) limited comparisons showed that cold in-place recycled mixtures generally have greater moduli and fatigue lives than conventional hot mixes at similar void contents.

Since 1984, Oregon has used cold in-place recycling (CIR) techniques as one alternative to conventional practices for the rehabilitation of asphalt concrete pavements. Experienced paving personnel constructed the 1984 projects using trial-and-error procedures. In 1985 Oregon first attempted a formal mix design for the cold recycled mixtures. Because of the initial success of these early projects, Oregon State University (OSU) and the Oregon State Highway Division (OSHD) initiated a study in 1986 to develop an improved mix design procedure and construction guidelines for cold in-place recycling (*1*). Ths study was continued in 1988.

One of the purposes of the study was to develop a sample preparation procedure for cold recycled mixtures with the intent of using the samples for mix design purposes. To validate the procedure, selected mix properties of field cores were compared with those of laboratory-prepared samples. To accomplish this, two of the seven CIR projects selected for the 1986 field study were also selected for the laboratory study. At the time of construction of these two projects, laboratory samples were prepared from the millings. These samples, along with field cores from the two projects, were tested for mix properties (modulus, fatigue, and stability) 3, 15, 27, and 48 months after construction.

T. Scholz, D. F. Rogge, and R. G. Hicks, Department of Civil Engineering, Oregon State University, Corvallis, Oreg. 97331. D. Allen, Oregon Department of Transportation, Bend, Oreg. 97708.

The laboratory and field studies are described and the mix property test results are presented for two of the seven CIR projects included in the 1986 construction season. A comparison between laboratory and field test results from 1986 to 1990 is given, as well as a comparison between CIR field mixes and conventional hot mixes. Also included are significant conclusions resulting from this test program.

FIELD STUDY

This section presents the results of the field study on two of the seven test sections evaluated in the 1986 OSU/OSHD study. Figure 1 shows location and construction information for the two projects (Warm Springs and Lake of the Woods). Both projects are on two-lane, medium-volume highways (1,750 to 2,850 average daily traffic). The Warm Springs test section had an average to soft (15 to 90 penetration at 77°F) asphalt before the CIR; the Lake of the Woods secton had a very hard and oxidized asphalt (4 to 5 penetration at 77°F). Field cores from the recycled projects were used for the field study, and recycled asphalt pavement (RAP) millings from the distressed pavement were used for the laboratory study.

Description of Field Study

Field cores were obtained from the Warm Springs and Lake of the Woods test sections in fall 1986, 1987, 1988, and 1989 (approximately 3, 15, 27, and 39 months after construction). Six 4-in. cores were extracted from each project. (The field cores were cut dry using air because use of cooling water tends to reemulsify the emulsified asphalt in the recycled cores, causing the core to soften and break down.) Three of the cores from each project were used for resilient modulus (ASTM D4123) and fatigue tests (*2*); the three remaining cores were used to test Marshall stability and flow (ASTM D1559).

Test Results

The results of mix property tests performed on the field cores from the two projects are summarized in Table 1. All results represent the average of three tests. The resilient modulus tests were conducted at 23°C (73°F), at a dynamic loading frequency of 1 Hz, at a dynamic load duration of 0.1 sec, and at a tensile strain of 100 microstrain ($\mu\varepsilon$). The fatigue tests were performed using the same loading conditions as for the

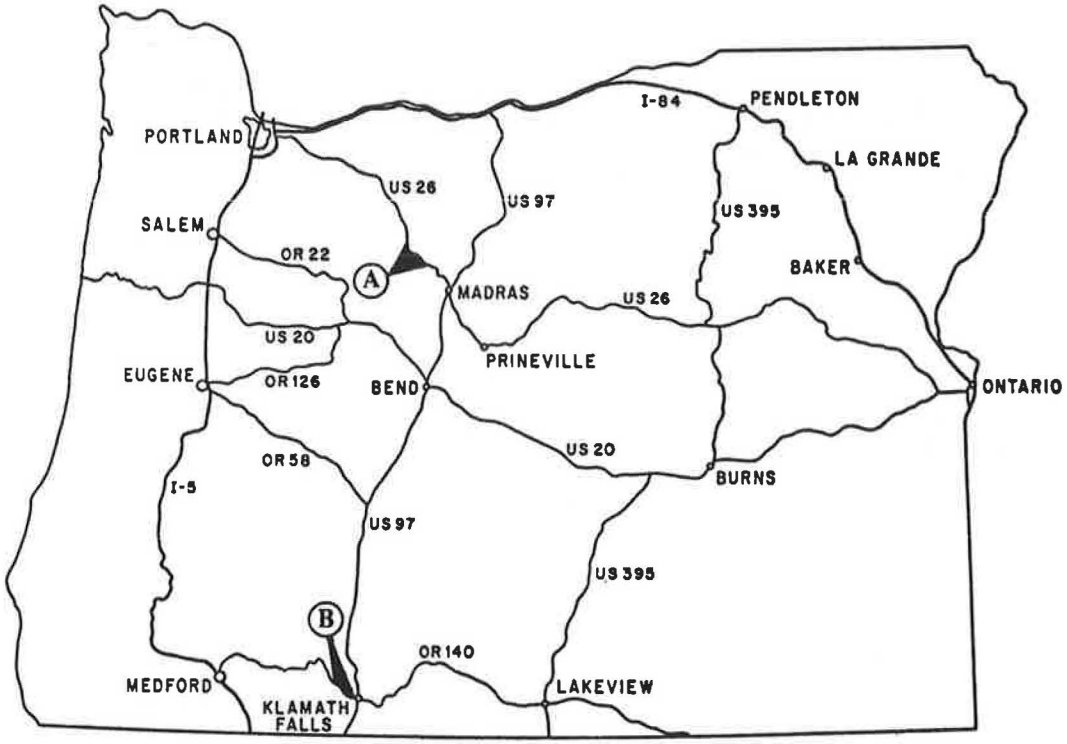

Unit	Project	Length (mi.)	Depth of CIR (in.)	Surface Treatment
A	MP 79.2-Wasco Co. Line (Warm Springs Hwy)	17.3	2-4	Polymer Chip Seal
B	Lakeshore Dr.-Greensprings Jct. (Lake of the Woods Hwy)	6.36	2.5-4	Chip Seal

FIGURE 1 Project location and construction information.

TABLE 1 SUMMARY OF FIELD CORE TEST RESULTS

Emulsion/ Water Content (%)	Test Period	Percent Voids	Average Resilient Modulus (ksi)	Average Fatigue Life (reps)	Average Marshall Stability (lb)	Average Flow (in./100)
a) MP 79.2-Wasco Co. Line (Warm Springs)						
1.0/2.4	Fall 1986	12.8	305 (243)	11,030 (5,053)	694 (80)	59 (5.7)
	Fall 1987	7.4	242 (15)	50,010 (17,709)	861 (81)	19 (3.0)
	Fall 1988	11.7	377 (30)	53,965 (12,800)	1,110 (22)	21 (1.5)
	Summer 1990	7.4	526 (8)	150,000+	1,811 (71)	17 (2.1)
b) Lakeshore Dr.-Greensprings Jct. (Lake of the Woods)						
1.8/1.6	Fall 1986	10.9	513 (107)	5,863 (4,354)	605 (100)	29 (13)
	Fall 1987	15.7	504 (62)	34,261 (5,536)	614 (27)	19 (0.6)
	Fall 1988	14.6	530 (16)	78,731 (13,847)	1,170 (43)	24 (3.8)
	Summer 1990	13.0	727 (58)	250,000+	1,597 (134)	17 (1.2)

Note: Parentheses contain standard deviation

resilient modulus tests, with an initial tensile strain of 100 $\mu\varepsilon$. Marshall stability tests were performed at 60°C (140°F) and at a load rate of 2 in./min.

The results indicate that the modulus, although initially remaining relatively constant, increased substantially after 3 years for both test sections, as shown in Figure 2a. Fatigue values, although initially very low for both sections, increased significantly over time (Figure 2b). This increase in fatigue resistance is attributed to improved cohesive properties of the asphalt cement due to additional curing over time.

As shown in Figure 3a, the stabilities increased over time for both test sections: the Warm Springs section shows a rel-

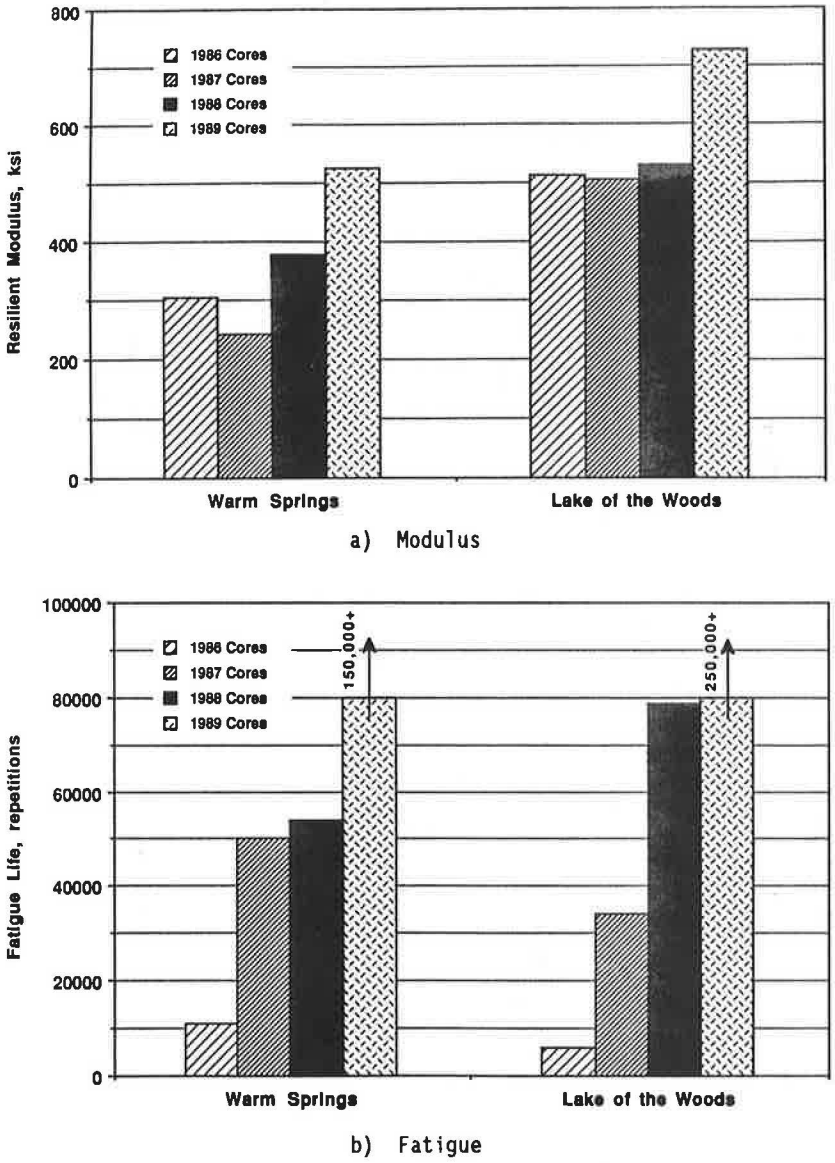

FIGURE 2 Modulus and fatigue results for field samples.

atively constant increase over time, and the stabilities for the Lake of the Woods section initially remained the same and then increased significantly. The flow values for the Warm Springs section were initially very high but leveled off to a relatively constant value; the values for the Lake of the Woods section decreased slightly or remained relatively constant over time (Figure 3b). Again, the increases in stabilities and decreases in flow values are attributed to improved cohesive properties of the asphalt cement due to additional curing of the recycled mix.

LABORATORY STUDY

This section presents the results of the laboratory study on the Warm Springs and Lake of the Woods test sections. The laboratory study is described and the mix property test results are summarized.

Description of Laboratory Study

A laboratory study program was undertaken on materials taken from the test sections on the Warm Springs and the Lake of the Woods highways in order to investigate the effects of emulsion content, curing time, and compactive effort. The recycled materials were collected and compacted at the same time as the cold recycling construction (July 1986 for Lake of the Woods, August 1986 for Warm Springs), which ensured a RAP gradation and existing asphalt content as in the in situ recycled pavement (Table 2).

The design emulsion content used to fabricate the 2.5-in.-thick by 4-in.-diameter briquets was the same as that used in the field during construction (1 percent for Warm Springs, 1.9 percent for Lake of the Woods). Additional samples were fabricated with the design emulsion content, the design minus 0.5 percent, and the design plus 0.5 percent. Thus, for the Warm Springs section, which had a design emulsion content

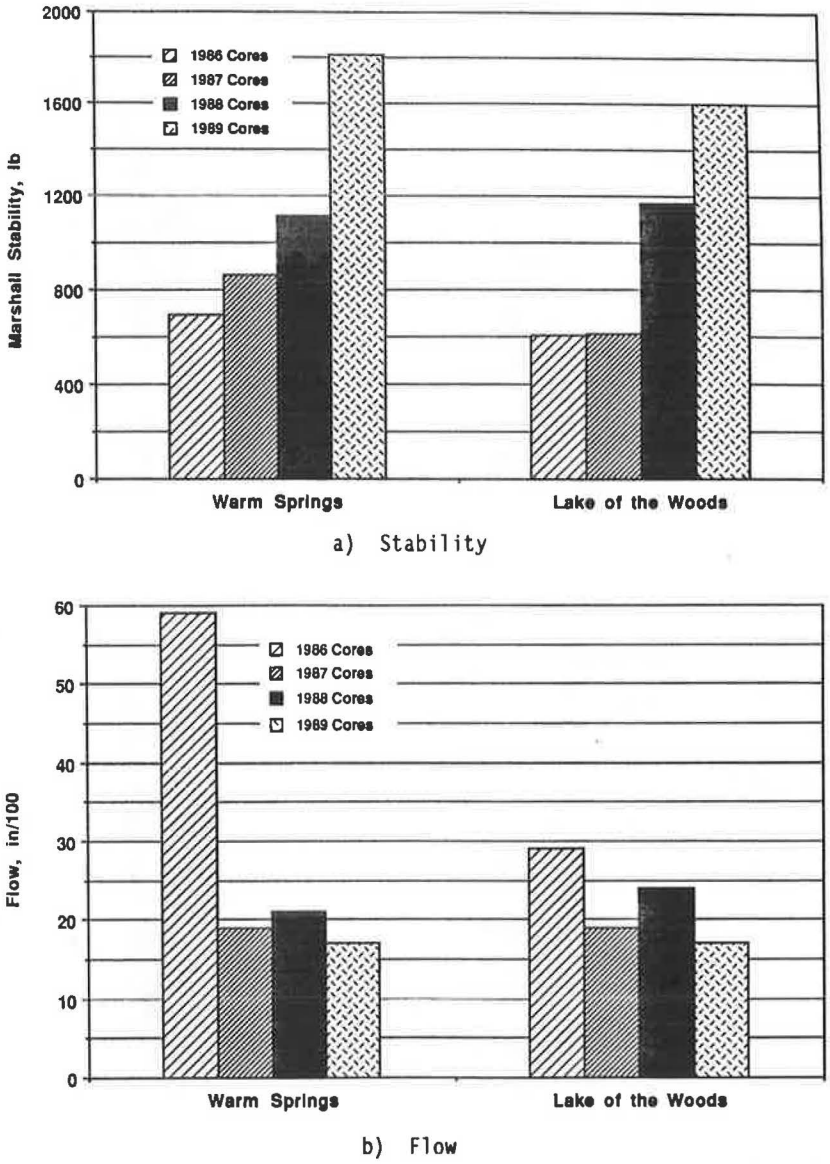

FIGURE 3 Marshall stability and flow results for the field cores.

of 1.0 percent, briquets were fabricated with 0.5 percent, 1.0 percent, and 1.5 percent added emulsion. Similarly, for the Lake of the Woods section, briquets were fabricated with 1.4 percent, 1.9 percent, and 2.4 percent added emulsion, with the design content being 1.9 percent.

The total liquids (emulsion and water) for all briquets fabricated with RAP from the Warm Springs section was held constant at 4.0 percent. Thus, for example, if the added emulsion content was 1.0 percent, the added water content was 3.0 percent. This same criterion was attempted for the Lake of the Woods section. However, during the preparation of samples with 1.4 percent emulsion, using 2.6 percent water produced a dry mix. To mitigate this problem, the total liquid content was increased to 4.5 percent, resulting in more workable and better-adhering mixtures. The total liquid content is the minimum quantity of liquids required for adequate dispersion of emulsion; insufficient liquid content results in a dry, unworkable mixture, and a total liquid content that is too high results in instability during compaction. Thus, once prescribed, the total liquid content was held constant to avoid problems during sample preparation. Incidentally, this philosophy is used in actual field construction.

Table 3 summarizes the number of samples prepared for each emulsion content; the mix property tests for the fall 1986, 1987, 1988, and summer 1990 test periods; and the schedule for each test period. Twelve samples per emulsion content were required for the remaining mix property tests (three samples per test period) because the fatigue and stability tests are destructive.

The procedure used to fabricate the samples is shown in Table 4. All mixing, curing, and compaction are performed at 60°C (140°F). A total compactive effort of 2,250 ft-lb is used during compaction (i.e., 150 blows using a 10-lb hammer with an 18-in. freefall). This relatively low compactive effort was necessary to achieve air void levels similar to those of CIR pavements in the field. Following specimen fabrication,

TABLE 2 RAP GRADATIONS AND ASPHALT CONTENTS

	MP 79.2-Wasco Co. Line (Warm Springs)			Lakeshore Dr.-Greensprings Jct. (Lake of the Woods)			
	1	2	Avg.	1	2	3	Avg.
% Passing							
1 in.	96	94	95	98	84	93	92
3/4 in.	88	90	89	96	81	90	89
1/2 in.	75	77	76	89	74	83	82
3/8 in.	61	62	62	79	65	74	73
1/4 in.	44	46	45	61	50	57	56
#4	33	36	34	48	40	46	45
#10	11	3	7	21	18	21	20
#40	1.7	2.2	2.0	6	6	7	6
#200	0.4	0.6	0.5	2.0	2.0	1.8	1.9
Extracted Asphalt Properties							
Content, %	5.4	5.7	5.6	4.6	4.4	5.1	4.7
Penetration @ 77°F, dmm	15	90	52	4	4	5	4
Viscosity @ 140°F, p.	18,067	2,693	10,380	100,000+	100,000+	100,000+	100,000+
Viscosity @ 25°F, cS	852	374	613	2,572	2,920	1,987	2,493

TABLE 3 NUMBER OF SAMPLES PREPARED AND TEST SCHEDULE FOR LABORATORY STUDY

Project Name	Emulsion/Water Content (%)	Resilient Modulus and Fatigue	Marshall Stability and Flow
a) Number of Samples Prepared			
MP 79.2- Wasco Co. Line (Warm Springs)	0.5/3.5	12	9
	1.0/3.0	12	9
	1.5/2.5	12	9
Lakeshore Dr.- Greensprings Jct. (Lake of the Woods)	1.4/2.6	12	9
	1.4/3.1	12	9
	1.9/2.6	12	9
	2.4/2.1	12	9
b) Test Schedule Per Test Period*			
MP 79.2- Wasco Co. Line (Warm Springs)	0.5/3.5	3	3
	1.0/3.0	3	3
	1.5/2.5	3	3
Lakeshore Dr.- Greensprings Jct. (Lake of the Woods)	1.4/2.6	3	3
	1.4/3.1	3	3
	1.9/2.6	3	3
	2.4/2.1	3	3

*Four Test Periods: Fall 1986, 1987, 1988, and Summer 1990

TABLE 4 SAMPLE PREPARATION PROCEDURE USED TO FABRICATE TEST SPECIMENS FOR LABORATORY STUDY

1		Split the millings into approximately 3500 gram batches. This size of sample makes three to four 2.5-in. high by 4.0-in. diameter specimens.
2		Screen the sample over a 1-in. sieve. Reduce all material retained on the 1-in. sieve using a hammer or chisel such that 100% passes the 1-in. sieve.
3		Heat the samples and emulsion to 60 ± 1°C (140 ± 1.8°F) for 1 hour prior to mixing.
4		Add water to the millings in the appropriate portion based on the air dry weight of the millings (e.g., % water = % total liquids - % added emulsion). Thoroughly mix the water into the millings by hand.
5		Add the emulsion to the pre-moistened millings using the recommended content (the added emulsion is based on the air dry weight of millings). Thoroughly mix the emulsion into the millings by hand.
6		Spread the material in a 305 × 432 mm (12 × 17-in.) baking pan and cure for 1 hour at 60 ± 1°C (140 ± 1.8°F) to simulate the average time elapsed between paver laydown and initial compaction during actual construction.
7		Mold the samples using the standard Marshall procedure (ASTM D-1559) to produce 64 mm (2.5-in.) high briquets as described below.
	a	Preheat molds to 60 ± 1°C (140 ± 1.8°F).
	b	Compact the mixture with 50 blows per side using a 44 N (10 lb) hammer having a 457 mm (18-in.) freefall.
	c	Remove the filter papers from each side of the briquets.
	d	Cure overnight at 60 ± 1°C (140 ± 1.8°F) and recompact with 25 blows per side using the 44 N (10 lb) hammer.
	e	Lay the molds on their end and cure the briquets for 24 hours at 60 ± 1°C (140 ± 1.8°F) prior to extrusion.
	f	Extrude the briquets with a compression testing machine.
	g	Lay the briquets on their side to maximize surface exposure and cure for 72 hours at room temperature prior to testing.

the samples were stored at 25 ± 2°C in the laboratory before testing.

Test Results

Tests were performed on two groups of the laboratory-prepared samples as follows: (a) resilient modulus and fatigue samples, and (b) Marshall stability and flow samples.

Resilient Modulus and Fatigue Samples

For each test period (fall 1986, 1987, 1988, and summer 1990) resilient modulus tests were performed on three samples of each emulsion content. Fatigue tests were performed on these samples during the first three test periods. Modulus and fatigue tests were conducted under the same conditions as those used for the field cores.

The results of the modulus and fatigue tests are summarized in Table 5. All results represent the average of the three samples tested for each emulsion content. The maximum modulus for the Warm Springs section occurs at the design emulsion content of 1.0 percent, except for the first year's test results. Similarly, the maximum modulus for the Lake of the Woods section occurs at the design emulsion content of 1.9 percent, as well as at design minus 0.5 percent with the total liquids of 4.5 percent (i.e., 1.4/3.1 percent). For both

TABLE 5 SUMMARY OF LABORATORY SAMPLE TEST RESULTS

Project	Emulsion/ Water Content (%)	Test Period	Air Voids (%)	Average Resilient Modulus (ksi)	Average Fatigue Life	Average Marshall Stability (lbs)	Average Flow (in./100)
MP 79.2- Wasco Co. Line (Warm Springs)	0.5/3.5	Fall 1986	14.4	528	33,560	409	25
		Fall 1987	11.5	319	33,080	441	27
		Fall 1988	14.8	203	24,811	526	50
		Summer 1990	17.1	219	*	515	27
	1.0/3.0	Fall 1986	11.8	374 (60)	18,673 (7,015)	612 (?)	59 (?)
		Fall 1987	11.2	346 (99)	31,780 (2,653)	694 (98)	24 (4.5)
		Fall 1988	9.7	221 (28)	30,373 (9,330)	1,116 (144)	23 (3.6)
		Summer 1990	12.7	473 (55)	*	1,173 (24)	23 (5.1)
	1.5/2.5	Fall 1986	11.7	260	23,530	518	24
		Fall 1987	12.3	299	30,102	585	35
		Fall 1988	9.6	237	28,730	531	18
		Summer 1990	14.6	409	*	847	34
Lakeshore Dr.- Greensprings Jct. (Lake of the Woods)	1.4/2.6	Fall 1986	18.7	383	35,540	409	20
		Fall 1987	19.3	511	21,958	511	25
		Fall 1988	17.2	324	43,985	758	29
		Summer 1990	15.9	375	*	955	19
	1.4/3.1	Fall 1986	17.6	466	91,260	681	18
		Fall 1987	16.0	604	61,337	1,160	22
		Fall 1988	17.8	426	81,223	1,190	30
		Summer 1990	18.2	555	*	1,446	27
	1.9/2.6	Fall 1986	17.7	457 (98)	39,333 (10,874)	928 (?)	57 (?)
		Fall 1987	17.0	603 (74)	59,269 (25,899)	861 (17)	32 (1.2)
		Fall 1988	15.2	412 (56)	82,059 (19,597)	1,307 (228)	17 (1.5)
		Summer 1990	17.4	780 (33)	*	1,236 (285)	26 (7.2)
	2.4/2.1	Fall 1986	19.6	408	117,320	613	40
		Fall 1987	19.2	437	58,158	451	32
		Fall 1988	19.0	289	69,046	758	18
		Summer 1990	22.9	492	*	1,038	24

*Fatigue tests were not performed on the laboratory samples in Summer 1990
Note: Parentheses contain standard deviations

sections, the modulus decreased slightly or remained about the same when the emulsion content was increased or decreased from the design content (see Figure 4a). This finding is true of all four test periods except for the first year's results for the 0.5 percent emulsion content on the Warm Springs section. The unexpected drop in moduli within each emulsion content between 1987 and 1988 test periods is unexplained; possible reasons include operator or measurement error and variability in the mix.

As shown in Figure 4b, the fatigue life of the samples from the Warm Springs section remained relatively constant over the first three test periods (fatigue tests were not conducted during the fourth test period). Consequently, there is no definite trend that shows which emulsion content provides the best fatigue resistance. The fatigue results for the Lake of the Woods section show considerable variation within each emulsion content as well as between emulsion contents. However, it is evident that the 1.4/3.1 percent emulsion/water content provides better fatigue resistance than does the 1.4/2.6 percent emulsion/water content. That is, the mix having more water had better fatigue resistance. This finding may indicate that the greater amount of water provided a more thorough dispersion of the emulsion throughout the mixture.

Marshall Stability and Flow Samples

During each test period, three samples from each emulsion content were tested for Marshall stability under the same conditions as those of the field core tests. The results of these tests are shown in Table 5. All results represent the average of the three samples. As shown in Figure 5a, the maximum stability occurs at the design emulsion content for the Warm Springs section for each test period. The maximum stability of the Lake of the Woods section occurs at the design emulsion content for three of the four test periods; the exception was the 1987 results in which the maximum stability occurred at the 1.4/3.1 percent emulsion/water content (design minus 0.5 percent).

The flow values generally reflect the stability values for the Warm Springs section in that low flows generally occur at the design emulsion content (see Figure 5b). However, for the Lake of the Woods section, trends in the flow values are indiscernible due to the erratic nature of the results.

COMPARISON OF RESULTS: LABORATORY VERSUS FIELD

A major purpose of this study was to compare selected mix properties of the field cores with those of the laboratory-prepared samples in order to develop a procedure for preparing laboratory samples. Because both the field cores and laboratory samples were from the same RAP, the significant differences between the two are the method of compaction, temperature during cure, moisture during cure, and traffic densification. The actual age of the two mixes (field cores versus laboratory specimens) differs by approximately 1 month: the field cores were tested 3, 15, 27, and 48 months after construction, and the laboratory samples were prepared im-

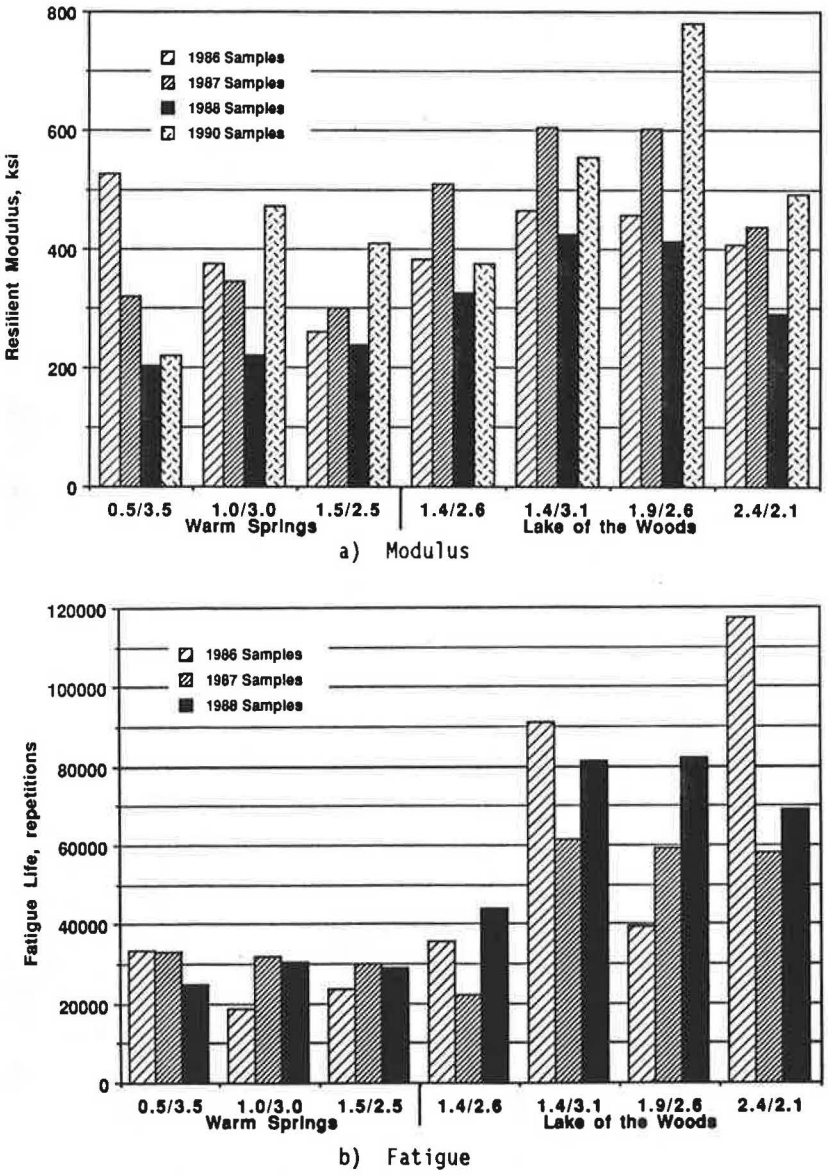

FIGURE 4 Modulus and fatigue results for laboratory samples.

mediately after the pavement was recycled and were tested 4, 16, 28, and 49 months after fabrication using an ambient cure condition (i.e., 25 ± 2°C). The reason for the difference in ages is that the testing of the field cores required 1 month to complete.

Summary of Results

The results of tests made on both field cores and laboratory-prepared samples are summarized in Table 6. The results for the laboratory samples are those with the design emulsion contents (1.0 percent for Warm Springs, 1.9 percent for Lake of the Woods). Figures 6–8 compare test results for field core versus laboratory samples for percent voids, modulus, fatigue, Marshall stability, and flow.

To compare the results, statistical analyses were performed on the data obtained from each test method to determine, at a 5 percent significance level ($\alpha = 0.05$), whether the mean of the laboratory test results was equal to the mean of the field core test results (null hypothesis), with the alternative hypothesis being that the means are not equal. These analyses are summarized in Table 7. As indicated, the means were not found to be significantly different for the modulus and Marshall stability tests; the means for the fatigue and flow test results were found to be significantly different at the 5 percent significance level.

Discussion of Results

The comparison of test results for field cores versus laboratory samples generally indicate the following:

1. The voids of the laboratory-prepared samples are about the same as or slightly higher than those of the field cores

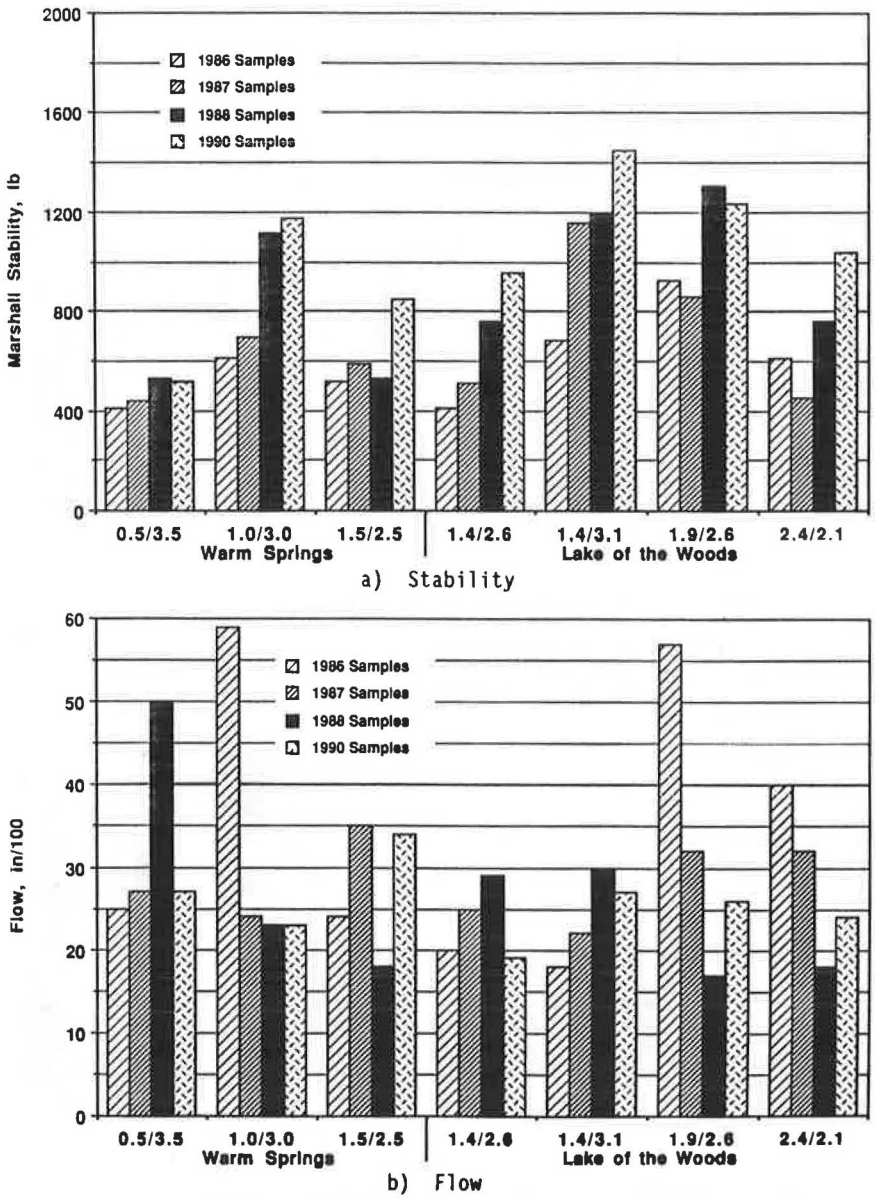

FIGURE 5 Marshall stability and flow results for laboratory samples.

(Figure 6). The air void contents for the laboratory samples would be expected to remain essentially equal over time, while those for the field cores would be expected to decline. The erratic nature of the results suggests errors in measurement or variability of the mix. Nevertheless, the compactive effort used in preparation of the laboratory samples appears to be at about the correct level.

2. The laboratory-prepared sample modulus values are not significantly different from those of the field core modulus values at the 5 percent significance level (see Figure 7a).

3. In general, the comparison of fatigue lives between field cores and laboratory samples is, at best, fair (the means are significantly different at a 5 percent significance level but not at a 1 percent significance level). The fatigue lives of the Warm Springs field cores are generally greater (except initially) than those of the laboratory samples, as shown in Figure 7b. The opposite is true of the results for the Lake of the Woods section; the fatigue lives of the laboratory samples are greater than those of the field cores, except for the 1988 test results in which the fatigue lives are essentially equal. The differences in fatigue lives between field cores and laboratory samples may be due to the significant differences in curing temperatures.

4. The comparison of Marshall stabilities between field cores and laboratory samples are, in general, good (the means are not significantly different at the 5 percent significance level). As shown in Figure 8a, the stabilities of the laboratory samples for the Warm Springs section compare well with those of the field cores. The stabilities of the laboratory samples for the Lake of the Woods section, however, are generally greater than those of the field cores.

5. Except for the first year's test results, the flow values of the laboratory samples compare well with those of the field

TABLE 6 SUMMARY OF TEST RESULTS (LABORATORY VERSUS FIELD)

Specimen Type	Emulsion/ Water Content (%)	Test Period	Percent Voids (%)	Average Resilient Modulus (ksi)		Average Fatigue Life (reps)		Average Marshall Stability (lb)		Average Flow (in./100)	
a) MP 79.2-Wasco Co. Line (Warm Springs)											
Laboratory Sample	1.0/3.0	Fall 1986	11.8	374	(60)	18,673	(7,015)	612	(?)	59	(?)
		Fall 1987	11.2	346	(99)	31,780	(2,653)	694	(98)	24	(4.5)
		Fall 1988	9.7	221	(28)	30,373	(9,330)	1,116	(144)	23	(3.6)
		Summer 1990	12.7	473	(55)	*		1,173	(24)	23	(5.1)
Field Core	1.0/2.4	Fall 1986	12.8	305	(243)	11,030	(5,053)	694	(80)	59	(5.7)
		Fall 1987	7.4	242	(15)	50,010	(17,709)	861	(81)	19	(3.0)
		Fall 1988	11.7	377	(30)	53,965	(12,800)	1,106	(22)	21	(1.5)
		Summer 1990	7.4	527	(8)	150,000+		1,811	(71)	17	(2.1)
b) Lakeshore Dr.-Greensprings Jct. (Lake of the Woods)											
Laboratory Sample	1.9/2.6	Fall 1986	17.7	457	(98)	39,333	(10,874)	928	(?)	57	(?)
		Fall 1987	17.0	603	(74)	59,269	(25,899)	861	(17)	32	(1.2)
		Fall 1988	15.2	412	(56)	82,059	(19,597)	1,307	(228)	17	(1.5)
		Summer 1990	17.4	780	(33)	*		1,236	(285)	26	(7.2)
Field Core	1.8/1.6	Fall 1986	10.9	513	(107)	5,863	(4,354)	605	(100)	29	(13)
		Fall 1987	15.7	504	(62)	34,261	(5,536)	614	(27)	19	(0.6)
		Fall 1988	14.6	530	(16)	78,731	(13,847)	1,171	(43)	24	(3.8)
		Summer 1990	13.0	727	(58)	250,000+		1,597	(134)	17	(1.2)

*Fatigue tests were not performed on the laboratory samples in Summer 1990
Note: Parentheses contain standard deviations

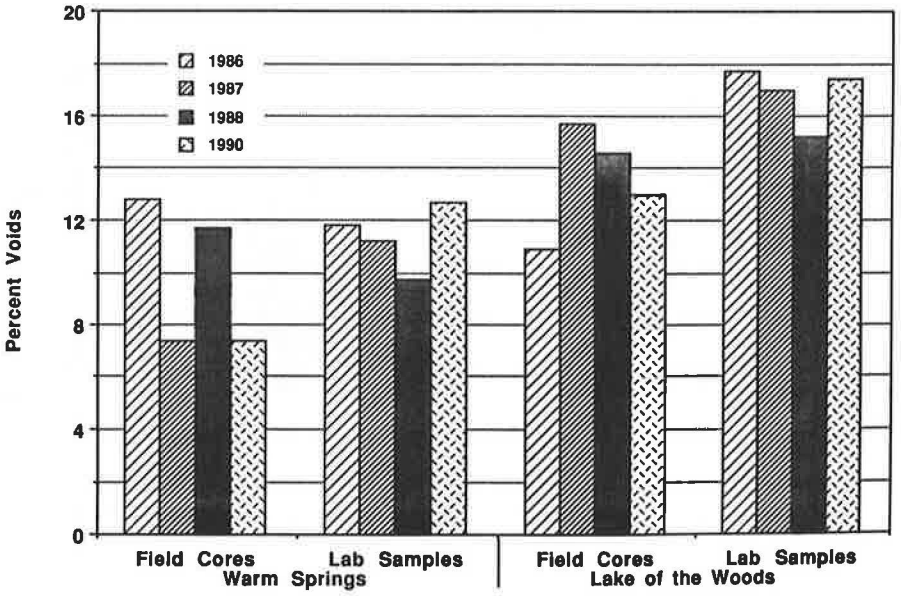

FIGURE 6 Comparison of void contents—field cores versus laboratory samples.

cores for both sections (Figure 8b). However, overall, the means were found to be significantly different at the 5 percent significance level.

COMPARISON OF CIR VERSUS CONVENTIONAL HOT MIXES

This secton compares the resilient modulus and fatigue of CIR mixtures and conventional hot mixes. The results of tests performed on cores from the Warm Springs and Lake of the Woods sections are shown in Table 8 along with results of tests performed on conventional hot mixes (*3,4*). The hot mixes are a Class B mix (*5*), with 5 to 6 percent asphalt intentionally compacted to acquire high air void contents. The results of tests performed on these mixes were chosen for the comparison because these mixes have void contents similar to those of the CIR mixes and were tested under similar conditions. The results in Table 8 are shown graphically in Figure 9.

The CIR mixes, which typically have high voids, show little change in mix properties with significant changes in void contents. Figure 9a clearly shows that significant changes in void content (up to 5.4 percent) have little effect on the modulus of either CIR project. Similarly, Figure 9b shows that, for the Warm Springs project, the fatigue life can be essentially

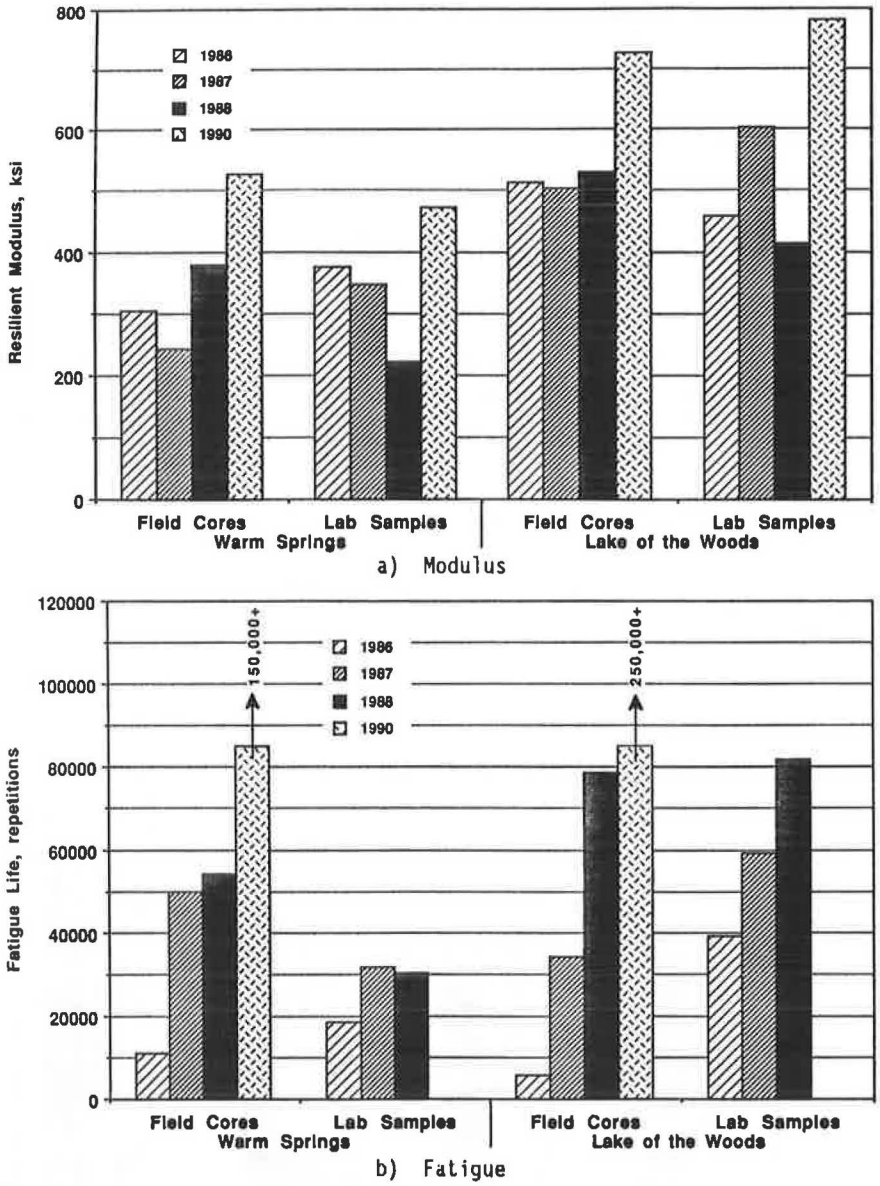

FIGURE 7 Comparison of modulus and fatigue results—field cores versus laboratory samples.

equal at significantly different void contents *or* significantly different at nearly equal void contents. The latter finding also holds true for the Lake of the Woods section. The significant increases in fatigue life are more likely caused by long-term softening of the original binder in the pavements than by increases or decreases in void content.

The void content of the hot mixes, however, has a clear and significant effect on the mix properties. As shown in Figure 9a, the modulus decreases appreciably with increased void content. Figure 9b shows the same trends for fatigue—decreased fatigue with increased void content—but the effect is not as dramatic as with the modulus.

These plots indicate that the CIR mixes generally have slightly higher modulus values and significantly greater fatigue lives relative to the hot mixes at similar void contents. This finding may indicate that CIR mixes behave more like open-graded mixes than dense-graded mixes.

CONCLUSIONS

The following conclusions appear to be warranted from this study:

1. The sample preparation procedure that was developed allows fabrication of specimens from RAP that closely simulate the void content of the pavements in the field.
2. Moderate deviations (± 0.5 percent) from the design emulsion content generally have little effect on the modulus of laboratory-prepared specimens. This finding is also true of

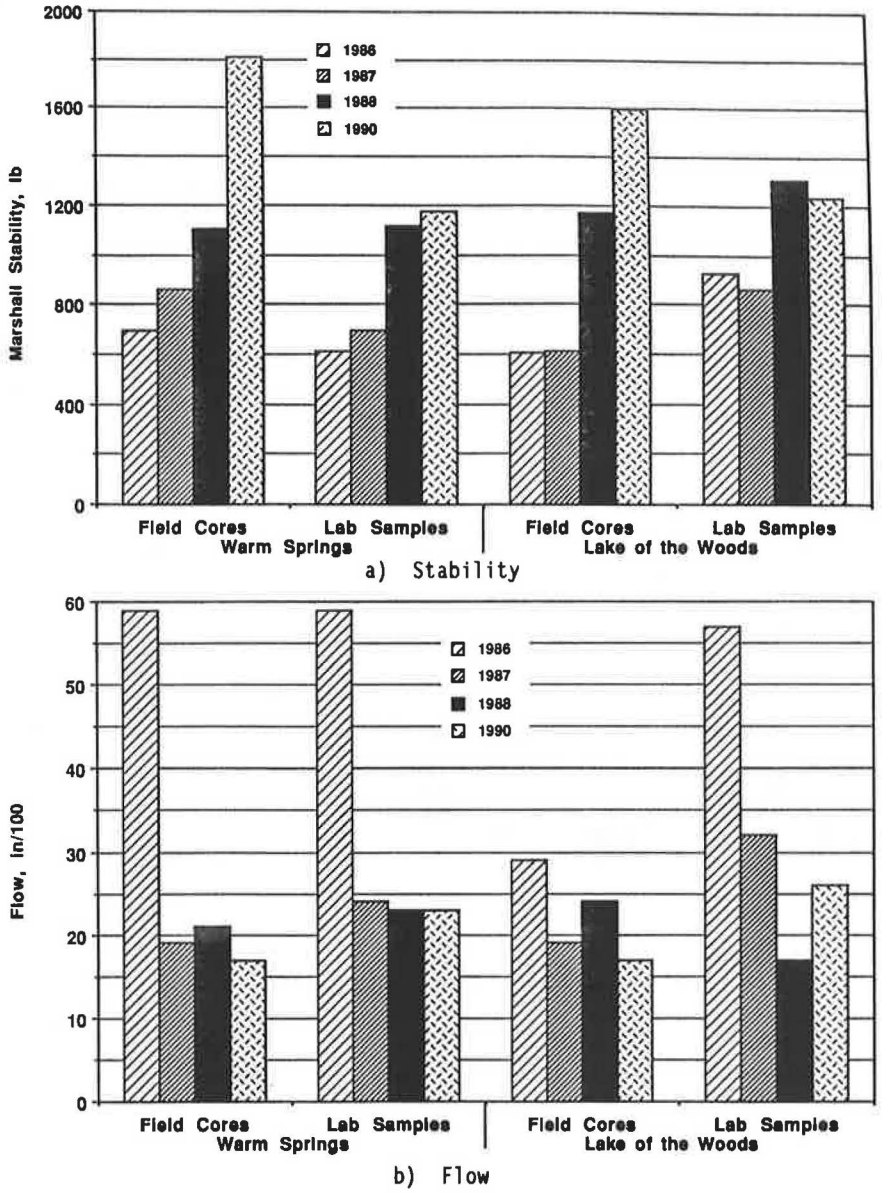

FIGURE 8 Comparison of Marshall stability and flow values—field cores versus laboratory samples.

TABLE 7 SUMMARY OF STATISTICAL ANALYSIS (LABORATORY VERSUS FIELD)

Test	Section	F	$F_{crit.}$ $\alpha = 0.05$	Significant Difference ?	P-value
Modulus	Warm Springs	0.056	4.49	No	P > 0.05
	Lake of the Woods	0.039	4.49	No	P > 0.05
Fatigue	Warm Springs	5.403	4.75	Yes	0.01 > P > 0.05
	Lake of the Woods	8.102	4.75	Yes	0.01 > P > 0.05
Marshall Stability	Warm Springs	1.897	4.75	No	P > 0.05
	Lake of the Woods	0.008	4.75	No	P > 0.05
Flow	Warm Springs	7.048	4.75	Yes	0.01 > P > 0.05
	Lake of the Woods	10.227	4.75	Yes	0.001 > P > 0.01

TABLE 8 CIR VERSUS HOT-MIX TEST RESULTS

Mix Type	Project	% Voids	Resilient Modulus (ksi)	Fatigue Life
CIR	Warm Springs	7.4	242	50,010
		11.7	377	53,965
		12.8	305	11,030
	Lake of the Woods	10.9	513	5,860
		14.6	530	78,731
		15.7	504	34,261
Hot Mix	Castle Rock-Cedar Creek	8.2	466	44,209
		13.2	238	10,426
		14.4	163	6,853
	Warren-Scappoose	8.0	736	9,166
		11.6	265	8,366

the Warm Springs fatigue specimens. However, for the Lake of the Woods section, the emulsion content significantly affected the fatigue life of the laboratory specimens. The effect of emulsion content is clearly indicated by the Marshall stabilities although no clear trends are evident by the flow values. Thus, from these observations, the Marshall stability appears to be the best test for design purposes.

3. The modulus and fatigue results from the fall 1986 test period (3 to 4 months after the pavements were constructed), when used as mix design criteria, predict an initial emulsion content of 0.5 percent for the Warm Springs section and 1.4 percent for the Lake of the Woods section. The fall 1986 Marshall stability test results predict 1.0 percent and 1.9 percent emulsion contents (those used in the field) for the Warm Springs and Lake of the Woods sections, respectively. When

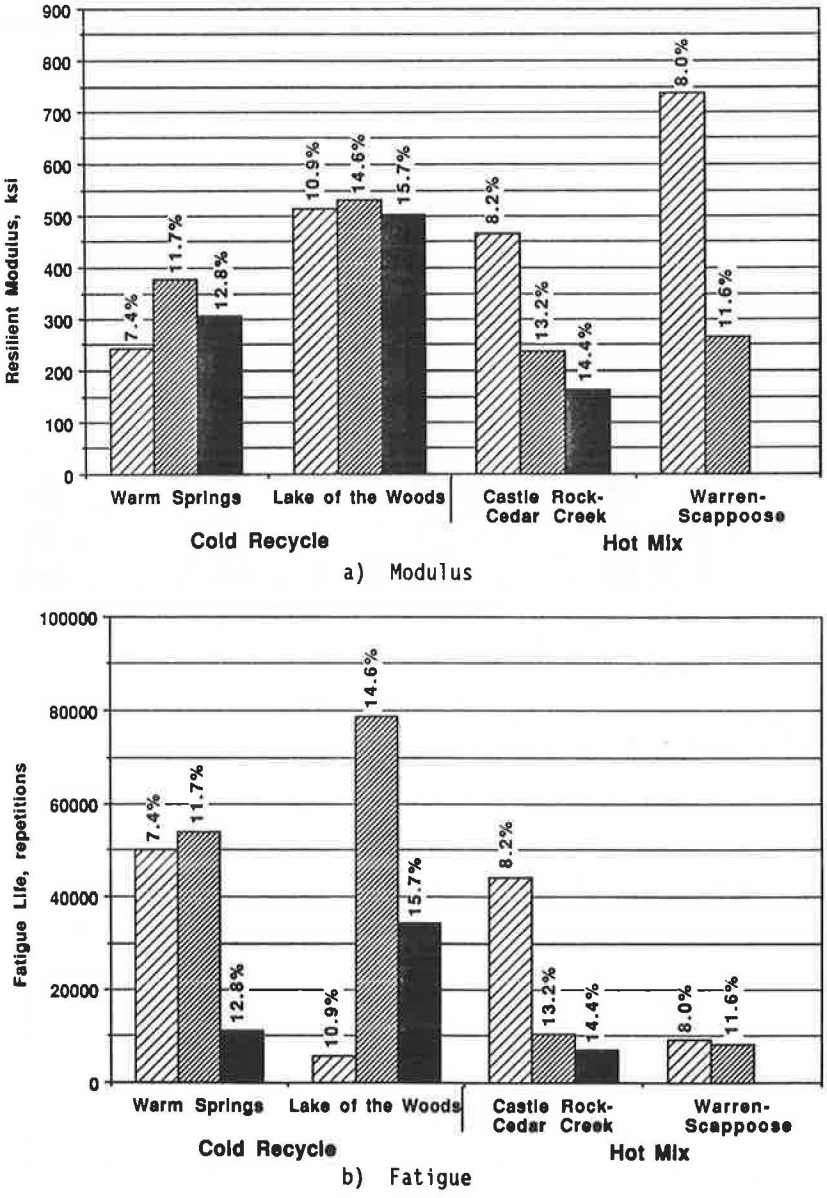

FIGURE 9 Comparison of CIR versus hot-mix modulus and fatigue test results (percentages are air void contents).

consideration is given to stabilities and flow values together, a 1.4 percent emulsion content might be used for the Lake of the Woods section. In short, only the Marshall stability predicted the emulsion content that was used in the field.

4. In general, the mix property test results of laboratory-prepared samples compare well with those of the field cores. In particular, the modulus and Marshall stability results show a good comparison, while the comparison of the fatigue and flow results is, at best, fair.

5. At similar void contents, CIR mixes generally have slightly greater modulus values and significantly greater fatigue lives relative to conventional hot mixes intentionally compacted to acquire high air void contents. This finding indicates that CIR mixes can provide a significant contribution to the pavement structure.

6. Total liquids content must be adequate to disperse the emulsion throughout the mix. There was an adverse effect on material properties (Figures 4 and 5) when Lake of the Woods specimens were prepared with insufficient addition of water (4 percent total liquids).

ACKNOWLEDGMENTS

The authors are grateful for the cooperation of the Oregon State Highway Division Region 4 field staff in Bend, Oregon, and to the personnel in the State Materials Laboratory in Salem, Oregon. Special appreciation is extended to Randy Davis, David Foster, and Patty Jo Walters of Region 4 and to Glenn Boyle and the staff in the Materials and Research Section of the Oregon State Highway Division. The authors are also indebted to John Morgan of Oregon State University, who assisted in the laboratory testing progam as well as in writing this paper. The financial support provided by the Oregon Department of Transportation and FHWA is gratefully acknowledged. The paper has not yet been reviewed by FHWA.

REFERENCES

1. R. G. Hicks et al. *Development of Improved Mix Design and Construction Procedures for Cold In-Place Recycled Pavements.* Interim Report, Vols. I and II. Report FHWA-OR/RD-87-06. FHWA U.S. Department of Transportation, 1987.
2. T. Scholz et al. *Repeatability of Testing Procedures for Resilient Modulus and Fatigue.* Report FHWA-OR/RD-89-09. FHWA, U.S. Department of Transportation, Sept. 1989.
3. J. L. Walter et al. *Impact of Variations in Material Properties on Asphalt Pavement Life—Evaluation of Warren-Scappoose Project.* Interim Report. FHWA/OR-81-7. FHWA, U.S. Department of Transportation, Dec. 1981.
4. J. L. Walter et al. *Impact of Variation in Material Properties on Asphalt Pavement Life—Evaluation of Castle Rock–Cedar Creek Project.* Interim Report. Report FHWA/OR-81-6. FHWA, U.S. Department of Transportation, Dec. 1981.
5. W. J. Quinn et al. *Mix Design Procedures and Guidelines for 1. Asphalt Concrete; 2. Cement-Treated Base; 3. Portland Cement Concrete.* Report MLTS-87-0002. Oregon Department of Transportation, Salem, April 1987.

Analysis of Crack Propagation in Asphalt Concrete Using Cohesive Crack Model

YEOU-SHANG JENQ AND JIA-DER PERNG

A cohesive crack model, which is similar to the Dugdale-Barenblatt model, was proposed to simulate the progressive crack development in asphalt concrete. Tensile strength, fracture energy, and the stress-separation relationship are the basic material properties associated with this model. To evaluate the material properties, indirect tensile tests and three-point bend tests were performed. From these experimental results, the effects of temperature on Young's modulus, the fracture energy, and the indirect tensile strength were evaluated. To determine the stress-separation relationship, a numerical simulation (or curve-fitting method) was used. Using the material properties obtained from the experimental study, temperature effects on different fracture parameters (i.e., critical stress intensity factor and critical J-integral) were studied. The theoretical predictions were found to be in good agreement with the available experimental results. This finding also indicates the potential applications of the proposed model in evaluating the performance of asphalt concrete pavements.

Asphalt concrete is composed of brittle inclusions (aggregates) and viscous matrix (asphalt cement). Because of the viscous matrix, asphalt concrete behaves like a viscoelastic material. As a result, the stress-strain response depends on the loading rate and the environmental temperature. A basic understanding of the time-dependent response of asphalt concrete can be qualitatively obtained by the use of rheological models. The simplest model is the Maxwell model, which consists of a spring (providing the elastic response) and a dashpot (providing the viscous response) connected in series. A more realistic representation of actual behavior of asphalt concrete can be modeled using the Burger model (*1*). In general, the strain (ε) of a viscoelastic material such as asphalt concrete can be expressed as a function of time (t), temperature (T), and loading rate $\dot{\sigma}$. That is,

$$\varepsilon = \varepsilon(t,T,\dot{\sigma}) \tag{1}$$

However, it should be noted that Equation 1 is valid only for undamaged materials. To model crack propagation in asphalt concrete, a separate criterion is necessary.

FRACTURE CRITERIA

Selection of fracture criteria, which can be used to estimate the fracture strength and service life of a structure, is an important aspect of pavement design. For example, the existence of joints and cracks often causes stress concentration as well as a redistribution of stress. As a result, the failure strength predicted using a conventional strength criterion—namely, that a material will fail if the tensile strength is exceeded—may not be reliable and may overestimate the actual strength of the structure. Therefore, to properly estimate the fracture resistance of asphalt concrete, a fracture mechanics concept must be incorporated.

The distribution of the stresses in front of a crack tip (σ_{ij}) (only Mode I tensile condition is considered here) can be expressed by the following equation:

$$\sigma_{ij} = \frac{K_I}{(2\pi x)^{1/2}} + \text{higher order terms} \tag{2}$$

where

x = distance from the crack tip,
K_I = Mode I stress intensity factor, and
σ_{ij} = near tip stresses.

K_I is a function of the applied load, the crack length, and the shape of the specimen. Equation 2 indicates that the stresses around the crack tip are square-root singular. This also implies that a material with a crack cannot sustain any applied load if one assumes the strength criterion. However, it has been observed that a material with flaws or sharp cracks still has the ability to resist a certain amount of applied loads. This observation clearly indicates that a conventional strength criterion is not appropriate in estimating the crack resistance of asphalt concrete.

To overcome the drawbacks of strength criteria, Griffith (*2*) proposed a constant surface energy concept in 1921. He proposed that a brittle body fails because of the presence of many internal cracks or flaws that produce local stress concentration. He stated that the elastic body under stress must transfer from an undamaged state to a damaged state by a process during which a decrease of the potential energy takes place. He also stated that fracture instability is reached when the increase in surface energy, which is generated by the extension of the crack, is balanced by the release of elastic-strain energy in the volume surrounding the crack. For an infinitely large plate with an initial crack length of $2a$ and subjected to a uniform tension, σ_0, Griffith's energy criterion for crack propagation can be presented mathematically as

$$\delta U \geq \delta U_{SE} \tag{3}$$

where δU is the decrease in potential energy due to increased crack surface and δU_{SE} is the increase in surface energy due to increased crack surface.

Department of Civil Engineering, Ohio State University, Columbus, Ohio 43210.

The expression for the critical stress (σ_c) at which a crack will propagate based on the Griffith energy criterion can be written as

$$\sigma_0 = \sigma_c \text{ (crack driving force = fracture resistance)} \quad (4)$$

and

$$\sigma_c = \left(\frac{2\tau E}{\pi a}\right)^{1/2} \quad (5)$$

where τ is surface energy per unit area, and E is Young's modulus.

According to Irwin (*3*), the following relation can be derived between the Mode I stress intensity factor (K_I) and the energy release rate (G):

$$K_I = (EG)^{1/2} \text{ for plane stress case} \quad (6)$$

$$K_I = \left(\frac{EG}{1-\nu^2}\right)^{1/2} \text{ for plane strain case} \quad (7)$$

Because the energy release rate is two times that of the Griffith surface energy, the critical stress intensity factor (K_{Ic}) and critical energy release rate (G_c) can be used as crack propagation criteria.

The Griffith energy criterion is based on linear-elastic fracture mechanics (LEFM) assumptions, that is, there is no (or negligible) plastic deformation in the material. However, for most materials, inelastic deformation such as plastic deformation always takes place. Thus, the Griffith criterion must be modified for materials with significant inelastic deformation. Orowan (*4*) and Irwin and Kies (*5*) concluded that even a slight plastic flow that occurs in the brittle fracture case will absorb a great amount of additional energy required to create new surfaces.

Irwin and Kies also recognized that the plastic energy dissipated in material is much higher than the surface energy dissipated. Therefore, they proposed that the surface energy can be neglected when compared with plastic energy. To simulate this type of nonlinear energy dissipation, a cohesive crack model was proposed by Dugdale (*6*) and Barenblatt (*7*).

Dugdale Model

To simulate the plastic fracture process observed in a thin metal plate, Dugdale (*6*) proposed a model that assumed that the length of the plastic zone is much larger than the thickness of the sheet and that the plastic zone is a yielded strip ahead of the crack tip. The material is assumed to be elastic—perfectly plastic so that the stress within the yielded strip equals the yield strength (σ_y). Dugdale also postulated that the effect of yielding is to increase the crack length by the extent of the plastic zone, as shown in Figure 1 for a finite length crack in an infinite medium subjected to a uniform remote stress (σ_0). Within the yielded strip (a_c), the opening of the crack faces is restrained by the closing pressure (or yield stress) (σ_y). The length (d) of this strip can be determined from the condition that the stress field is nonsingular.

By superposing the solutions for the uncracked sheet loaded by a remote tension (σ_0), and for the cracked sheet with

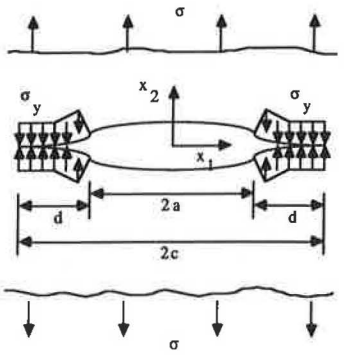

FIGURE 1 Dugdale model.

remote loading and with pressure $p_2(x) = \sigma_0$ for $|x| \leq a$ and $p_2 = \sigma_0 - \sigma_y$ for $a \leq |x| \leq c$ on the crack surface (Figure 1), Dugdale came to an expression for the length of the plastic zone:

$$d = 2a \cdot \sin^2\left(\frac{\pi\sigma_0}{4\sigma_y}\right) = \frac{\pi}{8}\left(\frac{K_I}{\sigma_y}\right)^2 \quad (8)$$

He found very good agreement between the measured lengths of the plastic zones in steels from experimental results and the predictions based on Equation 8 for σ_0 as large as $0.9\sigma_y$. It should be noted that the specific energy dissipation for crack formation in this model is unbounded, which is not a reasonable assumption for most materials.

Barenblatt Model

As in the Dugdale model, Barenblatt (*7*) proposed that a cohesive force acts across a fracture process zone ahead of the real crack tip. However, unlike the yielding consideration assumed by Dugdale, the cohesive force in the Barenblatt model is from molecular force consideration, and the cohesive force depends on the opening displacement along the crack. As a result, specific energy dissipation for crack formation is bounded, which is a more realistic assumption.

The cohesive crack concept was later successfully extended by Hillerborg et al. (*8*) to study nonlinear fracture process in portland cement concrete.

COHESIVE CRACK MODEL FOR ASPHALT CONCRETE

To properly model the crack propagation in asphalt concrete, a cohesive crack model, which is similar to the Dugdale-Barenblatt model, is proposed. Some fundamental concepts and basic assumptions regarding the proposed cohesive crack model are discussed first.

Basic Assumptions

To simulate the fracture process using the Dugdale-Barenblatt cohesive crack model, the following assumptions were made:

1. The process zone starts to develop at one point when the first principal stress reaches the tensile strength f_t.
2. The process zone develops perpendicular to the direction of first principal stress.
3. The properties of the materials outside the process zone are governed by stress-strain (σ-ε) relation (e.g., Equation 1 or Figure 2).
4. The material in the process zone is able to transfer stress, and the stress-transferring capability depends on its opening according to the stress-separation (σ-w) curve shown in Figure 3. In addition, this stress-separation relationship depends on the loading rate and the service temperature.

Based on this assumption, the specific energy dissipation can be shown to be bounded, which is a reasonable assumption. An example of the closing pressure along this process zone can be modeled as nonlinear spring coupled with dashpots (see Figure 4).

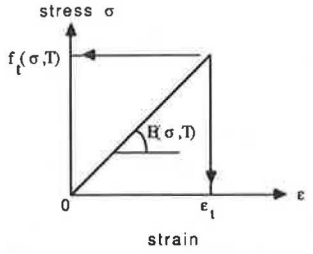

FIGURE 2 Straight line approximation of the σ-ε curve for asphalt concrete.

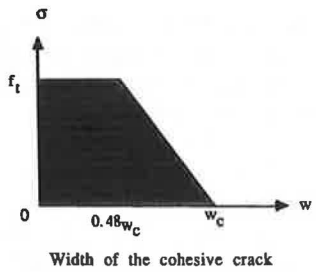

FIGURE 3 Bilinear simulation of σ-w curve for asphalt concrete.

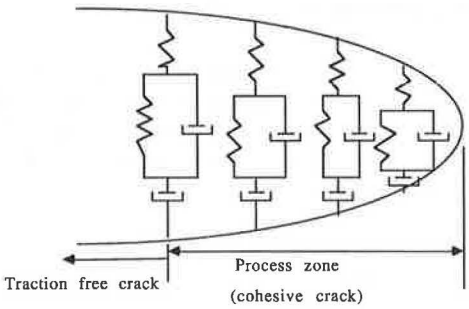

FIGURE 4 Cohesive crack modeled by Burger model.

To obtain the theoretical results using the proposed cohesive crack model, a numerical method such as finite element methods must be applied.

Numerical Formulation

For simplicity, a notched beam is used to demonstrate the numerical formulation. Consider a notched beam with a preexisting crack up to node n subjected to a load P in the midspan, as shown in Figure 5. It is assumed that the process zone will develop along a straight plane, which is reasonable for Mode I crack propagation. When the beam is loaded, by introducing the closing stresses over the crack, one can analyze the progressive crack development in the beam.

In the calculation process, the stresses acting across the cohesive crack were replaced by equivalent nodal forces. These forces can be determined according to the stress-separation (σ-w) curve when the width at the cohesive crack zone is known. As shown in Figure 5, when the first node reaches its tensile strength, the opening at the first node is still equal to zero, that is, $\sigma_1 = f_t$, $w_1 = w_2 = \ldots = w_{n-1} = 0$. From this, one can determine the first point, which corresponds to the crack initiation point of the load-load line deflection (P-δ) curve and the load-crack mouth opening displacement (P-CMOD) curve.

When the crack starts to propagate, as shown in Figure 6, the first node is opened and the second node is assumed to

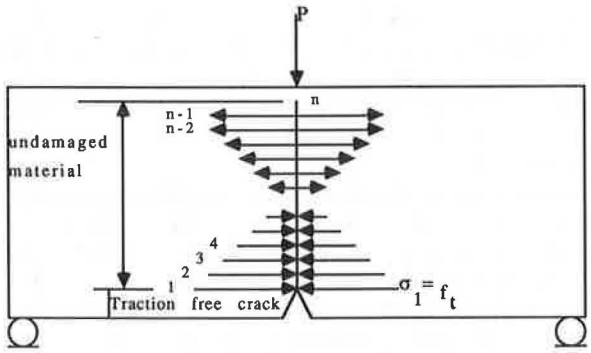

FIGURE 5 Schematic illustration of first step of numerical calculation.

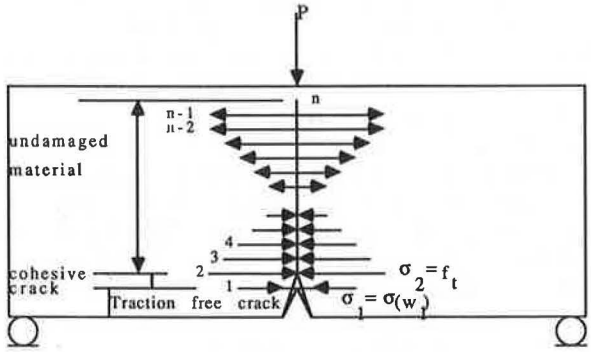

FIGURE 6 Schematic illustration of second step of numerical calculation.

reach the tensile strength. At this point the boundary conditions can be expressed as $\sigma_2 = f_t$, $w_2 = w_3 = \ldots w_{n-1} = 0$, $w_1 \neq 0$, $\sigma_1 = \sigma(w_1)$. The system equations are nonlinear because of the stress-separation constraint, that is, σ_1 depends on the value of w_1, and w_1, on the other hand, is affected by the magnitude of σ_1. Therefore, an iteration process is needed for this step.

Following the same procedure, the progress of the crack propagation can be analyzed and the complete P-δ curve and P-CMOD curve can be generated. More detailed numerical formulation is given elsewhere (*9*).

MATERIAL PROPERTIES

An experimental program is designed to evaluate the material properties associated with the proposed model. The tensile strength, the fracture energy, and Young's modulus were determined using Marshall tablets and beam specimens.

Asphalt Concrete Mix

The asphalt cement used in this study is AC-20 grade, which was purchased from the Koch Company in Ohio. The aggregates are natural gravel and natural sand obtained locally. The gradation of the aggregate satisfies the requirement of 404 mix specified by Ohio Department of Transportation (*10*). The mixing temperature is 300°F, and the compaction temperature is 280°F. A medium traffic condition was assumed; thus, for the asphalt tablets the number of compaction blows at each end of the specimen is 50. The optimum asphalt content according to Marshall mix design is 5.15 percent. This optimum asphalt content was used to produce the asphalt tablets and the beam specimens. The asphalt tablets were used for Marshall stability tests and indirect tensile tests. The beams were used for the three-point bend tests. Some of the beams were sawcut with notch-depth ratios of 0.2, 0.4, and 0.6. The beam specimens are 15 in. long, 2.9 in. high, and 3 in. wide. The asphalt tablets are 4 in. in diameter and 3 in. high.

The tablets were prepared according to the Mix Design Method for Asphalt Concrete (MS-2) recommended by the Asphalt Institute for Marshall stability tests (*11*). The same mixing procedures were used to prepare the beam specimens. However, the beam specimens were compacted statically using a Forney testing machine by applying 10 cycles of static force to the surface of the beams. This procedure ensured that the density of the beam was similar to that of the asphalt tablets.

Indirect Tensile Tests

To measure the tensile strength of asphalt concrete, indirect tensile tests were performed (*12*). The indirect tensile tests were carried out at five temperatures: 18°F, 36°F, 75°F, 104°F, and 140°F. In the 18°F and 36°F cases, the tablets were put in the refrigerator for 1 day to reach the required temperature before testing. In the 104°F and 140°F cases, the tablets were wrapped with a plastic sheet, placed in a plastic bag, and then conditioned in the water bath for 6 hr. An MTS Systems Corporation testing apparatus was used in all of the tests. Displacement control was used to get a complete load versus load-line deflection curve. The loading rate was fixed at 0.03 in./min for the indirect tensile tests. Using this loading rate, the indirect tensile test for each asphalt tablet was finished within 10 min. Thus, the temperature change during the testing process was assumed to be negligible. The applied load and load-line deflection were monitored and recorded by an X-Y recorder. Based on the measured peak load, the indirect tensile strength can be measured and expressed as

$$f_t = \frac{2P_{\max}}{\pi DH} \tag{9}$$

where

$P_{\max}$ = measured peak load,
H = thickness of the tablet,
D = diameter of the tablet, and
f_t = indirect tensile strength.

Since the work done to fracture the specimen is equal to the area under the complete load versus load-line deflection, the fracture energy (G_F) can be expressed as

$$G_F = \left[\int_0^{\delta_{\max}} P(\delta)d\delta\right]/(HD) \tag{10}$$

The area under the P-δ curve was calculated using a planimeter.

Three-Point Bend Test

Figure 7 shows the three-point bend testing setup. The applied load and the load-line deflection were also recorded by an X-Y recorder. From the initial slope of the load-deflection curve, one can determine the modulus of elasticity. The loading rate for this test was 0.125 in./min, and the notch-depth ratios were 0.2, 0.4, and 0.6. Because the area under the load-deflection curve and the work done by the self-weight of the beam are the total energy consumed to break the beam, the fracture energy (G_F) for the beam specimens can be calculated as

$$G_F = \left[\int_0^{\delta_{\max}} p(\delta)d\delta + \frac{1}{2}Mg\delta_{\max}\right]/[(b - a)W] \tag{11}$$

where M is the mass of the beam and g is acceleration of gravity.

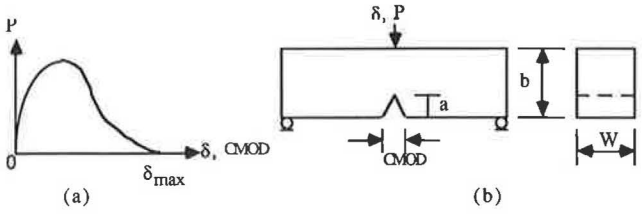

FIGURE 7 Typical P-δ and P-CMOD curves for three-point bend test.

Test Results

The results for indirect tensile tests and three-point bend tests are summarized in Tables 1 and 2. Table 1 shows that the indirect tensile strengths at different temperatures obtained from this study are comparable to the results reported by Kennedy and Hudson in 1968 (*12*). As reported by Kennedy and Hudson, the loading rate, as well as temperature, significantly affects the indirect tensile strength. A higher loading rate, as well as a lower temperature, will result in higher indirect tensile strength. Thus, the experimental results obtained from the present study (loading rate = 0.03 in./min) were judged to be reasonable (Figure 8). It can also be noted that the fracture energy increases as the temperature decreases, indicating that more energy is needed to fracture asphalt concrete at a lower temperature. This observation, at first sight, does not seem to be reasonable because asphalt concrete generally is more brittle at a lower temperature. It should be emphasized that it is the overall change of material properties that causes the brittleness of asphalt concrete observed at low temperatures. This phenomenon will be explained in the parametric study.

The fracture energy (G_F), critical stress intensity factor (K_{Ic}), and net flexural tensile strength (f_t^{net}) for different notch-depth ratios (a/b = 0.2, 0.4, and 0.6) obtained from the three-point bend tests are listed in Table 2. From this experimental study, the following material properties were extracted and are used in the present study:

1. Tensile strength (f_t): The tensile strengths obtained from the indirect tensile tests at different temperatures are used as inputs for tensile strength.
2. Fracture energy (G_F): Because of the end compressive effect of the asphalt tablets, multiple cracks were produced in the indirect tensile specimen test. As a result, the fracture energy obtained from the indirect tensile tests is higher than that obtained from the three-point bend test (Tables 1 and 2). It is therefore appropriate to select the fracture energy

TABLE 1 RESULTS OF INDIRECT TENSILE TESTS

Temp. (°F)	Specimen No.	Indirect tensile strength (f_t) (psi)	Fracture Energy (G_F) (lb/in)	Avg. f_t (psi)	Avg. G_F (lb/in)
18	0-37	293.81	18.41	305.4	19.98
	0-38	309.56	20.94		
	0-39	324.45	20.33		
	0-40	293.94	20.24		
36	0-28	183.15	17.63	189.16	18.66
	0-29	156.17	18.03		
	0-41	213.26	18.19		
	0-42	204.06	20.74		
75	0-20	70.40	9.53	63.39	8.71
	0-21	63.21	9.3		
	0-22	64.59	9.63		
	0-23	57.19	8.14		
	0-24	61.58	6.95		
104	0-33	14.07	1.65	13.70	1.54
	0-34	13.23	1.39		
	0-35	13.80	1.59		
140	0-30	3.70	0.295	3.62	0.276
	0-31	3.53	0.259		
	0-32	3.63	0.274		

TABLE 2 RESULTS OF THREE-POINT BEND TESTS (T = 75°F)

a/b ratio	Specimen No.	P_{max}[1] (lbs)	Net flexural strength	Critical stress intensity factor K_{Ic}, psi$\sqrt{in}$	Fracture Energy G_F[2] (lb/in)	Contribution[3] to G_F due to self-weight
0.2	B-0-10	177.2	203.34	173.99	2.94	0.292
	B-0-9	151.2	183.28	154.68	2.78	0.297
0.4	B-0-8	77.2	159.65	129.17	1.90	0.300
	B-0-7	64.8	128.69	105.18	2.00	0.385
0.6	B-0-6	21.2	98.64	67.51	1.33	0.456
	B-0-5	29.8	144.49	97.87	1.42	0.400
Average			153.02	121.40	2.06	0.355

1. If the self-weight of the beam is considered, an extra 5.45 lbs (i.e., one half of the weight of the beam) must be added to P_{max}.
2. Fracture energy values without the contribution of self-weight.
3. Contribution of self-weight to the fracture energy values.

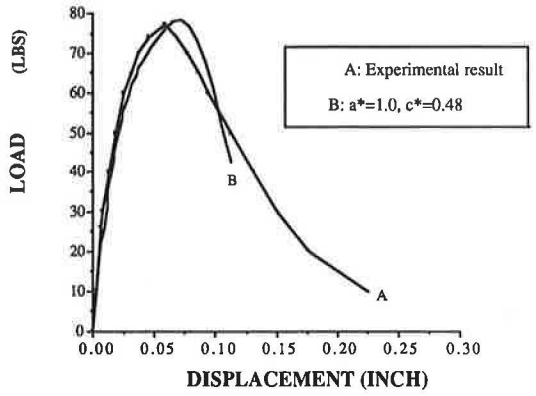

FIGURE 8 Numerical simulation of load versus load-line displacement for $a^* = 1.0$ and $c^* = 0.48$.

obtained from the three-point bend tests instead of that obtained from the indirect tensile test. However, because only the $T = 75°F$ case was performed for three-point bend tests, an alternative method is used to derive the fracture energy-temperature relationship. It was assumed that the temperature effect on G_F is the same for both indirect tensile tests and three-point bend tests. Thus, the fracture energy (G_F) of three-point bend tests can be derived as

$$G_F = 0.355 \times 10^{(1.3226 + 0.0018T - 0.0001187T^2)} \text{ lb/in.} \quad (12)$$

3. Young's modulus (E) and Poisson's ratios (ν): The Young's modulus at different temperatures can be estimated from the initial slope of the P-δ curves obtained from the indirect tensile tests as well as three-point bend tests. Young's modulus (E) was calculated using the linear-elastic fracture mechanics formulas and can be expressed as

$$E(T) = 10^{(5.93906 - 0.0142T)} \text{ psi} \quad (13)$$

Table 3 summarizes the material properties along with the characteristic length [$L_{ch} = G_F \times E/(f_t)^2$]. The effect of asphalt concrete temperature on Poisson's ratios is also included (*13*). It is worth noting that the characteristic length (L_{ch}) is a better indicator for the ductility (or brittleness) of asphaltic materials. It can be shown that the larger the characteristic length, the more ductile the material.

Determination of Stress-Separation Curve (σ-w) for Asphalt Concrete

One can determine the stress-separation relationship from a direct uniaxial tensile test. However, the experimental setup for a direct uniaxial tensile test is very sophisticated and the test results may not be reliable because of possible eccentricity involved in the experimental setup. As a result, an indirect method is used to determine the stress-separation relationship in the present study. Because the actual stress-separation relationship is not known a priori, possible stress-separation relationships were considered by varying the values of a^* and c^*, as shown in Figure 9. By choosing different values of a^* and c^*, the w_c value must be adjusted so that the fracture energy (or area under the curve) will remain the same. A bilinear relationship is used in the present study for simplicity; one can, of course, assume a more complex relationship for the stress-separation curve.

By trying different combinations of a^* and c^*, 25 bilinear σ-w curves with the same fracture energy (G_F) were generated. The values used in the 25 combinations were $a^* = 0.2$, 0.4, 0.6, 0.8, and 1.0 and $c^* = 0.1$, 0.3, 0.5, 0.7, and 0.9.

Figure 10 shows that the predicted load versus load-line deflection response is very sensitive to the shape of the stress-separation (σ-w) curve. It was found that the experimental result can be better reproduced using $a^* = 1.0$ and $c^* = 0.48$, as shown in Figure 8. There are no available data to assess the effects of asphalt grade, aggregate types and gradation, and different additives on the values for a^* and c^*.

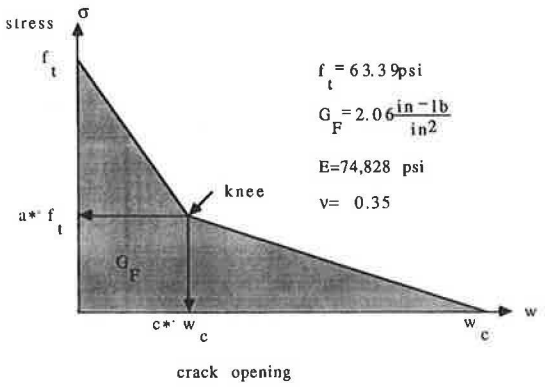

FIGURE 9 Bilinear stress-separation curve for numerical simulation.

TABLE 3 SUMMARIES OF MATERIAL PROPERTIES USED IN PRESENT STUDY

Temperatures (°F)	18	36	75	104	140
Tensile strength f_t (psi)	305.4	189.16	63.39	13.70	3.62
Fracture Energy G_F (lb/in)	4.726	4.413	2.06	0.364	0.065
Young's modulus E (Ksi)	483	268	75	29	9
Poisson's ratio	0.13	0.25	0.35	0.46	0.48
Characteristic length, L_{ch} (in)	24.45	33.03	38.36	56.22	44.31

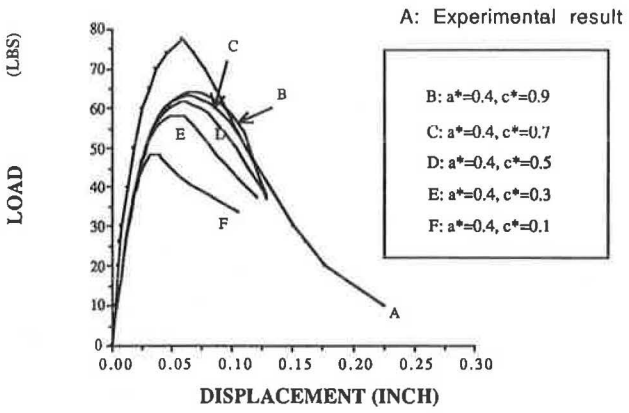

FIGURE 10 Numerical results of load-deflection curves using different stress-separation relationships.

An experimental program at Ohio State University is evaluating these effects.

Using the same stress-separation relationship, the load-deflection curves obtained for different notch-depth ratios (0.4 and 0.6) were found to be satisfactory. It can be concluded that the proposed stress-separation relationship is acceptable and that more experimental data, of course, are needed to obtain a more accurate relationship.

Development of the Process Zone

The stress distribution of the process zone at different loading stages is shown in Figure 11 for a notch-depth ratio of 0.2. The process zone starts to develop when the load is applied. It can be observed that at Stage 1, a small process zone has already developed. Note that no stress exceeds the maximum tensile strength (f_t) along the process zone. At the second stage, the cohesive crack propagates and the process zone is extended. When the peak load is reached (Stage 3), the stress distribution is quite different compared to the linear-elastic one. Nevertheless, the material along the process zone is still able to transfer stress even after the peak load is reached, and the traction free crack will not propagate until the fourth stage is reached.

Temperature Effects on *P*-δ and *P*-CMOD Curves

As shown in Figure 12, the behavior or asphalt concrete becomes more brittle when the temperature decreases; that is, the peak load is reached at a much smaller deformation at lower temperatures. This low-temperature–enhanced brittleness is mainly caused by the increase of Young's modulus and tensile strength values. Although the tensile strength, as well as the fracture energy, is higher at lower temperatures, for the same amount of thermal contractions and deformation (or displacement), asphalt concrete is more susceptible to thermal cracking during winter because of the brittleness enhanced by lower temperatures.

Temperature Effects on Fracture Parameters

By knowing the peak load value obtained from the proposed cohesive crack model, one can also calculate the critical stress intensity factor (K_{Ic}) at different temperatures.

The model prediction shown in Figure 13a indicates that the higher the temperature, the lower the critical stress intensity factor will be. This trend was also reported by Karakouzian (*14*) (see Figure 13b).

Among the various fracture parameters, the J-integral proposed by Rice in 1968 has been widely used (*15*). The J-integral is defined as a path-independent contour integral representing a nonlinear elastic energy release rate. By using the load versus load-line deflection curve obtained from the model, one can measure the area under the curve up to the peak load for different notch-depth ratios. Based on these measurements, U_T and thus J_{Ic} can be determined (*9*). Unlike the critical stress intensity factor, the critical J-integral was found to increase with temperature up to about 40°F and then decreases for much higher temperature (Figure 14a). A similar experimental observation was also reported by Dongre et al. (*16*), as shown in Figure 14b. It is, however, difficult to make conclusions for temperatures higher than 40°F because of the large dispersion observed in the experimental data. More experimental results are needed to verify the theoretical prediction at a higher temperature range.

With the proposed model and the aid of finite element analysis, one can also analyze the crack resistance of a pavement structure. For example, the effects of seasonal and daily thermal cycles, thermal gradients, thermal contraction of concrete slabs, and joint faulting on the performance of asphalt concrete overlay can be objectively analyzed, and the mechanisms that cause premature pavement failure can be better understood. Research results on these effects will be presented elsewhere.

CONCLUSIONS

1. By using the cohesive crack model, progressive crack development in asphalt concrete can be properly simulated. The effects of temperature on the crack resistance of asphalt concrete pavements can thus be objectively evaluated.
2. Based on the proposed model, the effect of temperature on the fracture toughness K_{Ic} can be correctly predicted. However, no definite conclusion can be made about the critical J-integral based on the theoretical predictions and the available experimental results.
3. In this study, the stress-separation (σ-w) relationships were determined using a back-calculation method and were assumed to be the same for various temperatures. To correctly evaluate the effect of temperature on the stress-separation curve, a direct uniaxial tensile test should be performed under different temperatures.
4. The proposed cohesive crack model is very promising in evaluating the temperature effect on the viscoelastic fracture response of asphalt concrete pavements.

ACKNOWLEDGMENTS

Partial support provided by the Ohio Department of Transportation and Illinois Tool Works, Inc., is gratefully appreciated.

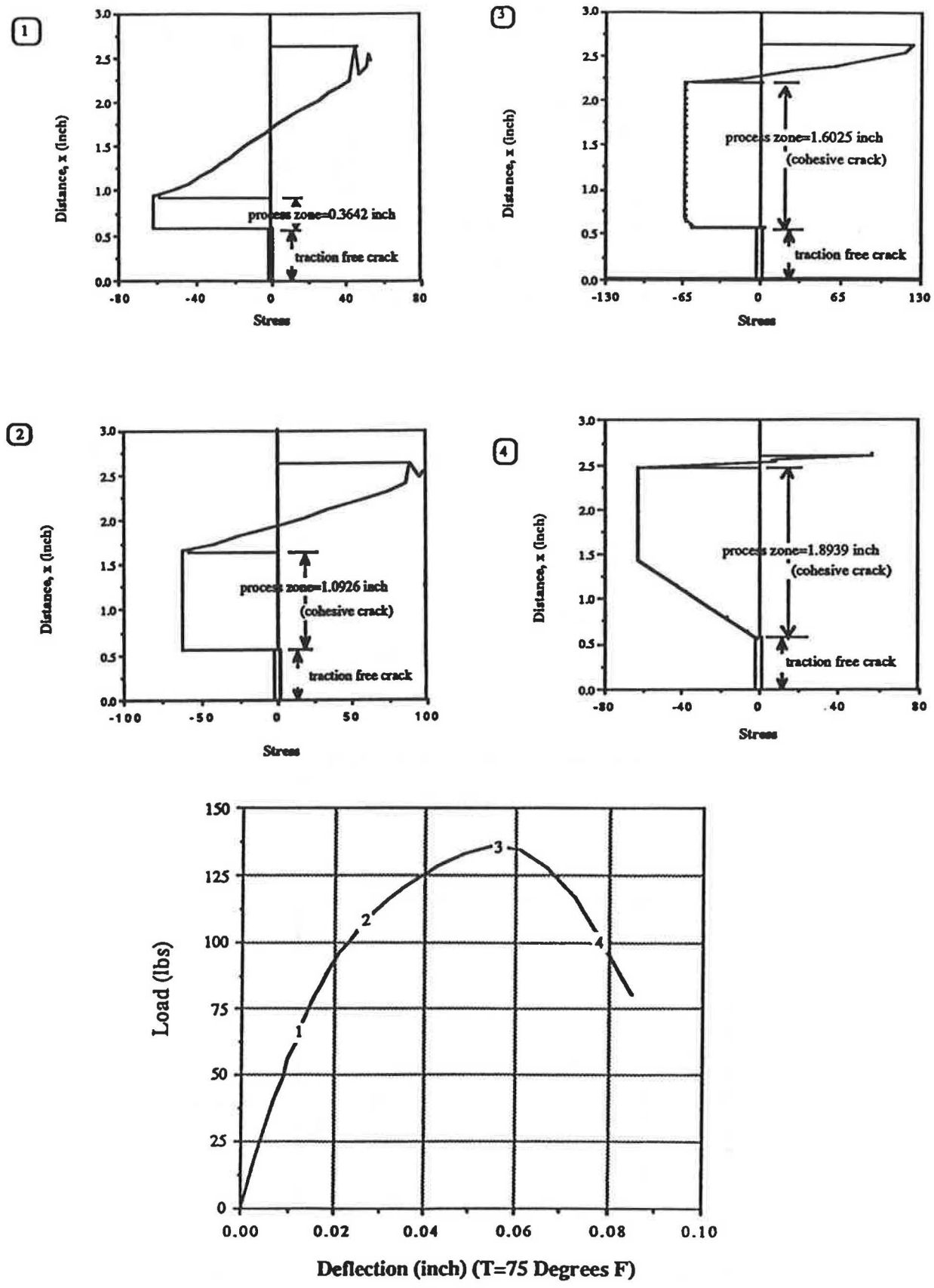

FIGURE 11 Development of process zone at different loading stages.

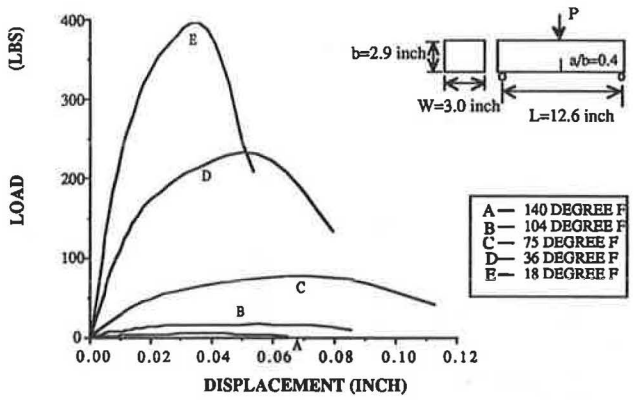

FIGURE 12 Effects of temperature on load-deflection curve ($a/b = 0.4$).

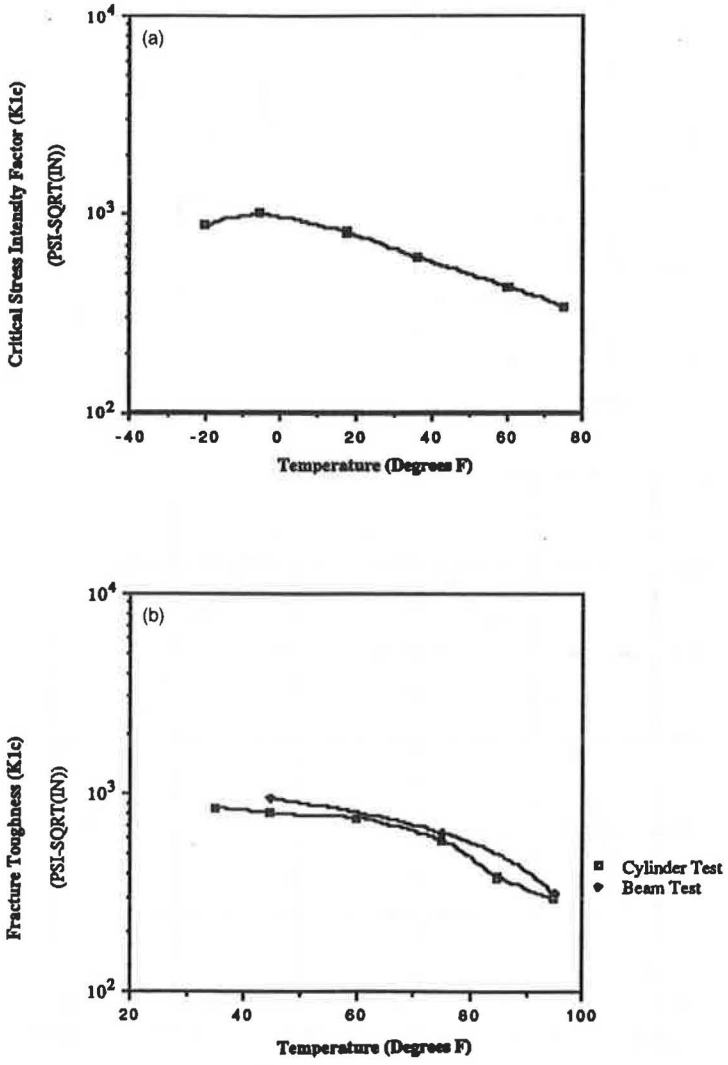

FIGURE 13 Effects of temperature on critical stress intensity factors (K_{Ic}). (a) Theoretical predictions (b) Experimental results

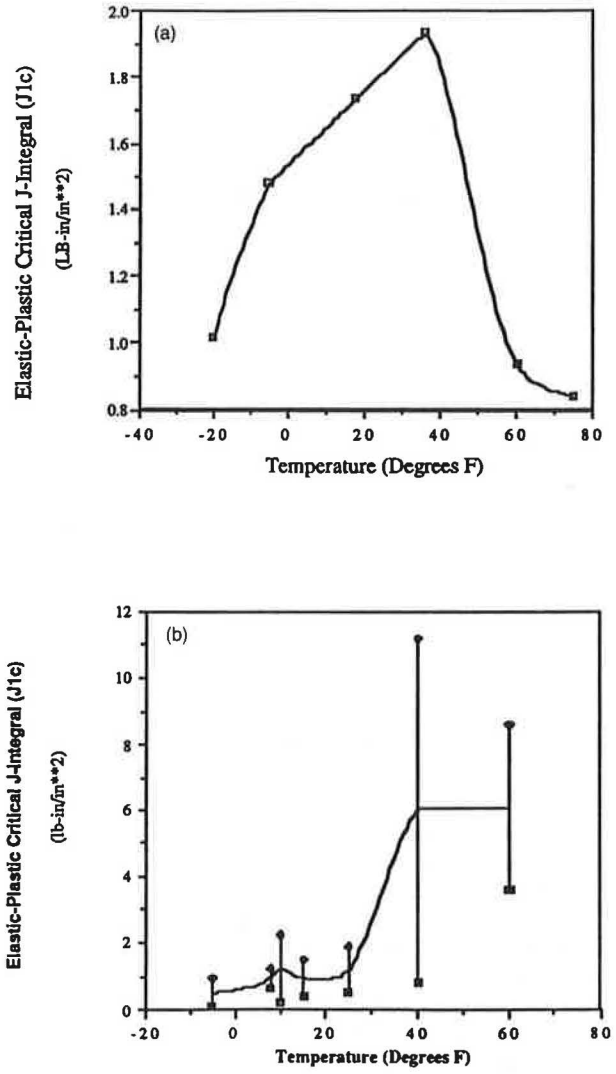

FIGURE 14 Effects of temperature on critical J-integral. (a) Theoretical predictions (b) Experimental results

REFERENCES

1. S. F. Brown. *Time-Dependent Behaviour of Bituminous Material.* Creep of Engineering Materials. Senior Lecture in Civil Engineering, University of Nottingham, England, 1978.
2. A. A. Griffith. Theory of Rupture. *Proc., 1st International Congress in Applied Mechanics*, 1924.
3. G. R. Irwin. Analysis of Stresses and Strains Near the End of a Crack Traversing a Plate. *Journal of Applied Mechanics*, Transaction ASME, Vol. 79, 1957, pp. 361–364.
4. E. Orowan. Energy Criterion of Fracture. *Welding Journal Research Supplement*, March 1955, pp. 157–160.
5. G. R. Irwin and J. A. Kies. Critical Energy Rate Analysis of Fracture Strength. *Welding Journal Research Supplement*, Vol. 33, 1954, pp. 193–198.
6. D. S. Dugdale. Yielding of Steel Sheets Containing Slits. *Journal of the Mechanics and Physics of Solids*, Vol. 8, 1960, pp. 100–108.
7. G. I. Barenblatt. The Mathematical Theory of Equilibrium of Crack in Brittle Fracture. *Advances in Applied Mechanics*, Vol. VII, 1962, pp. 55–129.
8. A. Hillerborg, M. Modeer, and P. E. Petersson. Analysis of Crack Formation and Crack Growth in Concrete by Means of Fracture Mechanics and Finite Elements. *Cement and Concrete Research*, Vol. 6, No. 6, Nov. 1976, pp. 773–782.
9. J. D. Perng. *Analysis of Crack Propagation in Asphalt Concrete Using a Cohesive Crack Model.* M.S. thesis. Department of Civil Engineering, Ohio State University, Columbus, 1989.
10. *Construction and Material Specification.* Department of Transportation, State of Ohio, Columbus, Jan. 1987.
11. *Mix Design Methods for Asphalt Concrete and Other Hot-Mix Types.* Manual Series No. 2, Asphalt Institute, May 1984.
12. J. W. Kennedy and W. R. Hudson. Application of the Indirect Tensile Test to Stabilized Materials. In *Highway Research Record 235*, HRB, National Research Council, Washington, D.C., 1968, pp. 36–48.
13. E. J. Yoder and M. W. Witczak. *Principles of Pavement Design.* John Wiley and Sons, Inc., New York, 1975.
14. M. Karakouzian. *A Simplified Method for Material Testing and Design of Pavement Systems.* Ph.D. dissertation. Ohio State University, Columbus, 1978.
15. J. R. Rice. A Path Independent Integral and the Approximate Analysis of Strain Concentration by Notches and Cracks. *Journal of Applied Mechanics*. Vol. 35, 1968, pp. 379–386.
16. R. Dongre, M. G. Sharma, and D. A. Anderson. Development of Fracture Criterion for Asphalt Mixes at Low Temperatures. In *Transportation Research Record 1228*, TRB, National Research Council, Washington, D.C., 1989, pp. 94–105.

Investigation of Rutting Potential Using Static Creep Testing on Polymer-Modified Asphalt Concrete Mixtures

NEIL C. KRUTZ, RAJ SIDDHARTHAN, AND MARY STROUP-GARDINER

In recent years, polymer-modified asphalt mixtures have been increasingly used in the construction of flexible pavements. These products have gained popularity because of their ability to increase pavement performance in both cold and hot environments. The increased elasticity from the polymer imparted to the mixtures at cold temperature increases the pavement's ability to resist thermal cracking. The increased stiffness, as well as the increased elasticity, of these mixtures at warm temperatures has shown an improved resistance to rutting. The increased resistance to rutting in warm climates was of particular interest for construction projects in the hot desert climate of southern Nevada. To investigate the potential benefits of these polymer-modified materials, the Nevada Department of Transportation (NDOT) placed six polymer-modified experimental test sections between Los Vegas, Nevada, and the Arizona border in December 1989. The University of Nevada, Reno, in conjunction with NDOT, developed a research program to rank the rutting potential of the various mixtures and the increased rutting potential in the presence of moisture. Conclusions from this research were that strains observed in creep testing depend on the location of instrumentation and boundary conditions imposed on the sample. Results showed that a ranking of the materials (lowest to highest strain) was the same for 8-in.-high samples instrumented over the center third or over full depth. A finite element analysis showed that the magnitude of strains observed depends on the area of instrumentation. End friction in the sample can give rise to substantial difference in the creep strain measurements made. Conclusions also indicate that the permanent strains after moisture conditioning appear to be a good indicator of possible moisture damage.

In recent years, polymer-modified asphalt mixtures have been increasingly used in the construction of flexible pavements. These products have gained popularity because of their ability to increase pavement performance in both cold and hot environments. The increased elasticity from the polymers imparted to the mixtures at cold temperature increases the pavement's ability to resist thermal cracking. The increased stiffness and increased elasticity of these mixtures at warm temperatures have improved resistance to rutting. The increased resistance to rutting in warm climates is particularly important for construction projects in the hot desert climate of southern Nevada.

To investigate the potential benefits of these polymer-modified materials, the Nevada Department of Transportation (NDOT) placed six polymer-modified experimental test sections between Las Vegas, Nevada, and the Arizona border in December 1989. The University of Nevada, Reno in conjunction with NDOT developed a research program to rank the rutting potential of the various polymer-modified mixtures and the increased rutting potential in the presence of moisture.

Civil Engineering Department, SEM, Room 105, University of Nevada, Reno, Nev. 89557.

RESEARCH PROGRAM

The objectives of the research program were to

1. Evaluate differences between the various polymer-modified mixtures;
2. Evaluate the impact of moisture on the rutting potential of the mixtures; and
3. Undertake a limited investigation of the impact of sample size and instrumentation location.

NDOT collected samples behind the paver from each of the six experimental test sections placed on I-15 between the Arizona state line and 5.3 miles east of the state line (toward Las Vegas). The variables between the test sections were limited to the binder; both the aggregate source and gradation remained constant.

Permanent deformation (i.e., creep) characteristics were measured using a static unconfined creep test currently under development for adoption by ASTM. Both 4-in.-diameter by 8-in.-high (typical triaxial cell size) samples and 4-in.-diameter by 2.5-in.-high (conventional mix design size) samples were prepared. Deformation was measured over both the full depth and center third of the 8-in. samples. The deformation of the 2.5-in. samples was measured over the full depth only.

The impact of moisture on the permanent deformation was evaluated using the Lottman accelerated conditioning procedure for only the 8-in. samples.

MATERIALS USED IN CONSTRUCTION

The binders used in each of the sections were

- AR4000-R,
- AC-20-RL (L indicates low modifier content),
- AC-20-RH (H indicates high modifier content),
- AC-20-PM,
- AR4000-PM, and
- AC-20-P (control section).

AC-20-R was designated the control section because it is the product currently used by NDOT.

The modifiers used for each of the test sections were listed as proprietary; as of the writing of this paper, specific information has not been released.

The aggregate gradation met a Type II NDOT specification; this is similar to the ASTM D3515 dense-mixture specification of ¾-in. maximum nominal size.

SAMPLE PREPARATION AND TEST METHOD

Sample Preparation

Loose-mix materials were sampled by NDOT during construction and delivered to the university in sealed canisters. This material was reheated and split into individual 1,100-g samples. Each sample was then reheated to 230°F for 2 hr prior to compaction. All samples were compacted with a California kneading compactor using sufficient compactive effort (30 blows at 250 psi) to produce samples with air voids between 6 and 8 percent.

The 8-in. samples were compacted in three lifts of 1,100-g batches placed consecutively on top of each other. Approximately 2.5 in. of the sample was built with each lift. Each lift received the same compactive effort (30 blows at 250 psi). After compaction, samples were placed in a 140°F oven for 1½ hr prior to the application of a 5,000-lb leveling load.

The 2.5-in samples (conventional mix design size) consisted of one 1,100-g batch compacted with 30 blows at 250 psi before being placed in a 140°F oven for 1½ hr prior to the application of a 11,600-lb leveling load.

All samples, regardless of size, were extruded and cooled to 77°F. The heights and bulk specific gravities were then determined according to ASTM D3549 and D2726, respectively.

Creep Testing

The creep test selected was a uniaxial, static, unconfined test. A Satec "Cats" closed-loop system was used for all creep tests. The testing setup for 2.5-in. and 8-in. samples is shown in Figure 1. Sample ends were well greased with a graphite-based lubricant prior to the seating of the loading platens in order to reduce friction between the sample and the platen.

All tests consisted of a static preconditioning followed by a static load. Preconditioning consisted of the application of a 628.5-lb (50-psi) step load for 2 min followed by a 5-min rest period. Testing started immediately at the end of this rest period and consisted of another 628.5-lb (50-psi) static step load applied for 60 min. This step was followed by a 15-min rest period to allow for elastic recovery. Vertical deformations were measured continuously for all samples, but the location of instrumentation varied for the different sample sizes. All samples were tested at 77°F.

The 2.5-in. samples were instrumented over the entire height of the sample with two linear variable differential transducers (LVDTs) placed 180 degrees apart (Figure 1 (*top*)). These deformations were electronically averaged and recorded every 60 sec throughout the test.

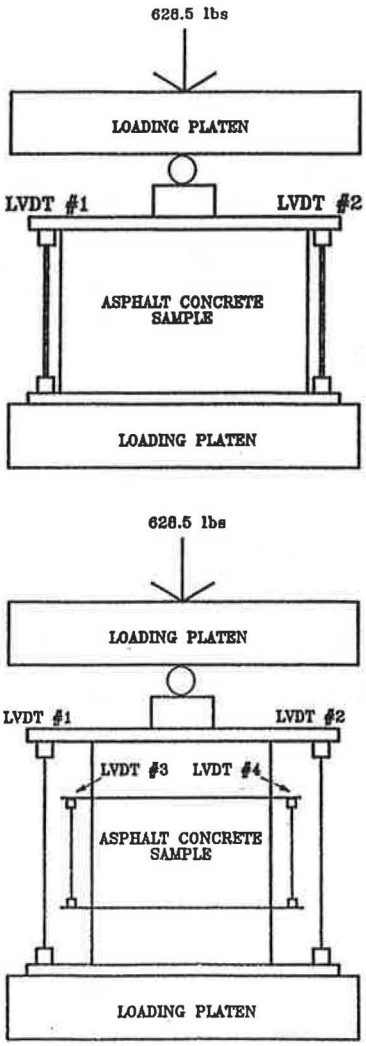

FIGURE 1 Test setup for conventional (*top*) and unconventional (*bottom*) size samples.

The 8-in. samples were instrumented in two locations: (a) over the entire height of the sample, and (b) over the center 3 in. In each location, the deformations were measured on both sides of the sample, 180 degrees apart (Figure 1 (*bottom*)). These deformations were electronically averaged and recorded every 60 sec throughout the test.

The data were then used to calculate compressive strains over the instrumented length:

$$\varepsilon(t) = [(d(t)/H_o)]$$

where

$\varepsilon(t)$ = strain at time t, in./in.;
H_o = original height of the sample or gauge length, in.; and
$d(t)$ = deformation over the instrumented length at time t, in.

This equation was used for both unconditioned and moisture-conditioned samples.

Moisture Conditioning

Selected samples were moisture conditioned consistent with Lottman's procedure for accelerated conditioning used to determine the retained strengths of asphalt concrete materials (*1*). Briefly, this procedure consists of immersing the samples in water and applying a vacuum of 24 in. Hg for 10 min to achieve a minimum of 90 percent saturation. Samples are wrapped in plastic and placed in a 0°F freezer for a minimum of 15 hr. Samples are then unwrapped and transferred to a 140°F water bath for 24 ± 0.5 hr and immediately placed in a 77°F water bath for 2 hr in order to cool to test temperature.

TESTING PROGRAM

A total of seven samples from each of the six test sections were prepared: three 8-in. samples were tested unconditioned, two 8-in. samples were tested after moisture conditioning, and two 2.5-in. samples were tested unconditioned. The number of samples was restricted because of the limited quantity of material on hand. Although the number of samples was not ideal, sufficient data were obtained to estimate standard deviation, variance, and coefficient of variation as well as to evaluate the differences between the binders.

ANALYSIS OF UNCONDITIONED TEST RESULTS

8-in. Samples

Instrumented over the Full Depth

Typical test results over the duration of both the loading and unloading period are shown in Figure 2. The ranking (lowest to highest permanent deformation) of the various materials was as follows:

Binder	*Avg Permanent Strain*
AC-20-RL	0.002636
AC-20-RH	0.003166
AR4000-R	0.005519
AC-20-PM	0.008942
AC-20-P (Control)	0.011277
AR4000-PM	0.011364

It appears that AC-20-RL and AC-20-RH behave similarly. It also appears that AC-20-RL and AC-20-RH and AR4000-R could be expected to exhibit less rutting in the field than either AC-20-P or AR4000-PM.

For the 8-in. samples instrumented over the full depth, within-sample set variance was calculated and an average variance was determined (Table 1). The resulting within-sample set standard deviation (i.e., square root of the average variance) was 0.002175 strain.

Instrumented over the Center Third

The typical data collected over the duration of both the loading and unloading period are shown in Figure 3. The data recorded over the center third for a set of three samples of the same material are much more variable than those recorded over the full depth. After an examination of the test setup, it was concluded that the method of mounting the third-point LVDTs made the electronics sensitive to both machine vibrations and drafts. The impact from drafts can be seen in the discontinuity of the one line; this phenomenon was evident once in most of the sets of three. Therefore, for the analysis, the data with this discontinuity were removed from the data base.

The ranking (lowest to highest permanent deformation) of the various materials for the remaining set of two samples was as follows:

Binder	*Avg Permanent Strain*
AC-20-RL	0.001785
AC-20-RH	0.002263
AR4000-R	0.003529
AC-20-PM	0.004844
AC-20-P (Control)	0.009385
AR4000-PM	0.010131

This ranking is identical to that obtained for the full-depth instrumentation, even with the increased fluctuation of the third-point readings. The conclusions are also similar: the AC-20-RL and AC-20-RH behave similarly, and the AC-20-RL and AC-20-RH, and the AR4000-R could be expected to exhibit less rutting in the field than either the AC-20-P or the AR4000-PM.

For the 8-in. samples instrumented over the center third, within-sample set variance was calculated and an average variance was determined (Table 2). Only two of the three samples tested were instrumented over the center third. The resulting within-sample set standard deviation (i.e., square root of the average variance) was 0.002799 strain.

2.5-in. Samples

Instrumented over the Full Depth

For the 2.5-in. samples instrumented over the full depth, within-sample set variance was calculated and an average variance was determined (Table 3). Graphical representation of a typical set of samples is shown in Figure 4. The resulting within-sample set standard deviation (i.e., square root of the average variance) was 0.000889 strain. The ranking (lowest to highest permanent deformation) of the various materials was as follows:

Binder	*Avg Permanent Strain*
AC-20-P (Control)	0.001924
AR4000-R	0.002574
AR4000-PM	0.003272
AC-20-RL	0.003507
AC-20-RH	0.003514
AC-20-PM	0.004243

The ranking of lowest to highest permanent deformation is considerably different from that obtained from either method of instrumenting the 8-in. samples. The AC-20-P and the AR4000-PM mixtures exhibited the most deformation when 8-in. samples were tested and the lowest strains when 2.5-in. samples were used. The AC-20-RL, AC-20-RH, and the AR4000-R exhibited essentially identical permanent deformation characteristics when the 2.5-in. samples were used for testing.

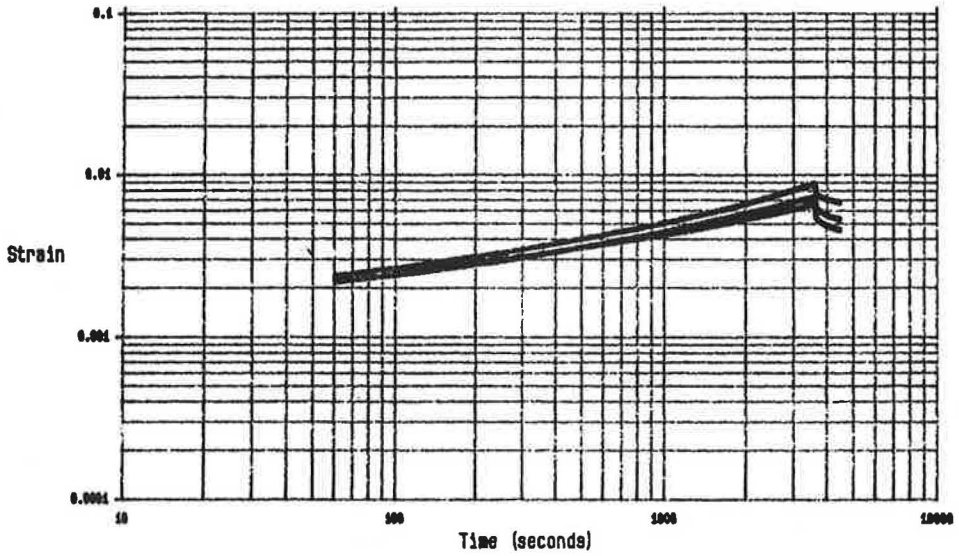

FIGURE 2 Graphical representation of typical set of three unconventional samples, full-depth strain.

TABLE 1 STATISTICAL ANALYSIS OF PERMANENT DEFORMATION FROM 8-in. SAMPLES, FULL-DEPTH STRAIN

Sample Set	Test Number			Ave. Perm. Strain	Variance	Standard Deviation
	1	2	3			
AR4000-R	0.005286	0.006727	0.004545	0.005519	1.23E-06	0.001109
AC-20-RL	0.003920	0.002911	0.002669	0.003166	4.40E-07	0.000663
AC-20-RH	0.000684	0.003314	0.003911	0.002636	2.95E-06	0.001716
AC-20-PM	0.004957	0.008993	0.012877	0.008942	1.57E-05	0.003960
AR4000-PM	0.008019	0.011110	0.014964	0.011364	1.21E-05	0.003479
AC-20-P	0.009452	0.010769	0.013610	0.011277	4.52E-06	0.002125
AVERAGE				0.007151	6.15E-06	0.002175

TABLE 2 STATISTICAL ANALYSIS OF PERMANENT DEFORMATION FROM 8-in. SAMPLES, CENTER THIRD STRAIN

Sample Set	Test Number		Ave. Perm. Strain	Variance	Standard Deviation
	1	2			
AR4000-R	0.003016	0.004042	0.003529	5.26E-07	0.000725
AC-20-RL	0.002427	0.001143	0.001785	8.24E-07	0.000907
AC-20-RH	0.002540	0.001987	0.002263	1.53E-07	0.000391
AC-20-PM	0.003261	0.006427	0.004844	5.01E-06	0.002238
AR4000-PM	0.006013	0.014249	0.010131	3.39E-05	0.005823
AC-20-P	0.004641	0.014129	0.009385	4.50E-06	0.006709
AVERAGE			0.005322	1.42E-05	0.002799

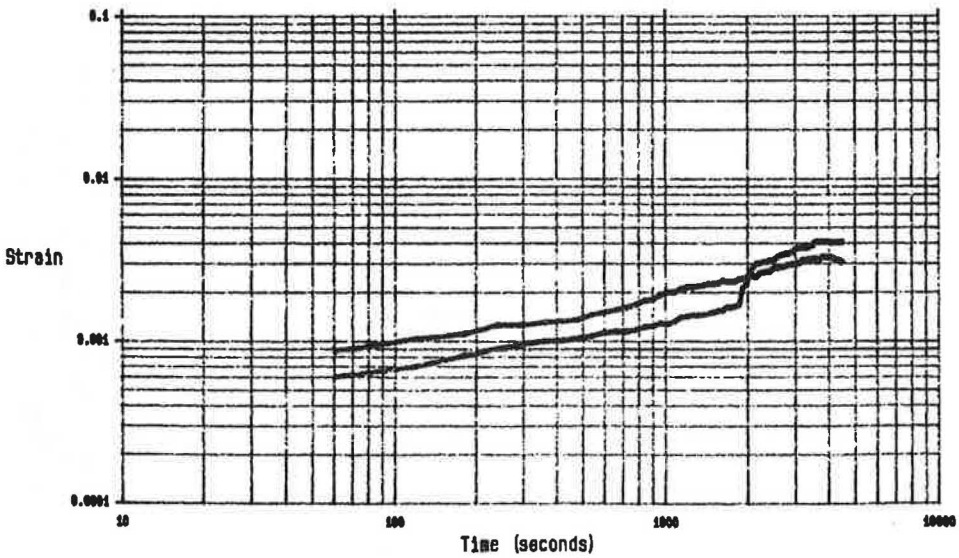

FIGURE 3 Graphical representation of typical set of two unconventional samples, center third strain.

TABLE 3 STATISTICAL ANALYSIS OF PERMANENT DEFORMATION FROM 2.5-in. SAMPLES, FULL-DEPTH STRAIN

Sample Set	Test Number		Ave. Perm. Strain	Variance	Standard Deviation
	1	2			
AR4000-R	0.002045	0.003103	0.002574	5.60E-07	0.000748
AC-20-RL	0.004154	0.002661	0.003407	1.11E-06	0.001055
AC-20-RH	0.002707	0.004321	0.003514	1.30E-06	0.001141
AC-20-PM	0.004127	0.004360	0.004243	2.71E-08	0.000164
AR4000-PM	0.003354	0.003191	0.003272	1.33E-08	0.000115
AC-20-P	0.000429	0.003419	0.001924	4.47E-06	0.002114
AVERAGE			0.003155	1.25E-06	0.000889

Comparison of Test Results for the Two Sample Sizes

While instrumenting an 8-in. sample over either the full depth or the center third generates the identical ranking of the materials, testing the 2.5-in. samples generates a completely different, almost reverse, ranking. Historically, the height-to-width ratio of axially compressed specimens has been 2:1 because of the effect of end constraints. Based on this information, an assumption was made that the testing from the 8-in. samples would generate the more accurate reflection of relative ranking of the material. Once this decision was made, the impact of end constraint influence on the deformation measurements over both the full depth and the center third of the sample needed to be assessed. A finite element method was chosen to perform this analysis.

FINITE ELEMENT ANALYSIS OF 8-in. SAMPLE

A preliminary investigation into the effects on nonuniform stress/strain field in the 8-in. sample using the finite element method was undertaken. If the stress/strain conditions developed under the imposed loading are uniform within the sample, the strain results from both measurements (full depth and center 3 in.) should be the same. When the asphalt concrete sample is axially loaded using the closed-loop testing system, the stresses and strains developed at various points in the sample vary depending on the boundary conditions at the top and bottom of the sample. The nonuniform stress/strain field in the sample may be responsible for the difference in strain measurements obtained for the whole sample and at the middle of the sample. A preliminary investigation using the finite element method into the nonuniform stress/strain field in the sample is presented below.

Finite Element Descritization and Loading

Different boundary conditions between the sample and the top and bottom loading plates can exist. They are

1. No-slip interface condition (Case 1),
2. Smooth interface condition (Case 2), and
3. Partial slip at the interfaces (Case 3).

The third case can be viewed as an intermediate condition between Case 1 and Case 2. Though a coating of lubricant is used at the top and bottom of the sample, smooth interface conditions may not be present. The stress/strain field developed under all three boundary conditions can be calculated using the finite element method.

The finite element method has been successfully used in many engineering problems to evaluate stresses, strains, and deformations of bodies subjected to loading. This method is a very effective tool because it takes into account the variability in the geometry and properties of the materials and the

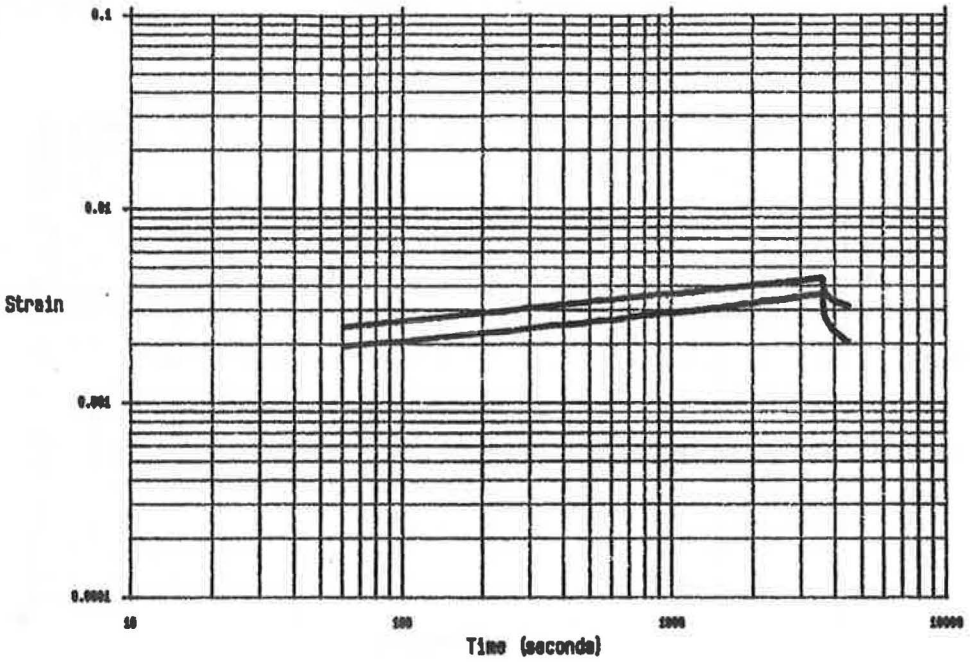

FIGURE 4 Graphical representation of typical set of three conventional samples, full-depth strain.

various boundary conditions. In this method, the entire domain of interest is assumed to be an assembly of a finite number of elements that are connected at the nodal points. By assuming a reasonable variation for displacements within an individual element, it is possible to generate a load-displacement relationship for the entire domain.

A widely used finite element-based program, IMAGES-3D (*2*), was used to analyze the sample behavior under axial loading with the three types of boundary conditions. The axisymmetric finite element descritization and the boundary conditions are shown in Figures 5 and 6. The entire sample was divided into 580 elements of 0.25 in. × 0.1 in. in size. In Case 1 (see Figure 6) the bottom nodes have freedom to move only vertically, thus simulating a no-slip condition at the interface. At the top face, the nodes are fixed. In Case 2, the top and bottom nodes are free to move without resistance (smooth condition) in the radial direction. On the other hand, the third case represents partial slip in which the interface resistance is obtained by multiplying the applied pressure by the coefficient of friction (μ). A value of 0.1 was used in this paper. Material properties in terms of Young's modulus (E) and Poisson's ratio (ν) are necessary to use the finite element program. Representative values of E = 300,000 psi and ν = 0.35 were used. Table 4 gives sample properties and loading used in the computer runs. In all cases, a vertical pressure of 50 psi was applied at the bottom face.

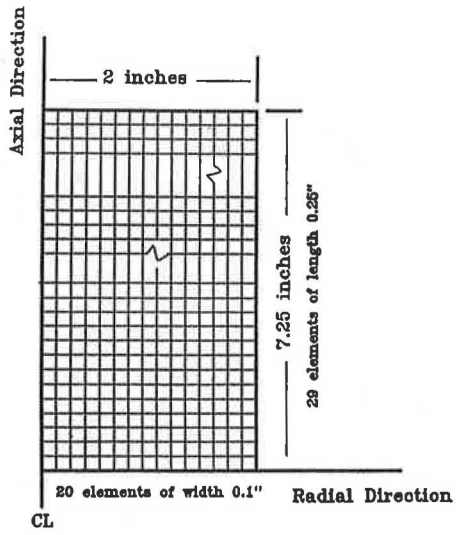

FIGURE 5 Axisymmetric finite element descritization (580 elements, 630 nodes).

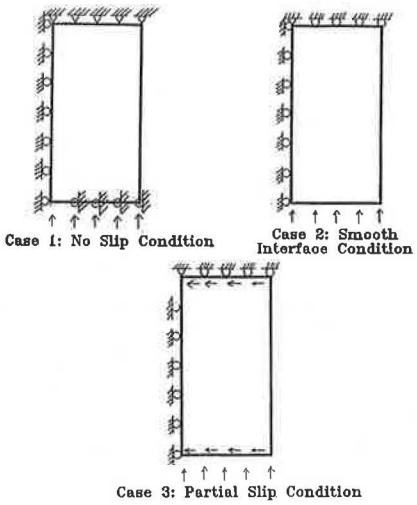

FIGURE 6 Boundary conditions used with the finite element analysis.

Analysis of Finite Element Method Results

The IMAGES-3D program gives displacements at the nodes and stresses and strains at the middle of the elements. The nodal displacements can be used to compute average strains in the sample between any two points. The overall compressive strain in the sample $(\varepsilon_Z)_s$ can be calculated using

$$(\varepsilon_Z)_s = [(u_{top})_{ave} - (u_{bot})_{ave}]/L$$

where $(u_{top})_{ave}$ and $(u_{bot})_{ave}$ are the average vertical displacements at the top and bottom of the sample, and L is the sample length. A similar procedure can be adopted to compare compressive axial strain at the middle of the sample, $(\varepsilon_Z)_m$ using displacements given by the program at two points separated by 3 in. near the middle of the sample. These strain values are shown in Table 5 for all three cases considered in the study. Using the element strain data, it is possible to evaluate the range of maximum and minimum principal normal strains and shear strains in the sample. These values are also shown in the table.

A number of observations can be made from the results in the table. In Case 2 (smooth interface), the strain field in the

TABLE 4 SAMPLE PROPERTIES AND LOADING

Sample Size	
Sample Length	7.25 inches
Sample Radius	2 inches
Material Properties	
Young's Modulus	300,000 psi
Poisson's Ratio	0.35
Loading	
Vertical Pressure	50 psi
Coefficient of Friction	0.1

TABLE 5 RESULTS FROM FINITE ELEMENT ANALYSIS

Computed Strain Response	Case #1	Case #2	Case #3
Axial Composition for Whole Sample (ave.) (10 -6 m/m)	162	167	165
Axial Compressive Strain at Middle of Sample (ave) (10 -6 m/m)	173	167	170
Range of Maximum Principal Strain (10 -6 m/m)	99 to 185	167 to 167	128 to 176
Range of Minimum Principal Strain (10 -6 m/m)	-7 to -74	-58 to -58	-22 to -62
Range of Maximum Principal Shear Strain (10 -6 m/m)	266 to 107	225 to 225	237 to 153

Computed Normal Strain is Considered Positive

sample is uniform and therefore gives identical results for strains computed based on end displacements and those computed using the middle-of-sample displacements. However, there are differences between the strain values in the other two cases (Cases 1 and 3). The difference is within 6.8 percent. Larger compressive strains are obtained when using the middle-of-sample displacements. It should be noted that Case 3, which is a partial friction case, gives results between Case 1 (no slip) and Case 2 (smooth) in all categories.

The range of principal strains (normal and shear) gives a measure of the nonuniformity. In Case 2, the strain field is again uniform, while Cases 1 and 3 give nonuniform strain field. The ranges obtained for strain values in Cases 1 and 3 are quite wide. For example, in Case 1, the maximum principal shear strain range is 107 to 266 μ. In other words, the strain difference between any two points in the sample can differ by as much as 2.5 times. In Case 3, which may be a more realistic representation of the testing conditions, the difference is within 1.6 times.

It is clear from the finite element studies that the nonuniform stress conditions can be present if smooth sample end conditions do not exist. However, though friction may be present, the analysis indicates that the compressive strains obtained for the whole and middle of the sample differ only by a small percentage. It should be recalled that the finite element analysis is based on linear-elastic properties for asphalt concrete. It may be argued that viscoelastic behavior in the asphalt concrete may be responsible for the difference in strain measurements. Though asphalt concrete is viscoelastic, the behavior immediately after the application of the load is linear elastic.

It should be noted that the creep behavior monitored long after the load application can result in much different strain measurements for the whole sample and middle of the sample. This is because the creep behavior, which is mainly a time-varying shear behavior (*3*), varies from point to point in the sample. The difference in shear behavior is brought on by the nonuniform shear strain field present in the sample. The strain obtained for the whole sample is caused by creep behavior of the entire sample; the strain in the middle is caused by creep behavior of the middle region. This is why the difference in strain measurements is not uniform from the start to finish of the creep sample.

ANALYSIS OF MOISTURE-CONDITIONED TEST RESULTS

Previous research conducted for NDOT (*4*) showed that moisture sensitivity, a typical problem for Nevada mixtures, could contribute to increased permanent strain. Because of the limited amount of materials, only 8-in. samples were tested after moisture conditioning. Two samples from each of the six experimental test sections were subjected to moisture conditioning before testing. The resulting data for the full depth and the center 3 in. are shown in Tables 6 and 7. To reduce the number of variables in the experiment, the method of instrumentation, load, and temperature were consistent with the unconditioned data base.

TABLE 6 STATISTICAL ANALYSIS OF PERMANENT DEFORMATION FROM 8-in. SAMPLES, MOISTURE-CONDITIONED, FULL-DEPTH STRAIN

Sample Set	Test Number		Ave. Perm. Strain	Variance	Standard Deviation
	1	2			
AR4000-R	0.009810	0.006646	0.008228	5.01E-06	0.002237
AC-20-RL	0.008715	0.008661	0.008688	1.09E-09	0.000033
AC-20-RH	0.007116	0.007533	0.007324	6.25E-08	0.000255
AC-20-PM	0.009108	0.009304	0.009206	1.92E-08	0.000138
AR4000-PM	0.008611	0.007532	0.008071	4.37E-07	0.000660
AC-20-P	0.010328	0.006149	0.008238	8.73E-06	0.002954
AVERAGE			0.008292	2.38E-06	0.001046

TABLE 7 STATISTICAL ANALYSIS OF PERMANENT DEFORMATION FROM 8-in. SAMPLES, MOISTURE-CONDITIONED, CENTER THIRD STRAIN

Sample Set	Test Number		Ave. Perm. Strain	Variance	Standard Deviation
	1	2			
AR4000-R	0.011839	0.005497	0.008668	2.01E-05	0.004484
AC-20-RL	0.008728	0.006487	0.007607	1.88E-06	0.001372
AC-20-RH	0.005263	0.005550	0.005406	3.09E-08	0.000175
AC-20-PM	0.006491	0.009632	0.008061	4.93E-06	0.002221
AR4000-PM	0.006504	0.007432	0.006968	3.23E-07	0.000568
AC-20-P	0.007686	0.004670	0.006178	4.55E-06	0.002132
AVERAGE			0.007148	5.30E-06	0.001825

Instrumented Over the Full Depth

After moisture conditioning, the ranking of the mixtures was as follows:

Binder	*Avg Permanent Strain*
AC-20-RH	0.007324
AR4000-PM	0.008071
AR4000-R	0.008228
AC-20-P (Control)	0.008238
AC-20-RL	0.008688
AC-20-PM	0.009206

Although the ranking has changed from the unconditioned test results, there is so little variation between the results that there is essentially no difference between the permanent deformation characteristics of the mixtures. Therefore, all mixtures could be expected to exhibit similar rutting distress in the presence of moisture. Previous research has shown that the permanent deformation characteristics after moisture conditioning vary greatly between construction projects; therefore it is hypothesized that the "stripping" potential of the aggregate, not the binder, is the governing factor. Therefore, mixtures prepared with the same aggregate source and gradation, but with different binders, could be expected to exhibit similar permanent deformation characteristics after moisture conditioning.

The within-sample set variance for full-depth and center third instrumentation was calculated and an average variance was determined. The resulting standard deviations were 0.001046 and 0.001825, respectively.

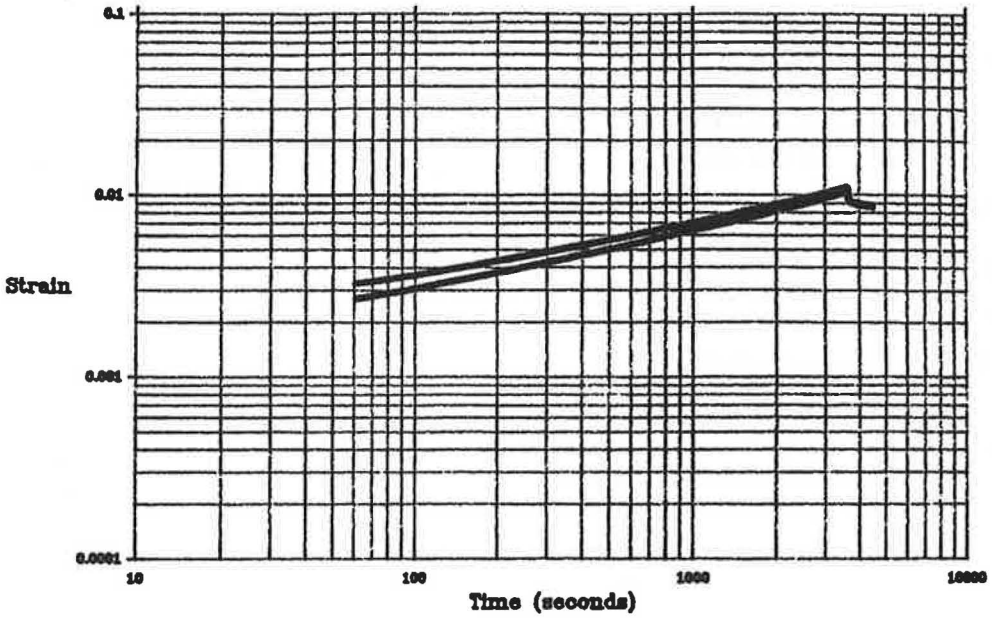

FIGURE 7 Graphical representation of typical conditioned unconventional samples, full-depth strain.

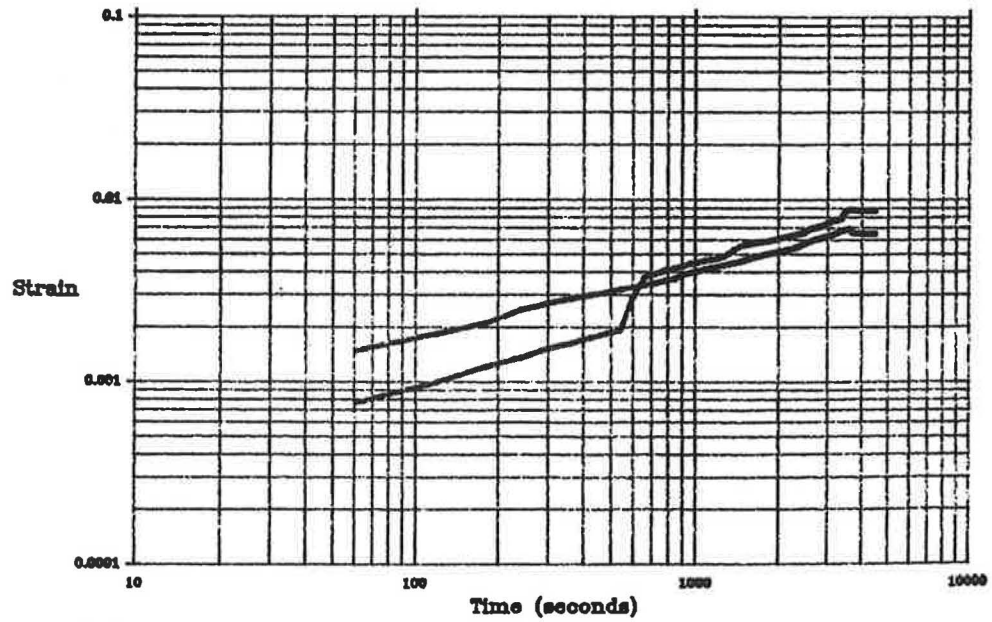

FIGURE 8 Graphical representation of typical unconventional samples, center third strain.

Figures 7 and 8 show typical ranges of data for each area of instrumentation (full depth and center 3 in.). Again, the discontinuity occurring on one of the center third data sets can be seen.

Instrumented Over the Center Third

After moisture conditioning, the ranking of the mixtures was:

Binder	*Avg Permanent Strain*
AC-20-RH	0.005406
AC-20-P (Control)	0.006178
AR4000-PM	0.006968
AC-20-RL	0.007607
AC-20-PM	0.008061
AR4000-R	0.008668

Although the ranking has changed from both the full-depth instrumentation and the unconditioned test center point results, there is still little variation between the results.

The within-sample set variance for full-depth and center third instrumentation was calculated and an average variance was determined. The resulting standard deviations were 0.001825 and 0.002799, respectively.

CONCLUSIONS

The following conclusions can be drawn:

1. The ranking of lowest to highest permanent strain for the various binders used in this project was the same for 8-in. samples instrumented over either the full depth or the center third of the sample.
2. There was no correlation between the relative ranking obtained from the 8-in. and the 2.5-in. data.
3. The finite element analysis of the 8-in. sample configuration showed that:
   - The strains observed in creep testing depend on the location of instrumentation and boundary conditions imposed on the sample; and
   - The presence of friction at the ends can result in nonuniform stress/strain fields in the sample. The end friction can give rise to a substantial difference in creep strain measurements made at the ends (full depth) and center of the sample.
4. Moisture conditioning the 8-in. specimens and then determining the permanent deformation resulted in a fairly consistent permanent deformation for all mixtures, regardless of binder.
5. The research conducted in this program consisted of a very small data base because of the limited availability of material. Future research should be conducted to confirm any conclusions suggested here.

ACKNOWLEDGMENT

The authors would like to thank the Nevada Department of Transportation for its continued commitment to improved pavement performance and the advancement of the research connected with this goal.

REFERENCES

1. R. P. Lottman. *NCHRP Report No. 246: Predicting Moisture-Induced Damage to Asphaltic Concrete*. TRB, National Research Council, Washington, D.C., May 1982.
2. *IMAGES-3D—Interactive Microcomputer Analysis and Graphics of Engineering Systems–Three Dimensional*, Version 1.6. Celestial Software, Inc., Berkeley, Calif., Sept. 1988.
3. J. M. De Sousa. *Dynamic Properties of Pavement Materials*. Ph.D. thesis. University of California, Berkeley, Nov. 1986.
4. N. C. Krutz and M. Stroup-Gardiner. Relationship Between Permanent Deformation of Asphalt Concrete and Moisture Sensitivity. In *Transportation Research Record 1259*, TRB, National Research Council, Washington, D.C., 1990, pp. 169–177.

Material Characterization and Inherent Variation Analysis of Asphaltic Field Cores

WILLIAM O. HADLEY

A knowledge of the variation in fundamental engineering properties of the construction materials is essential to a comprehensive evaluaton of the performance of various road sections. This study supports the Louisiana Experimental Base Project, an in-service experimental road project that aids in an evaluation of design-performance characteristics of a number of experimental test sections. The expected variation in the static and resilient (fatigue) properties of the materials in the layers of the pavement structure can provide an inherent variation data base from which continuing evaluation and analysis of pavement behavior and performance of these layers could be undertaken. A material characterization and inherent analysis of a resilient (fatigue) test program was undertaken to establish the magnitude, scope, and expected variation in fundamental engineering properties of laboratory-prepared specimens and field cores of the asphaltic materials used in the wearing, binder, and black base layers of the test sections of the base project. Variation analyses were completed for such fundamental properties as modulus, Poisson's ratio, and fatigue cycles to failure. Regression analysis techniques were also used to quantify those factors that significantly affect the fatigue life of the various construction materials used in the Louisiana Experimental Base Project. This information, when combined with the in-service performance results from the base project, should improve knowledge of the important mix variables affecting the fundamental engineering-performance properties and result in improvements in quality control measures.

A knowledge of the magnitude, scope, and expected variation in the fundamental engineering properties of the construction materials used in pavement structural sections is essential to a comprehensive evaluation of the performance of roadway sections. This study supports the Louisiana Experimental Base Project, an in-service experimental road project that aids in an evaluation of design-performance characteristics of a number of experimental test sections.

GENERAL

A repetitive (fatigue) testing program had two goals: to establish the magnitude and scope of inherent variation in the fundamental resilient properties of field cores representative of in-service conditions (Table 1), and to develop material characterization information from laboratory specimens (Table 2) of the three types of asphaltic materials (wearing, binder, and black base materials) used in the Louisiana Experimental Base Project.

Regression analysis techniques were used to quantify those factors that significantly affect the fatigue life of the various construction materials used in the Louisiana Experimental Base Project. This information, when combined with the in-service performance results from the base project, should improve knowledge of the important mix variables affecting the fundamental engineering-performance properties and could lead to improvements in quality control measures.

Texas Research and Development Foundation, 2602 Dellana Lane, Austin, Tex. 78746.

Louisiana Experimental Base Project

The Louisiana Experimental Base Project is situated on a portion of US-71–167, which accommodates a moderate volume of mixed vehicular traffic. To ensure that the flow of traffic would not be affected by its experimental status, the base project was completed as a part of a construction project upgrading US-71–167 to a four-lane facility.

The terrain at the base project is generally flat with poor drainage. The subgrade material is basically a fine-grained soil ranging from a silty clay loam to a heavy clay. The range in mean ambient air temperature is approximately 39°F (40°C) to 84°F (29°C), and the mean annual rainfall is approximately 55 to 60 in. (140 to 150 cm).

The projected average daily traffic at the time of construction was 7,990 vehicles, including approximately 15 percent trucks. All test sections were included in a portion of a newly constructed two-lane roadway adjacent to an existing two-lane highway.

The base project consists of 18 test sections: 14 experimental sections, and 4 control sections (Figure 1). The factors investigated in the project included three base types, three pavement design lives, and two surface thicknesses.

Each test section is approximately 550 ft (168 m) long with a 50-ft (15-m) transition zone interconnecting each adjacent test section. The randomization scheme for locating the various test sections included a complete randomization of the 10- and 15-year design sections but limited randomization of the 5-year sections. The latter sections were grouped together to allow for maintenance of the 5-year design sections at the same time. Detailed information on the construction of the base project is available from the Louisiana Department of Transportation (*1*).

TABLE 1 RESILIENT (FATIGUE) TESTING PROGRAM—FIELD CORES

PAVEMENT LAYER	TEST TYPE	VARIATION EVALUATED	FUNDAMENTAL MATERIAL PROPERTIES ESTIMATED
Wearing, Binder, and Black Base	Repetitive Indirect Tensile Test	Longitudinal - 10′ spacing Longitudinal - 1′ spacing Lateral - 4′ spacing Lateral - 1′ spacing Depth - vertical Stress levels - 11 to 39 psi	N_f, Cycles to Failure E_r, Resilient Modulus μ_r, Resilient Poisson's Ratio ϵ_r, Resilient Tensile Strain S_r, Resilient Applied Tensile Stress

TABLE 2 RESILIENT (FATIGUE) TESTING PROGRAM—LABORATORY-PREPARED ASPHALT SPECIMENS

PAVEMENT LAYER	TEST TYPE	FACTORS EVALUATED		FUNDAMENTAL MATERIAL CHARACTERISTICS ESTIMATED
		TYPE	LEVELS	
Wearing, Binder, and Black Base	Repetitive Indirect Tensile Test	Mix Variables: a)Asphalt content b)Gradation c)Compaction temperature d)Age at test e)Stress level	1)Wearing 3.9-4.9% 2)Binder 3.7-4.7% 3)Black base 3.5-4.5% Varies with layer type 235, 250, 275, 300, 314°F 35, 56, 112, 224, 343 days 10.1, 14.9, 22.9, 30.9, 35.7 psi	N_f, Cycles to Failure E_r, Resilient modulus μ_r, Resilient Poisson's Ratio ϵ_r, Resilient Strain S_r, Resilient Stress

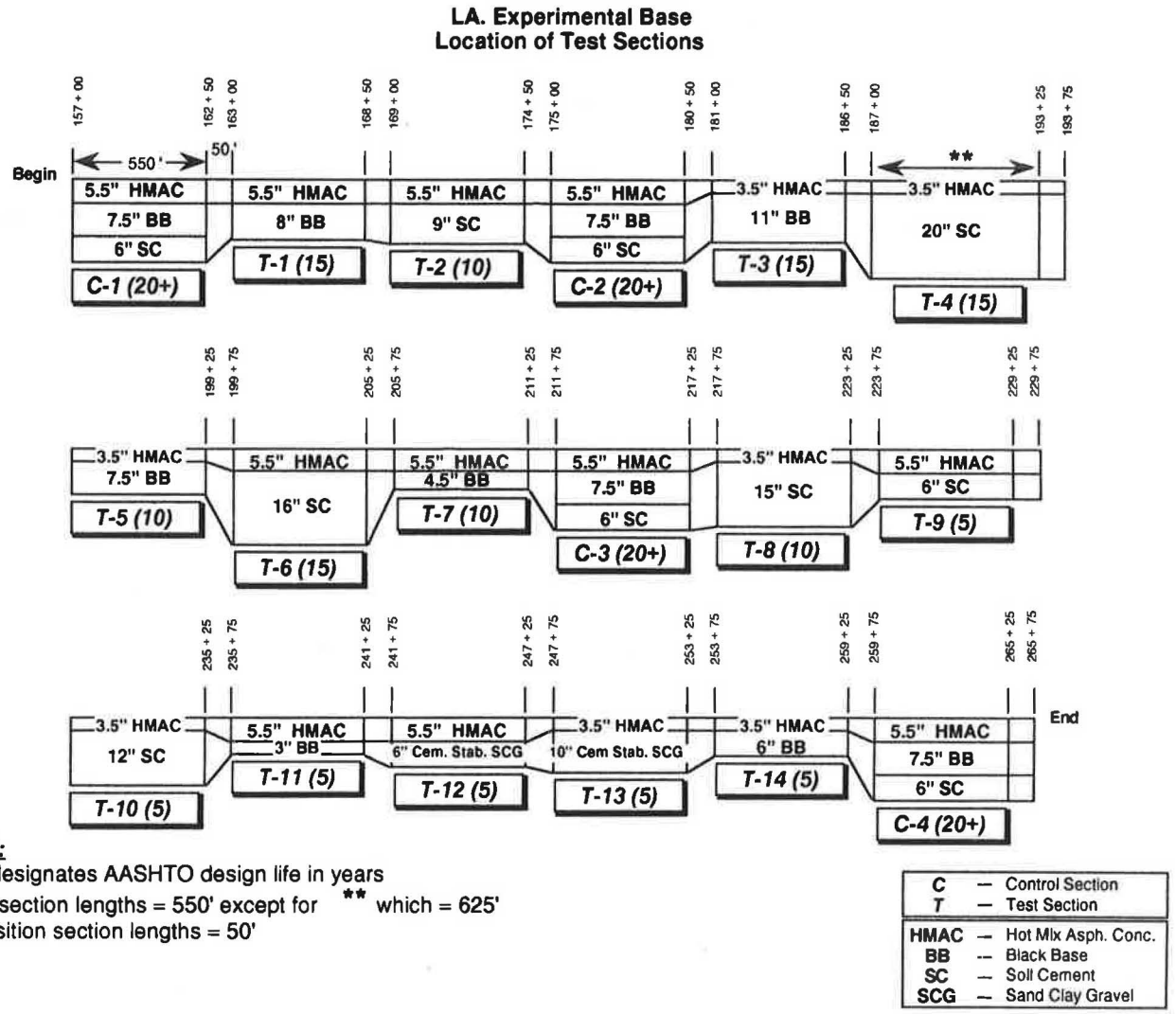

FIGURE 1 Experimental base project layout.

Field Coring Plan

The coring plan established for the Louisiana Experimental Base Project is shown in Table 3. The plan provided for an investigation of the variability in material properties of the various pavement materials used throughout the base project. The coring plan allowed for variational analysis in the longitudinal (along the road), lateral (across the road), and vertical (depth into pavement) directions. In addition, the plan included various spacings of the coring locations to provide for evaluation of inherent variation within close spacings (± 1 ft) and larger spacings (± 10 ft).

The fundamental engineering properties investigated in this phase included resilient modulus, resilient Poisson's ratio, and Log N_f (cycles to failure). Because the specimens were field cores, the only variable that could actually be varied was the tensile stress repeatedly applied to the specimens during the fatigue test. The properties associated with the cores—such as air voids, density, voids in mineral aggregate, and asphalt content—could be only measured, not established as a fixed value. All tests were conducted at a test temperature of 75°F (24°C) and 1 Hz (sinusoidal waveform).

INHERENT VARIATION ANALYSIS

The inherent variation estimates were obtained from field cores at an approximately similar position, depth, spacing, and material type. The estimates of the inherent variation in the resilient fundamental engineering properties are shown in Tables 4–6 for wearing course, binder course, and black base field cores. Within the tables, the variations are broken down into longitudinal at 1-ft spacing (A), longitudinal at 10-ft spacing (B), lateral at 1-ft spacing (C), lateral at 4-ft spacing (D), and depth (E, for binder and black base only).

Statistical comparisons of inherent variation in the longitudinal and lateral directions allowed the four sets of variations to be pooled. This operation provided better estimates of the in-service inherent variation in the resilient modulus,

TABLE 3 RANDOMIZED CORE PLAN

SECTION DESIGNATION	DESIGN LIFE YRS	SAMPLING DIRECTION AND GROUPING	STATION	LANE	COMMENTS
Control 1	20	longitudinal	160 + 24	outside	outside
		within	160 + 25		wheel path
			160 + 26		
Test 1	15	longitudinal	166 + 74	inside	outside
		within	166 + 75		wheel path
			166 + 76		
Test 2	10	longitudinal	171 + 15	outside	outside
		among	171 + 25		wheel path
			171 + 35		
Control 2	20	longitudinal	178 + 15	outside	outside
		among	178 + 25		wheel path
			178 + 35		
Test 3	15	lateral	185 + 75	outside	9' Rt of CL
		within	185 + 75		10' Rt of CL
			185 + 75		11' RT of CL
Test 4	15	lateral	192 + 25	outside	9' Rt of CL
		within	192 + 25		10' Rt of CL
			192 + 25		11' Rt of CL
Test 5	10	lateral	199 + 00	inside	2' Lt of CL
		among	199 + 00		6' Lt of CL
			199 + 00		10' Lt of CL
Test 6	15	lateral	202 + 00	inside	2' Lt of CL
		among	202 + 00		6' Lt of CL
			202 + 00		10' Lt of CL
Test 7	10	longitudinal	205 + 99	outside	outside
		within	206 + 00		wheel path
			206 + 01		
Control 3	20	lateral	213 + 50	inside	2' Lt of CL
		among	213 + 50		6' Lt of CL
			213 + 50		10' Lt of CL
			213 + 50	outside	2' Rt of CL
			213 + 50		6' Rt of CL
			213 + 50		10' Rt of CL
Test 8	10	longitudinal	221 + 40	outside	outside
		among	221 + 50		wheel path
			221 + 60		

TABLE 3 (*continued on next page*)

TABLE 3 (*continued*)

SECTION DESIGNATION	DESIGN LIFE YRS	SAMPLING DIRECTION AND GROUPING	STATION	LANE	COMMENTS
Test 9	5	longitudinal	227 + 99	inside	outside
		within	228 + 00		wheel path
			228 + 01		
Test 10	5	longitudinal	231 + 49	outside	outside
		within	231 + 50		wheel path
			231 + 51		
Test 11	5	longitudinal	237 + 90	outside	outside
		among	238 + 00		wheel path
			238 + 10		
Test 12	5	lateral	245 + 00	outside	2' Rt of CL
		among	245 + 00		6' Rt of CL
			245 + 00		10' Rt of CL
Test 13	5	longitudinal	251 + 99	outside	outside
		within	252 + 00		wheel path
			252 + 01		
Test 14	5	lateral	257 + 00	outside	2' Rt of CL
		among	257 + 00		6' Rt of CL
			257 + 00		10' Rt of CL
Control 4	20	lateral	261 + 50	outside	9' Rt of CL
		within	261 + 50		10' Rt of CL
			261 + 50		11' Rt of CL

Poisson's ratio, and fatigue life of the wearing, binder, and black base layers. The pooled results are shown in Table 7.

There were significant differences in the variances of the pooled longitudinal and lateral data and the depth data. The varation with depth was significantly greater than the variation in the longitudinal and lateral directions; therefore, the two variances must be considered separately. This finding implies more variation in the vertical direction (depth in the pavement) than in the lateral and longitudinal directions. The inherent variation estimates in the vertical direction are shown as the bottom rows of Tables 5 and 6 for the binder and black base cores, respectively. As noted previously, no data were available for vertical direction variability in the wearing course; however, it is believed that the estimates for the binder course cores could be used for this purpose.

INHERENT VARIATION COMPARISONS

A compilation of the available information on the fundamental engineering properties of the asphaltic field cores has been prepared. The means and standard deviations for resilient modulus, resilient Poisson's ratio, measured resilient strain, and Log N_f of the various asphaltic materials are shown in Table 8. This information was subsequently used in completing several statistical comparisons among the various types of field cores (i.e., surface, binder, and black base).

Comparisons between the field core results of wearing and binder materials and binder and black base materials established whether there were significant differences in means and variances. If there were no significant differences, the results could be combined and any subsequent use of the data could be simplified (i.e., wearing and binder courses could be considered as one layer for a layered theory evaluation).

Comparisons between wearing and binder course materials are shown in Table 9. There was no significant difference in the resilient Poisson's ratio, but there were significant differences in the other material properties. In general, the property values for the wearing course were 9 to 14 percent higher than for the binder course. It is therefore concluded that the fundamental engineering properties of the wearing and binder course materials are generally different and that the two materials must be considered separate entities in any subsequent analysis or in any layered theory type evaluation.

TABLE 4 FUNDAMENTAL MATERIAL PROPERTY VARIATION IN FATIGUE-RESILIENT RESULTS—FIELD CORES OF WEARING COURSE MATERIALS

		RESILIENT MODULUS		RESILIENT POISSON'S RATIO		LOG OF CYCLES TO FAILURE	
TYPE VARIATION	DESIGN LEVEL	MEAN SQUARES	DEGREES FREEDOM	MEAN SQUARES	DEGREES FREEDOM	MEAN SQUARES	DEGREES FREEDOM
A - longitudinal	1,2 *	1.885677	3	0.013197	3	0.004135	3
direction @ 1'	3						
spacing	4	2.762354	6	0.007888	6	0.137140	6
		2.470128	9	0.009658	9	0.092805	9
B - longitudinal	1,2	2.185220	2	0.005924	2	0.174753	2
direction @ 10'	3	0.061894	4	0.001851	4	0.096129	4
spacing	4	5.471106	2	0.024194	2	0.025457	2
		1.945029	8	0.008455	8	0.098114	8
C - lateral	1,2	0.961149	2	0.001075	2	0.041346	2
direction @ 1'	3						
spacing	4	———	–	———	–	———	–
		0.961149	2	0.001075	2	0.041346	2
D - lateral	1,2	3.100015	6	0.015089	6	0.203137	6
direction @ 4'	3	3.564450	1	0.003961	1	0.006705	1
spacing	4	2.549280	1	0.000578	1	0.089535	1
		3.089228	8	0.011884	8	0.164383	8
E - none available							

* Design Level	Test Sections	Design Life
1	C1, C2, C3, C4	Control (20 year)
2	T1, T3, T4, T6	15 Year
3	T2, T5, T7, T8	10 Year
4	T9, T10, T11, T12, T13, T14	5 Year

Similar comparisons in the fundamental engineering properties of binder and black base field cores yielded essentially the same results. In this comparison, the modulus and Poisson's ratio values for the two material types could be combined; however, because there were significant differences in Log N_f, the two material types must be considered separately in any subsequent analyses. The property values for the binder materials were generally 5 to 9 percent higher than for the black base materials (Table 10).

One of the perplexing problems associated with experimental analysis and evaluations based on laboratory-prepared specimens is the uncertainty of the premise that the results are applicable to field conditions. In order to obtain information concerning the existence of a correlation between field and laboratory core results, statistical comparisons were completed between the resilient properties of laboratory specimens and field cores for wearing (Table 11), binder (Table 12), and black base (Table 13) materials. In general, statistically significant differences were found between the resilient-fatigue results for the laboratory and field cores.

However, there was a consistent difference between the field and laboratory cores, indicating a correlation between

TABLE 5 FUNDAMENTAL MATERIAL PROPERTY VARIATION IN FATIGUE-RESILIENT INDIRECT TENSILE TEST RESULTS—FIELD CORES OF BINDER COURSE MATERIALS

TYPE VARIATION	DESIGN LEVEL	RESILIENT MODULUS MEAN SQUARES	RESILIENT MODULUS DEGREES FREEDOM	RESILIENT POISSON'S RATIO MEAN SQUARES	RESILIENT POISSON'S RATIO DEGREES FREEDOM	LOG OF CYCLES TO FAILURE MEAN SQUARES	LOG OF CYCLES TO FAILURE DEGREES FREEDOM
A - longitudinal	1,2	0.422602	4	0.001099	4	0.002644	4
direction @ 1'	3	1.705175	2	0.012951	2	0.079551	2
spacing	4	1.488872	6	0.005270	6	0.156679	6
		1.169499	12	0.005160	12	0.092479	12
B - longitudinal	1,2	1.362684	2	0.004576	2	0.045163	2
direction @ 10'	3	0.071368	2	0.002688	2	0.416775	2
spacing	4	0.425921	2	0.015864	2	0.009743	2
		0.619991	6	0.007709	6	0.157227	6
C - lateral	1,2	0.649841	8	0.008500	8	0.156221	8
direction @ 1'	3						
spacing	4	———	–	———	–	———	–
		0.649841	8	0.008500	8	0.156221	8
D - lateral	1,2	0.367963	4	0.003655	4	0.224174	4
direction @ 4'	3	0.013057	2	0.013129	2	0.082499	2
spacing	4	1.012517	4	0.001686	4	0.116597	4
		0.554803	10	0.004762	10	0.152808	10
E - depth -	1,2	8.180508	20	0.000325	20	0.006539	20
vertical	3	0.124130	7	0.000019	7	0.018656	7
	4	3.637503	7	0.000213	7	0.043754	7
		5.586517	34	0.000239	34	0.016696	34

* Design Level	Test Sections	Design Life
1	C1, C2, C3, C4	Control
2	T1, T3, T4, T6	15 Year
3	T2, T5, T7, T8,	10 Year
4	T9, T10, T11, T12, T13, T14	5 Year

them. For the three materials, the engineering property estimates for the field cores ranged from 9 to 20 percent higher than those for the laboratory cores. The differences could very well be the difference in age (and probably mixture properties) between the core specimens (approximately 2½ years) and the laboratory specimens (from 1 month to a year). The differences between field and laboratory specimens were 13 to 15 percent, 9 to 14 percent, and 12 to 20 percent for wearing, binding, and black base materials, respectively.

ANALYSIS OF VARIANCE: FATIGUE LIFE

The analysis of variance results for the logarithm of fatigue life (i.e., Log N_f) of all combined asphaltic core data are shown in Table 14.

From these results, it can be ascertained that the fatigue life (explicitly the logarithm of fatigue life) of asphalt field cores is significantly influenced by or correlated with four main effects and one interaction. The fatigue life will generally

TABLE 6 FUNDAMENTAL MATERIAL PROPERTY VARIATION IN FATIGUE-RESILIENT INDIRECT TENSILE TEST RESULTS—FIELD CORES OF BLACK BASE MATERIALS

		RESILIENT MODULUS		RESILIENT POISSON'S RATIO		LOG OF CYCLES TO FAILURE	
TYPE VARIATION	DESIGN LEVEL	MEAN SQUARES	DEGREES FREEDOM	MEAN SQUARES	DEGREES FREEDOM	MEAN SQUARES	DEGREES FREEDOM
A - longitudinal	1,2*	0.163828	4	0.004661	4	0.038723	4
direction @ 1'	3						
spacing	4	———	–	———	–	———	–
		0.163828	4	0.004661	4	0.038723	4
B - longitudinal	1,2	4.059316	3	0.038379	3	0.083409	3
direction @ 10'	3						
spacing	4	———	–	———	–	———	–
		4.059316	3	0.038379	3	0.083409	3
C - lateral	1,2	1.122110	4	0.010111	4	0.047001	4
direction @ 1'	3						
spacing	4	———	–	———	–	———	–
		1.122110	4	0.010111	4	0.047001	4
D - lateral	1,2	1.192811	5	0.005342	5	0.022983	5
direction @ 4'	3	2.509904	5	0.020342	5	0.077305	5
spacing	4	2.198857	6	0.006119	6	0.115570	6
		1.981670	16	0.010321	16	0.074679	16
E - depth -	1,2	8.785102	9	0.000275	9	0.074251	9
vertical	3	8.483081	1	0.006728	1	0.029905	1
	4	———	–	———	–	———	–
		8.754900	10	0.000920	10	0.069816	10

* Design Level	Test Sections	Design Life
1	C1, C2, C3, C4	Control (20 Year)
2	T1, T3, T4, T6	15 Year
3	T2, T5, T7, T8,	10 Year
4	T9, T10, T11, T12, T13, T14	5 Year

be greater for higher modulus values, lower applied percent stress levels, higher voids in mineral aggregate, and lower asphalt contents. In addition, a combination of low asphalt content and high percent stress, or high asphalt content and low percent stress, would result in a longer fatigue life.

REGRESSION EQUATIONS: FATIGUE LIFE

The centered data approach was used to develop an overall regression equation for the logarithm of fatigue life (log N_f) of asphaltic field cores using a stepwise regression technique (Table 15). The terms included in this equation correspond to those factors and their interactions found to be of practical engineering significance in the analysis of variance.

Regression analyses were also conducted to develop relationships between Log N_f and logarithm of measured tensile strain for the wearing course, binder, and black base materials. These relatonships are shown in Table 15 as Equations b, c, and d. Although the coefficient of determination values for the equations listed in Table 15 range from 0.524 to 0.723,

TABLE 7 COMBINED VARIATION ESTIMATES (LATERAL AND LONGITUDINAL DIRECTIONS) OF FATIGUE-RESILIENT INDIRECT TENSILE TEST RESULTS—FUNDAMENTAL MATERIAL PROPERTIES OF FIELD CORES

	WEARING COURSE		BINDER COURSE		BLACK BASE	
MATERIAL PROPERTY	MEAN SQUARES	DEGREES FREEDOM	MEAN SQUARES	DEGREES FREEDOM	MEAN SQUARES	DEGREES FREEDOM
Resilient modulus	2.477981	26	0.814305	35	1.885708	26
Resilient Poisson's Ratio	0.009684	26	0.006394	35	0.013052	26
Log of Cycles to Failure	0.116074	26	0.138027	35	0.069060	26

TABLE 8 COMPILATION OF INHERENT VARIATION INFORMATION OF FATIGUE-RESILIENT INDIRECT TENSILE FIELD CORES—OVERALL SAMPLE VARIABILITY (INCLUDING VERTICAL VARIABILITY)

	WEARING SURFACE			BINDER COURSE			BLACK BASE		
MATERIAL PROPERTY	MEAN	MEAN SQUARE	DEGREES FREEDOM	MEAN	MEAN SQUARE	DEGREES FREEDOM	MEAN	MEAN SQUARE	DEGREES FREEDOM
Resilient Modulus, 10^5 psi	6.147	2.4780	26	5.272	3.1658	69	4.986	3.9022	35
Resilient Poisson's Ratio	0.321	0.0097	26	0.326	0.0036	69	0.331	0.0100	35
Measured * Resilient strain, μin/in	129.7	74.6	50	158.6	96.5	100	144.7	59.6	57
Log of Cycles to Failure	4.2488	0.1161	26	3.8679	0.0782	69	3.5669	0.0712	35

* Overall strain variability (i.e., includes all tests conducted).

all four equations have acceptable fit and can be considered adequate for prediction purposes. These four equations can then be used to estimate the fatigue life individually for each of the in-service asphaltic materials.

CONCLUSIONS

The findings and conclusions of this study are limited to the types of asphalt materials considered in this study. On the basis of the data and the analysis described earlier, the following general conclusions were made:

1. The variations in the fundamental resilient engineering properties of cores in the longitudinal (along the road) and lateral (across the road) directions were essentially the same and could be pooled. The variations in material properties with depth, however, were significantly different and could not be combined. Therefore, the variations in fundamental resilient engineering properties in vertical and horizontal di-

TABLE 9 COMPARISON OF INHERENT VARIATION OF WEARING COURSE AND BINDER COURSE (FIELD)

MATERIAL PROPERTY	WEARING SURFACE			BINDER COURSE			SIGNIFICANT DIFFERENCE IN	
	MEAN	MEAN SQUARE	DEGREES FREEDOM	MEAN	MEAN SQUARE	DEGREES FREEDOM	VARIANCE	MEAN
Resilient Modulus, 10^5 psi	6.147	2.4780	26	5.272	3.166	35	Yes	Yes
Resilient Poisson's Ratio	0.321	0.0097	26	0.326	0.0064	35	Yes	No
Measured * Resilient strain, μin/in	129.7	74.6	50	158.6	96.5	100	Yes	Yes
Log of Cycles to Failure	4.2488	0.1161	26	3.8679	0.1380	35	No	Yes

* Overall combined variation in measured tensile strain (all specimens included).

** Mean property values of wearing course are 9 to 14% higher than for binder course (with exception of Poisson's ratio).

TABLE 10 COMPARISON OF INHERENT VARIATION OF BLACK BASE AND BINDER COURSE (FIELD)

MATERIAL PROPERTY	BLACK BASE			BINDER COURSE			SIGNIFICANT DIFFERENCE IN	
	MEAN	MEAN SQUARE	DEGREES FREEDOM	MEAN	MEAN SQUARE	DEGREES FREEDOM	VARIANCE	MEAN
Resilient Modulus, 10^5 psi	4.986	1.886	26	5.272	3.166	35	Yes	No
Resilient Poisson's Ratio	0.331	0.0131	26	0.326	0.0064	35	Yes	No
Measured * Resilient strain, μin/in	144.7	59.6	57	158.6	96.5	100	Yes	No
Log of Cycles to Failure	3.5669	0.0691	26	3.8679	0.1380	35	Yes	Yes

* Overall combined variation in measured tensile strain (all specimens included).

** Mean property values of binder course are 5 to 9% higher than black base values (with exception of Poisson's ratio).

TABLE 13 COMPARISON OF INHERENT VARIATION OF BLACK BASE (FIELD) AND BLACK BASE (LABORATORY)

MATERIAL PROPERTY	LAB *			FIELD			SIGNIFICANT DIFFERENCE IN	
	MEAN	MEAN SQUARE	DEGREES FREEDOM	MEAN	MEAN SQUARE	DEGREES FREEDOM	VARIANCE	MEAN
Resilient Modulus, 10^5 psi	3.982	0.9446	17	4.986	1.866	26	Yes	Yes
Resilient Poisson's Ratio	0.282	0.0113	17	0.331	0.013	26	No	No
Measured ** Resilient strain, μin/in	192.9	116.1	17	144.7	59.6	26	Yes	Yes
Log of Cycles to Failure	3.1375	0.0304	17	3.5669	0.0691	26	Yes	Yes

* Total variability in laboratory prepared specimens was utilized, since field core variability would include inherent as well as factor variability.

** Variability in all laboratory and field cores tested.

*** Mean property values for field cores are 12 to 20% higher than laboratory cores and measured strains are 33% less.

TABLE 14 COMBINED ANALYSIS OF VARIANCE FOR LOG N_f OF FATIGUE-RESILIENT INDIRECT TENSILE TEST RESULTS—ASPHALT FIELD CORES

SOURCE OF VARIATION	DEGREES FREEDOM	MEAN SQUARES	F VALUE	SIGNIFICANCE LEVEL	APPROXIMATE UNIT VARIATION
STL	1	62.72323	525.26	0.01	-0.602
ACxSTL	1	3.86714	32.38	0.01	-0.132
E	1	2.78582	23.33	0.01	+0.114
VMA	1	2.43992	20.43	0.01	+0.536
AC	1	2.29341	19.20	0.01	-0.184
Residual	141	0.75609			
Error	60	0.130814			

Factor Legend

AC - Asphalt Content

E - Modulus

STL - Stress level

VMA - Voids in mineral aggregates

TABLE 11 COMPARISON OF INHERENT VARIATION OF WEARING COURSE (FIELD) AND WEARING COURSE (LABORATORY)

MATERIAL PROPERTY	LAB *			FIELD			SIGNIFICANT DIFFERENCE IN	
	MEAN	MEAN SQUARE	DEGREES FREEDOM	MEAN	MEAN SQUARE	DEGREES FREEDOM	VARIANCE	MEAN
Resilient Modulus, 10^5 psi	5.217	0.9578	17	6.147	2.478	26	Yes	Yes
Resilient Poisson's Ratio	0.280	-0.113	17	0.321	0.010	26	No	No
Measured ** Resilient strain, μin/in	134.8	56.7	17	129.7	74.6	26	No	No
Log of Cycles to Failure	3.6817	0.0516	17	4.2488	0.1161	26	No	Yes

* Total variability in laboratory prepared specimens was utilized, since field core variability would include inherent as well as factor variability.

** Variability in all laboratory field cores tested.

*** Mean property values for field cores are 13 to 15% higher than laboratory cores and measured strains are 4% lower.

TABLE 12 COMPARISON OF INHERENT VARIATION OF BINDER COURSE (FIELD) AND BINDER COURSE (LABORATORY)

MATERIAL PROPERTY	LAB *			FIELD			SIGNIFICANT DIFFERENCE IN	
	MEAN	MEAN SQUARE	DEGREES FREEDOM	MEAN	MEAN SQUARE	DEGREES FREEDOM	VARIANCE	MEAN
Resilient Modulus, 10^5 psi	4.807	0.6898	17	5.272	3.166	69	Yes	No
Resilient Poisson's Ratio	0.288	0.0237	17	0.326	0.0036	69	Yes	No
Measured ** Resilient strain, μin/in	113.11	60.78	17	158.6	96.5	69	Yes	Yes
Log of Cycles to Failure	3.321	0.0689	17	3.8679	0.0782	69	No	Yes

* Total variability in laboratory prepared specimens was utilized, since field core variability would include inherent as well as factor variability.

** Variability in all laboratory and field cores tested.

*** Mean property values for field cores are 9 to 14% higher than laboratory cores and measured strains are 29% higher.

TABLE 15 REGRESSION ANALYSIS OF FATIGUE-RESILIENT INDIRECT TENSILE TEST RESULTS—ASPHALT FIELD CORES

a) LOG OF CYCLES TO FAILURE - COMBINED ANALYSIS

$$L_{Nf} = 3.9647 + 0.3042\left[\frac{\text{Log E} - 0.7075}{0.1549}\right] - 0.6995\left[\frac{\text{Log STS} + 0.79053}{0.2209}\right]$$

$$+ 0.1219\left[\frac{\text{Log VMA} - 1.80441}{0.042}\right] - 0.2462\left[\frac{\text{Log AC} - 0.63501}{0.0239}\right]$$

$R^2 = 0.5275$ $\hat{S}_r = 0.6682$

b) LOG OF CYCLES TO FAILURE - WEARING COURSE

$$\text{Log}_{Nf} = 9.67 - 2.650 \text{ Log } (\epsilon)$$

$R^2 = .659$ $\hat{S}_r = .4410$

c) LOG OF CYCLES TO FAILURE - BINDER COURSE

$$\text{Log}_{Nf} = 8.736 - 2.255 \text{ Log } (\epsilon)$$

$R^2 = .524$ $\hat{S}_r = .5110$

d) LOG OF CYCLES TO FAILURE - BLACK BASE

$$\text{Log}_{Nf} = 9.779 - 2.925 \text{ Log } (\epsilon)$$

$R^2 = .723$ $\hat{S}_r = .259$

E = Resilient modulus (10^5 psi) ϵ = Measured tensile strain, μin/in

STS = Applied tensile stress, psi VMA = Voids in mineral aggregates, %

AC = % Asphalt content

rections must be considered separately (i.e., analogous to a anisotropic condition). In fact, the variability will be greater in the vertical direction.

2. Comparisons of the fundamental engineering properties of the various asphaltic material indicate that the wearing, binder, and black base are significantly different and must be considered as separate material groups (i.e., statistical populations) in any subsequent analysis.

3. Although there were significant differences in the mean resilient properties of the asphaltic laboratory specimens and field cores, there appeared to be a correlation between the two sets of data. For the wearing, binder, and black base materials, the engineering properties of the field cores ranged from 9 to 20 percent greater than those of the laboratory cores. These differences could very well be explained by differences in age at time of test. This correlation indicates that the properties of laboratory-prepared specimens can be used as indicators of the in-service material properties.

4. The inherent variation and fatigue life information developed in this study constitutes a materials variation data base that will be useful in the performance, evaluation, and analysis of the Louisiana Experimental Base Project, as well as other in-service pavement sections.

REFERENCE

1. J. W. Lyon, Jr. *Louisiana Experimental Base Project.* Report 1. Office of Highways, Research and Development Section, Louisiana Department of Transportation, Baton Rouge, Nov. 1979.

New Technique To Measure Moisture in Hot-Mix Asphalt Concrete Nondestructively

IMAD L. AL-QADI AND PETER E. SEBAALY

A new technique was developed to measure the moisture content in hot-mix asphalt concrete. The technique involves measuring the dielectric properties of the hot-mix asphalt concrete using electromagnetic waves in the microwave range of 12.4 to 18.0 GHz. Using the dielectric property measurements, the moisture content can be calculated. This study used piedmont gravel and limestone aggregates in dense-graded and open-graded cases. One type of asphalt cement was studied exclusively because three types of asphalt were found to have almost the same dielectric properties. Asphalt content, surface smoothness, and specimen thickness were also found to have no effect on the measured dielectric properties. The study considered the different void ratios that had noticeable effects on the microwave reflection measurements. However, the presence of water in the mixes overshadowed the effects of all other factors on the dielectric properties of the mix. Regression models were developed to predict the volumetric moisture content. The study suggested a model that was found to be a function of the dielectric properties of dry and wet hot-mix asphalt concrete. Therefore, in practice, several cores are essential to obtain the in situ dry dielectric properties of hot-mix asphalt concrete.

The strength of hot-mix asphalt concrete is drawn from the bonding between the asphalt cement and the aggregate. The existence of moisture in asphalt concrete causes major damage to the asphalt cement–aggregate bonding and therefore reduces the overall strength of asphalt concrete pavements. This phenomenon is referred to as "stripping." The presence of excess moisture affects both resilient modulus and fatigue life; in general, it reduces the pavement life.

As part of the research to prevent the weakening of asphalt concrete pavements caused by the existence of moisture, this study attempted to measure moisture content using electromagnetic waves at the microwave frequency range. Microwave wavelengths are typically 10^5 times larger than optical wavelengths. Indeed, microwaves behave much like light waves in that they travel in the same manner and according to the same physical laws; they are reflected by metallic objects, are absorbed by some dielectric materials, are transmitted without significant absorption through other dielectric materials, and change directions when traveling from one dielectric material into another. Because microwaves can penetrate many nonmetals, information can be obtained about material composition, density, state of cure, and moisture content. This information can be obtained from the amplitude and phase measurements of wave transmitted and/or reflected by the specimen.

The microwave was used in this study as a nondestructive testing (NDT) technique to detect the moisture content in asphalt concrete pavements without contact. The water molecule possesses a permanent dipole moment; that is, its electrical properties might be simulated to first order as arising from a fixed positive charge and fixed negative charge, separated by a certain distance. The molecule also possesses a polarizability as a result of an additional dipole, which is induced by an electric field and is proportional to its magnitude. Although the composition of the asphalt concrete can influence its dielectric properties, water dipoles have the greatest influence on these properties. The changes in the asphalt concrete dielectric properties can be monitored indirectly through the ability of microwaves to detect changes in complex dielectric constant.

The dielectric properties of asphalt concrete depend on the proportion and state of the water component in the mixture, as well as the polarization and conductivity of the other component or components (*1*). The water molecule, at microwave frequencies, is unique in having an extremely high dielectric constant and loss tangent. Water will absorb several thousand times more microwave energy than a similar volume of almost any perfectly dry material. Therefore, microwaves can be used to monitor the moisture content of many materials instantaneously and continuously.

The use of electromagnetic waves in pavement NDT started in the 1960s. Over the past two decades, extensive studies on the microwave signature of soil moisture have been reported (*2–4*). The capabilities of microwave remote sensing in detecting moisture in soils have been investigated through experimental studies since the early 1970s. As a result of these investigations, the role of microwave scattering became well recognized. However, most of the studies were performed on thin soil specimens using conductors.

Electromagnetic waves have also been used in rigid pavements, using pulse radar. The use of short-pulse radar for subsurface exploration has received considerable attention, especially during the past decade. Short-pulse radar has been used in a variety of subsurface applications, including measurement of pavement thickness, void detection, reinforcement detection, and delamination. The transmitted wave form of ground-penetration radar is usually a very narrow pulse, 1 ns and 1 GHz central frequency. Although short-pulse radar represents a major change in the application of new tech-

I. L. Al-Qadi, Department of Civil Engineering, Virginia Polytechnic Institute and State University, 200 Patten Hall, Blacksburg, Va. 24061. P. E. Sebaaly, Department of Civil Engineering, University of Nevada, Reno, Nev. 89557.

nology to evaluate rigid pavement distress, its application is still under investigation because of current limitations. This method depends largely on the user's interpretation. Also, the imaginary part of the complex dielectric constant is neglected in the evaluation process, which might undergo a significant change if the pavement is wet. However, Clemena used electromagnetic waves to detect the water content of fresh concrete mixes using both reflection and transmission methods (*5*). Although the transmission method gave more accurate and more precise results than the reflection method, the transmission method is unfeasible and impractical for field applications (*1*).

The use of electromagnetic waves for NDT of asphalt concrete pavements has not been well investigated. Few studies have been made on the dielectric properties of asphalt cement (*6*), and many studies have been made on the dielectric behavior of aggregates (*1,7*). Only very limited investigations have been conducted regarding the dielectric properties of asphalt concrete (*8–10*).

The first radar in the swept frequency mode was built by Lundien in 1970–1971, using a frequency range of 0.5 to 8.0 GHz (*11*). The results obtained from 2.0 to 8.0 GHz were found to be 200 to 300 percent out of calibration compared with the data in the range of 0.5 to 2.0 GHz. Although the antennas used were huge, very high, and unfocused, the research in the laboratory and field represented a new era in using electromagnetic waves as an NDT technique in asphalt concrete.

THEORY OF ELECTROMAGNETIC WAVES

The dielectric constant of a material is a measure of the extent to which the electric charge distribution in the material can be distorted by applying an electrical field. Based on their dielectric constants materials are classified as lossless, complex, or lossy. The pavement materials are considered to be poor conductors or dielectric. Therefore, the penetration of this material (which is considered low-loss material) is possible. The complex dielectric constant is usually presented as

$$\varepsilon^* = \varepsilon_0 (\varepsilon' - j\varepsilon'') \tag{1}$$

where

ε^* = complex dielectric constant,
ε_0 = vacuum dielectric constant (8.84×10^{-12} farad/m),
ε' = real part of ($\varepsilon^*/\varepsilon_0$) associated with the ability of dielectric material to store energy,
ε'' = imaginary part of ($\varepsilon^*/\varepsilon_0$) associated with the dielectric losses that occur in the material, and
$j = (-1)^{1/2}$.

In practice, the normalized complex dielectric constant (ε_r) is used; it is called the relative dielectric constant, or simply the dielectric constant, and is defined by

$$\varepsilon_r = \varepsilon^*/\varepsilon_0 = \varepsilon'(1 = j\tan\delta) \tag{2}$$

where $\tan\delta$ is the loss tangent ($\varepsilon''/\varepsilon'$).

In this study, the dielectric properties of asphalt concrete were calculated from the measured microwave reflections. The microwaves used were in the Ku band (12.4 to 18.0 GHz). A uniform plane wave is normally incident on a specimen backed by a metal plate. The metal plate is used because of its complete reflection. Therefore, a finite specimen theory can be used (*10*). The complex reflection coefficient S_{11} is related to the complex relative dielectric constant. Because the asphalt concrete material is nonmagnetic, the following equation can be obtained:

$$S_{11} = \frac{[jZ_s \tan(\beta_d) - Z_0]}{[jZ_s \tan(\beta_d) + Z_0]} \tag{3}$$

where

Z_s = impedance in specimen = $Z_0/(\varepsilon^*)^{1/2}$,
Z_o = impedance in vacuum,
d = specimen thickness, and
β = phase constant.

Because $Z_s/Z_o = 1/(\varepsilon^*)^{1/2}$, the following equation can be developed:

$$S_{11} = \frac{[j\tan(\beta d) - (\varepsilon^*)^{1/2}]}{[j\tan(\beta d) + (\varepsilon^*)^{1/2}]} \tag{4}$$

ε^* is found iteratively from Equation 4. The iterative procedure is based on finding the zeros of an error function from the measured and calculated values of the complex reflection coefficient:

$$E_r = |S_{11}^m - S_{11}^c| \tag{5}$$

where S_{11}^m equals the measured values of the complex reflection coefficient, and S_{11}^c equals the calculated values of the complex reflection coefficient.

A program was developed in this study to find the roots of a complex function. The program required a good initial estimate of the dielectric constant, which is a function of light speed, the frequencies corresponding to two successive minimums from the reflection coefficient-frequency relationship, and the specimen thickness. The initial estimate of the loss factor depends on successive local minimums and maximums of the reflection coefficients, the obtained real dielectric constant, and the specimen depth.

When water exists in the specimens, the material has a high loss factor and becomes difficult to measure using this method. Therefore, an infinite theory may be used, in which the specimen is assumed to be a lossy material or very long (*10*). In this case, the reflection coefficient (S_{11}) is related to the complex dielectric constant according to the following relationship:

$$\varepsilon^* = \left(\frac{1 - S_{11}}{1 + S_{11}}\right)^2 \tag{6}$$

EXPERIMENTAL SYSTEM

The system used in this study consisted of an HP8510B network analyzer, synthesized sweeper, and focused antenna as shown in Figure 1. The HP8510B network analyzer is a high-

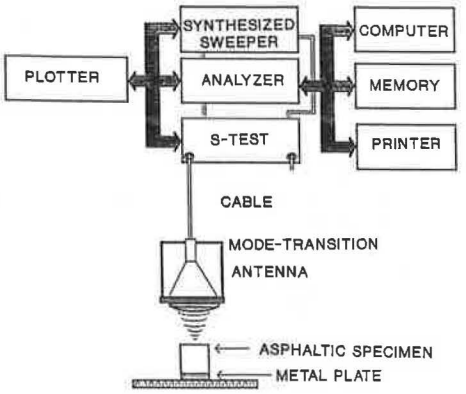

FIGURE 1 Schematic diagram of measurement system used in study.

performance vector receiver that gives accurate and repeat able measurements of S_{11}. Measurement by the HP8510B network analyzer is actually made in the frequency domain and transformed mathematically into the time domain by calculating the inverse Fourier transform. The frequency domain reflection measurement is a composition of the responses of all of the discontinuities present in the material tested. The source is phase-locked at each measurement frequency under the control of the HP8510B network analyzer. The synthesized sweeper generates the microwave signals in a sweep mode at 801 frequency points. The antenna consists of a conical feed horn and two back-to-back planoconvex dielectric lenses mounted in a conical horn antenna. The combination of lenses produces a plane wave with an approximate spot size of one free-space wavelength at a focal distance of 30.45 cm. The system used 0.01 watt power.

The difficulties usually encountered in measuring the dielectric properties in free space are the suppression of unwanted reflections, the launching of a plane wave in a limited space, and the diffraction from the edges of the specimen. A free-space calibration was adopted to overcome these limitations. The calibration of the measurement system shown in Figure 1 was performed in two steps. First, the rectangular wave guide calibration was conducted between the analyzer and the mode of transition. Then the other calibration was performed on the reflection coefficient data obtained from the metal plate placed at the focus of the antenna (free-space S_{11} calibration). Time domain response was used to apply gating on the transformed frequency domain. Taking a Fourier transform of a gated time domain response (from the top and bottom of the specimen), as shown in Figure 2, gives the reflection data obtained from the specimen only. The correct reflection coefficient, obtained after the calibration, is the ratio of uncalibrated reflections obtained after time domain gating from the metal-backed specimen and the metal plate.

A standard material (0.384-cm-thick glass plate) with known response was used to verify the calibration procedure. Figures 3 and 4 show the variation of the calculated and measured values of $|S_{11}|$ and ϕ (the real and phase of reflection coefficient) for metal-backed glass. The calculated values were obtained by using $\varepsilon^* = 4.38 - j0.02365$. It was found that the measurement accuracy of $|S_{11}|$ and ϕ is ± 0.2 dB and ± 6 degrees, respectively (dB $= -20 \text{ Log } |S_{11}|$). After performing the calibration, the maximum error in $|S_{11}|$ and ϕ for the dry asphalt concrete specimen was found to be ± 1 percent and ± 14 percent, respectively; for the wet specimen, it was found to be ± 5.7 and ± 20 percent, respectively. This error is acceptable considering that the ratio of the loss factor of the wet specimen to the loss factor of the dry specimen is 4:7.

TEST MATERIALS

The test materials used are part of the group of materials under investigation by the Strategic Highway Research Pro-

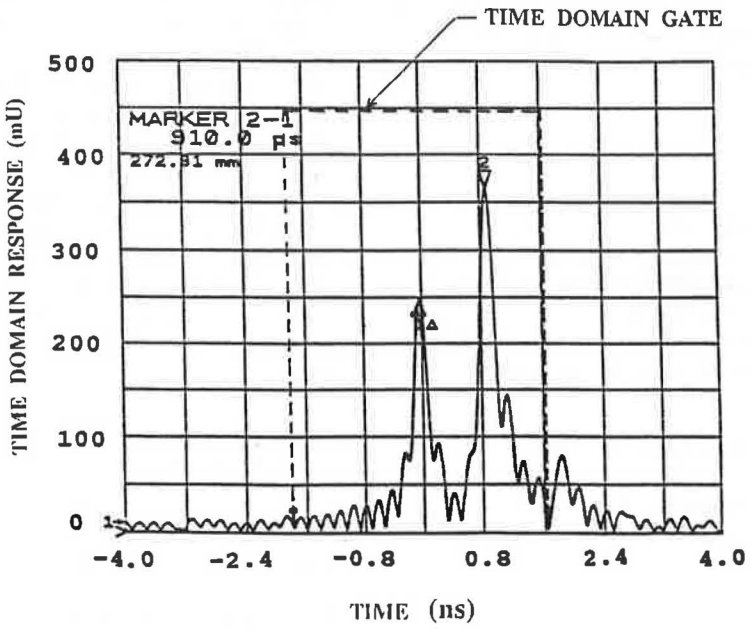

FIGURE 2 Typical time domain response of asphalt concrete specimen backed by metal plate.

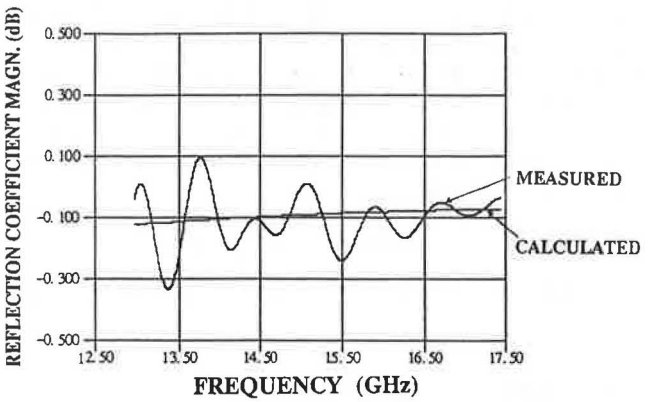

FIGURE 3 Calculated and measured values of $|S_{11}|$ in decibels for 0.384-cm-thick glass plate.

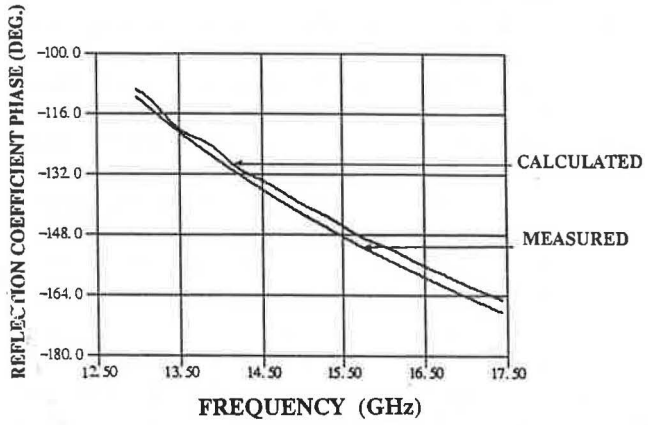

FIGURE 4 Calcualted and measured phase values of S_{11} in degress for 0.384-cm-thick glass plate.

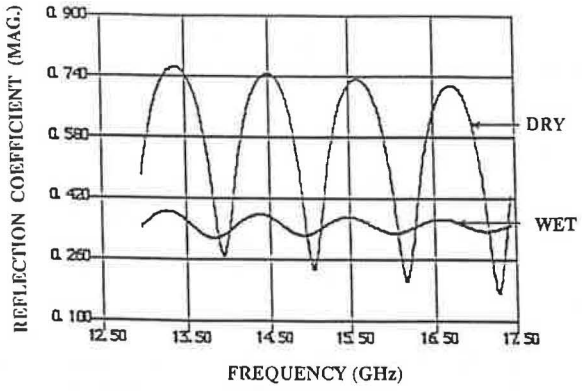

FIGURE 5 Typical reflection coefficient–frequency relation for dry and wet asphalt concrete specimens.

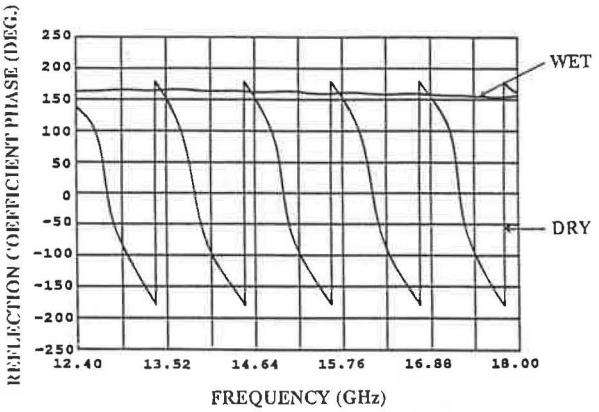

FIGURE 6 Typical phase-frequency relation for dry and wet asphalt concrete specimens.

gram. Two kinds of aggregates were used: low-absorption aggregates (limestone) and high-absorption aggregates (piedmont gravel). Each type of aggregate was used in two gradation forms, dense-graded and open-graded. The dielectric properties of three types of asphalt—Conoco AR4000, Witco AR4000, and Shamrock AC-20—were measured. However, because the measured dielectric properties of these types of asphalt cements were almost the same, only Conoco AR4000 was used in the study. Asphalt concrete specimens were prepared using a kneading compactor for different air void contents, thicknesses, asphalt contents, aggregates, and aggregate gradations.

EXPERIMENTAL RESULTS AND DISCUSSION

The laboratory rest results were obtained at 801 frequency points, each representing an average of 128 measurements. The overall measurements were taken over 30 sec for each test. The measurements consisted of the reflection coefficient and phase as a function of frequency. Figure 5 shows a typical reflection coefficient-frequency relation for dry and wet asphalt concrete specimens; Figure 6 shows a typical phase-frequency relation for dry and wet asphalt concrete specimens. The dielectric constants were calculated over a frequency range of 12.96 to 17.44 GHz. From experience, it is known that the greatest possibility of error occurs at the beginning and end of the frequency band measurements.

The dielectric constants (real and imaginary parts) were calculated over 641 frequency points for each specimen. It was found that the dielectric properties did not vary significantly over the frequency band used. Therefore, the effect of frequency on the calculated dielectric properties was assumed negligible for both dry and wet specimens. Thus, an average dielectric constant and loss factor were used for the specific frequency band. The maximum coefficient of variation obtained was 5 percent.

The real relative dielectric constants of the three types of asphalt cement—Conoco AR4000, Witco AR4000, and Shamrock AC-20—were found to be 2.65, 2.68, and 2.67, respectively. The loss tangents for the three types were found to be 0.0104, 0.0094, and 0.0086, respectively. These results are different from the results obtained for asphalt cement by the Air Force Materials Laboratory (AFML), which showed that the magnitude of the dielectric constant was 2.46 at frequencies of 1, 3, and 8.5 GHz (*6*). The loss tangent results are also different from those found by AFML (which were between 0.0017 and 0.0019). However, the results obtained in this study are in agreement with the results obtained by the Colorado Department of Highways, where the dielectric

constant magnitude was 2.6; no information was given about the loss tangent (*12*). These results indicate that the asphalt cement type does not affect the dielectric constant magnitude of the asphalt concrete mixture and might have a minor effect on the loss factor. Also, the asphalt content of the mixture was found to have no effect on the measured dielectric properties of the mix. This conclusion was reached by measuring the dielectric properties of six specimens having the same characteristics but with different asphalt cement contents. The three asphalt cement contents tested were 4.5, 5.0, and 5.5 percent.

The dielectric properties of aggregates were studied for particle sizes less than 75 μm. In this case, the wavelength of the microwaves was larger than the particle size. The magnitude of the dielectric constants was found to be 4.23 for limestone and 3.20 for piedmont gravel. However, the loss tangent was found to be 0.0318 for limestone and 0.0346 for piedmont gravel.

The specimen surface roughness was found to have no effect on the dielectric properties obtained. Many specimens were tested on both the bottom face and the top face, which was leveled by 1,000 psi compression force after compaction. Specimen thickness was also tested and showed an insignificant effect on the measured dielectric properties of the mixture. Three thicknesses were tested for open-graded limestone asphalt concrete mix: 6.35, 10.16, and 15.24 cm.

After the initial study, it was decided that only the aggregate type and gradation and the air void content have significant effects on the dielectric properties of the asphalt concrete mixture. Therefore, each specimen, with different aggregates, gradation, and air void content, was exposed to three stages of microwave reflection measurements. In the first stage, the specimen was dry. In the second stage, the specimen was vacuum-saturated for 20 min at a vacuum pressure of 25 psi and soaked in water for 2 hr. In the third stage of microwave measurements, the specimen was vacuum-saturated for 90 min at a vacuum pressure of 25 psi and soaked overnight in water. All vacuum-saturated and microwave measurements were performed at 23°C. The amount of water in the specimen was measured by the weight differential method.

The dielectric properties of water were measured at the center of the frequency band used, 15.2 GHz. The water in the asphalt mixture was assumed free and its dielectric properties were determined using the Cole-Cole equation (*1*). The water dielectric constant was 63.34, and the loss tangent was 29.66.

A statistical regression study was performed to correlate the moisture content measured by the microwave technique with the amount of water determined by the weight differential method. The independent variables were the thickness of the specimen, the specimen's air void content, the type of aggregate, the aggregate gradation, the specimen surface smoothness, the dielectric constant magnitude, the loss factor, the difference in the dielectric constant magnitude between the dry and wet specimen, and the difference in loss factor between the dry and wet specimen. The dependent variable was the measured volumetric moisture content. The type of aggregate, aggregate gradation, and surface smoothness were expressed as binary (0 or 1).

The correlation method was used to measure the associations between the variables, and R-squared values were obtained by constructing regression analysis for all possible combinations of the independent variables. The R-squared results show that the difference in the dielectric constant magnitude between dry and wet measurements for a given specimen is the most important factor affecting the R^2-value. If all the independent variables are included in a statistical model, the model is expressed as

$$Y = 0.217 + 0.002A + 0.122B - 0.442C + 8.378E - 0.017F + 0.794G + 0.098H + 6.735I + 1.090J \quad (7)$$

where

Y = volumetric moisture content,
A = specimen thickness,
B = specimen air void content,
C = dielectric constant magnitude,
E = loss factor $\times 10^4$,
F = surface smoothness: 0 for relative rough and 1 for relative smooth,
G = aggregate type: 0 for limestone and 1 for piedmont gravel,
H = gradation type: 0 for open-graded and 1 for dense-graded,
I = difference in dielectric constant magnitude between dry and wet specimens, and
J = difference in loss factor between dry and wet specimens.

The R^2-value for the above model was 95.3 percent and the root mean square error (root MSE) was 0.417. The results of this model are shown in Figure 7. Although this model has good correlation, it is difficult to obtain in situ information about some of the independent variables, such as the air void content. Also, the study showed that the existence of water overshadowed all other effects. Therefore, the following model was developed as a function of the difference of dielectric properties between the dry and wet specimens:

$$Y = 0.620 + 6.136I + 6.873J \quad (8)$$

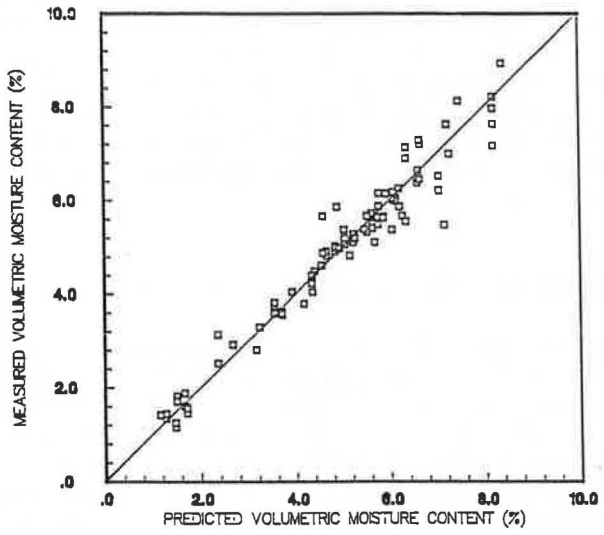

FIGURE 7 Measured versus predicted volumetric moisture content using Equation 7.

R^2 for the above model is 83.2 percent, and the root MSE is 0.758 (Figure 8). This model can be used to estimate the in situ moisture content of asphalt concrete pavement. It requires the measurement of the dry dielectric properties of a few cores from the test site. It is believed that the model shown in Equation 8 is simple and that it is feasible to obtain its parameters. Also, this model is feasible for field application.

FINDINGS AND CONCLUSIONS

This study resulted in the following findings and conclusions:

1. The reflection coefficient and phase amplitude are good indicators of water presence in asphalt concrete mixtures.
2. The information obtained using the free-space setup in the reflection method can be used to calculate the dielectric properties of the asphalt materials.
3. The three types of asphalt cement tested in this study—Conoco AR4000, Witco AR4000, and Shamrock AC-20—have almost the same dielectric properties. However, limestone was found to have a higher dielectric constant magnitude than piedmont gravel and almost the same loss tangent.
4. The difference in dielectric properties between dry and wet asphalt mixtures was found to correlate very well to the volumetric moisture content.
5. The volumetric moisture content in an asphalt concrete mixture can be predicted with an R^2-value of 96.2 percent and a root MSE of 0.560.

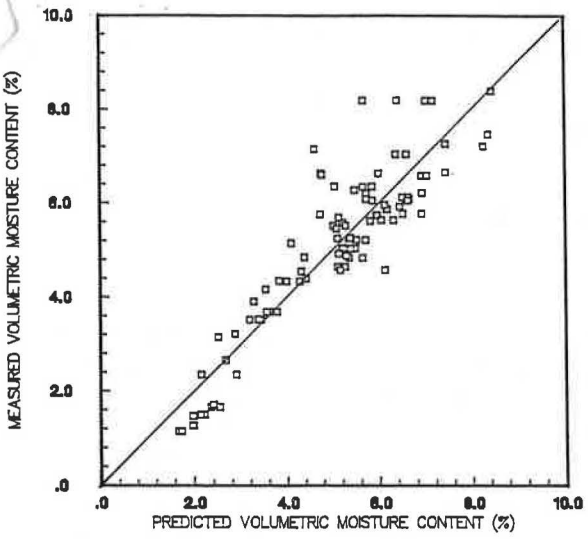

FIGURE 8 Measured versus predicted volumetric moisture content using Equation 8.

6. Because of difficulties encountered in measuring the air void content in the field, a statistical model was developed in which the volumetric moisture content is a function of dry and wet asphalt mixture dielectric properties. The developed model has an R^2-value of 83.2 percent and a root MSE of 0.758.

ACKNOWLEDGMENT

This paper is based on research performed at the Pennsylvania Transportation Institute, Pennsylvania State University.

REFERENCES

1. J. B. Hasted. *Aqueous Dielectrics*. Chapman and Hall, Ltd., London, England, 1973, pp. 235–267.
2. M. I. Skolink. *Introduction to Radar*. McGraw-Hill, New York, 1962.
3. R. F. Goodrich, B. A. Harrison, B. Kleinman, and T. B. A. Senior. Studies in Radar Cross Sections XLVII Diffraction and Scattering by Regular Bodies-1. In *The Sphere*, ARCRL 62-40. Contract 19(604) 6655. U.S. Air Force; Cambridge Research Laboratories, Bedford, Mass.; University of Michigan, 1964.
4. R. W. Newton. *Microwave Remote Sensing and Its Application to Soil Moisture Detection*. Technical Report RSC-81. Remote Sensing Center, Texas A&M University, College Station, 1977.
5. G. G. Clemena. *Determining Water Content of Fresh Concrete by Microwave Reflection or Transmission Measurement*. Final Report. Virginia Transportation Research Council, Charlottesville, in cooperation with FHWA, U.S. Department of Transportation, Aug. 1987.
6. W. B. Westphal and A. Sils. *Dielectric Constant and Loss Data*. Technical Report AFML-TR-72-39. Air Force Materials Laboratory, Air Force Systems Command, Wright-Patterson Air Force Base, Ohio, April 1972.
7. A. R. Von Hippel. *Dielectric Materials and Applications*. Chapman and Hall, Ltd., London, England, 1954, pp. 63–70.
8. W. H. Stiles, F. T. Ulaby, and E. Wilson. *Backscattering Response of Roads and Roadside Surfaces*. Contract No. 07-5688. University of Kansas Center for Research, Inc., Jan. 1979.
9. I. L. Al-Qadi, D. K. Ghodganokar, V. V. Varadan, and V. K. Varadan. Detecting Water Content of Asphaltic Cement Concrete by Microwave Reflection and Transmission Measurement. Presented at 91st Annual Meeting of the American Ceramic Society, Indianapolis, Ind., April 1989.
10. I. L. Al-Qadi. *Detection of Moisture in Asphaltic Concrete by Microwave Measurements*. Ph.D. thesis. Pennsylvania State University, University Park, 1990.
11. J. R. Lundien. *Determining Presence Thickness and Electrical Properties of Stratified Media Using Swept Frequency Radar*. Technical Report M-72-4. U.S. Army Engineer Waterways Experiment Station, Vicksburg, Miss., Nov. 1972.
12. Colorado Department of Highways. *Evaluation of Dielectric Measurement Apparatus for Determining Pavement Density*. Final Report. Colorado Department of Highways, Planning and Research Division, in cooperation with FHWA, Bureau of Public Roads, U.S. Department of Transportation, July 1969.

Effect of Temperature and Mixture Variables on Fatigue Life Predicted by Diametral Fatigue Testing

Y. R. KIM, N. P. KHOSLA, AND N. KIM

One of the major objectives in the Strategic Highway Research Program Project A-003A, Performance Related Testing and Measuring of Asphalt-Aggregate Interactions and Mixtures, is to develop accelerated performance-related tests for asphalt aggregate systems that successfully model construction and service conditions. Controlled-stress diametral fatigue testing was conducted at North Carolina State University to evaluate the influence of temperature and mixture variables on fatigue life of asphalt concrete mixtures with RB (MRL code) aggregates. The resilient modulus testing fixture developed by MTS Systems Corporation in accordance with ASTM D4123 was used with the MTS closed-loop servohydraulic system. Diametral fatigue test results plotted on a logarithmic scale of recoverable horizontal deformation and number of cycles to failure showed a good agreement with the historic trend of the fatigue data. The analysis of variance test results indicated that all the factors investigated in this research significantly affected the fatigue performance of asphalt concrete. In summary, the fatigue resistance was improved by increasing asphalt content and reducing air void contents. The effect of temperature on the fatigue performance of asphalt concrete determined by using recoverable horizontal strain was opposite to that determined by using maximum total horizontal strain. Asphalt concrete with a softer binder resulted in longer fatigue life. Furthermore, the temperature susceptibility of asphalt binder had a pronounced effect on the fatigue life of asphalt concrete mixtures.

Fatigue cracking is one of the major distresses occurring in asphalt concrete pavements. A significant amount of effort has been made to predict the fatigue life of asphalt concrete pavements by laboratory testing under simulated environmental conditions. This effort has produced various types of test configurations and a considerable amount of laboratory data evaluating effects caused by different environmental conditions and mixture variables.

One of the major objectives of the Strategic Highway Research Program Project A-003A, Performance Related Testing and Measuring of Asphalt-Aggregate Interactions and Mixtures, is to develop accelerated performance-related tests for asphalt-aggregate systems that successfully model construction and service conditions. As one of the subcontractors of this project, North Carolina State University is responsible for evaluating the feasibility of the diametral fatigue test as a standardized fatigue testing method.

Department of Civil Engineering, North Carolina State University, Box 7908, Raleigh, N.C. 27695-7908.

The advantages of diametral fatigue test are as follows:

1. The test is relatively simple to conduct;
2. Sample fabrication is easy;
3. The same test configuration has been standardized by ASTM to determine indirect tensile strength and resilient modulus of asphalt concrete;
4. Failure is initiated in a region of relatively uniform tensile stress; and
5. Stress and strain solutions are readily available.

Regardless of these advantages, the sensitivity of test results to environmental conditions and mixture variables must be proved in order for the test to be a standardized method. The test results also must be consistent with historically available data from laboratory testing, test tracks, and field trials.

In this research, diametral fatigue testing was performed on dense-graded asphalt concrete samples at varying temperatures and mixture conditions. The mixture variables investigated in this research include temperature susceptibility of asphalt cement, asphalt content, air void content, and asphalt type.

MATERIALS

Asphalt Cement

Two asphalts used in this research were AAK-1 and AAG-1 asphalts (MRL codes). These asphalts were selected because of their vastly different compositional and temperature-susceptibility characteristics. From the penetration-viscosity-temperature plot, AAG-1 asphalt was found to be more temperature-susceptible than AAK-1 asphalt (*1*).

Two levels of asphalt content for each asphalt (by weight of aggregate) were determined at the University of California, Berkeley, as follows:

AAK-1 (%)		*AAG-1 (%)*	
Low	*High*	*Low*	*High*
5.1	5.7	4.9	5.5

The lower asphalt content was determined using a modification of standard Hveem (ASTM D1560) procedure, and the higher asphalt content was determined by the U.S. Army Corps of Engineers (Marshall) 75-blow procedure (ASTM D1559) (*1*). The higher asphalt content exceeded the lower

asphalt content by about 0.6 to 0.7 percent (by weight of aggregate).

Aggregates

The aggregates used in this research were RB aggregates (MRL code). The selected gradation and ASTM D3515 specification limits are shown in Figure 1. Wet-sieve analysis was conducted to meet this gradation. The detailed sieve analysis procedure can be found elsewhere (*1*).

SPECIMEN PREPARATION AND COMPACTION

Mixing and Curing

The optimum mixing temperatures for two asphalts were selected from a Bitumen Test Data Chart as follows (*1*) [t°F = (t°C ÷ 0.55) + 32]:

Asphalt Type	*Mixing Temperature (°F)*
AAG-1	284
AAK-1	300

The optimum temperatures correspond to a viscosity of 170 ± 20 cSt (*1*).

The asphalt was heated for distribution to small cans (first heating). The asphalt in the small cans to be used for mixing (second heating) was heated at the appropriate mixing temperature. It was stirred periodically to ensure uniform heating. The sample was discarded if it was not used within 3 to 3.5 hr from the start of heating. The heating of the asphalt was done once and was continuous.

Once the asphalt and aggregate were heated at the mixing temperature, they were mixed for 4 min inside a steel bowl. After mixing, the asphalt concrete was placed in an oven maintained at 140°F (60°C) for 15 hr. This curing operation allows any asphalt absorption by the aggregate to take place before compaction or any other use of the mix. More detailed information on mixing and curing can be found elsewhere (*1*).

Compaction

Cured mixtures were compacted at 240°F (116°C) using the gyratory testing machine designed by the U.S. Army Corps of Engineers. One degree of gyratory angle was used to produce briquets 2.5 in. (6.35 cm) high and 4 in. (10.16 cm) in diameter. Two levels of compaction effort were introduced to mixtures in order to produce specimens with two air void contents, 4 and 8 percent, determined in accordance with ASTM D1188.

TEST METHOD

Test Apparatus

The 810 Materials Testing System (MTS) with the 458.20 MicroConsole was used in this research. This servohydraulic system has a closed-loop control. The testing apparatus was provided by MTS Systems Corporation (*2*) and was originally designed for the determination of resilient modulus of asphalt concrete in accordance with ASTM D4123. The schematic presentations of this fixture are shown in Figures 2–4. The fixture was installed inside an environmental chamber in which temperature could be maintained within ±1°F for extended periods.

Horizontal and vertical displacements were measured by extensometers designed by MTS Systems Corporation with full-scale travels of 0.15 in. (0.381 cm) and 0.16 in. (0.4064 cm), respectively. Ranging the transducers to 10 percent of

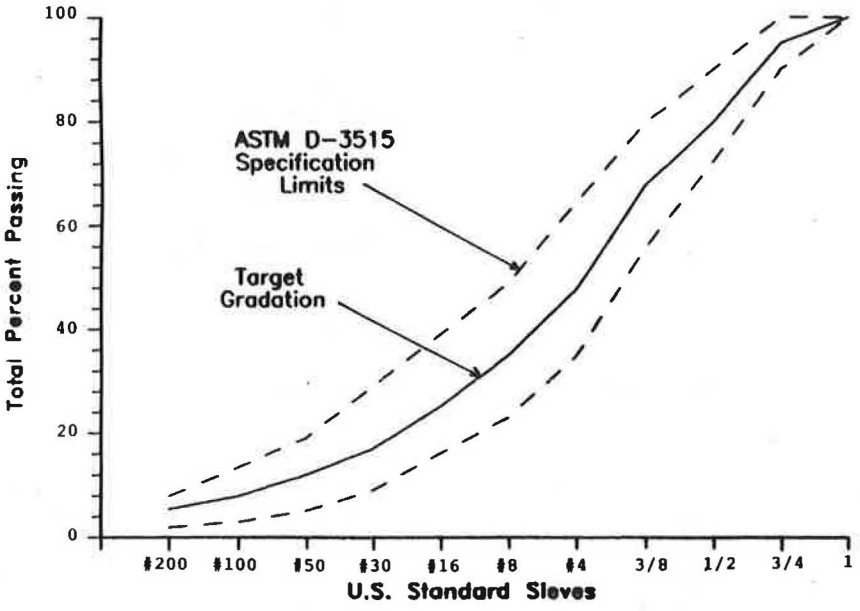

FIGURE 1 Target gradation for RB aggregates after wet-sieve analysis.

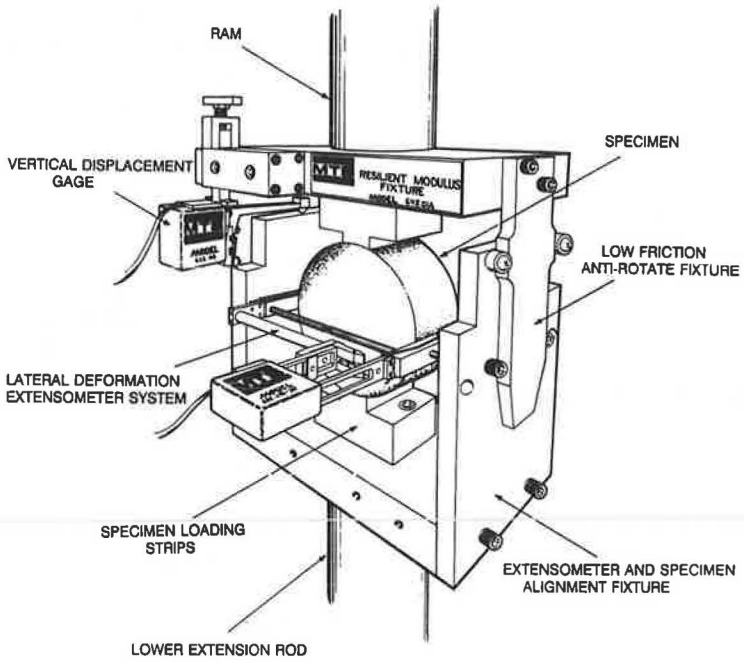

FIGURE 2 Diametral fatigue-testing fixture and extensometers.

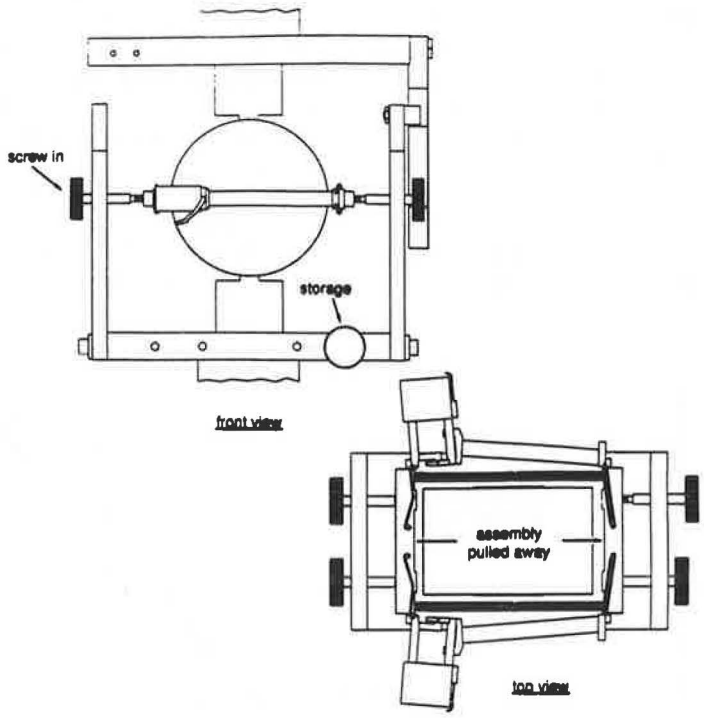

FIGURE 3 Positioning of side brackets using thumbscrews.

full scale calibrates the output to a finer-scale travel and allows higher-resolution measurements of small deformations.

The diametral device consists of two extensometers with gauge-length extenders and two specimen-adapter brackets as shown in Figure 2. The brackets are machined to the same radius as the specimen and remain in contact with the specimen all along the thickness. This design allows each bracket to measure the maximum deformation instead of measuring local deformation caused by point contact with a linear variable differential transducer, which is used in some diametral tensile test fixtures. The device is located on the specimen by guiding pins with the same lengths that extend from the side

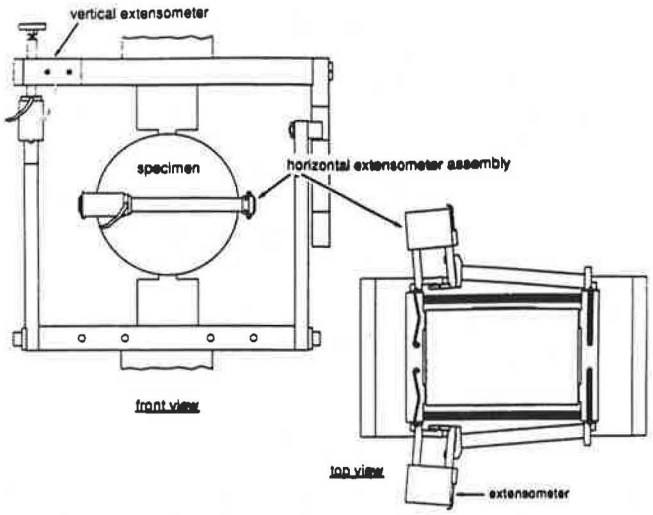

FIGURE 4 Setup ready for testing with spring-loaded extensometers.

of the fixture (Figure 3). When the brackets are pulled away completely, the equal distance between the brackets and the specimen ensures that the center line of the specimen is parallel to the direction of the upper and lower loading strips. Also, because the brackets are placed at the sides of the specimen and guided by pin screws through the holes in fixed side walls, this fixture gives more precise control over the vertical locations of the brackets.

Once the test starts, the low-friction antirotate bar in the upper fixture (Figure 2) prevents possible rotation of the actuator due to repetitive loading. Another advantage of this fixture is that improper measurements caused by "rocking" of the specimen can be minimized. Because the extensometers are attached to the specimen by springs (Figure 4), extraneous deformation caused by rigid-body rotation cannot affect the deformation measurements.

Test Protocol

Four factors were investigated in this research: asphalt type, asphalt content, air void content, and testing temperature. The experimental design is shown in Table 1.

Haversine load with a 0.1-sec load duration and 0.5-sec rest period was repeated until the specimen "failed." The stress amplitude was kept constant throughout testing, and horizontal and vertical deformations were recorded at the 200th cycle. Two load levels, low and high, were used; these load amplitudes induce the failure of the specimen under a specific condition at about 100,000 and 10,000 cycles, respectively.

Horizontal tensile strain (ε_x) in the indirect tensile specimen under the line loading can be determined from

$$\varepsilon_x = \frac{2P}{E\pi td}\left[\frac{(1 + 3\mu)d^4 - 8x^2d^2(1 + \mu) + 16x^4(1 - \mu)}{(d^2 + 4x^2)^2}\right] \quad (1)$$

where

P = load amplitude applied (lb),
E = elastic modulus of specimen (psi),
t = thickness of specimen (in.),
d = diameter of specimen (in.),
μ = Poisson's ratio of specimen, and
x = distance from center line of specimen (in.).

Integrating Equation 1 along the diameter of the specimen obtains the following equation for the horizontal deformation (δ_H):

$$\delta_H = \frac{P}{tE}\left(\frac{4}{\pi} - 1 + \mu\right) \quad (2)$$

To find the largest horizontal strain that occurs in the middle plane, x in Equation 1 is replaced with 0 to get:

$$\varepsilon_0 = \frac{2P(1 + 3\mu)}{E\pi td} \quad (3)$$

where ε_0 is horizontal strain in the middle plane.

In spite of the temperature and stress-level dependency of Poisson's ratio, this study used a value of 0.35 as suggested in ASTM D4123. Equating Equations 2 and 3 obtains the following equation for a 4-in.-diameter specimen:

$$\varepsilon_0 = 0.5235\delta_H \quad (4)$$

Therefore, the recoverable horizontal strain in the middle plane can be determined from

$$\Delta\varepsilon_0 = 0.5235\Delta\delta_H \quad (5)$$

Failure Criteria

The fatigue life of the specimen predicted from the laboratory testing is significantly influenced by the definition of the "failure." According to the earlier study by Scholz (*3*), the failure

TABLE 1 EXPERIMENTAL DESIGN FOR DIAMETRAL FATIGUE TESTS

Asphalt Type	Asphalt Content	Air Voids	Temperature
0	0	0	0
1	0	0	0
0	1	0	0
1	1	0	0
0	0	1	0
1	0	1	0
0	1	1	0
1	1	1	0
0	0	0	1
1	0	0	1
0	1	0	1
1	1	0	1
0	0	1	1
1	0	1	1
0	1	1	1
1	1	1	1

Asphalt Type: 0 = AAK-1, 1 = AAG-1

Asphalt Content: 0 = Low, 1 = High

Air Voids: 0 = 4 ± 0.5%, 1 = 8 ± 0.5%

Temperature: 0 = 32°F (0°C), 1 = 68°F (20°C)

in diametral fatigue testing occurs when the permanent horizontal deformation reaches between 0.28 in. (0.71 cm) and 0.36 in. (0.91 cm). It was recommended that the lead-based foil tape attached on the specimen and the fatigue shut-off wiring for the MTS could automatically stop the testing when the permanent horizontal deformation reached the failure criteria. Preliminary testing was performed under various conditions to determine unified failure criteria for the controlled-stress diametral fatigue tests conducted in this research project.

Throughout the preliminary testing, horizontal deformation was monitored and plotted against the number of cycles (Figures 5 and 6). Irrespective of the test temperature and the applied load, it was found that the horizontal deformation increased dramatically after a value of 0.1 in. of horizontal deformation. Even though the dramatic increase in horizontal deformation occurred earlier than a value of 0.1 in. (0.25 cm) in some cases [e.g., tests done at 32°F (0°C), shown in Figure 5], the difference in the number of cycles between the point where dramatic increase in horizontal deformation occurred and the point with the horizontal deformation equal to 0.1 in. (0.25 cm) was relatively small. It was thus concluded that the failure of the material in the controlled-stress diametral fatigue testing can be described as the moment when the total horizontal deformation reaches 0.1 in. (0.25 cm).

The greatest advantage of having failure criteria at 0.1 in. (0.25 cm) of horizontal deformations is that the fatigue test can be automatically stopped using the MTS limit detector without any additional devices or mechanisms. The limit detector automatically turns off the hydraulic pressure when the horizontal extensometer reading becomes larger than the preset limit, horizontal deformation of 0.1 in.

DISCUSSION OF TEST RESULTS

The recoverable horizontal strain during unloading of 200th cycle was plotted against the number of cycles to failure on a log-log scale. A linear behavior between logarithms of the recoverable horizontal strain and the number of cycles to

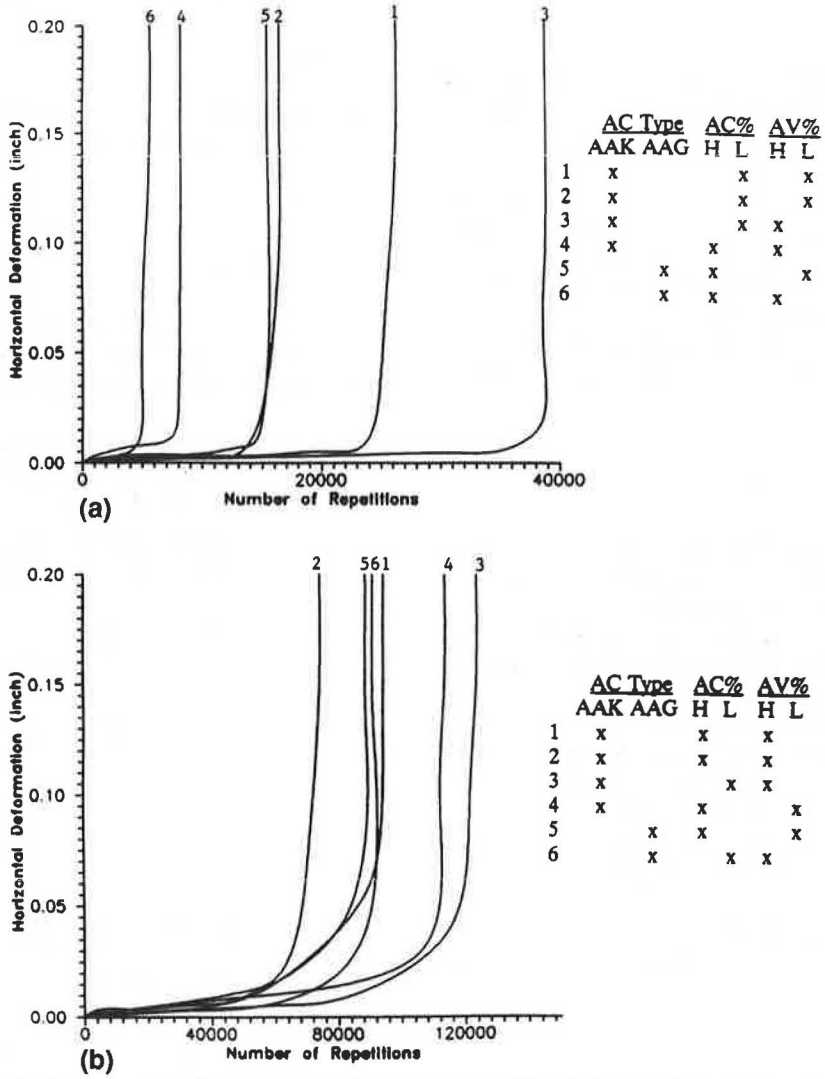

FIGURE 5 Growth of horizontal deformation at 32°F (0°C) at (a) high stress level and (b) low stress level.

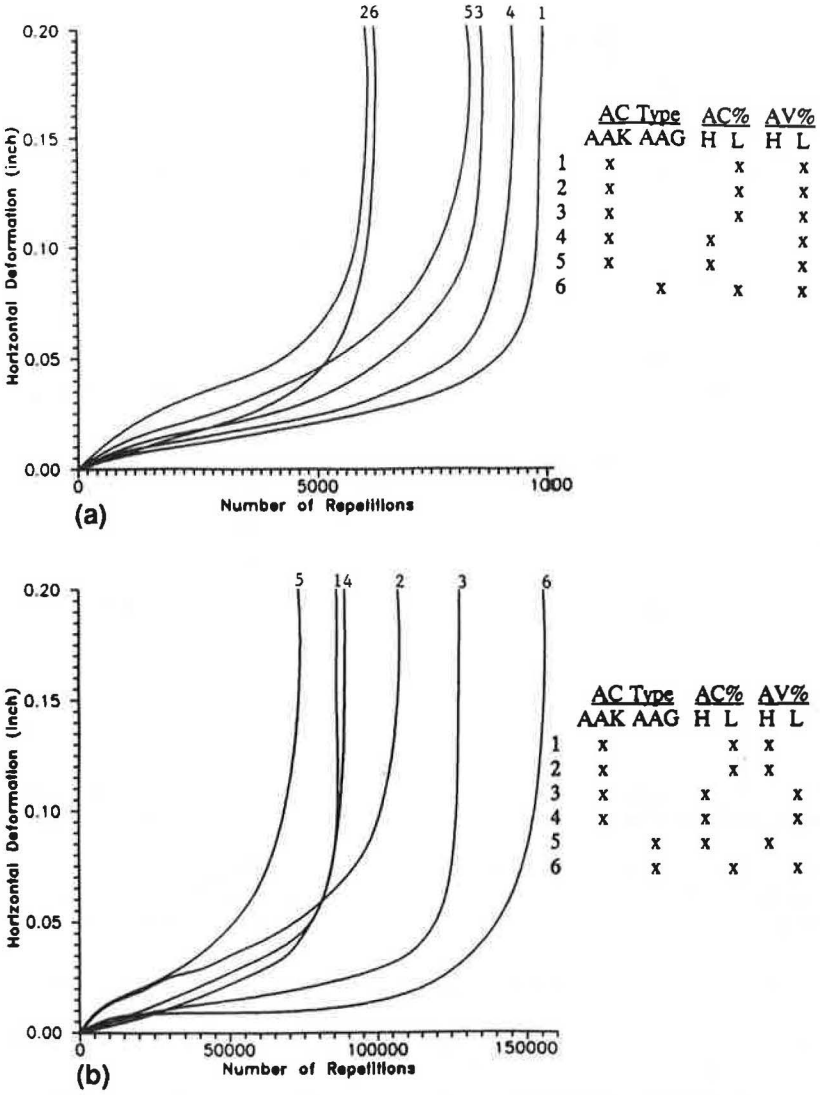

FIGURE 6 Growth of horizontal deformation at 68°F (20°C) at (a) high stress level and (b) low stress level.

failure confirmed the following power form of the fatigue model:

$$N_f = K_1\left(\frac{1}{\varepsilon_t}\right)^{K_2} \tag{6}$$

where

N_f = number of cycles to failure,
ε_t = tensile strain in asphalt concrete, and
K_1, K_2 = regression constants.

The entire test results in accordance with the experimental design in Table 1 are plotted in Figures 7 and 8, and a summary of K_1 and K_2 values are shown in Table 2. Generation of each data point required one test on one sample; for each test condition, four to six data points were required to fit a straight line using a regression analysis.

The same approach was followed using the maximum total horizontal strain at the 200th cycle in lieu of using recoverable horizontal strain in the ordinate of the plots. However, the figures with the maximum total horizontal strain in the ordinate did not demonstrate the effect of temperature and mixture variables as distinctively as Figures 7 and 8 did with the recoverable horizontal strains. Also, as shown in Figure 9, the variation of fatigue data from the best-fit line in the figures was generally smaller when the recoverable horizontal strain was used. The reason for the better role of recoverable horizontal strain is probably because the recoverable horizontal strain does not consider the plastic behavior of materials. Therefore, it was decided to use the recoverable horizontal strain to evaluate the effect of temperature and mixture variables on fatigue life of asphalt concrete.

The analysis of variance (ANOVA) tests for equality of slopes and intercepts of lines were conducted to statistically support the observations from the figures on the significance of different factors on fatigue performance. Test results indicated that all the interactions among factors were statistically insignificant. Therefore, a summary of ANOVA test results is shown in Table 3 for only four independent factors. The intercept in Table 3 is the intercept at the number of cycles to failure equal to 1,000 cycles. The use of intercept at

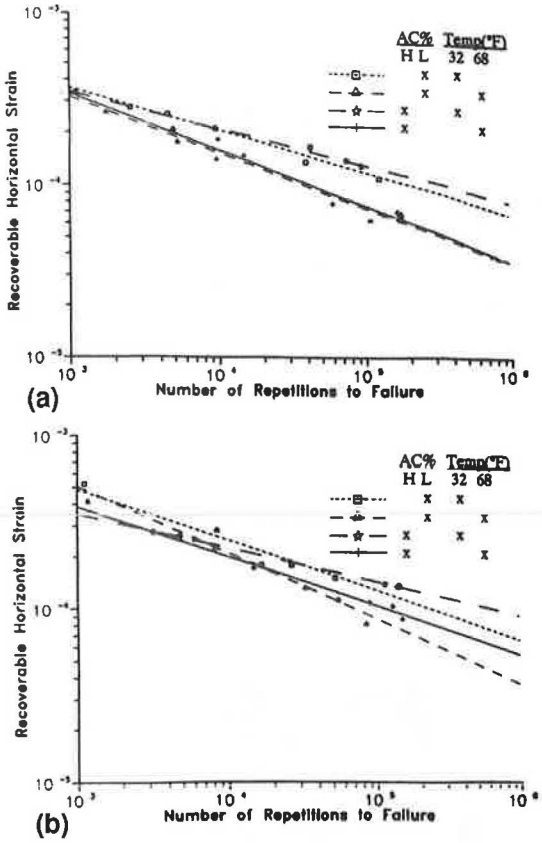

FIGURE 7 Diametral fatigue test results of AAK-1 asphalt mixtures with (a) high air void content and (b) low air void content.

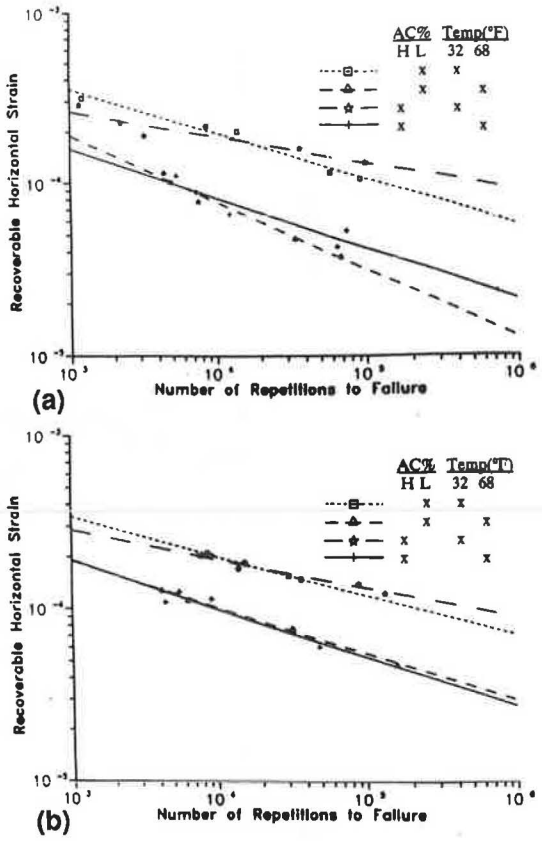

FIGURE 8 Diametral fatigue test results of AAG-1 asphalt mixtures with (a) high air void content and (b) low air void content.

1,000 cycles was necessary to compare findings from the figures and from ANOVA test results.

The ANOVA test procedure uses the *F*-value as the test statistic to test the null hypothesis that all the slopes or intercepts are the same. The level of significance for this test is the probability of having an *F*-value larger than the calculated *F*-value from a data set for the factor in question. A smaller value of this probability implies the heavier weight of the sample evidence for rejecting the null hypothesis. For example, in Table 3, a level of significance of $p = 0.0299$ on slope from asphalt content shows more evidence for the rejection of the null hypothesis, the slopes are the same, than does the statistical test on air voids with $p = 0.5725$. That is, a lower *p*-value means that the effect of the tested factor on a dependent variable (slope or intercept) is more significant.

The statistical results in Table 3 indicate that all four factors investigated in this study had a significant effect on slope or intercept or both. The following sections discuss the effect of individual factor on fatigue performance by using the engineering judgment from the figures and by comparing statistical test results. Normally, factors with a *p*-value less than 0.05 are considered to have a very significant effect on a dependent variable.

Effect of Temperature

The effect of temperature on the fatigue life of asphalt concrete with different mixture variables is shown in Figures 7 and 8. A significant effect of temperature on the fatigue performance was observed and was well supported by the *p*-values of 0.0041 and 0.0043 for slope and intercept in Table 3.

In Figures 7 and 8, the lines representing test data at 32°F (0°C) fall above the lines representing test data at 68°F (20°C), which contradicts a typical trend found from the plots of logarithms of initial bending strain versus number of cycles to

TABLE 2 SUMMARY OF K_1 AND K_2 VALUES

Sample ID abcd*	K_1	K_2
0000	3.00×10^{-9}	3.484
0001	1.90×10^{-8}	2.646
0010	3.82×10^{-13}	4.184
0011	1.00×10^{-8}	3.145
0100	1.01×10^{-15}	5.208
0101	7.71×10^{-10}	3.546
0110	2.07×10^{-14}	4.808
0111	1.40×10^{-8}	3.125
1000	5.40×10^{-13}	4.405
1001	1.64×10^{-11}	3.704
1010	7.51×10^{-11}	3.802
1011	2.85×10^{-7}	2.564
1100	7.95×10^{-19}	5.952
1101	5.76×10^{-11}	3.559
1110	2.72×10^{-21}	6.579
1111	8.70×10^{-11}	3.436

Note: *a = Asphalt Type b = Asphalt Content
c = Air Voids d = Temperature

Levels of each factor are presented in Table 1.

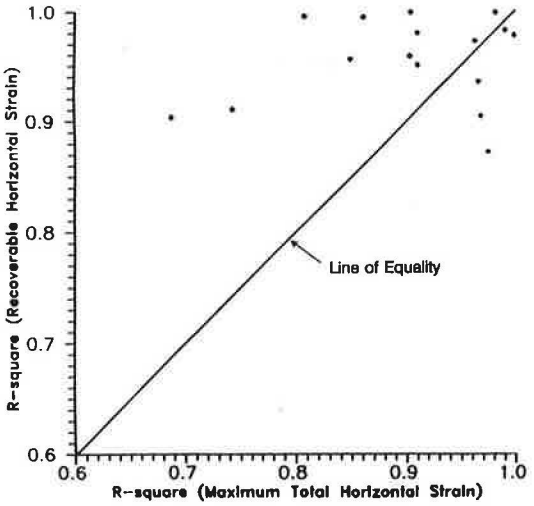

FIGURE 9 Comparison of R^2 values based on recoverable horizontal strain and maximum total horizontal strain.

TABLE 3 SUMMARY OF ANOVA TEST RESULTS

	Level of Significance (p-value)	
	Dependent Variable	
Factor	Slope	Intercept[a]
Asphalt Type	0.3044[b]	0.0004
Asphalt Content	0.0299	0.0303
Air Voids	0.5725[b]	0.0485
Temperature	0.0041	0.0043

[a] The values are the intercepts at the number of cycles to failure equal to 1000 cycles.

[b] These values are considered to be insignificant.

failure from beam flexural tests. When the fatigue test data in Figure 7a were replotted in terms of maximum total horizontal strain and number of cycles to failure as shown in Figure 10, the lines for 32°F (0°C) and 68°F (20°C) test data fell in the reverse order of Figure 7a. The reason for this contradiction is that the major portion of total deformation at 32°F (0°C) is elastic (i.e., recoverable) while the elastic portion of total deformation at 68°F (20°C) is relatively small compared to that at 32°F (0°C).

Therefore, it was concluded that the asphalt concrete layer at 68°F (20°C) fails earlier than that at 32°F (0°C) for a given *recoverable* horizontal strain and vice versa for a given *maximum total* horizontal strain. These findings are in agreement with the research work by Ruth and Olson (*4*) in which they determined the elastic strain from incremental stress test and dynamic fatigue test using indirect tensile mode and concluded that the asphalt concrete has a greater resistance to larger elastic strains at lower temperatures. Also, the comparison between flexural fatigue data and indirect tensile fatigue data showed contradictory results. Ruth and Olson (*4*) stated that the reason for this contradiction was related to the method of testing. Because the beam specimen was returned to its original position after application of each loading cycle, the measured elastic strain was excessive and not indicative of the actual dynamic elastic response of the material.

Kennedy (*5*) demonstrated that the fatigue characteristics obtained using the repeated-load indirect tensile test were comparable to the results obtained from other tests only if the biaxial state of stress in the indirect tensile test was accounted for. Therefore, care must be exercised in using the fatigue data presented in this paper as input to performance prediction models based on the data from beam flexural fatigue tests, such as the fatigue-cracking model used in the VESYS analysis. If the slopes and intercepts determined from Figures 7 and 8 were used in the VESYS analysis, the prediction would result in shorter fatigue life at the higher temperature. An effort was made to develop relationships between the fatigue constants based on these two strains so that the fatigue constants (K_1 and K_2) can be applied based on the recoverable horizontal strain to the fatigue-cracking model based on the maximum total horizontal strain. These relationships are shown in Figures 11 and 12. The correction factors for K_1 and K_2 were developed as follows based on the entire data set excluding one outlier shown in Figures 11 and 12:

$$K_{1,\mathrm{TOT}} = 5245.5\ K_{1,\mathrm{REC}}^{0.821} \qquad R^2 = 0.601$$

$$K_{2,\mathrm{TOT}} = 0.0039 + 0.747\ K_{2,\mathrm{REC}} \qquad R^2 = 0.596 \qquad (7)$$

where

$K_{i,\mathrm{TOT}}$ = K_i based on maximum total horizontal strain,
$K_{i,\mathrm{REC}}$ = K_i based on recoverable horizontal strain, and
i = 1, 2.

These relationships must be used with great caution because of poor R^2 values and sensitive influence of these parameters on fatigue life of asphalt concrete.

Effect of Temperature Susceptibility

Figures 7 and 8 show the effect of temperature susceptibility of asphalt binder on the fatigue life of asphalt concrete mixture. AAK-1 asphalt is less temperature-susceptible then AAG-1 asphalt, and comparison between Figures 7a and 7b for AAK-1 asphalt mixtures and Figures 8a and 8b for AAG-1 asphalt mixtures with varying other conditions proves that the fatigue life of mixtures with AAK-1 asphalt is less temperature-susceptible than that of mixtures with AAG-1 asphalt. That is, the lines for 32°F (0°C) and 68°F (20°C) in Figure 8 are further apart than those in Figure 7, which shows greater temperature susceptibility of fatigue performance of mixtures with AAG-1 asphalt.

In order to statistically support this observation, fatigue data were divided into two sets by asphalt type, and the ANOVA test was performed on each data set. The results are as follows:

	Level of Significance	
Asphalt Type	*Slope*	*Intercept*
AAK-1	0.0116	0.8762
AAG-1	0.0185	0.0007

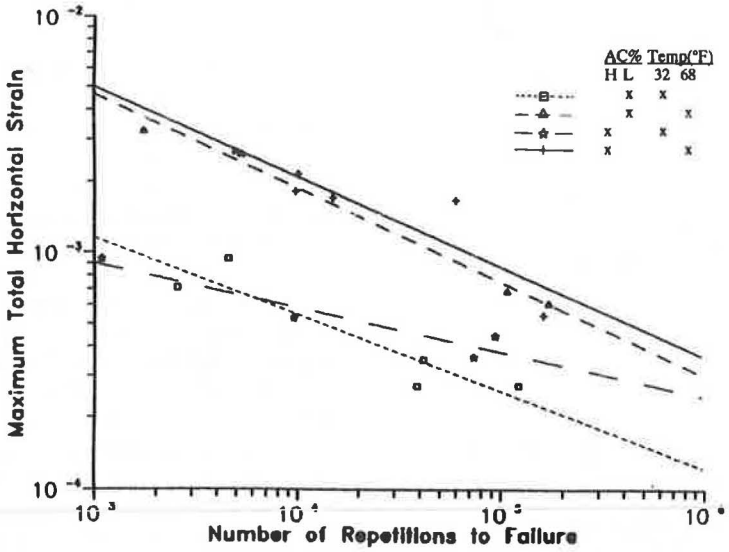

FIGURE 10 Diametral fatigue test results corresponding with Figure 7a (maximum total horizontal strain versus number of cycles to failure).

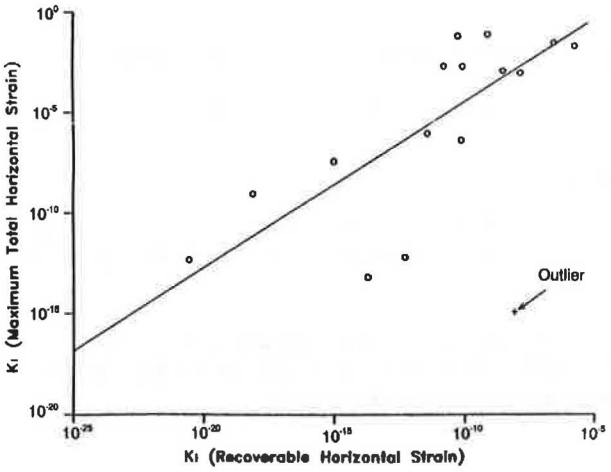

FIGURE 11 Relationship of K_1 values based on recoverable horizontal strain and maximum total horizontal strain.

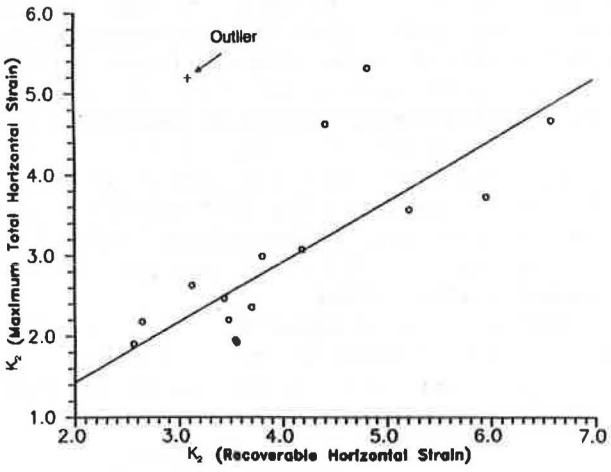

FIGURE 12 Relationship of K_2 values based on recoverable horizontal strain and maximum total horizontal strain.

The level of significance (p-value) of temperature on the slope remains almost the same for both asphalts; the level of significance of temperature on the intercept becomes much greater with AAG-1 asphalt than with AAK-1 asphalt. That is, the effect of temperature on the shift of fatigue lines is more significant with AAG-1 asphalt, which verifies the observation made from Figures 7 and 8.

Effect of Asphalt Content

The ANOVA test results shown in Table 3 indicate that the effect of asphalt content was significant for both slope and intercept. It was observed from Figures 7b and 8a that the increase in asphalt content reduced the slope of the fatigue line. However, the 0.6 percent increase in asphalt content did not make a significant difference in Figures 7a and 8b. This result might be explained by the test results reported by Barksdale (*6*). The fatigue properties of asphalt concrete base course mixes used by the Georgia Department of Transportation were measured using a rectangular beam specimen supported on an elastic rubber subgrade. The influence of asphalt content was evaluated for the mixture with 4.8 percent optimum asphalt content based on the Marshall mix design method. It was found that an increase in asphalt content from 4.25 to 4.5 percent increased the fatigue life by 350 percent and that an increase in asphalt content from 4.5 to 4.75 percent increased the fatigue life by 95 percent. Barksdale concluded that the improvement in fatigue resistance by increasing a specific percentage of asphalt content became less significant as the higher asphalt content was used. Because the asphalt contents used in this study are optimum contents from the modified Hveem mix design method (5.1 percent for AAK-1 asphalt and 4.9 percent for AAG-1 asphalt) and high asphalt contents, which were 0.6 percent higher than the optimum, the effect of increased asphalt content was not significant in some test conditions.

In order to identify the significance of the factors at different levels of temperature, fatigue data were divided into

two sets based on test temperature. The ANOVA tests were then conducted on each data set to investigate the significance of the factors (including asphalt type, asphalt content, and air voids) on slope or intercept at different temperatures. The results are shown in Table 4. According to the results in Table 4, the effect of asphalt content on both slope and intercept is much more significant at 32°F (0°C) than at 68°F (20°C). That is, a 0.6 percent increase in asphalt content in the mixture will provide more resistance to fatigue cracking at 32°F (0°C), which is the temperature range where fatigue cracking is of great concern.

Effect of Air Void Content

To clearly demonstrate the effect of air void content on fatigue life, the test data in Figures 7 and 8 were regrouped as shown in Figures 13 and 14. Figure 13 shows the data at 32°F (0°C), and Figure 14 shows them at 68°F (20°C). It was concluded that the effect of air void content on the fatigue life of the dense-graded asphalt concrete at 32°F (0°C) in Figure 13 was not as pronounced as at 68°F (20°C) in Figure 14. This observation was well supported by the statistical test results in Table 4 because the *p*-values of air voids on both slope and intercept were much smaller at 68°F (20°C) than at 32°F (0°C).

This behavior can be explained on the basis of crack initiation and propagation processes. As shown in Figure 5, the growth in horizontal deformation at 32°F (0°C) is almost negligible until a certain point, and then the growth becomes suddenly chaotic—which results in a complete failure of the specimen. Meanwhile, the growth in horizontal deformation at 68°F (20°C) in Figure 6 is more gradual. Therefore, one can easily draw a conclusion that the crack initiation is the major process at 32°F (0°C) and the crack propagation becomes more important as test temperature increases. With this concept as a background, it can be concluded that the effect of air void content on fatigue life at 68°F (20°C) is more pronounced than at 32°F (0°C) because, at the higher temperature, the failure is governed by crack propagation through void coalescence. In some materials with relatively strong bonding between matrix and reinforcing particles compared to particle strength, a large spherical cavity could decrease the stress concentration and, therefore, crack propagation rate. Conversely, when reinforcing particles are bonded to matrix relatively weakly compared to particle strength, which is the case of asphalt concrete, higher air void content provides better probability of void coalescence, faster crack propagation, and therefore, shorter fatigue life. Meanwhile, at 32°F (0°C), the difference in the air void content may not influence the fatigue resistance because the failure is mainly governed by the crack initiation process.

TABLE 4 EFFECTS OF ASPHALT TYPE, ASPHALT CONTENT, AND AIR VOIDS ON FATIGUE PERFORMANCE AT DIFFERENT TEMPERATURES

	Level of Significance (p-value)					
	Asphalt Type		Asphalt Content		Air Voids	
Temperature	Slope	Intercept	Slope	Intercept	Slope	Intercept
32°F (0°C)	0.1610	0.0325	0.0118	0.0289	0.8676	0.2028
68°F (20°C)	0.6358	0.0012	0.2311	0.2651	0.4495	0.0995

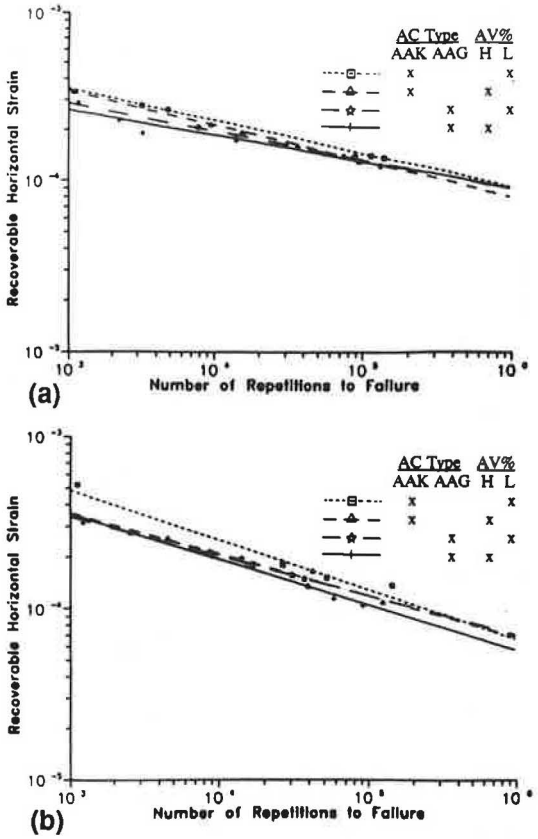

FIGURE 13 Diametral fatigue test results at 32°F (0°C) with (a) high asphalt content and (b) low asphalt content.

Effect of Asphalt Type

Figures 13 and 14 show the effect of asphalt type on the fatigue performance of asphalt concrete. Mixtures with AAK-1 asphalt demonstrated higher resistance to fatigue than did mixtures with AAG-1 asphalt. Also, the difference in fatigue resistance of two asphalt mixtures is more pronounced at 68°F (20°C) than at 32°F (0°C). Table 4 shows the level of significance of asphalt type on slope and intercept at two different temperatures. Statistical results showed insignificant effect of asphalt type on slope at both temperatures, whereas the effect of asphalt type on intercept becomes more significant at 68°F (20°C) than at 32°F (0°C).

This behavior can be explained by comparing the penetration values of two asphalts at both temperatures. The following penetration values were extrapolated from the Bitumen Test Data Chart (penetration-viscosity-temperature chart) (*1*) [t°F = (t°C ÷ 0.55) + 32]:

Asphalt Type	*At 32°F*	*At 68°F*
AAK-1	8	49
AAG-1	3	33

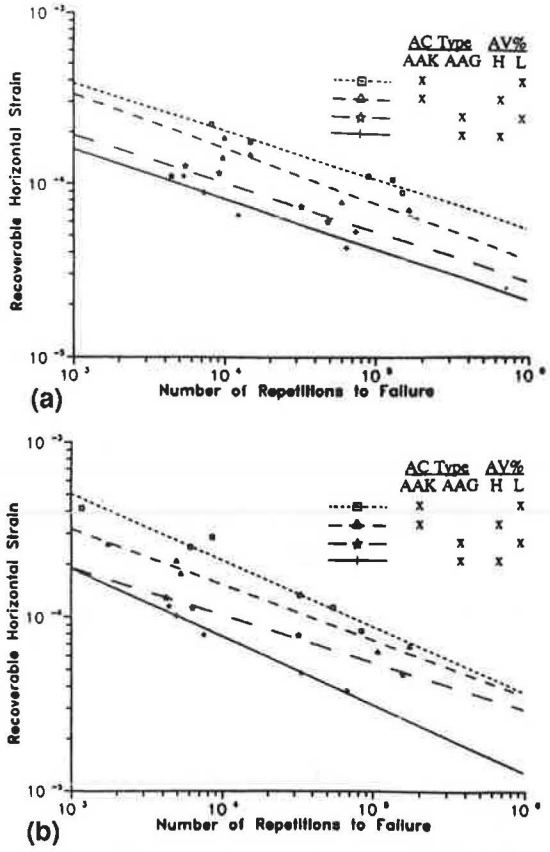

FIGURE 14 Diametral fatigue test results at 68°F (20°C) with (a) high asphalt content and (b) low asphalt content.

Within the temperature range studied in this research, AAK-1 asphalt is a softer binder which provides greater resistance to fatigue cracking. The difference in penetration values of both asphalts becomes greater at 68°F (20°C) than at 32°F (0°C). Therefore, the effect of asphalt type on the resistance to fatigue is more significant at 68°F (20°C) than at 32°F (0°C), as observed from Figures 13 and 14 and from the statistical test results.

CONCLUSIONS

It was proved that the diametral fatigue testing can be a promising tool in evaluating the fatigue performance of asphalt concrete under varying temperature and mixture variables. Within the limits of this study, the following principal conclusions can be drawn:

1. The value of 0.1 in. (0.25 cm) of maximum total horizontal deformation was found to be an appropriate failure criterion of the mixtures irrespective of the variables studied in this research.
2. The effect of mixture variables on fatigue life was better shown in the plots using recoverable horizontal strain.
3. Statistically, the effect of asphalt content was proved to be significant, although the data in some test conditions could not demonstrate the effect clearly. An increase of 0.6 percent above the optimum asphalt content statistically showed more significant improvement in fatigue resistance at 32°F (0°C) than at 68°F (20°C).
4. Assuming constant Poisson's ratio at different temperatures, it was found that temperature has significant effect on the fatigue life. For the given *recoverable strain*, lower temperature results in the longer fatigue life. For the given *maximum total strain*, the reverse is true.
5. An increase in air void content shortens the fatigue life with a more pronounced effect at 68°F (20°C) than at 32°F (0°C).
6. Temperature susceptibility of the asphalt binder has a pronounced effect on the fatigue life of asphalt concrete.
7. Asphalt concrete mixtures with a softer binder demonstrate the higher resistance to fatigue.

ACKNOWLEDGMENT

The authors are grateful to the Strategic Highway Research Program for its support and sponsorship of this research.

REFERENCES

1. J. Harvey. *Asphalt Concrete Specimen Preparation Protocol—SHRP Asphalt Project A-003A, Version 2.0.* University of California, Berkeley, May 1990.
2. C. E. Fairhurst, Y. R. Kim, and N. P. Khosla. Resilient Modulus Testing of Asphalt Specimens in Accordance with ASTM D4123-82. Presented at RILEM 4th International Symposium, Budapest, Hungary, Oct. 1990.
3. T. Scholz. *Evaluation of Cold In-Place Recycling of Asphalt Concrete Pavements in Oregon.* M.S. thesis. Oregon State University, Corvallis, 1989.
4. B. E. Ruth and G. K. Olson. Creep Effects on Fatigue Testing of Asphalt Concrete. *Proc., Association of Asphalt Paving Technologists*, Vol. 46, 1977.
5. T. W. Kennedy. Characterization of Asphalt Pavement Materials Using the Indirect Tensile Test. *Proc., Association of Asphalt Paving Technologists*, Vol. 46, 1977.
6. R. D. Barksdale. Practical Application of Fatigue and Rutting Tests on Bituminous Base Mixes. *Proc., Association of Asphalt Paving Technologists*, Vol. 47, 1978.

Effect of Loading Magnitude on Measured Resilient Modulus of Asphaltic Concrete Mixes

JAMAL A. ALMUDAIHEEM AND FAISAL H. AL-SUGAIR

The diametral resilient modulus test is a procedure by which the resilient or elastic modulus of asphalt mixes can be determined. The resilient modulus is used as a fundamental input parameter in the layer theory for flexible pavements design. In the 1986 *AASHTO Guide for Design of Pavement Structures*, the basis for materials characterization is the elastic or resilient modulus. The diametral resilient modulus test uses the repeated-load indirect tensile strength. ASTM D4123-82 recommends that the resilient modulus (M_r) be measured by applying stresses with magnitudes in the range of 10 to 50 percent of the indirect tensile strength of the specimens. It has been observed that the measured M_r-value depends on the percentage of indirect tensile strength used. For example, the value of M_r obtained by testing at a load of 10 percent indirect tensile strength will be different than that obtained by testing at a load of 30 percent indirect tensile strength. A comprehensive test program investigated the previous observation. To ensure that the difference between the M_r-values measured under various loadings is not statistical, several identical specimens were cast and the M_r-value for a particular loading was found by averaging the results. Also, three different asphalt contents were used to see if the change in M_r is affected by the percentage of asphalt in the mix. The results indicate that the M_r value measured using ASTM D4123-82 depends on the percentage of indirect tensile strength used as the load for testing. Also, the difference in the M_r-value was found to be less for mixes with higher asphalt contents.

Several empirical methods have been developed for characterizing asphaltic materials. These methods are useful for the comparison of materials under specific conditions. Several empirical correlations have also been recommended. However, these correlations are generally valid only for conditions similar to those under which the values were originally developed.

Several test procedures and theories for determining the different moduli of asphalt mixtures have been developed. Among these moduli are Young's modulus, the resilient modulus, the complex modulus, the modulus obtained from the Shell nomograph, and the dynamic modulus. Among these moduli, the resilient modulus has gained popularity as a means of evaluating the response of asphaltic mixtures to loads. In the 1986 *AASHTO Guide for Design of Pavement Structures*, the basis for material characterization is the resilient modulus (*1*). The values of the resilient modulus (M_r) can be used to evaluate the relative quality of materials as well as the input value for pavement design or pavement evaluation and analysis. The diametral resilient modulus test is a nondestructive test which allows the testing of the specimen under different conditions to eliminate the specimen-to-specimen variation. This test is basically a repetitive load test using the stress distribution principles of the indirect tensile test (*2*). In its current form, the diametral resilient modulus test consists of compacting mix specimens, conducting a density-void analysis on compacted and loose specimens, and testing the compacted specimens for their resilient moduli. Details of the test procedure and equipment required are documented in ASTM D4123-82.

Although ASTM D4123-82 is a standard test procedure, it is observed that the M_r-value is affected by different test conditions (*3,4*), particularly the loading magnitude. Therefore, in this study the effect of the loading magnitude on the measured resilient modulus is investigated for asphalt mixes with different asphalt contents. In order to eliminate the statistical variations that may affect the results, a large number of replicate specimens are used.

MATERIALS USED

The aggregate used in this study are the product of the Cercon crusher plant north of Riyadh, Saudi Arabia. The aggregates were sieved; the grain size distribution is shown in Table 1, and the gradation curve is shown in Figure 1. The aggregate gradation selected for this study was recently adapted by the Ministry of Communications (MOC) of Saudi Arabia, in an attempt to control permanent deformation (*5*). Routine tests were performed on the aggregates; the results are summarized in Table 2 along with the specification used in the testing.

The asphalt cement used in this study had a 60/70 penetration grade and was produced by the Riyadh refinery. The asphalt was brought in 20-L containers and separated after heating into 1/2-L cans. The properties of asphalt cement were evaluated; the results are shown in Table 3. The test method used and the specification limits set by MOC (*5*) are also shown in Table 3.

MARSHALL MIX DESIGN

All specimens were prepared according to the Marshall method of mix design using 75 blows of the automatic Marshall compactor on each side. Table 4 shows the Marshall mix design criteria adapted by MOC as a result of changing the aggregate

Department of Civil Engineering, King Saud University, P.O. Box 800, Riyadh 11421, Saudi Arabia.

TABLE 1 GRADATION OF AGGREGATES USED

Sieve size	Percent passing	Tolerance	Job mix Formula
(3/4")	100	+/- 6.0	100.0
(1/2")	76-92	+/- 6.0	84.0
(3/8")	64-79	+/- 5.0	71.5
(#4)	41-56	+/- 5.0	48.5
(#10)	23-37	+/- 4.0	30.0
(#40)	7-20	+/- 4.0	3.5
(#80)	5-13	+/- 3.0	9.0
(#200)	3-8	+/- 1.5	5.5

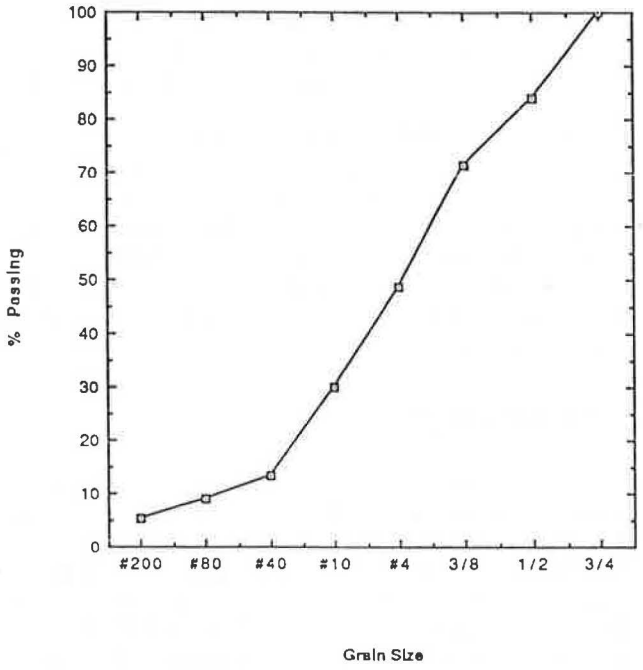

FIGURE 1 Gradation curve of aggregates used.

gradation. Standard cylinders 4 in. (102 mm) in diameter and 2.5 in. (64 mm) in height were prepared at five levels of asphalt cement content, namely 3, 3.5, 4, 4.5, and 5 percent of the total weight of the mix. The results of the Marshall mix design are summarized in Figure 2. The calculated optimum asphalt content is approximately 4 percent. This content was calculated according to the mix design methods for asphalt concrete mixes recommended by the Asphalt Institute (*6*). However, the asphalt content corresponding to 5.5 percent air void content was used because it represents the midpoint between the upper and lower range of the specifications set by MOC (*5*). Also, according to Jimenez (*7*), the amount of asphalt to be used is limited to the amount that will furnish a film thickness ranging from 6 to 12 microns if asphalt absorption is consid-

TABLE 2 PHYSICAL PROPERTIES OF AGGREGATES USED

Test No.	Property	Designation	Results
1.	Bulk Specific Gravity of Coarse Aggregate		2.550
2.	Bulk Specific Gravity (Saturated Surface Dry) of Coarse Aggregate	ASTM C-127-84	2.607
3.	Apparent Specific Gravity of Coarse Aggregate	AASHTO T-85-81	2.672
4.	Percent Absorption		1.783
5.	Bulk Specific Gravity of Fine Aggregate		2.507
6.	Bulk Specific Gravity (Saturated Surface Dry) of Fine Aggregate	ASTM C-128-84	2.514
7.	Apparent Specific Gravity of Fine Aggregate	AASHTO T-84-81	2.695
8.	Percent Absorption	AASHTO T-84-81	2.775
9.	Specific Gravity of Filler Dust	ASTM D-854-83 AASHTO T-100-70	2.690
10.	Percent loss by Los Angeles Abrasion Grading	ASTM C-131-76	
		AASHTO T-96-77	24.0
11.	Soundness by Sodium Sulfate Solution	C-88-83	
	Percent loss in Coarse Aggregate		3.2
	Percent loss in Fine Aggregate	AASHTO T-104-77	3.3
12.	Sand Equivalent	ASTM D2419-79 AASHTO T-176-73	49.2

TABLE 3 PROPERTIES OF ASPHALT CEMENT USED

Property	Test method AASHTO/ ASTM	Test result	MOC* specificatic
Original Asphalt			
Penetration @ 25°C, 100 gm, 5 second (0.1 mm)	T49/D5	62.3	min 60-max 70
Kinematic viscosity @ 130°C (cst)	T201/ D2170	415	min 200
Absolute viscosity @ 60°C (Poises)	T201/ D2171	3064	-
Softening point (°C)	T53/D36	52.5	
Ductility @ 25°C, 5 cm/min, (cm)	T51/D113	+100	min 100
Flash point (°C)	T48/D92	323	min 232.2
Fire point (°C)	T48/D92	350	-
Specific gravity	T228/D70	1.033	-
Loss on heating (%)		0.016	0.8 max
Residue from TFOT**			
Penetration, @ 25°C, 100 gm, 5 second (0.1 mm)	T49/D5	36.5	-
Retained penetration, % of original		58.6	min 52
Kinematic viscosity @ 135°C (cst)	T201/ D2170	56.6	-
Absolute viscosity @ 60°C (poises)		6249	-
Ductility @ 25°C, 5 cm/min, (cm)	T51/D113	94.4	-

* MOC = Ministry of Communication, Kingdom of Saudi Arabia.
** TFOT = Thin Film Oven Test.

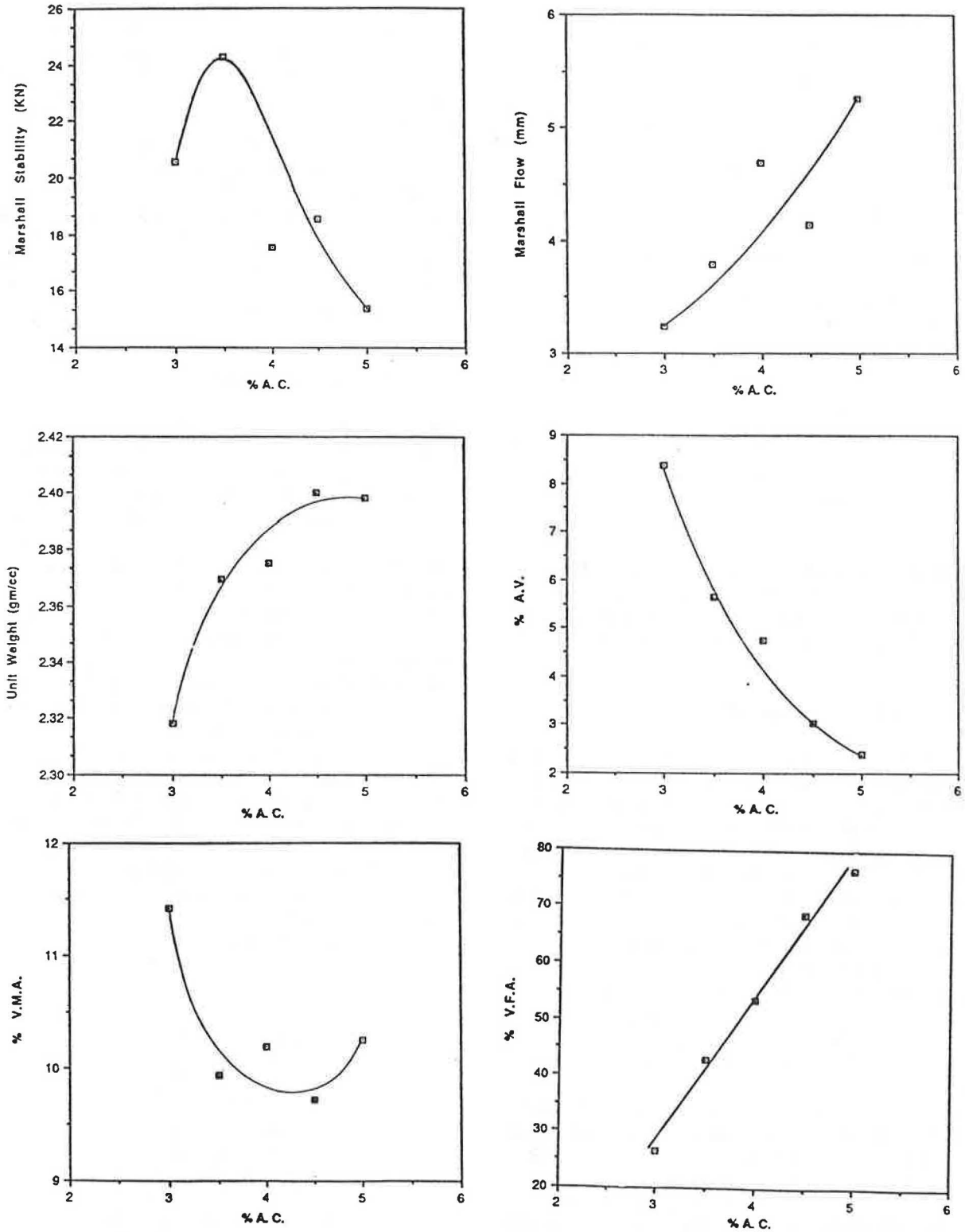

FIGURE 2 Marshall mix design results.

TABLE 4 MOC DESIGN CRITERIA

		LIMITS	
		Wearing Course	Base Course
1.	Voids in Mineral Aggregates	15	13
2.	Air Voids (%)	4 - 7	5 - 8
3.	*Mixing Temperature for Marshall Test	160+/-5C	150+/-5C
	Compaction Temperature for Marshall Test	145+/-5C	145+/-5C
4.	** Marshall Stability (kg) (min)	1000	1000
	Note: Marshall Stability should not vary by more than +/-200 kgs. from design value.		
5.	Marshall flow (mm)	2 - 3.5	2 - 3.5
6.	Hveem Stability (min)	40	40

Note: * = Based on use of 60/70 grade penetration asphalt.
** = At 60 deg. C.

ered. The minimum asphalt content that will yield this film thickness is 4.5 percent as calculated by the procedure presented by Jimenez (*7*). Therefore, it was decided in this study to consider three asphalt contents, namely 4, 4.5, and 5 percent.

STRENGTH CHARACTERISTICS

The Marshall method of mix design for hot mixes was used to prepare the required number of specimens at each asphalt content selected. For each asphalt content, 20 specimens were prepared. Half of the specimens were tested after being subjected to moisture conditioning, herein called wet specimens; the other half were tested at normal (dry) environmental conditions. Each specimen was tested on three different axes 60 degrees apart, thus obtaining a total of 30 measurements for each asphalt content and environmental condition. The prepared specimens were dry cured in an oven at 60°C (140°F) for 72 hr before testing. This process minimized the effect of strength gain due to asphalt aging (hardening), especially for specimens to be studied after moisture conditioning. This curing condition was found to be enough to reach a stabilized condition (*8,9*).

In this study, the 20 specimens prepared at each asphalt content were used as follows: 5 specimens for each asphalt content were used to determine the value of the dry indirect tensile strength, and 10 specimens were used to determine the dry M_r-values. After testing, the 10 specimens, along with the 5 remaining specimens, were soaked under water at 60°C for 24 hr. This procedure was very practical in evaluating the moisture susceptibility of asphalt mixtures (*8,9*). The five extra specimens were used to evaluate the wet indirect tensile strength, the other 10 specimens were used to evaluate the wet M_r-values.

The loading magnitudes were selected to ensure that the applied stresses were within the range of 10 to 30 percent of the indirect tensile strength of the specimens. The upper limit was reduced from the 50 percent indirect tensile strength recommended by ASTM D4123-82 to 30 percent to ensure that stresses within the samples did not exceed the elastic range. To study the differences in the M_r-values due to choosing a different loading magnitude, four levels of pulsating load were used, namely, 225, 350, 475, and 600 lb (1.003, 1.561, 2.118, and 2.676 kN, respectively). Table 5 gives the exact percentages of indirect tensile strength of the applied load for both dry and wet specimens. The room temperature was kept constant at 25°C throughout the period of testing by conducting the test inside a controlled temperature chamber. Before any readings were taken, a minimum of 50 load repetitions were applied to the specimen to properly seat the loading strips on the specimen and to allow the deformation to stabilize.

RESULTS AND DISCUSSION

The values of the dry resilient modulus tests are shown in Figure 3. Each value of M_r in Figure 3 is an average of 30 values of M_r measured from 10 specimens, 3 values from each specimen. Figure 3 shows that the value of M_r decreases with increasing the asphalt content. The important observation in Figure 3 is that the M_r-value measured is higher for a lower level of load. The largest difference is at 4 percent between the M_r-values at load levels 225 lb (1.003 kN) and 600 lb (2.676 kN). The larger value is about 15 percent higher than the lower one. This difference will be even greater if a higher percentage of indirect tensile strength is used (for example 50 percent indirect tensile strength), as the trend shows clearly

Figure 4 shows the M_r-values obtained from the wet resilie modulus tests. Again, the M_r-values are the average of values. The M_r-values are also higher for lower load leve The largest difference is about 11 percent. However, the wet M_r-values are generally higher than the dry values. This could be explained by one or both of the following reasons:

1. The M_r test is dynamic with short-duration pulsating loads. This may cause the water inside the moisture-conditioned specimens to develop pore pressure and thus increase the resilient modulus value measured.

TABLE 5 EXACT PERCENTAGES OF INDIRECT TENSILE STRENGTH OF THE APPLIED LOADS

Load (lbs)		A.C.%		
		4	4.5	5
225	Dry	10.51	10.64	10.84
	Wet	10.00	10.79	11.15
350	Dry	16.36	16.45	16.86
	Wet	15.55	16.78	17.40
475	Dry	22.20	22.61	22.89
	Wet	21.11	22.78	23.54
600	Dry	28.05	28.38	28.91
	Wet	26.66	28.77	29.73

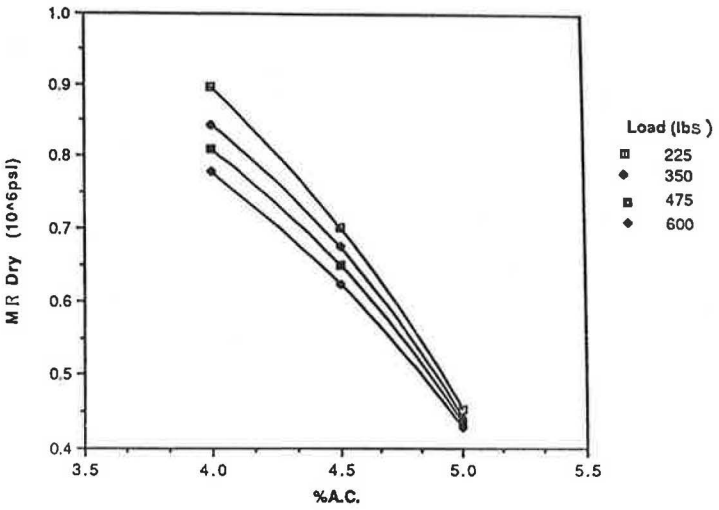

FIGURE 3 Dry resilient modulus versus asphalt content measured under different loading magnitudes.

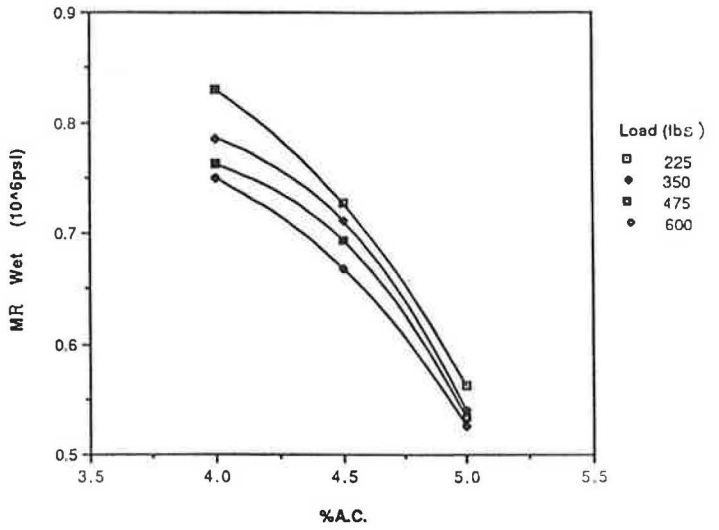

FIGURE 4 Wet resilient modulus versus asphalt content measured under different loading magnitudes.

2. The wet specimens were tested wet, which may have caused a drop in temperature due to evaporation. This drop in temperature may yield a higher M_r-value.

The results make it clear that the M_r-values obtained from the diametral resilient modulus test depend on the percentage of indirect tensile strength used as load. Because a larger load yields a smaller M_r-value, it is clear that a larger load should be used in the test because a smaller value of M_r results in a more conservative design.

CONCLUSIONS

The results indicate that the standard test for determining the resilient modulus of asphaltic concrete mixes depends on the magnitude of load used. Because a smaller M_r-value results in a conservative design, it is recommended that a large percentage of indirect tensile strength should be used when testing for the M_r-value. This would be a load level closer to 50 percent of the indirect tensile strength of the specimen. This is particularly important for mixes with low asphalt contents.

ACKNOWLEDGMENTS

The authors would like to acknowledge the assistance of Abdullah Al-Agil during the testing program. Also, the help of the staff and technicians of the Transportation Laboratory at the College of Engineering, King Saud University, is gratefully acknowledged.

REFERENCES

1. *AASHTO Guide for Design of Pavement Structures*. AASHTO, Washington, D.C., 1986.
2. E. Yoder and M. Witczak. *Principles of Pavement Design*, 2nd ed. John Wiley and Sons, New York, 1975.
3. J. Heinicke and T. Vinson. Effect of Test Condition Parameters on IRM. *Journal of Transportation Engineering*, Vol. 114, No. 2, 1988, pp. 153–172.
4. B. Anani, F. Balghunaim, and S. Swailmi. Effect of Field Control of Filler Contents and Compaction on Asphalt Mix Properties. *Transportation Research Record 1217*, TRB, National Research Council, Washington, D.C., 1989, pp. 29–37.
5. *General Specifications for Roads and Bridges Construction; Revised 1987*. Circular No. 2403. Ministry of Communications, Riyadh, Saudi Arabia, 1987.
6. *Mix Design Methods for Asphalt Concrete*. Manual series No. 2 (MS-2) Asphalt Institute.
7. R. Jimenez. Control of Aggregate Gradation for Asphaltic Concrete, *Proc., 3rd IRF Middle East Regional Meeting*, Vol. 5, 1988, pp. 27–40.
8. R. Almuqayyad. *A Laboratory Evaluation of Moisture-Induced Damage to Asphalt Mixes Used in Riyadh Streets*. M.Sc. thesis, King Saud University, Riyadh, Saudi Arabia, 1990.
9. M. Alajmi. *An Evaluation of Short Term Curing of Asphalt Concrete Mixes*. Research Report 89-05-02, Department of Civil Engineering, King Saud University, Riyadh, Saudi Arabia, 1990.